Laboratory and Field Investigation on Characteristics and Removal Mechanisms of Phosphorus from Wastewater via a Carbonation Process and Apatite

THIS THESIS IS SUBMITTED IN PARTIAL FULFILMENT OF THE REQUIREMENTS FOR THE DEGREE OF DOCTOR OF PHILOSOPHY (PhD)

By

Ban Alkhazraji

B.Sc., M.Sc.

Cardiff School of Engineering

September 2019

Abstract

Phosphorus (P) is a crucial element in the aquatic ecosystem for all livings. The removal of phosphorus from wastewater is primarily to reduce the potential for eutrophication in receiving waters. However, most P removal technologies do not represent an economically viable route and have been developed for use at larger wastewater treatment plants that have rigorous monitoring and in-house operating expertise. Smaller treatment plants often do not have these facilities, which is problematic because there is concern that P releases from small treatment systems may have a more significant environmental impact than previously believed (Bunce et al. 2018). This research is a laboratory and field project involving the investigation of a carbonation process using limestone to remove P from wastewater and include an investigation of the effectiveness of two industrial apatite media. Phosphorus removal using a carbonation process and limestone media to provide calcium ions and precipitation process experimented under various operation conditions of reaction time, carbon dioxide flow rate, aeration flow rate, solution composition, and initial P concentration during laboratory experimentation. Application of this process was designed, constructed and commissioned in West Bonvilston treatment works, a Dŵr Cymru Welsh Water site. The laboratory system of the proposed process showed effective P removal with a range of different P solution compositions and a range of initial P concentrations. The lowest P concentration left in solution was 0.6 mg/l which is lower than the Urban Wastewater Treatment Directive lower control limit of 1 mg/l.

Further study on the precipitate collected from the laboratory system with XRD and total carbon analysis indicated that the form of the precipitate depends on initial P concentration and it's a mix between calcium carbonate and calcium phosphate at high initial P concentration. The results of the laboratory study also showed that precipitation is the dominant removal mechanism. Carbonation stage has been identified as the limiting factor within the field trial. Ca concentration recorded in the field trial was lower than in the laboratory system. pH recorded during aeration stage within the field system was also not high enough to encourage precipitate to occur.

Phosphorus removal by the two apatite media (pellets) in field trial was determined. Overall, the results have shown that both pellets are effective in removing almost 100% phosphate under a relatively low P loading rate. Mechanism of P removal by these pellets is likely to be precipitation as both media release high Ca concentration at high pH.

Acknowledgements

Finishing this doctoral thesis has been a truly life-changing experience for me and it would not have been possible to undertake without the support and guidance that I received from many people.

With my deepest gratitude, I would like to thank my supervisor, Dr Devin Sapsford for giving me the opportunity to undertake this research project under his supervision and guidance. I would not be the researcher I am today without his support, suggestions, valuable discussions and continuous provisions that benefited me much in completion and success of this study.

Special thanks to Dr. Talib Mahdi, for his continued encouragement and specific help on supporting ideas and editing technical works on different aspects of the field part of this thesis.

I would like to express my thanks to Victoria Wilson, Craig Davey, Gemma Hall and Mike Davies from Dŵr Cymru Welsh Water (DCWW) and Patrick Hawes, Stuart Widdowson, Chris Wainwright and Andy Freeman from ARM LTD.

I would like to thank Cardiff University technical staff, who helped me during my PhD journey, Jeffrey Rowlands and Marco Santonastaso for their efforts with me in laboratory work, and their great help during the field trial providing the required material and equipment and advises for experimental setup and maintenance. I would like to thank Carl from the concrete laboratory, Harry from the soil laboratory and Malcolm from the mechanical workshop for their help and contribution towards completing my field experimental setup. Special thanks to Michael Francis for his effort in providing the CO_2 supplier for the field trial.

I am also thankful to those special people who we worked together in the same office for the past three years of my life at Cardiff University, for their support, advice, help and all those nice moments we have spent together Sahar and Safaa. I am particularly thankful to my friends Arwa, Mai and Noha for their continuous encouragement, support and help.

Special thanks to my dearest and most precious mother for her support, encouragement and love. It is never enough to just say 'Thank-you' but please accept my great and sincere appreciation for what you have done for me. My greatest thanks go to my husband (Ali) who was always there encouraging me to overcome all the barriers and my kids (Mena, Sadeer, and Aiya) who make everything and every moment in my life shine brighter, and for their continuous support, prayers and love. Thank you and I love you all very much.

Ban Alkhazraji
September 2019

Contents

List of Figures

List of Tables

Chapter 1: Introduction

1.1 Motivation

phosphorus is a material of great importance for many applications in different fields. About 90% of phosphate is used to produce fertilizers and detergents, and the rest is used in other specific applications such as animal feed, water treatment, food and beverages, dentistry, kinds of toothpaste, fire extinguisher and other different uses (Hanna et al. 2008). Most of the used phosphates, from the agricultural and detergent fields, finally end in the water environment. Such a situation results in pollution of the water environment which leads to more stringent environmental regulations in different countries to reduce phosphate concentration. Phosphorus has been identified as a growth limiting nutrient for algae in aquatic systems. Issues associated with eutrophication include an extraordinary growth of algae and aquatic plants, decreased water transparency, impoverishment of dissolved oxygen levels, increased fish mortality, and more frequent incidence of toxic phytoplankton. These factors not only complicate the use of the water in the water supply of residential areas and enterprises but also affect natural processes taking place in reservoirs (Sabliy et al. 2019). Therefore, eutrophication related water quality deterioration could have very substantial negative economic effects, for example, higher treatment costs and health hazards due to algal toxins for drinking water (Letshwenyo 2014; Huang et al. 2017). The aim behind phosphorus removal from domestic wastewater is primarily to reduce the potential for eutrophication in receiving waters as a global environmental concern, especially with waters worldwide experiencing significant increases in P concentrations and is mandated and widespread in many countries (Lürling and Oosterhout 2013; Yu and Paul Chen 2015). The US Environmental Protection Agency classified eutrophication as the most significant overall source of impairment of the nation's rivers and streams, lakes and reservoirs, and estuaries; while in the EU, approximately 50% of all lakes have total P (TP) at levels which form a risk of eutrophication (Mayer et al. 2013). In the UK, the Technical Advisory Group has advised that 65% of England's rivers fail current P limits with lakes being more sensitive to contamination (Wood et al. 2007). Conventional technologies widely used for P removal from wastewater like chemical precipitation and enhanced biological phosphorus removal, with chemical precipitation being most common through dosing of iron and / or aluminium salts. The base of these treatment approaches is to convert the state of phosphorus from soluble forms in wastewater streams to insoluble forms, either by using metal based coagulants to precipitate it or by incorporating it into biological biomass. Further, whilst it is possible to increase chemical dosing to attain low P concentration, the additional cost and the risk of overdose of Fe / Al by site operators, high metal

concentration and low pH leading to environmental harm and risks of large fines plus the health and safety risk associated with handling aqueous acidic or alkaline chemicals alongside with the water industry's drive towards chemical free treatment make it an undesirable option (Blaneyet al. 2007). Both these methods can require operator input which is particularly unfavourable at smaller WWTWs that only serve small populations. These smaller plants have a much higher cost per kilogram of phosphorus removed. For example, the average cost of chemical dosing per Kg of P to a target concentration of less than 1 mg/l is £146 for very small plant with population less than 2000, whereas the average cost to the same target concentration is £6 at large works of population more than 80000 (Ofwat 2015). Moreover, these technologies are either generate secondary sludge which needs to be disposed of, or they cannot be relied upon in certain cases. Such cases can include when aiming for low P concentration in final effluents, or when dealing with wastewater with highly variable characteristics. Significant progress has been made in developing some technologies for small-scale application. However, there is still a shortage of treatment technologies for P-removal at smaller scales, particularly sustainable and reliable options that demand minimal operating and maintenance expertise. In view of emerging regulatory pressure, investment should be made in developing new or adapting existing P-removal technologies, specifically for implementation at small-scale treatment works. An investigation into new techniques is therefore required, to enable the water industry to comply with the tighter consent limits and so protect the ecology of surface waters (Bunce et al. 2018).
This thesis presents work that investigates the potential of two different ways to remove phosphorus from wastewater. The first is the application of precipitation theory for the removal of phosphorus from wastewater via a carbonation process using limestone. The second way is by using two types of apatite media (pellets). Laboratory and field experiments were conducted to investigate the above.

1.2 Aim of Thesis

The combined aim of this study was to assess the performance of a carbonation precipitation process and the effectiveness of apatite media in eliminating phosphorus from wastewater. The method and the media should be suitable to be used in rural treatment works and such should have low energy and maintenance requirements. Furthermore, they should be able to be retrofitted to existing sewage treatment works plus the possibility of implementing such a process/media at a small-scale treatment works. The following objectives were developed to meet this aim:

- To determine the effect of CO_2 flow rate and duration on calcium carbonate dissolution in the presence and absence of phosphate ions.

- To determine the effect of subsequent aeration flow rate and duration on the pH and precipitation of calcium carbonate/calcium phosphate.
- To determine the effect of different lengths of quiescent conditions on any precipitate formed.
- To determine the effects of the presence of foreign ions on precipitate formation through the assessment of tap and real wastewater.
- To determine the minerology and bulk chemistry of precipitate formed by the process
- To determine the effect of foreign ions on bulk chemistry of the precipitate formed.
- To determine the mechanism through which phosphate is removed in the aeration and settling stages of the process through the determination of adsorption capacity, zeta potential, ESEM and XPS of the newly formed precipitate and undertake detailed physicochemical characterisation of any precipitates formed.
- To identify the key factors for removing phosphorus from wastewater using the process at full operational scale.
- To characterise the forms of P in real wastewater at the West Bonvilston site.
- To determine the minerology and bulk chemistry of an industrial media (apatite pellets) and the adsorption behaviour of these pellets.
- To determine the effectiveness of the two-industrial media (apatite pellets) in application for phosphorus removal from wastewater.

1.3 Organisation of Thesis

The thesis is presented as a collection of discrete chapters, all contributing to the research objectives in section 1.2.

Chapter 2 gives an extensive literature review that includes three main parts. The first part describes the background to the problems addressed by this thesis i.e. the driving forces of this study. The problems with phosphorus sources are discussed as are the increasing strains on current phosphorus removal technology at WWTWs. The second part discusses the theoretical background to the processes touched on in this thesis. The third part reviews work that has been carried out by others in related fields to this study. The phosphorus removal performances of other natural materials are discussed as well with other studies that have directly looked at the use of limestone to remove phosphorus are then evaluated.

Chapter 3 this chapter divided into two parts. The first part describes the material tested in this study and presents the experimental methods used to carry out the laboratory experiments. The second part describes field trials experimentation including the experimental setup and design details of Cardiff University field trial and ARM Limited (a privately owned company based in

Rugeley, Staffordshire. Established in 1947 as agricultural engineers, since 1980, the company specialised in the development and application of natural wastewater treatment systems using constructed wetlands technology) trial of using 2 types of apatite media to remove phosphorus from wastewater.

Chapter 4 presents the results and the discussion of the laboratory experiments according to an experiment plan shown in this chapter. The results and discussion of other economical ways to reduce the cost of the process are included in this chapter

Chapter 5 presents the results and the discussion of precipitate full characterisation and the investigation of the dominant removal mechanisms. This chapter also include the results and discussion of the laboratory work carried out on the apatite media supplied by ARM Ltd.

Chapter 6 presents the results and the discussion of Cardiff university and ARM Ltd field trials.

Chapter 7 an overall discussion of the findings presented in the previous chapters, surmises the key conclusions and recommendations for future work that this thesis has resulted in.

Chapter 2: Literature Review

2.1 Introduction

Phosphorus can be considered as one of the most critical nutrients for all livings and it is making a major contribution to the development of agriculture and industry. On the other hand, it has an essential role in biochemical functional groups for the growth of cells in plants including algae (Zhou et al. 2005). In many water environments, P is the limiting nutrient in inhibiting the excessive growth of algae. Consequently, disposal of phosphorus rich effluents into surface water such as lakes, rivers, reservoirs and estuaries promotes eutrophication (Hussain et al. 2011; Letshwenyo et al. 2014). Eutrophication results in oxygen depletion in surface waters leading to detrimental effects on aquatic life and water quality (Kang et al. 2018). Under low phosphorus concentrations, algae do not pose any problems for water treatment; however, blooms resulting from phosphorus enrichment can affect water treatment (Huang et al. 2017). Accordingly, stringent laws have been developed by bodies such as the European Union to control the level of P concentrations into receiving environments. The EU directive 91/271/EEC sets limits of total phosphorus in effluent wastewater of 1 or 2 mg P/l on an annual average basis in sensitive areas depending on the equivalent population of the discharge area. Mainly, there are two techniques currently employed by the UK water industry to remove phosphorus from wastewater: chemical and biological. The chemical removal method works by dosing iron or alum salts, which cause phosphorus to precipitate out of solution, settle, and be removed as sludge. Biological removal uses bacteria to incorporate phosphorus from solution into biomass, which is also settled and removed as sludge. Both techniques are successful at eliminating sufficient concentrations of phosphorus. However, enhanced techniques are required to be employed by the water industry to enable the necessary improvements in phosphorus removal to comply with the new legislation (Tahmazi et al. 2017).

This chapter reviews previously undertook research to verify the background issues for the work presented in this thesis. These issues derive from the pressure faced by the water industry in terms of P removal. The specific objectives of this chapter are: To explore and discuss in-depth, state of the art for P removal, To review the theoretical background of the removing process adopted in this study, To identify the gap in knowledge regarding P removal techniques. This chapter is split into the following sections:

Section 2.2: Background – presenting the role of phosphorus in nature and how anthropogenic sources can affect the aquatic environment. The problem of increasing pressure on current

phosphorus removal techniques at Wastewater Treatment Works (WWTWs). The control of phosphorus, both in terms of legislation and treatment methods at WWTWs.

Section 2.3: Theory – presenting the theoretical background to concepts used in this thesis.

Section 2.4: Related work – reviewing some of the alternative methods of phosphorus removal and draws out parts relevant to the current study.

Section 2.5: Chapter summary and conclusions.

2.2 Background

2.2.1 Phosphorus

Phosphorus is a highly reactive element, especially under oxidizing conditions, and never found in its free form in nature but almost always in its fully oxidized state as phosphate (PO_4^{3-}) (Corbridge 2016). At present, this phosphate is derived from non-renewable natural resources of rock. While it is acknowledged that energy and water issues must be addressed for meeting the future nutritional demands of a growing population, the need for securing phosphorus supply for fertiliser production has not been widely recognised (Cordell et al. 2009). Based on the most extreme predictions, phosphate rock reserves could be exhausted in the next 50 - 100 years (STEEN 1998; Martin 2010). The need for sustainable use of this valuable and finite resource is evidently becoming increasingly important.

2.2.2 Phosphorus in natural systems

Many researchers studied the chemistry of phosphorus compounds in aqueous solutions. Most works was done in the 60's and 70's as a theoretical support for chemical precipitation of phosphorus compounds. In natural water systems, P occurs in three different forms of soluble reactive phosphorus (SRP), soluble unreactive phosphorus (SUP) and particulate phosphorus (PP) (Sharpley and Haygarth 1991; Zhang et al. 2004; Faul et al. 2005; Paytan and McLaughlin 2007). The sum of SRP and SUP is called the total soluble phosphorus (TSP), and the sum of all P fractions is called the total phosphorus (TP). The distinction between the soluble and particulate fractions is usually separation on 0.45 µm filter with the soluble fraction passing through the filter (Paytan and McLaughlin 2007). The dissolved P species (i.e. $H_2PO_4^-$ and HPO_4^{2-}) are the dominant species in the aquatic environment (Paytan and McLaughlin 2007; Yoshimura et al. 2007). However, the abundance of this P form is generally dependent on the water quality parameters such as the pH value(Benitez-Nelson, 2000). The dissolved inorganic phosphorus (DIP), is a very important fraction as it is the most readily available P fraction to aquatic plants and often considered the most critical fraction contributing to accelerated eutrophication of surface waters. The dissolved inorganic phosphorus (DIP) is considered as a small proportion of TP transported with values of 0.01 to 0.025 mg/l (Meybeck 1993). However, being the most reactive fraction of TP (Froelich 1988), this fraction reacts with acid solutions containing molybdate ions to form a phosphomolybdate complex, which can develop a coloured molybdenum blue complex when reducing with ascorbic acid (Murphy and Riley 1962). This DIP includes orthophosphates the most significant form of inorganic phosphorus, inorganic condensed phosphates (polyphosphates) such

as pyrophosphates, tripolyphosphates and trimetaphosphates (Maher and Woo 1998). Common classes of phosphorus containing compounds in aquatic systems are shown in Table 2.1.

Table 2- 1: Classes of phosphorus containing compounds of importance in aquatic systems (from Snoeyink and Jenkins 1980)

Group	Species of Importance	Acid Ionization Constants (25°C)
Orthophosphate	H_3PO_4, $H_2PO_4^-$, HPO_4^{2-}, PO_4^{3-}, HPO_4^{2-} complexes	pK_{a1} = 2.1 pK_{a2} = 7.2 pK_{a3} = 12.3
Polyphosphates **Pyrophosphate**	$H_4P_2O_7$, $H_3P_2O_7^-$, $H_2P_2O_7^{2-}$, $HP_2O_7^{3-}$, $P_2O_7^{4-}$, $HP_2O_7^{3-}$ complexes	pK_{a1} = 1.52 pK_{a2} = 2.4 pK_{a3} = 6.6 pK_{a4} = 9.3
Tripolyphosphate	$H_3P_3O_{10}^{2-}$, $H_2P_3O_{10}^{3-}$, $HP_3O_{10}^{4-}$, $P_3O_{10}^{5-}$, $HP_3O_{10}^{4-}$ complexes	pK_{a3} = 2.3 pK_{a4} = 6.5 pK_{a5} = 9.2
Metaphosphates	$HP_3O_9^{2-}$, $P_3O_9^{3-}$	pK_{a3} = 2.1
Organic phosphates	Very many types, including phospholipids, sugar phosphates, nucleotides, phosphoamides, etc.	

2.2.3 Phosphorus sources in wastewater

Despite books and papers focused on phosphorus as a chemical compound e.g. (Corbridge 1966, and 1995) various studies focused on the fate of these compounds with a special emphasis on water and wastewater treatment based on the fact that phosphorus has a significant impact if it discharged to the water bodies in high concentrations. Original works were done by Stumm (1962); Stumm and Morgan (1970). These works were followed by many other papers e.g. (Jenkins et al. 1971; Goldsmith and Rubin 1980; Fytianos et al. 1998). The sources of phosphorus in wastewater vary from fertilizers (orthophosphates) to cleaning products (condensed phosphate) and from the breakdown of organic material such as bacterial cells (organic phosphorus)(De-Bashan and Bashan 2004). Most authors agree that orthophosphates are dominating over other phosphorus compounds in wastewater. Particulate phosphorus can be the

product of weathered material, incorporated into plant, animal or bacterial material or direct precipitation of inorganic phosphorus. Insoluble phosphorus is found adsorbed to particles or incorporated into amorphous and crystalline material. Additionally, soils and sediments contain P bound to iron or aluminium (Maher and Woo 1998; Maryutina 1999). Struvite ($MgNH_4PO_4$ $6H_2O$) and Vivianite ($Fe_3(PO_4)_2$ $8H_2O$) are two examples of specific minerals containing phosphorus. Polyphosphate accumulating organisms (PAOs) are used in wastewater treatment to hydrolyze and store poly-P and orthophosphate under anaerobic and aerobic conditions respectively (Mino et al. 1998). the chemical species of orthophosphate (H_3PO_4, $H_2PO_4^-$, HPO_4^{2-}, and PO_4^{3-}) vary with the pH of solution phase and with the nature of adsorption sites in the solid phase. The common forms of phosphorus in wastewater are orthophosphate (PO_4^{3-}), polyphosphates (polymers of phosphoric acid) and organically bound phosphates. The latter two forms gradually hydrolyse in water to the soluble ortho form and, therefore, it could be said that orthophosphate presents the principal form of phosphorus in wastewater (Ooi et al. 2017). Due to the reactivity of phosphate it bonds with many cations such as iron (Fe), aluminum (Al), and calcium (Ca) which form relatively insoluble compounds. The most common P compounds are oxyphosphorus compounds all of which contain phosphorus - oxygen connections. Oxyphosphorus compounds include orthophosphates, condensed phosphates, and organic phosphate esters (phosphorus - oxygen - carbon bonds)(Corbridge 2016).

2.2.4 Industrial uses of phosphorus

The modern world has generated an increasing demand for phosphorus, which has led to its increased extraction from minerals and consequently its increased discharge into the environment. The industry with the most considerable need for phosphorus is agriculture consuming 80-85% of total demand, the majority of this goes to the production of inorganic fertilizers with the remainder going into areas such as animal feed production (Martin 2010; Littler 2012). The second largest need for phosphorus comes from the detergent industry where phosphorus is used as a builder which assists in softening the water and establishing optimum cleaning conditions. Other industries that require phosphorus include metal surface treatment, flame retardation, fruit and vegetable processing and paper production (Littler 2012; Bowes et al. 2016).

2.2.5 Role of phosphorus in the eutrophication

The European legislation (Commission of the European Communities 1999) defined eutrophication as the enrichment of water by nutrients (mainly nitrogen (N) and phosphorus (P)),

resulting in an excessive growth of algae or floating plant mats and higher forms of plant life, thereby generating an undesirable disturbance to the balance of organisms present in the water and the quality of the water concerned.

During the algal bloom, floating thick mat of algae prevents light from reaching plants under the surface. When algal organisms die, they settle to the bottom, where bacteria that live in the sediments digest them. This mechanism leads to bacteria blooms in conjunction with an algal bloom, and thus oxygen consumption is increased leading to anoxia in poorly mixed bottom water. Over time, sediments release P that reinforces the eutrophication (Kagalou et al. 2008; Tahmazi et al. 2017).

Anthropogenic sources of phosphorous can be split into two categories, point and diffuse sources. Point sources are those that enter watercourses at a single point of discharge, these sources are typically wastewater treatment works, but will also include releases from the industry. Diffuse sources generally result from agricultural run-off where phosphorus from fertilizers and animal wastes can be washed into watercourses. The relative contribution from agriculture and domestic sewage to phosphorus in rivers varies depending on how urban or rural the catchment area is (Minstone and Parr 2002; Littler 2012).

2.2.6 Phosphorus legislation

Phosphorus has been controlled under EU legislation since 1975 when standards for drinking water abstraction were drawn up. The 1991 Urban Wastewater Treatment Directive also contained controls for phosphorus as did the Directive for Integrated Pollution and Prevention Control (IPPC) (1996). The WFD (A European directive which introduces a planning process to manage, protect and improve the water environment. It applies to all rivers including drains, ditches, lakes, estuaries, coastal water and groundwater) introduced in 2000 ensures the full integration of the economic and ecological perspectives in water quality and quantity management. Its key objective is to achieve, by 2015, good status for the over 111 000 surface waters (e.g. rivers, lakes, coastal waters) and the over 13000 groundwaters in EU territory. The WFD however allows for extensions to the 2015 deadline, provided they are limited to at most 2 further cycles (i.e. the present 2015, 2021 period, and the next 2021-2027 one), unless natural conditions prevent reaching the WFD objectives within the time limits set. Achieving “good status” means securing good ecological and chemical status for surface waters and good quantitative and chemical status for groundwaters, main sources of abstraction of drinking water. Under the WFD all watercourses will have to achieve “good” status, this will be mostly as close to a natural condition as possible, i.e., minimal anthropogenic influence. Rivers will be assessed

under both ecological and chemical categories, phosphorus, as a critical nutrient will be controlled under the WFD (2000/60/EC).

Legislations on the effluent from WWTPs have been created to reduce P discharges into the surrounding environment. The UK Environment Agency regulates wastewater treatment works by assessing the quality of the wastewater they discharge against set compliance limits. The regulation regarding total P discharge updated on 17 January 2019 states that the maximum allowable phosphorus release of 2mg/l from treatments sites with population equivalent of between 10 000 – 100 000 and a discharge of no more than 1 mg/l from plants with population equivalent of more than 100 000 as an annual mean and reduction of 80% of the TP influent is required.

2.2.7 Management of P within WWTPs

P occurs in a variety of forms within wastewater, and these vary throughout the wastewater treatment works (WWTWs) process (Patrick et al. 2017). Phosphorus in particulate forms is more easily and almost completely removed through clarification stages (Dueñas et al. 2003). Whereas dissolved P species, the organic and inorganic forms, need more targeted chemical or biological processes for their removal. Preliminary screening is firstly applied in WWTPs to remove larger particles followed by a primary treatment step. This involves the settlement and removal of suspended solids and organic fractions, which can be achieved by chemical addition or filtration (Tu and You 2014). Kim and Chung (2014) report that 17 – 26% of an inorganic total P, predominantly in particulate forms, can be transferred to primary sludge in the initial settlement at a WWTP. Secondary treatment, especially in larger WWTPs and those discharging to sensitive environments, is then applied. This can involve the addition of chemicals to promote the coagulation and flocculation of solids. Other than particulate P removed through secondary clarification, specific P removal techniques such as chemical precipitation or enhanced biological phosphorus removal (EBPR) can be integrated into the treatment process to target dissolved forms of P. Tertiary and advanced treatments are applied for the further removal or degradation of dissolved contaminants, especially when the treated water will be reused. Standard primary and secondary treatments often do not remove sufficient P to meet the required discharge concentration. Under the normal secondary treatment (the activated sludge process) around 31 – 48% of influent P can be transferred into sludge (Desmidt et al. 2015). With the P removed through primary settlement, this can leave approximately 50% of the total influent P load to be removed by enhanced P removal technique before discharging into a receiving water body.

2.2.8 Phosphorus removal techniques

Development of technologies to remove phosphorus started in response to the issue of eutrophication and the need to eliminate the excess phosphorus content from wastewater discharged to receiving waters and then to utilize this excluded phosphorus load in the way which is the most proper for the natural phosphorus cycle in nature. This policy should prevent surface waters against eutrophication-related problems. Phosphorus removal at WWTPs starts first with physical separation as some of the phosphorus will be bound up in the solid fraction, the soluble phosphorus is then removed by incorporation into the solid fraction using chemical precipitation, biological removal, or a combination of the two (Littler 2012). The technology involved with these processes is trusted and primarily understood.

Conventional technologies widely used for P removal from wastewater are chemical precipitation and enhanced biological phosphorus removal (Morse et al. 1998). Phosphorus removal by chemical precipitation is converting the dissolved P species into particulate form can be achieved by the addition of multivalent metal salts that form precipitates of sparingly soluble phosphates. The most common metals ions used are calcium Ca, aluminium Al (III), and iron Fe (II) and Fe (III) (Karunanithi et al. 2015). Calcium is generally used in the form of lime $Ca(OH)_2$ to remove P from the wastewater. Lime reacts in the water column with natural bicarbonate alkalinity to precipitate $CaCO_3$. The quantity of lime required for P removal depends on the alkalinity and the amount of P present in the wastewater to precipitate hydroxyapatite $Ca_{10}(PO_4)_6(OH)_2$ (Clark et al. 1997). Iron salts (Fe^{2+} and Fe^{3+}) and aluminium salts are commonly used to precipitate P from wastewater, and approximately one mole of aluminium or iron will precipitate one mole of P. The factors that affect the choice of chemical treatment for P removal include the P concentration level, suspended solids in wastewater, alkalinity, chemical cost, sludge treatment facilities, disposal methods and compatibility with other treatment processes (Clark et al. 1997). Chemical dosing is quite a flexible technology and can be implemented throughout the WWTPs. It can be used to remove phosphorus with the primary sedimentation sludge, it can be used within the activated sludge process where it carries the phosphorus out with the secondary sludge (co precipitation) and it can also be used as a tertiary treatment i.e. as a polisher which has the drawback of producing a chemically rich tertiary sludge (Morse et al. 1998). The majority of wastewater treatment plants in the UK used iron salts for chemical P removal. Iron salts are dosed in one or a combination of wastewater treatment stages to remove P and suspended solids (Carliell-Marquet et al. 2010).

Chemical P removal has many advantages over biological P removal: it is less sensitive to variation in influent characteristic, loading rate, and temperature changes. The sludge has a high P content

which can be used as a fertiliser. In addition, less time is required to achieve the chemical treatment, unlike the biological P removal in which the performance slowly improves with time as the microbial community matures. On the other hand, there are issues relating to dosing of ferric (Fe III) salts. If phosphorus discharge limits are below 2mg/l, then accurate and variable dosing is required. If the influent quality varies further operator input is required and the chance of overdosing increases which if happens can result in the ferric salts being discharged into the environment. Ferric chloride which is commonly used is corrosive and burns skin on contact and so there are many health and safety issues related to the use and storage of this chemical. The shortage of ferric salts has caused their price to rise and as the WFD is likely to put higher demands on this technology and so it will also put further strain on the already limited supply. The use of salts requires chemical storage and sludge treatment leading to increased costs which are strongly linked to the supply price of the different chemicals available.

Phosphorus removal by biological treatment which is performed in two ways (i) reedbeds, which work with bacterial decomposition of organic substances to nutrient uptake from the effluent flows, and this process requires a large land area and (ii) by using higher bacterial to P uptake. This process is used in large sewage treatment and depends on the ability to take up excessive P by polyphosphate-accumulating microorganisms (PAOs), via the process called enhanced biological phosphorus removal (EBPR). The stored P in the cells is removed from the liquid by sludge separating. The microorganisms are exposed to anaerobic and aerobic conditions in the mainstream (Clark et al. 1997).

Biological treatments also have issues related to their operation; they often require a steady supply of carbon. It can be hard to consistently remove phosphorus to a low effluent concentration and therefore biological treatment is often run with chemical dosing as a backup, thus retaining the problems associated with this. Biological treatment can be temperamental and so it is hard to achieve consistently low effluent levels. Both these favoured methods can require operator input which is particularly undesirable at smaller WWTPs that only serve small populations. These smaller plants have a much higher cost per kilogram of phosphorus removed (Ofwat 2017). The novel technique in development within this study seeks to offer a low energy, a passive treatment system that utilises relatively inexpensive materials (limestone) and involves no additional pre or post treatment. Furthermore, the treatment system will be able to be retro fitted to existing WWTPs.

2.2.9 P removal through reedbeds and reactive media

Constructed wetlands represent passive technology for enhanced solid removal and some associated biological degradation (Letshwenyo 2014). The technology is most commonly configured as a horizontal flow gravel bed. This involves the movement of inorganic P from the wastewater to the media, biofilm and plants although removal is known to be limited and insufficient to meet a 0.1 mg/l P standard (Brix et al. 2001). Enhancement of the technology has been proposed through the use of reactive media which are in contrast to traditional filtration systems, reactive media filters rely on P-sorption properties of certain materials to remove P in a targeted manner from wastewater, rather than using filter media solely for attachment of biomass (Bunce et al. 2018). In other meaning, it provides additional uptake through adsorption or precipitation due to the fact that P sorption capacity of the filter media which is dependent on the mineral content of the media is a crucial parameter for the p removal. Specifically, the presence of metals such as aluminium, calcium and iron has been used as a selection tool (Drizo et al. 2002; Arias et al. 2003; Wei et al. 2008; Cucarella et al. 2008). Calcium is considered a more critical component than iron or aluminium as under the pH conditions usually encountered adsorption/precipitation is thought to be limited such that precipitation of calcium phosphates is considered the main removal pathway (Chazarenc et al. 2007). The elemental composition, mineralogy and media size have been also identified as key parameters that influence media capacity (Drizo et al. 1999).

In recent years, many researchers have devoted their contribution to the development of effective media for phosphorus removal from wastewater (e.g.,Drizo et al. 2006; Shilton et al. 2006; Kõiv et al. 2010; Herrmann et al. 2014). These materials can be grouped into three main categories according to their origin: natural materials, industrial by-products, and man-made products (Johansson Westholm 2006).

Natural adsorbents material includes minerals and rocks (dolomite, bauxite, zeolite, opoka, limestone), soils and sediments like shell sand. Most of these materials have a high affinity for P binding because they are rich in aluminium, iron or calcium (Johansson Westholm 2006). Table 2.2 shows the application of natural materials for P adsorption from synthetic or real wastewater using batch and column experiments.

Natural materials are seen as readily available, cheap and safe for final disposal which makes using them as a reactive medium for P removal attractive. Despite the fact that many studies have investigated these materials in short and long-term experiments for P retention, it is difficult to compare their efficiency because of the differences in their inherent chemical and physical properties, particle size, solid to liquid ratio, agitation speed and time, temperature, pH, retention

time, hydraulic conductivity, initial P concentration, and P loading rate (Tahmazi et al. 2017). Most of these materials retain P via precipitation as calcium phosphate precipitates which depends on the Ca concentration availability, initial P concentration, solution pH, and contact time. It can be noted from Table 2.1 that the P adsorption capacities vary between 0.1 mg/g (Opoka) and 9.6 mg/g (shell sand). These values of P removal are affected by the chemical composition of the natural materials. It is reported that the chemical composition can inhibit the adsorption capacity (Drizo et al. 1999; Johansson Westholm 2006). The large particle sizes of these materials might restrict the required interaction between the phosphate ions and their chemical composition.

Constituents of industrial by-products which gives them high adsorption capacities are metal oxides of aluminium, iron and calcium. This makes these industrial by-products attractive to use as alternative adsorbents in wastewater processes. In addition, reusing by-products is also an important element of green engineering and sustainable design. When the by-products used as adsorbents are relatively inexpensive compared to commercial adsorbents. Table 2.3 lists the industrial by-products that have been examined for their ability for P adsorption using either batch or column experiments.

Using industrial by-products is attractive due to their high capacity for P retention. Their physical properties of small particle sizes and/or high porosity helps phosphate ions to fully contact with reactive surfaces of metals oxides (Tahmazi et al. 2017). Adsorption capacities vary between 0.469 mg/g for cement kiln dust material and 113.9 mg/g for red mud. This variation in P removal is mostly due to the variation in the experimental conditions, and the physical and chemical characteristics of the media.

Different Man-Made Products have been studied regarding their P adsorption capacity. These adsorbent materials include lightweight expanded aggregate, obtained by heating to a temperature up to 1000 °C e.g. Filtralite, LECA, Polonite and ion exchange fibers such as hybrid anion exchange (HAIX)-PhosXnp, granular ferric hydroxide (GFH), and hydrated ferric oxide (HFO)-coated sand. Most of the manufactured adsorbents contain a high content of Ca, Mg and metal hydroxide (Johansson Westholm 2006; Ádám et al. 2007; Li et al. 2009; Mayer et al. 2013). Table 2.4 shows some of these synthetic materials applied for P removal and recovery in different experiments conditions.

Anion exchangers are manufactured by the synthesis of poly-styrene matrices with amino groups to produce polymers with hydrophilic characteristics. They have a strong affinity for P binding in the presence of competing ions such as bicarbonate, chloride and nitrate (Blaney et al. 2007; Awual et al. 2011). These polymeric anion exchangers usually combine with the monovalent ($H_2PO_4^-$) and divalent (HPO_4^{2-}) phosphate forms (Kadlec and Wallace 2009).

There is an environmentally sound argument against using man-made products as the production of the substrates requires a large amount of energy (Johansson Westholm 2006). Other disadvantages of using these products are expense and commercial availability. However, the lack of P adsorption and selectivity, weak adsorption mechanisms, unable to regenerate the exhausted adsorbent or low regeneration performance, poor P recovery efficiency, and high operation cost have been the predominant reasons for continuing using the synthetic materials instead the other adsorbents types (Tahmazi et al. 2017).

Table 2- 2: Natural materials used for phosphorus removal

Material	Study type	Particle size (mm)	Mass (g)	Experimental conditions	Initial concentration (mg/l)	Main findings / removal mechanisms	Reference
Dolomite (Ca and Mg)	Batch	<0.425 and >0.180	0.2	-100 ml of P solution - 20, 40, and 60 °C at pH 7 -10, 15, 30, and 60 min contact time -90 to 150 rpm stirring speed	10 – 100 increased by 10	- Temperature affected negatively on P removal. -Slight increase in P removal with increase in pH. -15 to 30 min contact time was enough to reach adsorption equilibrium at high and low initial P concentration respectively. - Removal mechanism was physical interaction. - Structure and pore size distribution change with increasing temperature, leading to decrease its ability to retain P.	(Karaca et al. 2006)
Bauxite (Al, Fe oxides)	Batch	Mostly between	20	-60 rpm shaking speed for 24 h at 21°C - pH 5.9	2.5-40	- Adsorption capacity was 0.61 mg/g -The physical and chemical properties examined (pH, CEC,	(Drizo et al. 1999)

Material	Study type	Particle size (mm)	Mass (g)	Experimental conditions	Initial concentration (mg/l)	Main findings / removal mechanisms	Reference
	Column	6.8 and 12.6		-12 h retention time -25 g $P/m^3/d$ at first 40d -100 g $P/m^3/d$ used for an operation period	5,35 and 40	hydraulic conductivity, porosity, surface area) were not strongly linked with the observed P adsorption capacity -Maximum uptake was 0.335 mg/g	
Zeolite (hydrated aluminium silicate)	Batch	Ranging from 3-12	10	- 1000 ml solution with Initial P concentration of 5 mg/l -Shaking for 24 h at 21°C	5	-Removal efficiency of phosphate was slowly increased from pH 3 to 7 - Effect of co-existing ions indicated that phosphate removal was decreased remarkably by CO_3^{2-} - Maximum adsorption capacity was 9.1 mg/g	(He et al. 2016)
Apatite	Batch	2.5-10	35	- 700 of P solution of 8.0 pH and 1000 µs/cm conductivity	- ranged between 5 to 150	- Maximum adsorption capacity was 0.3 mg p/g apatite.	(Bellier et al. 2006)

Material	Study type	Particle size (mm)	Mass (g)	Experimental conditions	Initial concentration (mg/l)	Main findings / removal mechanisms	Reference
	Column			- 160 rpm stirring speed at 22 °C for 42 h -7.5 pH of P solution -0.7 l/d flow rate with up flow system -1.5 day retention time	30	- hydroxyapatite is the P removal form. -Complete P removal during first 15 days (mixture of apatite and limestone 1:1). -The removal declined to 65R until end of 39 days. -Removal mechanism is via crystallisation - 50% retention by lab column, field columns reduced P from10 to2 mg/l	
Wollastonite	Batch Column	--------	2	- 40 ml of P stock solution	5 and 10	- 90 % removal was obtained in the first 21h	(Brooks et al. 2000)

Material	Study type	Particle size (mm)	Mass (g)	Experimental conditions	Initial concentration (mg/l)	Main findings / removal mechanisms	Reference
				-Hydraulic retention time from 15 to 180 hours -Secondary wastewater, average 3.4 mg/l phosphorus		-> 80 % removal, rising to 96 % with longer contact (> 40 hours)	
Shell sand	Batch	3-7	3	-90 ml of P solution - 24 h shaking time	0-480	- Maximum P removal was 9.6 mg/g at initial P concentration of 480 mg/l.	(Ádám et al. 2007)
Opoka (mainly contain $CaCO_3$)	Batch	0-2	1	-50 ml of P solution with pH 7 -70 rpm shaking speed for 20 h at room temperature	5,10,15,20 and 25	-Removal efficiency inhibited by $CaCO_3$. -Maximum P uptake was 0.0 mg/g. -The dominant mechanism was the formation of Hydroxyapatite. The presence of the less reactive $CaCO_3$ in Opoka inhibits phosphorus removal when compared to minerals containing CaO	(Johansson and Gustafsson 2000)

Material	Study type	Particle size (mm)	Mass (g)	Experimental conditions	Initial concentration (mg/l)	Main findings / removal mechanisms	Reference
Limestone	Lab batch, column and field trials					- Lab columns removed 64%of P. During field trials performance decreased to18% removal. - Removal mechanism is via precipitation.	Shilton et al. 2006
Calcite	Batch	0.075		> 1-hour contact time	Artificial phosphate solutions.	-70 - 80 % removal at pH 7.5 – 8 -Complete removal possible (with high initial concentration and pH). -Not likely to remove the levels needed without adjusting pH. Need to trial with real wastewater	(Karageorgiou et al. 2007)

Table 2- 3: Application of industrial by-products for phosphorus removal

Material	Study type	Particle size (mm)	Mass (g)	Experimental conditions	Initial concentration (mg/l)	Main findings	Reference
Steel slag (mainly contains Ca)	Batch	< 2	2	50 ml of P stock solution and initial pH 5.2. - 200 rpm stirring speed for 2 h. -pH is ranging from 3.5 to 11.5 to study its effect. - to study the effect of adsorbent dose, 2, 4, 8, 16, 20, 40, 60, 80, and 100 g/l were used	5, 10, 30, 50, 75, 100, 125, 150, and 200 to study adsorption isotherm - 22.79 to study pH and adsorbent dose effect 1-3.4	-5.3 mg P/g slag of maximum adsorption capacity. - P removal increased with increasing temperature and adsorbent dose; and decreased with increasing initial P concentration. - P adsorption data fitted with Langmuir and Freundlich models. - P retention depends on Ca dissolution; making long-term experiments are necessitated to evaluate the material for future applications.	(Xiong et al. 2008)
	Column	< 2	6029	-Secondary effluent from WWTP with TP (1-3.4) mg/l. - 8.37 ml/min flow rate			

Material	Study type	Particle size (mm)	Mass (g)	Experimental conditions	Initial concentration (mg/l)	Main findings	Reference
						TP removal rate was 62 – 79 % while dissolved P removal was 71 – 82 %	
Blast furnace slag (mainly contain Ca and Si)	Batch	0.02-0.03	0.07	-50 ml of P stock solution. -different temperatures and pHs	180	-the dominant removal mechanism was chemical precipitation. -99% removal was achieved. -P removal influenced by pH, temperature and agitation rate.	(Oguz 2004)
Red mud	Batch	< 0.149	0.1	20 ml of P stock solution and pH range of 1 to 11. - 180 rpm shaking speed for 4 h.	0.31, 3.1, 15.5, 155, 775, 1550, and 3100	-99% maximum removal efficiency. -113.9 mg/g maximum adsorption capacity. Langmuir fitted better than other models.	(li et al. 2006)
Fly ash	Column	0.125-0.063	0.2	-50 ml of stock solution. -4, 10, 20 g/l of adsorbent with initial P concentration of	20,50 and 100	- > 99% P removal was achieved at 40ºC and PH 4, and P	(Ugurlu and Salman 1998)

Material	Study type	Particle size (mm)	Mass (g)	Experimental conditions	Initial concentration (mg/l)	Main findings	Reference
				20 mg/l - contact times were 5, 10, 15, 20, 25, and 30 min		concentration at equilibrium was 0.02 mg/l.	
Ochre	Batch	0.6 - 2		-48 hours -pH 7.2	1500 - 3000 mg/l phosphorus	-Final effluent levels < 1 mg/l phosphorus	(Heal et al. 2005)

Table 2- 4: The applied man-made adsorbents for P removal.

Material	Study type	Particle size (mm)	Mass (g)	Experimental conditions	Initial concentration (mg/l)	Main findings	Reference
Filtralite	Batch	0.5-4 Effective porosity 40%	3	- A 90 ml of P solution shook for 24h.	- A range of 0 - 480	At initial P concentration of 10 mg/l, P retention capacity was about 1.3 mg/g. -The adsorption behaviour became worse when the initial P concentration increased. - CaCO3, Ca-P, Mg-P precipitates were visible and identified on the media.	(Ádám et al. 2007)

Material	Study type	Particle size (mm)	Mass (g)	Experimental conditions	Initial concentration (mg/l)	Main findings	Reference
Polonite	Column	2-5.6	------	-A 10 cm diameter column filled with 50cm. - Loading rate of 530 L/m2.d, hydraulic conductivity 226 m/d, RT from 4 to 5 h.	Synthetic solution containing 10 mg/l.	- phosphate removal rate of 91% when using polonite to treat municipal wastewater over 1 year with a P-sorption capacity of 120 g/kg. -After the media saturated with P, it neEDX to replace with another fresh one, meaning that it is unable for regenerating.	(Renman and Renman 2010)
Portland Cement	Batch	- diameter of 20.8 microns.		-200ml batch tests with solids concentration of 10g/l	- initial phosphorus concentrations of 20-80mg/l.	- removing up to 27mg/g total phosphorus.	(Agyei et al. 2003)

2.2.10 Calcite

Calcite is a carbonate mineral and the most stable polymorph of calcium carbonate (Loste et al. 2003). Calcite, like most carbonates, will dissolve with most forms of acid. Calcite can be either dissolved or precipitated by groundwater, depending on several factors including the water temperature, pH, and dissolved ion concentrations. Although calcite has low solubility in cold water, acidity can cause dissolution of calcite and release of carbon dioxide gas. When conditions are right for precipitation, calcite forms mineral coatings that cement the existing rock grains together or it can fill fractures. When conditions are right for dissolution, the removal of calcite can dramatically increase the porosity and permeability of the rock, and if it continues for an extended period of time may result in the formation of caves.

Generally, $CaCO_3$ exists in a variety of polymorphic forms, of which there are three anhydrous crystalline polymorphs, calcite, aragonite and vaterite, and two well defined hydrated crystalline polymorphs, calcium carbonate hexahydrate ($CaCO_3.6H_2O$) and calcium carbonate monohydrate ($CaCO_3.H_2O$). An amorphous form of calcium carbonate also exists. When calcite precipitates, amorphous calcium carbonate forms first, then organises and dehydrates to form crystals (Meldrum 2003).

The $CaCO_3$ form that precipitates from aqueous solutions of Ca^{2+} and CO_3^{2-} ions depends on factors such as temperature, the concentration of reactants, duration of precipitation, the mixing rate, humidity and the trapped surface impurities. Studies have been made on the influence of water composition, temperature and water pH on the calco-carbonic system ($CaCO_3$-CO_2-H_2O) that leads towards $CaCO_3$ precipitation (Amor et al. 2004; Gal et al. 2002). For crystallisation to occur the solution must be supersaturated with respect to Ca^{2+} ions; however, supersaturation by itself is not sufficient to induce crystallisation. Crystallisation requires nucleation sites in the form of seeds or foreign matter in the solution. Usually nucleation is the controlling step, once the critical nuclei are formed, the crystallisation proceeds (Chong and Sheikholeslami 2001). The chemical reaction of $CaCO_3$ precipitation is shown in equation 2.1 below.

$$Ca^{2+} + HCO_3^- + OH^- = CaCO_{3\,(s)} + H_2O \qquad (2.1)$$

The solubility of calcium carbonate depends on the CO_2 content. Chong and Sheikholeslami (2001) provided the data on the distribution of CO_2 related ions and CO_2 gas in solution as a function of pH. Determining the correlation between P_{CO_2} and Ca^{2+} concentration is therefore one of the most direct ways of understanding the control factors in the calcium carbonate precipitation reaction. Hollett (2000)reported that according to calculated solubility products, calcite is theoretically the only stable phase at atmospheric pressure within 0-90°C temperature range. Calcite may

precipitate directly and under ambient temperature and pressure, aragonite and vaterite will transform to calcite if given enough time.

2.3 Theory

When limestone is dissolved in water in the presence of CO_2, this causes Ca^{2+} and CO_3^{2-} ions to be released into solution. When the volume of CO_2 in solution is reduced, the calcium ions are reprecipitated out of solution. However, instead of reforming with carbonate ions to form calcium carbonate, some or all of the CO_3^{2-} ions are replaced by PO_4^{3-} ions, which were also present in water, to form calcium phosphate (Kitano 1978; Ishikawa and Ichikuni 1981). this reaction can be seen in equation (2.2).

$$3Ca^{2+}_{(aq)} + 2PO_4^{3-}_{(aq)} = 3Ca_3(PO_4)_{2\,(s)} \qquad (2.2)$$

The basic mechanism of chemical phosphorus removal is precipitation followed by solids separation step such as settlement and/or filtration. Phosphorus precipitation is the transformation of the soluble phosphorus present in the wastewater as orthophosphate anion (PO_4^{3-}) to an insoluble chemical compound (salt) and the removal of these insoluble precipitates. Such a transformation occurs when a chemical agent bearing a proper cation, (Ca^{2+}) in the current study is added to the wastewater and reacts with the soluble phosphorus to form an insoluble orthophosphate salt. In practice more complex reactions are taking place, which involve coprecipitation and surface adsorption. The proposed chemical process inspired by the above facts is presented in Figure 2.1. In this instance, limestone chips provided the calcium source. This section presents the theoretical background of the concepts used in this thesis. Firstly, the theories relating to the material studied in this thesis are presented, this includes calcite dissolution and precipitation theories, the carbonate chemistry and phosphorus precipitation with calcite theories. Finally, theories relating to the removal mechanisms are then discussed with some of medias used for phosphorus removal are listed.

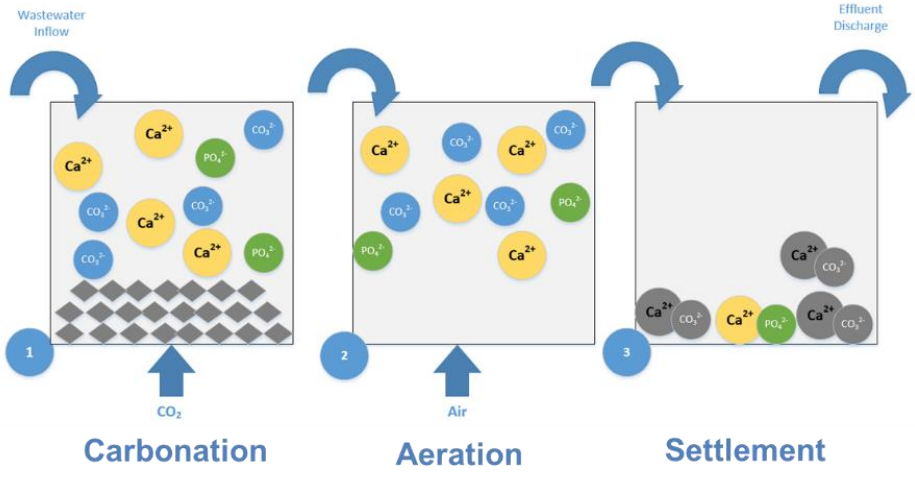

Figure 2- 1: Carbonate coprecipitation process

2.3.1 Carbonate chemistry

The carbonic species in water are: H_2CO_3, HCO_3^- and CO_3^{2-}. Carbon dioxide enters the water partly direct from the atmosphere, and partly with precipitation and other inputs, but largely due to infiltration through the soil as well as by the metabolic activity of the organisms in the water (Langmuir 1997; Panthi 2003). The carbon dioxide dissolved into water exist not only dissolved CO_2 but also as carbonic acid, H_2CO_3, which is then dissociated to H^+ and HCO_3^-(Panthi 2003). The following equilibrium has therefore to be considered:

The gas dissolution and carbonic acid formation are presented in equation (2.3) and (2.4) respectively.

$$CO_2(g) \rightleftharpoons CO_2(aq) \quad (2.3)$$

$$CO_2 + H_2O \rightleftharpoons H_2CO_3 \quad (2.4)$$

Dissolved CO_2 in the form of H_2CO_3 may lose up to two protons through the acid equilibria

$$H_2CO_3 \rightleftharpoons HCO_3^- + H^+ \quad (2.5)$$

$$HCO_3^- \rightleftharpoons CO_3^{2-} + H^+ \quad (2.6)$$

With ionisation constant,

$$K1 = \frac{[H^+][HCO_3^-]}{[H_2CO_3^*]} \quad (2.7)$$

Since a small fraction (≈0.25%) of the total CO_2 dissolving into water is hydrolysed to H_2CO_3, that fraction which is virtually unaffected by temperature and pH (Burau and Zasoski 2002). The concentration of carbonic acid [H_2CO_3*], which is the sum of the concentration of H_2CO_3 and dissolved CO_2 is given by equation (2.8):

$$[H_2CO_3^*] = [H_2CO_3] + [CO_2] \quad (2.8)$$

In a similar way the ionisation constant for HCO_3^- and CO_3^{2-}.

$$K2 = \frac{[H^+][CO_3^-]}{[HCO_3^-]} \quad (2.9)$$

The ionisation of water is conventionally written as:

$$H_2O = H^+ + OH^- \quad (2.10)$$

and the ionisation constant for this reaction is given by:

$$Kw = \frac{[H^+][OH^-]}{[H_2O]} \quad (2.11)$$

From experimental work K_w is found to be an extremely small quantity, 1.8×10^{-16} moles/liters at 25°C. As K_w is small, the fraction of H_2O that ionises is negligible compared with the unionised fraction. The unionised mass of H_2O can be taken as equal to the total water mass,

$$[H_2O] = \frac{mass\ of\ 1\ litre\ of\ water}{gram\ molecular\ weight} \quad (2.12)$$

= 1000/18

= 55.5 moles per litre

$[H^+] . [OH^-] = K \times [H_2O] = 1.8 \times 10^{-16} \times 55.5$

$= 1.0 \times 10^{-14}$

$[H^+] [OH^-] = K_w = 10^{-14}$ at 25°C

K_w is a function of temperature and ionic strength.

In pure water $[H^+] = [OH^-] = 10^{-7}$ moles per litre at 25°C

i.e pH = $-\log_{10} (H^+) = 7$ for pure water

Carbon dioxide exchange between water and atmosphere takes place until the partial pressure in the two phases is equal. During this process the pH in the water changes and there is a redistribution of dissolved carbonic concentrations. For equilibrium between dissolved and atmospheric CO_2 is defined by Henry's law as in equation (2.13):

$$[CO_2] = K'_{CO2} . P_{CO2} \quad (2.13)$$

K'_{CO2} is Henry's constant which is temperature dependent and P_{CO2} is partial pressure of CO_2 in the atmosphere.

Since the ratio $[H_2CO_3^*]/ [CO_2]$ is constant and temperature independent in temperature range 0°C to 50°C (Burau and Zasoski 2002),

$$[H_2CO_3^*] = K_{CO2} . P_{CO2} \quad (2.14)$$

The constant K_{CO2} is temperature dependent and given by two linear functions (Burau and Zasoski 2002)

$pK_{CO2} = 1.12 + 0.0138*t$ for the range 0°C to 35°C (2.15)

$pK_{CO2} = 1.36 + 0.0069*t$ for the range 35°C to 80°C (2.16)

As mentioned earlier in this section, that carbon dioxide enters the water through equilibrium with the atmosphere and during the equilibrium process between the atmospheric and dissolved CO_2 a change in pH would occur and that will result in redistribution of carbonic concentration (Panthi 2003).

2.3.2 Calcite dissolution and precipitation theory

There have been many different theories in the past trying to explain the theory behind the dissolution of calcite. In the first theory of Weyl (1958) approached by assuming that solution is in equilibrium with the calcite solids at the boundary layer and the dissolution process at the calcite surface is too fast, and the dissolution rate can be determined by mass transport from the boundary layer into the solution. Further progress was achieved by Curl et al. (1968.) who took into account the fact that conversion of physically dissolved CO_2 into H_2CO_3 is a slow process. These theories, however, all failed to take into account the mechanisms at the surface of the $CaCO_3$ rock. No significant progress was therefore achieved up to 1978 when Plummer et al. (1978) published a comprehensive investigation of dissolution rates of $CaCO_3$. , taking into consideration the ratio of the volume of the solution to the surface of the dissolving crystals so large that the conversion of CO_2 to H_2CO_3 was not rate limiting. Thus, the theory of Plummer et al. (1978) gives exact information on the chemical kinetics of surface-controlled dissolution of $CaCO_3$ by considering the dissolution rate as a function of the activities of the species Ca^{2+}, H^+, HCO_3^- and H_2CO_3 at the $CaCO_3$ surface.

Calcite dissolution is mainly controlled by the reactions occurring within the water, carbon dioxide and calcite system. The dissolution rate of calcite covered by a water film open to a CO_2 containing atmosphere is controlled by the chemical composition of the $CaCO_3$-H_2O-CO_2 solution at the water mineral interface. This composition can be determined by the Ca^{2+} concentration, conversion of CO_2 into H^+ and HCO_3^- in the solution, and by diffusional mass transport of the dissolved species like $Ca^{2+,}$ HCO_3, CO_2 and H_2CO_3 from and towards the phase boundaries. The $[Ca^{+2}]$ in solution (Dreybrodt, W. 1981; Zuddas and Mucci 1994), CO_2 loss (Zhang and Grattoni 1998), and pH (Inskeep and Bloom 1985) are considered to be the three dominant factors influencing calcium carbonate precipitation (Kaufmann and Dreybrodt 2007). The chemical reactions and processes responsible for the dissolution of calcite with respect to CO_2, are: (Langmuir 1997).

$$CaCO_3 + H^+ \leftrightarrow Ca^{2+} + HCO_3^- \quad (2.17)$$

$$CaCO_3 + H_2CO_3 \leftrightarrow Ca^{2+} + 2HCO_3^- \quad (2.18)$$

$$CaCO_3 + H_2O \leftrightarrow Ca^{2+} + HCO_3^- + OH^- \quad (2.19)$$

These reactions are termed attack by acid, CO_2 and water, respectively (Plummer and Busenberg 1982). Under certain conditions of pH and CO_2 pressure, one or another of these mechanisms may be dominant. The total dissolution rate is the sum of these three mechanisms. The rate in equation 2.19 is not affected by CO_2 while the rate of CO_2 attack, as seen in equation 2.18, increases with CO_2 pressure, and exceeds the water rate at a pressure of about 0.1 atm. The acid

attack rate, equation 2.17, is also affected by CO_2 addition, because CO_2 is a weak acid, through a shift of the pH to lower levels as CO_2 pressure increases.

The saturation state of water with respect to calcite is largely controlled by the flux of CO_2 gas into or out of that solution. Out gassing, which can take place whenever carbonated water with elevated P_{CO2} contacts a lower P_{CO2} atmosphere, increases the degree of saturation with respect to calcite (Holland et al. 1964; Langmuir 1971; Wigley and Plummer 1976). In flowing systems, the P_{CO2} of the water decreases in a downstream direction, and the degree of saturation with respect to calcite subsequently increases (Shuster and White 1971). Several field studies have shown that CO_2 can escape from the water and calcite will precipitate from the saturated solution (Dandurand et al. 1982; Herman and Lorah 1987; Hoffer-french et al. 1989; Dreybrodt et al. 1992). A certain critical degree of saturation must be achieved to pass the energy barrier to the formation of stable nuclei (Reddy et al. 1981; M.Lorah 1988) and laboratory studies of calcite crystallization kinetics have shown that the necessary ion activity product can be as much as ten times the equilibrium calcite solubility value (Ogino et al. 1987; Boudreau and Canfield 1993). Many laboratory experiments have been conducted to investigate the reaction kinetics of calcite in H_2O-CO_2 systems, for example (Usdowski 1979; Reddy et al. 1981; Walter and Morse 1985; Inskeep and Bloom 1985). Several different rate equations have been produced by these laboratory researchers to describe calcite dissolution and precipitation. House (1984) concluded that the hydration reactions of CO_2 may influence the precipitation rate and exchange with the atmosphere. The two hydration reactions are:

$$CO_2 + H_2O \rightleftharpoons H_2CO_3 \quad (2.20)$$

$$CO_2 + OH^- \rightleftharpoons HCO_3^- \quad (2.21)$$

These reactions cannot be considered instantaneous. For calcite precipitation from bicarbonate solutions, the rate of formation of CO_2 through the reaction:

$$Ca^{2+} + 2HCO_3^- \rightleftharpoons CaCO_{3(solid)} + CO_2 + H_2O \quad (2.22)$$

but the Plummer (1978) model is the only rate law which attempts to describe both calcite dissolution and precipitation at all solution pH and P_{CO2} values. The equation relates the net dissolution rate (R, in units of mass area^{1-} time^{1-}) of calcite to the activities (a,) of H^+, Ca^{2+}, HCO_3^-, H_2O, and H_2CO_3*

$$R = k_1a_{H+} + k_2a_{H2CO3*} + k3a_{H2O} - k4a_{Ca2+}\,a_{HCO3-} \quad (2.23)$$

where H_2CO_3* is (CO_2 (aq) + $H_2CO_3^0$) and the k's are rate constants.

The extent of separation of Ca by precipitation depends to a large extent on the solubility of its precipitate, which is in this study a carbonate salt. At the saturation or equilibrium concentration

of this salt an equilibrium exists between the solute ions and the solid phase as shown in the equation below:

$CaCO_{3(s)} \rightleftharpoons Ca^{2+} + CO_3^{2-}$ (2.24)

For which the equilibrium expression is:

$$K = \frac{[Ca^{2+}][CO_3^{2-}]}{[CaCO_3]s} \quad (2.25)$$

The activity of the solid phase is constant and hence the denominator in equation 2.25 can be combined with K

$[Ca^{2+}][CO_3^{2-}] = K_{sp}$ (2.26)

where K_{sp} is called the solubility product.

2.3.3 Phosphorus precipitation with calcite

In lakes the coprecipitation of phosphorus is an important self-cleaning mechanism and can result in the removal of as much as 97% of the phosphorus from the epilimnion (House 1990). Kleiner (1988) estimated that about 35% of the total phosphorus removal from the epilimnion of Lake Constance could be coprecipitated with calcite. The loss of CO_2 from a hard water by either transfer to the atmosphere or the metabolic activity of algae, phytoplankton or macrophytes may lead to the precipitation of calcium carbonate as calcite and the coprecipitation of solutes such as inorganic phosphorus (House 1990). Many reports have documented the precipitation of calcite in a range of different lakes at various trophic levels (e.g. Strong and Eadie 1978; Murphy 1983 and Stabel 1986). In streams and rivers, the precipitation of calcite usually occurs when a hardwater, which is supersaturated initially with CO_2 loses CO_2 to the atmosphere during its passage downstream and eventually precipitates calcite (Dandurand et al. 1982 and M.Lorah 1988).

The coprecipitation reaction is occurring naturally by the interaction between inorganic phosphorus and the calcite surface during crystal growth, followed by the incorporation of some of the surface phosphorus into the bulk structure as growth occurs (House et al. 1986; Karapinar et al. 2006). Inorganic phosphorus also inhibits the crystal growth of calcite and, depending on the supersaturation in the solution, may stop growth completely (House 1987). A similar observation was made by Montes-Hernandez et al. (2009) and the result of Alkattan et al. (2002)study illustrated that aqueous phosphate, which is also known to be a strong calcite dissolution inhibitor at neutral to basic pH, was found to also strongly inhibit calcite dissolution at acidic conditions and the degree of inhibition on calcite dissolution due to the presence of aqueous phosphate is likely not sufficient to affect most natural processes significantly. This means that as eutrophication of a lake increases and the soluble reactive phosphate

concentration increases, the self-cleaning mechanism is expected to be less effective as the precipitation reaction is progressively inhibited.

It has been generally observed that the concentration of dissolved reactive phosphate is significantly lower in sediments containing high weight percentages of calcium carbonate than in those containing small weight percentages of calcium carbonate (Serruya 1971; de Kanel and Morse 1978). The explanation usually given for this observation is that the surface of the calcium carbonate acts as an especially favourable site for the nucleation of a calcium phosphate of complex composition, but generally related to apatite. This explanation has been given support by the observation of carbonate-hydroxyapatite overgrowths on calcite in lake sediments and laboratory experiments in which apatite was precipitated on calcite (Stumm and Leckie 1970). In their experimental work, it was found that the kinetics of phosphate (orthophosphate) uptake on calcite indicated that chemisorption was the initial reaction. It was hypothesized that this was followed by a slow transformation of amorphous calcium phosphate to crystalline apatite and subsequent growth of the crystalline apatite. The rate of apatite crystal growth depended strongly on the phosphate to carbonate ion ratio. It was suggested that this was due to their competition for growth sites.

The formation of calcium phosphate salts in aqueous solutions takes place following the development of supersaturation (Song et al. 2002). There are a lot of factors which may control or influence the development of supersaturation and as a result influence the precipitation of calcium phosphates from solution, such as the concentrations of phosphate and calcium, the pH value due to its influence on base uptake of the precipitation reaction and the speciation of phosphate and calcium ions (Verbeeck and Devenyns 1992), the ionic strength, the impurities of solution (Feenstra and De Bruyn 1981; Melikhov et al. 1989; Lopez-Valero et al. 1992; Plant and House 2002). Moreover, temperature increase contributes to the solution supersaturation development because the sparingly soluble calcium phosphate salts have reverse solubility (Koutsoukos 1995; Song et al. 2002).It is still not very clear how these factors affect the precipitation of calcium phosphates and the extent of their influence, especially under the conditions of phosphate recovery from wastewater. Following the establishment of supersaturation nucleation takes place. Once the nuclei exceed a critical size, they grow further in the crystal growth proves which takes place on the active growth sites of the crystallites. Under proper physical and chemical environment and depending on the solution supersaturation, four well defined regions may be distinguished for the calcium phosphate system such as $CaHPO_4$. $2H_2O$ (dicalcium phosphate dihydrate, DCPD), $Ca_4H(PO_4)_3$.$2.5H_2O$ (octacalcium phosphate, OCP), $Ca_3(PO_4)_2$ (tricalcium phosphate, TCP) and $Ca_5(PO_4)_3OH$ (hydroxyapatite, HAP) may precipitate

from saturated solutions, among which HAP is thermodynamically the most stable one (Nancollas and Koutsoukos 1980; Kemenade and Bruyn 1987) and most common form of Ca-P precipitate and forms at high pH, typically greater than 10 (Rittmann et al. 2011). In slightly acidic calcium phosphate solutions, the monoclinic DCPD forms are dominant, OCP is formed by the hydrolysis of DCPD in solutions of pH 5 -6 and expected to be the more stable phases. However, these precipitated phases are thought to transform into more thermodynamically stable hydroxyapatite over time (Desmidt et al. 2015). When HAP precipitated in the presence of foreign ions substitutions calcium, phosphate and / or hydroxyls by some of these ions take place. When calcium phosphate is precipitated from highly supersaturated solutions an unstable precursor phase has been reported to form. This phase is known as the amorphous calcium phosphate (ACP). The composition of ACP appears to depend upon the precipitation conditions and is usually formed in supersaturated solutions at pH>7.0. These regions are shown Figure 2.2.

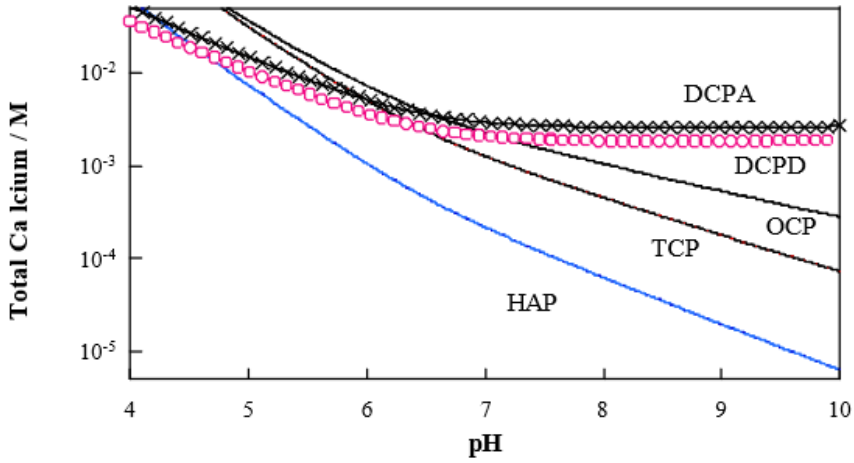

Figure 2- 2: Solubility isotherms of calcium phosphates. Calculated at 25ºC (Koutsoukos 1995)

As may be seen the driving force is the solution supersaturations, S, defined as:

$$S = \frac{IAP}{\mathrm{Ksp}} \tag{2.26}$$

where IAP is the ion activity product of the salt considered and K_{sp} the respective thermodynamic solubility product as explained in section 2.3.2.

In the case of hydroxides, solubilities can be calculated directly from the appropriate K_{sp} value if the pH is known. For phosphates, the calculation of solubility is complicated by its reaction in solution:

$$PO_4^{3-} + H_2O \Leftrightarrow HPO_4^{2-} + OH^- \tag{2.27}$$

For which the equilibrium expression is usually written in the form:

$$K = \frac{[H+][PO_4^{3-}]}{[HPO_4^{2-}]} \tag{2.28}$$

Solubility product values for a number of slightly soluble salts relevant to the present discussion are provided in Table 2.5.

Table 2- 5: Representative heterogeneous and complexation equilibria of phosphates with calcium (adapted from Snoeyink and Jenkins 1980)

Heterogeneous Equilibria		pK_{sp}
Calcite	$CaCO_{3(s)}$	+ 8.34
Calcium hydrogen phosphate	$CaHPO_4$ (s) ⇌ Ca^{2+} + HPO_4^{2-}	+ 6.66
Calcium dihydrogen phosphate	$Ca(H_2PO_4)_2$ (s) ⇌ Ca^{2+} + $2H_2PO_4^-$	+ 1.14
Hydroxyapatite	$Ca_5(PO_4)_3OH$(s) ⇌$5Ca^{2+}$+$3PO_4^{3-}$+OH^-	+ 55.9
β-Tricalcium phosphate	β-$Ca_3(PO_4)_2$ (s) ⇌ $3Ca^{2+}$ + $2PO_4^{3-}$	+ 24.0
Complexation Equilibria		pK
With orthophosphate	$CaHPO_4^0$ ⇌ Ca^{2+} + HPO_4^{2-}	+ 2.2
	$CaH_2PO_4^+$ ⇌ Ca^{2+} HPO_4^{2-} + H^+	− 5.6
With pyrophosphate	$CaP_2O_7^{2-}$ ⇌ Ca^{2+} + $P_2O_7^{4-}$	+ 5.6
	$CaHP_2O_7^-$ ⇌ Ca^{2+} + $HP_2O_7^{3-}$	+ 2.0
With tripolyphosphate	$CaP_3O_{10}^{3-}$ ⇌ Ca^{2+} + $P_3O_{10}^{5-}$	+ 1.8

At very high supersaturations calcium phosphate precipitates spontaneously, before reaching this region, it is possible to prepare solutions supersaturated with respect to calcium phosphate, but the precipitation takes place past the lapse of measurable induction times, following the establishment of the solution supersaturations. Moreover, it is possible to prepare calcium phosphate supersaturated solutions, which are stable. In these solutions, precipitation does not take place, unless they are seeded either with calcium phosphate seed crystals or with substrates which may function as templates for the selective overgrowth of calcium phosphates. The lower limit of this supersaturation range is the solubility of the calcium phosphate considered (S=1). Below this limit, dissolution takes place. It is thus reported that for pH 7.40 and a molar ratio of total calcium /total phosphate concentration equal to 1.66, at calcium concentrations of 10 mM spontaneous precipitation takes place and between 0.35 – 1.15 mg/l the precipitation takes place past the lapse of induction times. Below 0.35 mg/l the supersaturated solutions are stable for long periods of time. A considerable amount of the work done for the identification of calcium phosphate minerals which precipitates spontaneously has been based on the stoichiometric molar ratio of calcium to phosphate calculated from the respective changes in the solutions. This ratio has been found in several cases to be 1.45 ± 0.05 which is considerably lower than the value

of 1.67 corresponding to HAP which is generally implied as the precipitating mineral. A number of different precursor phases have been postulated to form including TCP, OCP and DCPD.

P content in recovered Ca-P precipitates can vary from 12 to 20% and can be assumed to have a higher solubility than that of well crystallised Ca-P (Cabeza et al. 2011). From a commercial viewpoint, however, the recovery of P in the form of Ca-P is beneficial since it has more diverse applications in the industry than struvite (Okano et al. 2013). Calcium phosphate mainly as hydroxyapatite, ($Ca_5(PO_4)_3OH$) reflects the composition of rock phosphate and should easily adopted as a secondary P source in existing industry and infrastructure (Song et al., 2006;Tervahauta et al. 2014). The speciation of the phosphate species is described by the following reactions (Liu et al. 2012).

$PO_4^{3-} + H_2O \leftrightarrow HPO_4^{2-} + OH^-$ pK = 1.68 (2.29)

$HPO_4^{2-} + H_2O \leftrightarrow H_2PO_4^- + OH^-$ pK = 6.79 (2.30)

$H_2PO_4^- + H_2O \leftrightarrow H_3PO_4 + OH^-$ pK = 11.67 (2.31)

$H_2O \leftrightarrow H^+ + OH^-$ pK = 14 (2.32)

The predominance of these species depends on the pH values of the aqueous medium as well as the concentration of the phosphate materials. According to the hydrolysis of the phosphates, it may expected to found $H_2PO_4^-$ and HPO_4^{2-} in the acidic or slightly base medium and PO_4^{3-} species becomes significant and exceeds that of HPO_4^{2-} in the basic medium and acts as a source of anions. The effect of pH on phosphate removal can be attributed to changes in the surface sites or speciation of phosphorus in solution as well as the dissolution of calcite and the degree of supersaturation and the type of precipitates formed. Figure 2.3 shows the phosphate distribution curves as a function of pH.

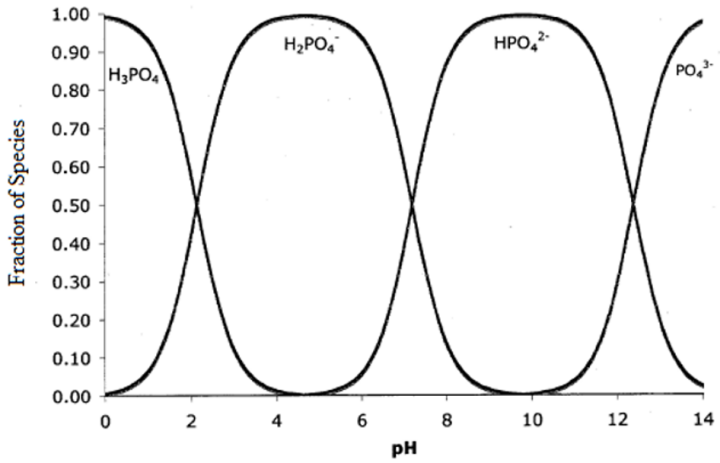

Figure 2- 3: Phosphate species distribution in water of varying pH

Phosphorus precipitation as calcium phosphate is achieved by adding lime ($Ca(OH)_2$) to the wastewater, raising the pH to about 10.5. The lime dose required to elevate the pH to this level

is a function of the wastewater alkalinity and may be approximated as 1.5 times the alkalinity as CaCO3. Thus, the calcium dose is not stoichiometrically related to the phosphorus concentration. While lime is a relatively low-cost chemical, the disadvantages of the lime process are that it produces a large amount of sludge residue and creates a too high pH for environmental discharge and low phosphate concentration could be achieved at a pH value in the range 8.5-9.5, this has not been found to be feasible under typical wastewater process operating conditions. In this study phosphorus precipitation as calcium phosphate is achieved by using limestone ($CaCO_3$) as a low-cost available source of calcium. While it would appear from the equilibrium solubility characteristics of calcium phosphates that a high phosphate concentration could be achieved at a pH value less than 9.

2.3.4 Effect of Carbon dioxide on calcite dissolution

An increase in carbon dioxide pressure in water has a significant effect on the solubility of limestone as it is a carbonate mineral. Lovell, (1973) found that at 16°C the alkalinity of water at atmospheric CO_2 pressure levels, which are around 387ppm is 50mg/l. this will increase to approximately 600mg/l, 790mg/l,880mg/l,1020mg/l and 1070mg/l for CO_2 pressure of 20%, 40%, 60%, 80% and 100% of total atmospheric pressure respectively. From this information, it was calculated that the equilibrium alkalinity of $CaCO_3$ increases as the cubed root of an increase in CO_2 levels in solution (Stumm & Morgan 1996). The reaction that is occurring when CO_2 dissolves limestone in water is shown in Equation below.

$$CaCO_3 + H_2O + CO_2 = Ca^{2+} + 2\ HCO_3^- \quad (2.33)$$

Limestone solubility also occurs naturally in natural water as shown in Equation below. Sibrell et al. (2007)found that the point at which the rate of $CaCO_3$ solubility due to increasing partial pressure of CO_2 will exceed this naturally occurring limestone dissolution is at about 0.1 atm. This is over 300 times the atmospheric pressure of CO_2.

$$CaCO_3 + H_2O = HCO_3^- + OH^- + Ca^{2+} \quad (2.34)$$

2.3.6 Phosphorus removal mechanisms

Phosphate removal by calcite often entails two processes: adsorption and precipitation. Separating these two processes is of great importance for the assessment of PO_4^{-3} stability after removal (Li et al. 2017). The kinetic data of Millero et al. (2001) showed that the phosphate uptake on carbonate minerals appears to be a multistep process. Adsorption was quite fast in the first stage (less than 30 min) followed by a much slower process (lasting more than 1 week). The dominant removal mechanism has been indicated to be influenced by initial PO_4^{3-} concentration,

reaction time and pH (Zhang et al. 2001; Xu et al. 2014). Particularly, when initial PO_4^{3-} concentration is lower than the required concentration for the precipitation of Ca-P solid compounds, it is theoretically impossible for precipitation to take place. A general consensus has affirmed that phosphate can be either adsorbed by calcite at low concentration or precipitated at high concentration(Liu et al. 2012; Perassi and Borgnino 2014). For instance, Ca-P precipitation was reported to be efficient when the P concentration exceeded 0.5 mg/l, below which adsorption became the key removal pathway (Kõiv et al. 2010b). Usually, adsorption is known to occur earlier than precipitation, though they may coexist in later reactions. While precipitation may happen after several hours or days. This can be attributed to the fact that the initial phosphate uptake onto calcite occurs via chemisorption, which is then followed by a slow transformation of amorphous calcium phosphate to crystalline apatite and can take place on limited number of sites when phosphate concentration is low (Stumm and Leckie 1970;de Kanel and Morse 1978); Karageorgiou et al. 2007). At high concentrations, the process starts with small amounts of phosphate adsorption followed by the precipitation calcium phosphate compounds such us hydroxyapatite, octacalcium phosphate, etc. The rate of apatite crystal growth depends strongly on the phosphate to carbonate ratio due to the competition for growth sites. (Yagi and Fukushi 2012) . Besides, another important indicator in calcite surface reaction study is pH and its effect on the net charge of calcite surface, calcite solubility and solution ion concentration such us Ca^{2+}, OH^-, HCO_3^- and CO_3^{2-}(Suzuki et al. 1986; Xu et al. 2014). The results of Perassi and Borgnino (2014) showed that phosphorus adsorption is dependent on pH; adsorption increases as pH decreases. However, there are several complex pathways due to competition and transformation of the precipitate from amorphous calcium phosphate to hydroxyapatite leading to conflicting reports and indications of the key requirements. Different P removal mechanisms have been reported for the same media as illustrated in Table 2.6.

Table 2- 6: Results from previous studies under different conditions showing removal mechanisms

Study Type	Initial PO_4^{3-} Con. (mg/l)	pH	Time (hr)	Amount of Calcite (g)	P Removal Mechanism	Reference
Batch	≤ 2.2 ≤ 7.5 ≤ 10 ≤ 10 ≥ 3 10	7.7 8.3 9.1 10.1 7.7 8.3	24	1	Adsorption Adsorption Adsorption Adsorption Precipitation Precipitation	(Li et al. 2017)
Batch	20	7-12	15 min	1	Adsorption	(Karageorgiou et al. 2007)
Batch	1.55		2-3	2	Adsorption	(Sø et al. 2011)
Batch	2	6-12	18	5	Adsorption	(Xu et al. 2014)
Batch	10	4.5, 7 and 9		1	Adsorption for low P concentrations and precipitation for high P concentration	(Perassi and Borgnino 2014)

Study Type	Initial PO_4^{3-} Con. (mg/l)	pH	Time (hr)	Amount of Calcite (g)	P Removal Mechanism	Reference
Batch	5-25 mg/l		24	1	P-sorption ranged from0.3–20mg/ kg Adsorption for low P concentrations and precipitation for high P concentration	(Johansson Westholm 2006)

2.4 Related work

Phosphorus removal from wastewater has become an important issue to control eutrophication and to solve the problem of phosphate shortage in natural resources (Cordell et al. 2011). There has been a considerable amount of research carried out into alternative methods of phosphorus removal. This section reviews some of this work. Firstly, papers that investigate calcite as a source of calcium used for phosphorus removal are addressed. These papers proved useful in planning the experiments carried out in support of this thesis, the optimum conditions and determining the dominant mechanism of phosphorus removal. Then papers that have looked at the application of the carbonation process in removing contaminants from water are reviewed. Finally, other novel techniques that have been used at Wastewater Treatment Works (WWTWs) to remove phosphorus are discussed.

2.4.1 Removal of phosphorus from wastewater by calcite

Plant and House (2002) studied the precipitation of calcite in the presence of inorganic phosphate. The results indicated that at dissolved phosphorus concentrations less than 4.46 mg/l, calcite precipitation can occur as long as the initial supersaturation with respect to calcite is sufficient to promote growth.

Hanna et al. (2008) studied the feasibility of calcite as a material rich with calcium, as adsorbent for phosphate removal from wastewater. Also, the optimum conditions and the removal mechanism were investigated. The calcite used contains 99.9% calcium. The initial solutions were adjusted to pH values equal to 7.5, 9, 10, 11, and 12. The results indicated that the efficiency of calcite to remove phosphates increases with pH values and reaches to their maximum value at pH 12. It is observed that for all phosphate concentrations, the efficiency of the calcite increases rapidly till 15 min and becomes slightly and nearly steady state after 20 min, so that the most suitable time of contact is equal to 15 min and independent on the concentration of the phosphate species. It is also observed that the adsorption capacity of calcite increased with increasing the initial phosphate concentrations.

2.4.2 Application of the carbonate coprecipitation process in removing other contaminants from water

The carbonate coprecipitation process occurs naturally in water bodies, acting a self-cleaning mechanism(House 1990). Much work has been undertaken to explore the reason behind calcite precipitation in water bodies (Murphy et al 1983; Hartley et al 1997) and research indicates that it is stimulated by dissolved carbon dioxide levels or pH. However, the application of

coprecipitation processes for the treatment of contaminated waters has not been as extensively investigated. Aziz and Smith investigated the use of a limestone rock filter for removing low concentrations of Mn from drinking water(Aziz and Smith, 1996). Sibrell et al. (2007) conducted a laboratory testing program to find the optimum conditions for the removal of Zinc and Manganese through carbonate coprecipitation (CCP) process using the pulsed limestone bed (PLB) process developed by researchers at the U.S. Geological Survey's Leetown Science Center (LSC) in Kearneysville, West Virginia, for treatment of acidic mine drainage. In the PLB process, limestone (calcium carbonate) is dissolved under pressure of carbon dioxide, and this gives the water an excess of bicarbonate alkalinity. Then calcite can be precipitated by air stripping the water to remove the carbon dioxide. The relevant key findings were that a higher flow rate of carbon dioxide during carbonation reduce the time required for calcium dissolving and precipitating. However, flow rate did not influence the equilibrium concentration of calcium, which at 22°C, was suggested to be 400 mg/l.

2.4.3 Other novel phosphorus removal techniques

The most advanced technology that can be applied to remove/recover phosphate from wastewater is precipitation as a calcium salt. The removal product is often calcium phosphate in different phases (Mekmene et al. 2009). In this section, other phosphorus removal methods that have the potential to replace current methods at WWTWs are listed.

Korchef et al. (2011) used the CO_2 degasification technique to recover phosphorus in the form of struvite from wastewater by precipitation of struvite ($MgNH_4PO_4 \cdot 6H_2O$). CO_2 removal from the aqueous solutions results to the increase of pH. Since the solution supersaturation with respect to struvite increases drastically upon increasing the solution pH, struvite precipitation and phosphate co precipitation are favoured.

Stumpf et al. (2008) looked at recovering essential phosphorus from digested sludge of a WWTP using a reactor which is performed as an airlift reactor for an improved mixing and stripping the dissolved CO_2 and separating the removed phosphate as a MAP-crystals.

2.4.4 Phosphorus removal in the form of Struvite

Early investigations on struvite known as (ammonium magnesium phosphate) crystallisation found that it will form naturally in wastewater when ammonium magnesium and phosphate occur in equal molar ratios of 1:1:1 under certain pH conditions (Doyle and Parsons 2002; Le Corre et al., 2009). The investigations also revealed that struvite is found to be very soluble in acidic conditions but only slightly soluble in alkaline conditions. For this reason, a pH of at least 8.5 is usually used in struvite crystallisation processes (Quintana et al. 2008).Jaffer et al. (2002) found

that 97% phosphorus removal as struvite can be achieved. Wang et al. (2005) found that the removal of phosphorus from wastewaters in form of struvite can produce overall sludge volumes of up to 49% less than when chemical phosphorus removal techniques are used. Saidou et al. (2009) studied the struvite precipitation by the dissolved CO_2 degasification technique where precipitation occurred following the degassing of the CO_2 by atmospheric air. The study found that for initial solution pH less than 6.5, no precipitation was observed. For initial solution pH greater than 6.5, the phosphorus removal through struvite precipitation could be improved by increasing the airflow rate up to 25 L min/l, or by increasing the initial pH for higher airflow rates. The study concluded that compared to traditional techniques of struvite precipitation such as stirring and aeration, the dissolved CO_2 degasification technique is promising since a high amount of phosphorus around (78%) could be removed at relatively short experiment time. Korchef et al., (2011) studied the precipitation of struvite ($MgNH_4PO_4 \cdot 6H_2O$) using the CO_2 degasification technique is investigated. The precipitation of struvite was done from supersaturated solutions in which precipitation was induced by the increase of the solution supersaturation concomitant with the removal of dissolved carbon dioxide. The study found that at a fixed phosphate concentration, the increase of magnesium concentration in solution to 510.4mg/l, decreased the precipitation pH and improved significantly the phosphate removal efficiency.

2.5 Chapter Summary

This chapter divided into 3 parts, the first part identified and explored the problems that are the driving forces behind the work presented in this thesis. The issues associated with excessive release of phosphorus to the environment were stated. The limitations of current phosphorus removal technologies were shown along with a discussion of the WFD and the extra strain that this may place on existing techniques. The second part has described the theories behind the concepts used in support of this thesis. This included theories relating to calcite dissolution and precipitation as well as the phosphorus coprecipitation with calcite. The removal mechanism theories were explained with a review of some papers who found adsorption as a dominating phosphorus removal mechanism, others found calcium phosphate dominant, many stating HAP as a likely end product. In general, low pHs were found to favour adsorption and high pHs and large amounts of soluble calcium to favour precipitation. The correlation of phosphorus removal with pH and soluble calcium levels, as described by many of the papers reviewed, will help identify the dominant phosphorus removal mechanism. The third part of this chapter has discussed papers in the field of phosphorus removal and picked out points that are particularly relevant to this study.

At the end of this chapter, it is worth mentioning that there was ongoing work on the proposed technique by Cardiff University in a laboratory and field scale in collaboration with Dŵr Cymru Welsh Water (DCWW). The results from continuous on-site testing showed that P can be removed successfully from Nash WWTP of Welsh Water from 7-9.5 mg/l to 1-4 mg/l with prolonged residence times.

Chapter 3: Materials and Methods

3.1 Introduction

This chapter focuses on the methodology of the laboratory experiments carried out in this study, describes the material and the equipment used within the lab system, lays out the experimental procedures and the analysis techniques. Materials and methods of the field systems (carbonation and apatite system) of this study are also included in this chapter. The laboratory investigations were carried out in the CLEER facility at Cardiff University. The batch experiments consisted of several scenarios, which were also carried out to give an indication of the behaviour of P removal before the experiments were carried out in the large field trial. Field trials were carried out in West Bonvilston treatment works, a Dŵr Cymru Welsh Water site. The chapter is split into the following sections:

Section 3.2: Laboratory system – describes the material used and the procedure implemented in the operation of the laboratory system.

Section 3.3: Laboratory methods – describes the method of samples collection, storage prior to analysis and sample analysis.

Section 3.4: Geochemical characterisation – describes the methods used for the identification of mineral phases and the geochemical characterisation of the precipitate. This includes X-Ray Diffraction (XRD), total carbon (TC), Environmental Scanning Electron Microscopy ESEM, Field Emission Gun Scanning Electron Microscopy (FEG-SEM), X-ray photoelectron spectroscopy (XPS), sequential extractions and zeta potential measurements (ZPC). A detailed description of the removal mechanism experiment is also included in this section.

Section 3.5: Field trial systems – describes the design, material used, and the procedure implemented in the operation of Cardiff university and ARM Ltd systems.

Section 3.6: Field methods – describes the measurement methods and analytical determination of the field samples.

Section 3.7: Chapter summary

3.2 Laboratory System

This part gives details of the laboratory system experiment, including materials, equipment, and procedure. The underlying chemical process utilised for phosphate removal within this study may be summarised in three steps:

- Carbonation: The wastewater influent passes through a limestone column in the presence of carbon dioxide this stimulates the dissolution of limestone.
- Aeration: air is passed through the wastewater solution to degas carbon dioxide out of solution, this stimulates the formation of calcium precipitates.
- Settlement: calcium precipitates settle to form a sludge.

3.2.1 Materials and equipment used in the experiments

Limestone is the principal material used during the lab experimentation and Cardiff university field trial of this study. The limestone chips were purchased from Tarmac LTD by the concrete laboratory of Cardiff University School of Engineering. Tests have been performed by Aziz et al. (2001) involving the use of limestone chips bed for the removal of heavy metals from wastewater, these experiments unanimously concluded that the removal percentage of these metals increased marginally with decreasing particle size and this is due to the greater surface area per volume of smaller diameter limestone chips available to come into contact with the effluent solution. However, as using limestone chips of small particle size diameters resulted in increasing restriction in the movement of gases in the column, the use of a limestone particle size between 2-5mm was selected for this experiment as shown in Figure 3.1.

Figure 3- 1: Limestone rocks used in the experiments

The proposed laboratory system of the carbonation process is shown in Figure 3.2. The system consisted of the following parts as shown in Figure 3.3 to apply the key stages of the process (carbonation, aeration and settlement as identified in section 3.2).

- Limestone reactor: this consisted of a plastic column. The limestone chips were elevated by 50mm by a plastic tray with 1mm apertures to allow CO_2 injection through an air stone attached to the outlet of the CO_2 pipe. The air stone was used to generate a mass of finer bubbles that are dispersed more evenly beneath the limestone column. A hole in the side of the column allowed for the insertion of CO_2 .
- CO_2 Cylinder: a CO_2 cylinder used to provide carbon dioxide in the first stage of the process.
- Aeration beaker: this consisted of a 1L beaker and an air tube ended with air stone to diffuse air inside the beaker.
- Settlement beaker: a 1L beaker used for precipitate to settle.

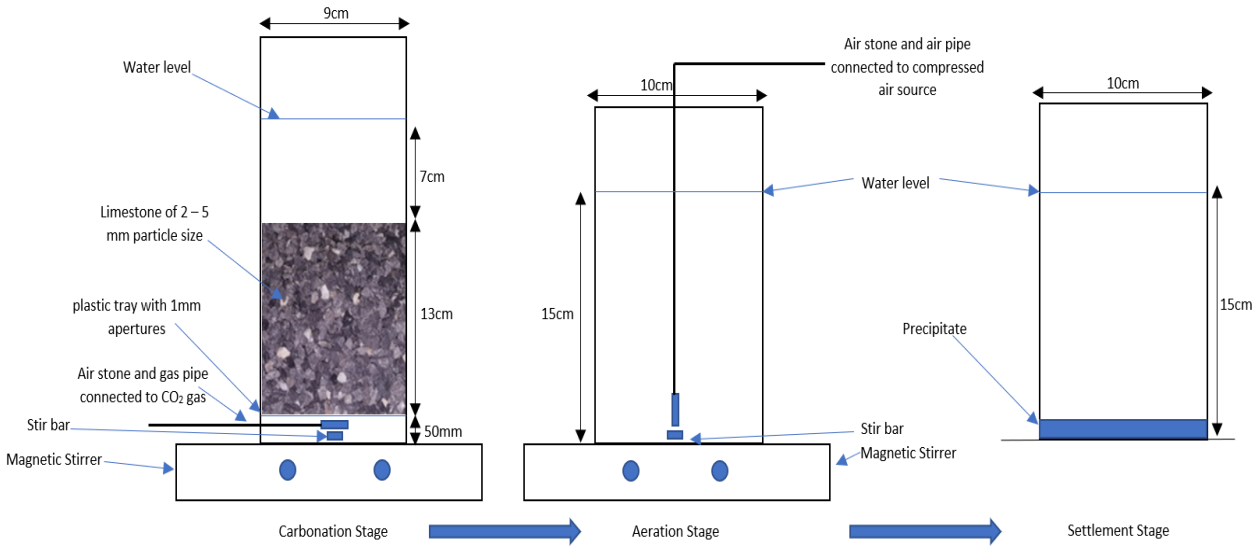

Figure 3- 2: Laboratory system of the carbonation process showing the three stages (carbonation, aeration and settlement

Figure 3- 3:Images of the lab system parts. (a) Limestone reactor (b) CO_2 cylinder (c) Aeration beaker with compressed air and (d) Settlement beaker

3.2.2 Lab work procedures

This part of the study gives details of the lab samples that were prepared, run and analysed where parameters controlling P removal process were investigated. This can be divided into three parts. The first part is the procedure performed prior experimentation. the second part is procedure performed during experimentation and the third part is experimentation performed after experimentation.

3.2.2.1 Procedure performed prior to experimentation

- Synthetic wastewater Preparation:

The stock solution used in these tests was prepared by dissolving 4.3871g potassium dihydrogen phosphate (KH_2PO_4) in 1 litre of deionised water to create a stock solution of 1g/l as total phosphorus. This solution was then stirred vigorously with a stir bar for 15 minutes on a magnetic stirrer plate to ensure that complete dissolution of the KH_2PO_4 crystals in the deionised water had occurred. This stock solution meant that relatively quick samples of the phosphorous solution could be made for each run during the experimentation. This was so that the stock could be diluted down to the desired concentration. Table 3.1 indicates the relative masses of the elements contained within KH_2PO_4; from these, the corresponding percentages of the elements within the soluble salt have been calculated. The percentage of phosphorous, in terms of mass, within KH_2PO_4 is 23%. Therefore, in order to produce a solution that contains 1000mg/l of phosphorous, a solution of 4348 mg/l of the salt was required.

Table 3- 1: Percentage distribution and relative masses of elements in KH_2PO_4

Element	Relative mass	Percent in KH_2PO_4 %
Potassium (K)	39	29
Hydrogen (H)	1	1
Phosphorus (P)	31	23
Oxygen (O)	16	47

- Limestone preparation

As mentioned earlier in this chapter that the limestone chips used in this study were purchased from Tarmac LTD by the concrete laboratory of Cardiff University School of Engineering. These

chips were initially 10mm in diameter and then they were reduced in size using a mechanical crusher then sieved to the required size of 2-5 mm. 1 Kg of these chips was washed before its use to remove any limestone dust from the surface to avoid any inaccurately high concentration of phosphate removal being obtained. A small amount of limestone chips was further crushed to a fine powder using a Labtech Essa air compressed grinder from which the chemical composition of the limestone chips was determined using XRD analysis (see section 3.4.1), the elements content using ICP (see section 3.3.5) and carbon content using Leco as detailed in (see section 3.4.2).

3.2.2.2 Procedures performed during system stages

- The first stage of the process which is the carbonation stage requires that the limestone come into contact with an elevated level of carbon dioxide in order to increase the solubility of the $CaCO_3$ chips in the wastewater. This resulted in the limestone chips being completely immersed in solution during the carbonation stage. Figure 3.2 shows the CO_2 injected into the bottom of the carbonation column below a bed of limestone chips. These chips are supported on top of a plastic mesh with one millimetre apertures. The carbonation column is placed on a magnetic stirrer with a stir bar placed in the column beneath the limestone bed. The solution was agitated continuously in order to make sure that uniform mixing of dissolved limestone in solution occurs. The CO_2 was pumped into the column from a pressurised cylinder while the rate at which the CO_2 is passed through the pipe and into the column is controlled by a CO_2 rotameter. A sample was taken before and after the carbonation stage to measure pH. A 20 ml sample was filtered using 0.45 µm membrane filter and analysed for Ca and P concentration. A range of carbonation time and flow rates were applied (see tables 4.3, 4.4, 4.5 and 4.6 Chapter 4).
- Following the CO_2 addition process, the solution was immediately removed from the carbonation column and placed in the aeration beaker. The solution was then injected with air controlled by an air rotameter as shown in Figure 3.2. The aeration beaker was also placed on a magnetic stirrer. A sample was taken at the end of aeration stage to measure pH. A 20 ml sample was filtered using 0.45 µm membrane filter and analysed for Ca and P concentration. A range of aeration time and flow rate were applied (see tables 4.3, 4.4, 4.5 and 4.6 Chapter 4).
- Once the air stripping of the batch of solution was complete, the solution was left to start the settlement stage, the suspended particles could settle to the bottom of the beaker as shown in Figure 3.2. A sample was taken at the end of settlement stage to measure pH.

A 20 ml sample was filtered using 0.45 µm filter and analysed for Ca and P concentration. A range of settlement time was applied (see tables 4.3, 4.4, 4.5 and 4.6 Chapter 4).

3.2.2.3 Procedures performed following experimentation

- pH

Values of pH were recorded for each of the samples extracted during the carbonation, aeration and settlement stages. This was carried out immediately after their removal from the batch test and another two pH readings after 24 and 48 hours of settlement. This was performed with a Severn multi Mettler Toledo with an expert pro pH probe, this was capable of a precision of three decimal places as shown in Figure 3.4. Prior to taking these readings, the pH meter was calibrated using pH buffer solutions of 4 and 7.

Figure 3- 4: pH meter

- Sample preservation

  Once pH was recorded, one drop of 20% nitric acid was added to each sample. The presence of nitric acid in these samples prevented any subsequent reactions occurring in them prior to ICP elemental analysis being performed. This was important to ensure that the concentrations of P and Ca ions dissolved in the sample at the time of its extraction from the batch solution.

- Filtration of samples

  After the settlement stage is finished, vacuum filtration was carried out on the precipitated solution to collect the precipitates. This is done using a 0.45-micron filter paper and a Buchner Funnel apparatus as shown in Figure 3.5.

Figure 3- 5: sample filtration

3.3 Laboratory Methods

This section gives details of sample storage and the laboratory analysis carried out on samples collected from laboratory and field experimentation.

3.3.1 Laboratory pH

For bench scale experiments, pH was measured using a Severn multi Mettler Toledo. This instrument was calibrated using two-point calibration (ph 4, 7) pH buffers were purchased from the manufacturer Hanna in compliance with operating instructions for Hanna combination meters HI-9828 and the laboratory instruments. Fresh buffers solutions were used each time instruments were calibrated. The remaining solutions were stored in the cool and dark. Only solutions that were within the expiry date were used.

3.3.2 Sample acidification

To make up 20 % (v/v) HNO_3 acid for acidifying samples, 20 ml of concentrated nitric acid was added to 80 ml of deionised water in volumetric measuring cylinder, the cylinder was inverted ten times to ensure sufficient mixing and labelled as a stock solution of 20 % (v/v) HNO_3. This was used for acidifying lab and field samples for the ICP-OES analysis.

3.3.3 Graded glassware, chemicals and Deionised Water

When accurate volumes were essential, i.e. in preparation of chemicals or reagents, grade A glassware was used exclusively. All chemicals used within this study were laboratory grade and obtained from either Fisher Scientific or Sigma Aldrich. All chemicals were used and stored in accordance with the material safety data sheets provided. High purity, sterile, 18 MΩ deionised water was used within all laboratory experiments and analysis.

3.3.4 laboratory glassware and equipment decontamination

Glassware and reusable laboratory equipment such as pipette tips, watch glasses and crucibles used in all laboratory experiments were washed with laboratory grade detergent prior to soaking in an acid bath of 10 % (v/v) HNO_3 solution for 24 hr. After this treatment, they were rinsed three times with tap water and subsequently three times using deionised water and left to air dry on clean paper towels before use.

3.3.5 Inductively Coupled Plasma- Optical Emission Spectroscopy (ICP- OES)

The analysis of the samples to determine total P and Ca concentrations were conducted in the CLEER facility at Cardiff School of Engineering using inductively coupled plasma- optical emission spectroscopy (ICP- OES). The instrument used was Perkin Elmer Optima 2100 DV with an AS90 plus auto sampler and a PC running Winlab 32 software. For the analysis of solids, 0.l g sample was gradually reacted with 3 ml of 10 % HCl and 3 ml of 10 % HNO_3 in a 1:1 ratio. The solution was placed in a microwave to digest (multi wave 3000- Anton Paar) and after cooling, the solution was diluted to 50 ml with deionised water before being filtered.

3.3.6 Orthophosphate analysis

Spectrophotometer used to determine the concentration of orthophosphate (PO_4-P) in this study. Spectrophotometry is an analytic method that measures the intensity of light of a specific wavelength passing through the sample. A colour complex is used and when photons of light encounter the analyte molecules, they are absorbed, thus reducing the intensity of the beam through the sample. To prepare the stock P solution, 219.5 mg of anhydrous potassium dihydrogen phosphate (KH_2P0_4) was dissolved in 1000 ml distilled water. The working P standard solutions of 0.2,0.5, 1, 5 and 10 mg/l were prepared from the stock solution by diluting it to the desired concentration using deionised water.

In order to prepare the reagent required for this method, 70 ml of 2.5 M H_2SO_4 was added slowly to a 400 ml volumetric flask of distilled water and then diluted to a volume of 500 ml. Twenty grams of ammonium molybdate solution $(NH_4)_6Mo_7O_{24}4H_2O$ were dissolved in 500 ml of distilled water. 1.76 g of 0.1 M ascorbic acid was dissolved in 100 ml of distilled water and 1.3715 g of $K(SbO)C_4H_40_6$ $1/2H_2O$ in 500 ml. To make 100 ml of combined reagent, all reagents above were mixed in the following order:

50 ml of sulphuric acid, 15 ml of ammonium molybdate, 30 ml of ascorbic acid and 5 ml of the potassium antimonyl tartrate solution. This combined reagent remains stable for approximately

8 hours. The combined reagent was prepared so that the P concentration in solution could then be analysed using the spectrophotometer at wavelengths of 880 to 882 nm. In order to obtain accurate P measurements, a preliminary test was conducted to calibrate the spectrophotometer (U- 1900 HITACHI), by measuring prepared standard solutions with known P concentrations. This calibration was carried out before the analysis of samples. The calibration curve used in measuring PO_4-P is shown in Figure 3.5.

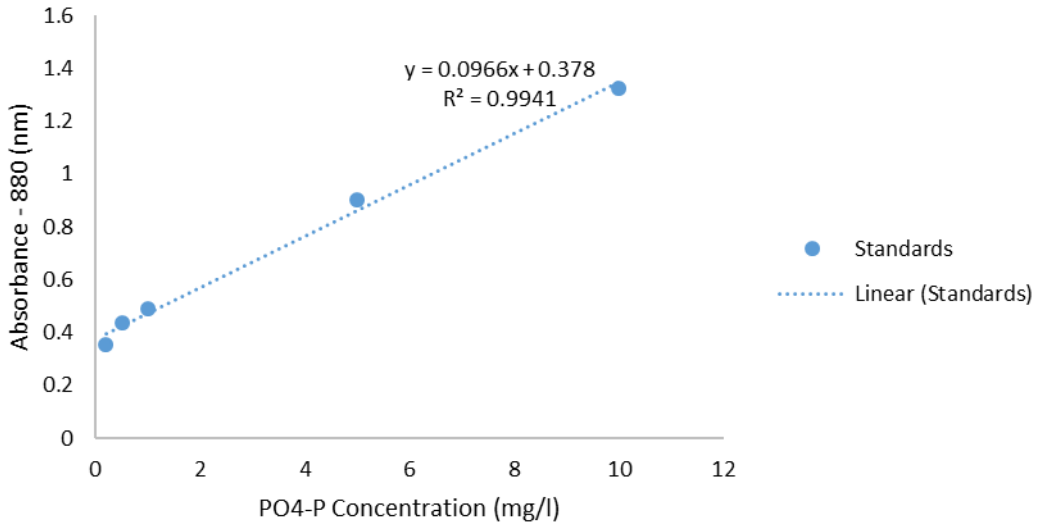

Figure 3- 6: Calibration curve for PO_4-P concentration

3.4 Geochemical characterisation

3.4.1 X-Ray Diffraction analysis - XRD

Analyses of the limestone chips being used during experimentation and the precipitated solids settled at the bottom of the settlement beaker was carried out using XRD analysis using a Philips PW 3830 X- ray instrument for analysis and determination of the main crystalline minerals present in the precipitate samples. Limestone chips were crushed to a fine powder using a mechanical crusher prior to this test. The sample of 0.1 mm thick was placed on the sample holder in the X-ray sample chamber and the scan run. After completing the scan, the data were exported to the software (X- pert high- score) for analysis. The mineral composition of the sample could then be identified by searching and matching the sample peaks with the known mineral peaks.

3.4.2 Total Carbon – TC

In order to measure the TC in the precipitate, a LECO (SC-144DR) analyser, were used in the CLEER facility of Cardiff School of Engineering. The total carbon (TC) was determined by placing 0.35 g

of samples in a ceramic boat with aluminium foil insert. The boat was then put into the furnace which was preheated at 1000 C°. The carbon infrared detection cell measured the CO_2 gas concentration, following thermal composition/ decomposition allowing the percentage value of TC to be determined by LECO analyser. Analysis using this instrument is accurate to within ± 10 %.

3.4.3 Environmental Scanning Electron Microscopy (ESEM) Analysis

ESEM analysis was used in this research to examine the mineralogical structure of the precipitates. Samples were analysed at Cardiff University School of Earth and Ocean Science. The instrument used was FEI XL 30 FG with a Peltier cooled specimen stage using Oxford Instruments INCA ENERGY X-ray analyser. The sample was coated with a layer of gold/palladium alloy in order to make the sample electrically conductive which prevents them from becoming charged during the scanning process. ESEM analysis was then performed. Backscatter images produced by ESEM help to distinguish between different minerals by producing different brightness levels for particles of varying density. Energy dispersive X-ray spectroscopy (EDX) was also carried out using SEM machinery to give the elemental composition of the substances being scanned.

3.4.4 Field Emission Gun Scanning Electron Microscopy FEG-SEM

FEG-SEM analysis was carried out at the Cardiff University School of Chemistry to produce colour maps of elemental distribution. The FEG-SEM facility is an ultra-high resolution Schottky field emission scanning electron microscope and is ideal for studying materials on the nanometre scale. Microscopy was performed on a Tescan Maia3 field emission gun scanning electron microscope (FEG-SEM) fitted with an Oxford Instruments $XMAX^N$ 80 energy dispersive X-ray detector (EDX). Images were acquired using the secondary electron and backscattered electron detectors. Samples were dispersed as a powder onto adhesive discs mounted onto aluminium stubs. The FEG-SEM can provide a high-resolution secondary electron (SE) and back scattered electron (BSE) imaging, instrument resolution of 3.5nm at 500V, 2.5nm at 1kV and 1.5nm at 10kV.

3.4.5 X-ray photoelectron spectroscopy XPS

XPS analysis was carried out at the Cardiff University School of Chemistry. XPS is an Ultra high Vacuum (UHV) technique and is suitable for the quantitative determination of elemental composition (atomic %) of elements in the surface region of solid sample. XPS involves irradiating the surface of interest with X-rays and analysing the energy of the emitted photoelectrons. Since these electrons have energies which are typically less than 1500 eV they interact strongly with the material under analysis and can therefore only escape from the top few atomic layers. The

binding energy of the core levels from which the photoelectrons are emitted are sensitive to the number of electrons in the valence band, and so the technique enables chemical state information to be obtained from the top few atomic layers of a surface. Analyses can be applied to all vacuum compatible solid materials whether they are conducting, semi-conductors or insulators. Layered samples may also be depth profiled in order to investigate the layer distribution. XPS is sensitive to all elements apart from hydrogen and helium and is highly surface sensitive with information typically arising from the top *ca*. 1-5 nm. Through measurement of the element peak areas and correction with the appropriate sensitivity factors.

3.4.6 Removal mechanisms

To thoroughly understand the removal mechanism, batch tests were conducted using 1g of calcite precipitate obtained from running the system using limestone chips and DI water only with no added P, shaken for 120 hr. Orthophosphate solutions were used throughout the adsorption tests. Initially, a stock solution of 100 ppm of orthophosphates was prepared by dissolving a certain amount of chemically pure K_2HPO_4 in deionized water. An aliquot of the stock solution was mixed with a certain volume of water so that a phosphate solution was prepared at the desired experimental concentration of 2 and 10 mg/l. pH values were adjusted using HCl and NaOH to 7, 8 and 9 due to their closeness to that of natural calcareous environment (Marschen et al. 1995; Chaturvedi and Sahu 2014). After the set time had elapsed, 0.45 µm filters were used to filter the suspension and the supernatants were analysed for Ca and P. The batch equilibrium adsorption tests for calcite precipitate were carried as detailed below:

1. 1g of calcite precipitate was weighed out on a balance capable of a precision up to 0.0001g.
2. Each 1g of calcite precipitate were placed in a 100ml polypropylene sample pot.
3. 100 ml of synthetic wastewater solutions were poured into the sample pots. Two initial P concentration of 2 and 10 mg/l were examined at three different initial pH values of 7, 8 and 9.
4. The sample pots were then fixed horizontally on the shaker table. The shaker table was set at 180 rpm to ensure good mixing and started.
5. At a certain time interval the samples were removed from the shaker table and vacuum filtered using 0.45µm cellulose nitrate membrane filters.
6. Samples were filtered in the order of lowest concentration to highest concentration to avoid contamination.
7. The pH of the filtered samples was carried out using a Severn multi mettler Toledo meter with an expert calibrated pro pH probe which is capable of a precision of three decimal places.
8. The samples were stored in the fridge until analysis by the ICP-OES for phosphorus and calcium.

3.4.7 Sequential extraction

A sequential extraction procedure adapted from Ruttenberg (1992) designed for phosphorus rich sediments, was performed on the samples. A summary of this procedure is presented in Table 3.2. The extraction by $MgCl_2$ was used in this experiment to remove the P attached or loosely sorbed on the sediment surface. This method has been widely used by a number of researchers (Sundareshwar et al. 1999; Coelho et al. 2004; Smith et al. 2006). Before experiments commenced, the wet precipitate samples were centrifuged at 2,500 rpm for 15 minutes to remove the pore water. The first stage was to extract the exchangeable or loosely sorbed P. Samples of wet precipitate weighing 0.5 g were placed into 50 ml centrifuge tubes and 10 ml of the 1M $MgCl_2$ solution was added. The tubes were shaken for 2 hours and centrifuged at 2500 rpm for 15 minutes. The supernatant was then filtered through a 0.45 µ filter membrane and the solution kept for analysis. Another 10 ml of $MgCl_2$ was added to the residue precipitate in the centrifuge tubes and the same process was repeated. The residue precipitate was washed with deionised water twice for 2 hr at 25°C, then shaken and centrifuged as described above. The second stage was to extract the Authigenic Apatite plus $CaCO_3$ bound P plus Biogenic Apatite. 10 ml of acetate buffer was added to the residue precipitate. The tubes were shaken for 6 hours and centrifuged at 2500 rpm for 15 minutes. The supernatant was then filtered. 10 ml of $MgCl_2$ was added to the residue precipitate in the centrifuge tubes and the same process was repeated for 2 hours each time. The residue precipitate was washed with deionised water twice for 2 hr at 25°C, then shaken and centrifuged as described above. The third stage of extraction was to extract Detrital Apatite plus another inorganic P. 10 ml of 1M HCl was added to the residue precipitate. The tubes were shaken for 16 hours and centrifuged at 2500 rpm for 15 minutes. The supernatant was then filtered as described above.

Table 3- 2: Summary of sequential extraction phases. Adapted from Ruttenberg (1992) and Smith et al. (2006)

Target Phase	Extractant Used	Extraction conditions
Exchangeable or loosely sorbed P	1. $MgCl_2$ (pH 8) 2. H_2O	1. 2h, 25°C 2. 2h, 25°C
Authigenic Apatite plus $CaCO_3$- bound P plus Biogenic Apatite	1. Acetate buffer (pH 4) 2. $MgCl_2$ (pH 8) 3. H_2O	1. 6h, 25°C 2. 2h, 25°C 3. 2h, 25°C
Detrital Apatite plus another inorganic P	1M HCL	16h, 25°C

3.4.8 Zeta potential analysis

Zeta potential is a measure of the magnitude of the electrostatic or charges repulsion/attraction between particles and it is one of the fundamental parameters known to affect stability. Its measurement brings detailed insight into the causes of dispersion, aggregation or flocculation, and can be applied to improve the formulation of dispersions, emulsions and suspensions. The zeta potential is measured with the Zetasizer Nano, Malvern that uses micro-electrophoresis/electrophoretic light scattering technology to measure the zeta potential and the electrophoretic mobility. The Zeta potential is measured as a function of pH, thus several samples at different pHs are produced by using 1g of calcite precipitate weighed out on a balance capable of a precision up to 0.0001g. Each 1g of calcite precipitate collected from running the proposed system with limestone chips and DI water only without added P were placed in a 100ml polypropylene sample pot. A 100 ml of synthetic wastewater solutions were poured into the sample pots. Three groups of samples were prepared the first group was calcite precipitate and DI only, the second and third group were calcite precipitate and P solution of 2 and 10 mg/l P. All groups were examined at initial pH values of 6,7, 8,9,10,11 and 12.

3.4.9 Particle size distribution

This test carried out on calcite precipitate collected from running the proposed system with limestone chips and DI only without added P. Testing was performed using a Malvern Mastersizer 3000 and Hydro EV sample dispersion unit. Along with the requisite software, this enables particle size to be measured via laser diffraction. Particle density and an estimated refractive index of the samples were inputted into the analysis program along with the refractive index of the dispersing media, in this case distilled water. Deionised water was also used for flushing and calibrating the apparatus for each sample tested. A small sample was added to the dispersion unit and cycled through the apparatus for analysis.

3.5 Field Trials Materials and Methods

Cardiff University (CU) in collaboration with Dŵr Cymru Welsh Water (DCWW) and ARM limited (a privately owned company based in Rugeley, Staffordshire. Established in 1947 as agricultural engineers, since 1980, the company specialised in the development and application of natural wastewater treatment systems using constructed wetlands technology) undertook a field trial aiming at trialling two techniques for the removal of Phosphorous from wastewater. This project was a pilot scale project which involves the trialling of innovative techniques for the treatment of

P on a DCWW waste treatment work site. The site chosen for the trial is West Bonvilston Wastewater Treatment Work.

3.5.1 Cardiff University system design

3.5.1.1 Site information

The West Bonvilston wastewater treatment work, one of Welsh Water sites was selected as the favourable location to construct the field trial for both techniques. Figure 3.7 shows the regional location of the site in relation to the city of Cardiff in South Wales. Figure 3.8 shows the site layout. Figure 3.9 shows treatment stages in West Bonvilston WwTW.

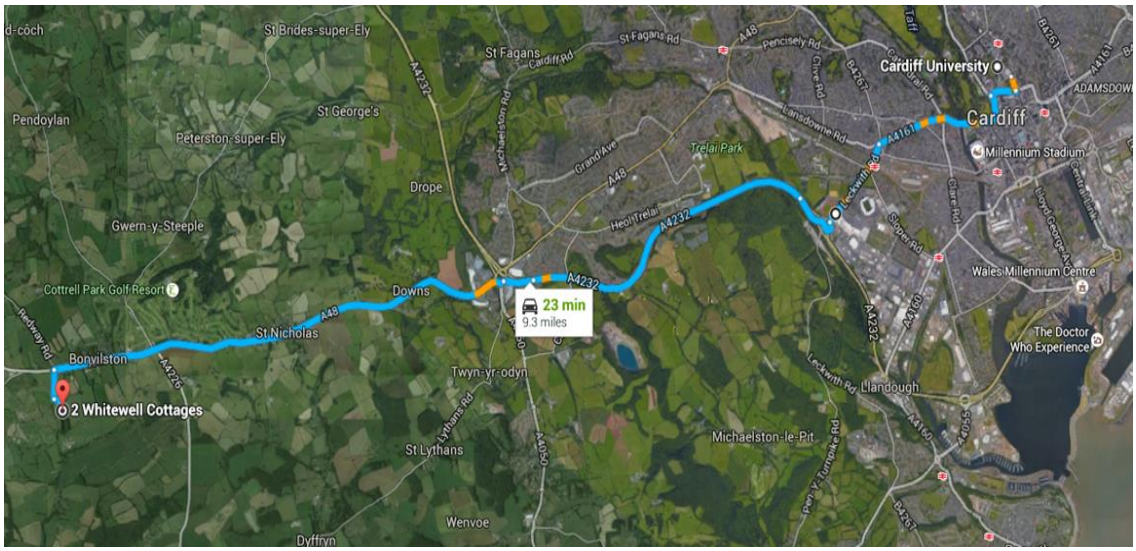

Figure 3- 7: Map showing the location of the West Bonvilston WwTW in relation to the city of Cardiff, South Wales, UK.

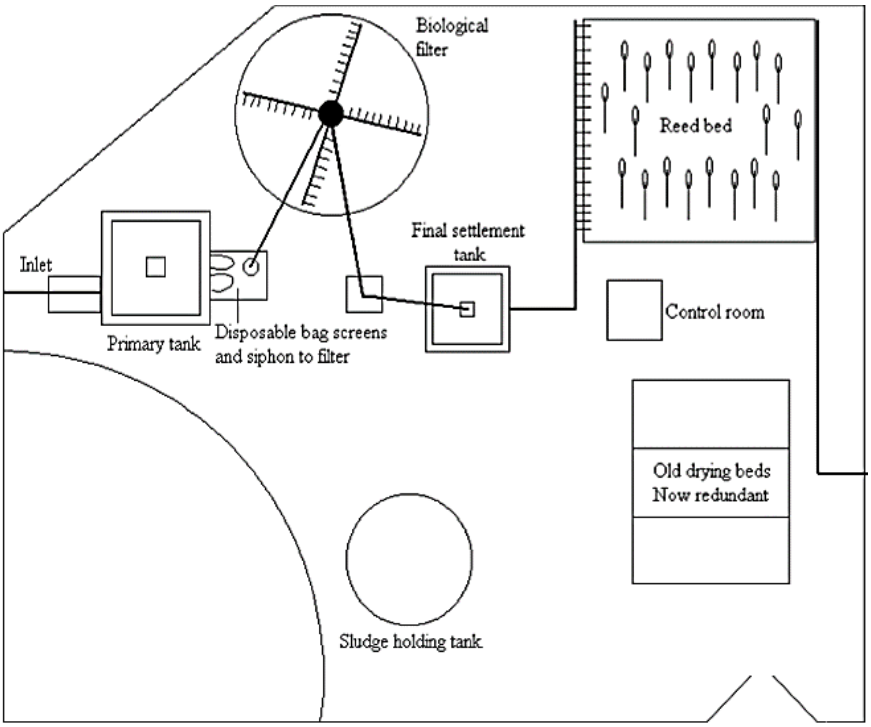

Figure 3- 8: West Bonvilston WwTW layout

(a) Inlet location

(b) Inlet

(c) Primary tank

(d) Biological filter

(e) Bag screen and siphon to biological filter

(f) Final tank

(g) Sludge holding tank

(h) Reed bed

Figure 3- 9: Treatment stages in West Bonvilston WwTW (a) Inlet location (b) Inlet (c) Primary tank (d) Biological filter (e) Disposable bag screen and siphon to biological filter (f) Final tank (g) Sludge holding tank (h) Reed bed

3.5.1.2 Design criteria

This section presents the design criteria used as a basis in the design of Cardiff university field system as listed in table 3.3. The field system consists of three stages as detailed in the following section.

Table 3- 3: System design criteria

Criteria	Justification
Ease of construction and maintenance	Field system design will allow easy maintenance by university technician team with limited technical expertise.
Ease of sampling and performance monitoring	Due to the research nature of this project and that extensive sampling will be undertaken, the design should include suitable systems for sampling and monitoring.
Hydraulic simplicity	Flow within the system should be kept as simplistic as possible to allow easy flow monitoring.
Adaptability	Should be a flexible enough design to allow the trial of differing support medias and parts for research purposes.
Budget	The cost of the build was limited by the constraints of the funding companies.

3.5.1.3 System design and operation

The field system was inspired from the lab system with some adaptations to maintain the criteria included in table 3.3 in terms of maintenance, flexibility, monitoring and budget. The system was designed, constructed and commissioned by the PhD candidate under Dr Devin Sapsford

supervision and with assistance provided by a number of Cardiff University technical staff in the construction stage and in collaboration with Welsh Water contractors. The system including three stages carbonation, aeration and settlement. A schematic layout of the system is shown in Figure.3.10. The system consists of the following:

- A **storage tank** placed upfront of the trial to collect wastewater from the final tank shown in Figure 3.11 (b) and feed both systems with untreated wastewater via 110V pumps.
- A **header tank** 1m^3 Intermediate Bulk Container (IBC) as shown in Figure 3.11 (c) to store the untreated wastewater for Cardiff University system prior to its use, this tank was provided with high and low float switches to control the pump in the storage tank, the header tank was connected to the limestone reactor via a hose with control valve to control the inlet flow to the limestone reactor and placed on a wall of 1m height to provide gravity flow from it to the limestone reactor.
- A **limestone reactor** consisted of a 1m^3 Intermediate Bulk Container (IBC) as shown in Figure 3.11 (e) to receive the coming wastewater from the header tank by gravity and a cylinder inside the IBC filled with 100 kg of limestone placed on the top of a gas diffuser connected to the CO_2 via gas pipe. The reactor also includes two 110V **water pumps** one to circulate the wastewater through the limestone reactor and the second one to transfer wastewater from the limestone reactor to the first aeration tank. The water in the cylinder can be considered as a batch treatment under elevated CO_2 pressure.
- The **CO_2** is provided by CO_2 bottles as shown in Figure 3.11 (d) connected to the plastic pipe which fed the limestone reactor via a regulator. The regulator is also connected to a gas flow meter (rotameter) to allow the measurement of CO_2 flow rate. The manifold cylinder pallets of CO_2 (MCP) was provided with trace heating to prevent the regulator from freezing.
- Two **Passive aeration tanks** on the top of each other placed on the wall of 1m height as shown in Figure 3.11 (f). This stage is different to the aeration stage that adapted during the lab experimentation, no compressed air source was used and instead two aeration tanks were used, the top tank is 400 L capacity provided with a series of holes made on the bottom side to transfer the wastewater to the second aeration tank which is an IBC tanks with 640 L capacity contains plastic media (pall rings 50mm) as shown in Figure 6.6(h) to promote efficient aeration by making the water flow trickling through it. The reason behind this change was to ensure lower cost for the trial by providing aeration without the need to use an air blower and examine effectiveness of a very simple aeration way in degassing the CO_2 and increase the pH level.

- A fill **drainpipe** connected to the outlet of the bottom aeration tank to transfer wastewater from the aeration tank to the holding tanks via holes.
- Two **holding tanks** of 2.25m width 4.5m length and 1m height as shown in Figure 3.11 (h) provided with wooden baffles as shown in Figure 3.12. The reason behind the use of this size of holding tanks was to achieve long residence time and ensure that the wastewater collected from the previous stage (aeration tanks) will have sufficient settlement time for the precipitate to form and remove phosphorus. These tanks were provided with wooden baffles used to increase the length of the water path so the water will spend more time in this stage rather than making a short cut to the end of the tank directly. The first zone of the holding tanks was filled with the same plastic media used in the aeration tank to provide a surface upon which the precipitation reaction can take place and easily collected as shown in Figure 3.11 (h) as it is very difficult to collect the precipitate from the base of the holding tanks with the covering sheets fixed to prevent the dilution effect caused by the rain.
- A **final collection tank** to receive the wastewater from the holding tanks and transfer it to the reedbed via pump as shown in Figure 3.11 (i).

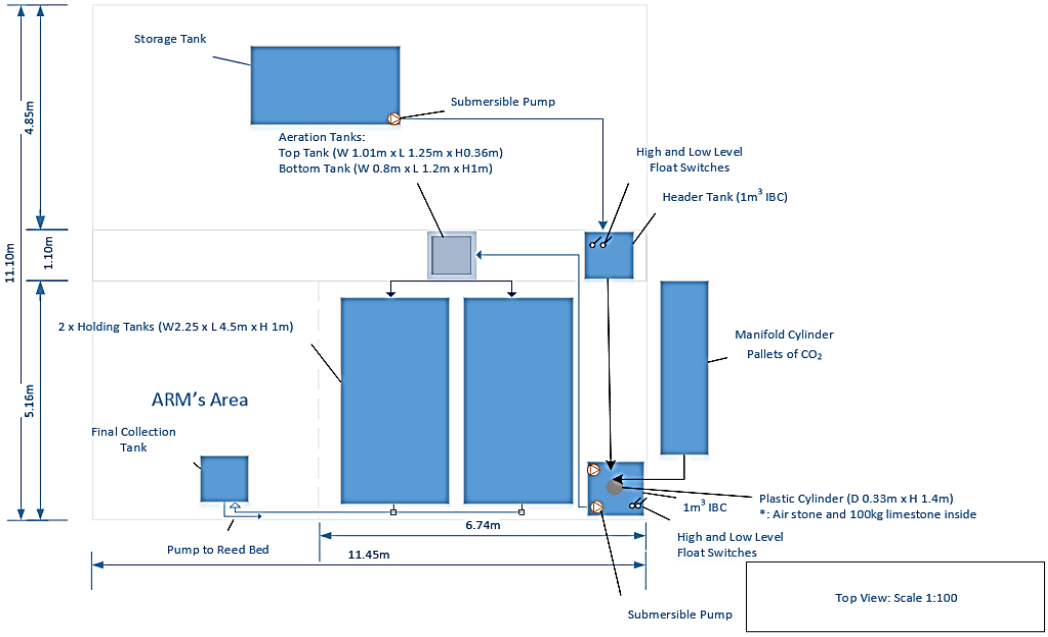

Figure 3- 10: Schematic layout of the field system

The carbonation stage starts when the untreated wastewater influent transfer from the header tank to the limestone reactor. the wastewater circulates through the limestone column by the circulation pump with CO_2 injected from the gas bottles at flow rate of 6 l/min. Approximate residence time of 50 min (40 min was the carbonation time applied through the lab system). **The**

aeration stage starts when wastewater transfers from the reactor to the top aeration tank then trickle through the plastic media in the second aeration tank for approximately 20 min (calculated from the beginning of the transfer to the first aeration tank until the drain of wastewater from the second aeration tank finished). **The Settlement stage** starts when the wastewater drained from the second aeration tank to the two holding tanks. The maximum residence time in the holding tanks was approximately 5 hr (calculated by a trace test). **Note** the residence time in the different stages is approximate. Figure 6.6(a-h) show the stages of Cardiff university field system

(a)Photo of Cardiff university system

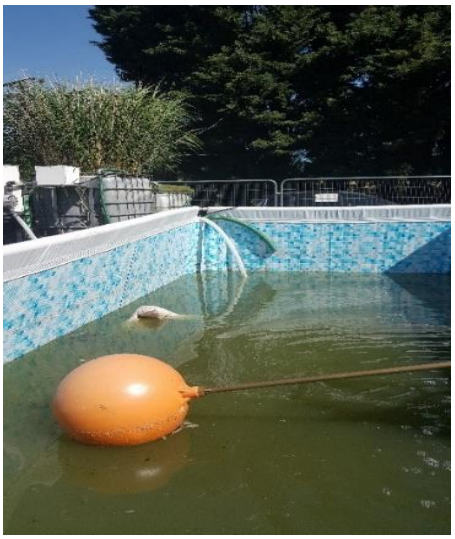

(b) storage tank

(c) Header tank

(d) CO_2 cylinders

(e) Limestone reactor

(f) Aeration Tanks

(g) Holding tanks

(h) Plastic media. (i) Final collection tank

Figure 3- 11: Cardiff system stages during experimentation. (a) Photo of the system (b) Storage tank (c) Header tank (d) CO_2 cylinders (e) Limestone reactor (f) Aeration Tanks (g) Holding tanks (h) Plastic media (i) Final collection tank.

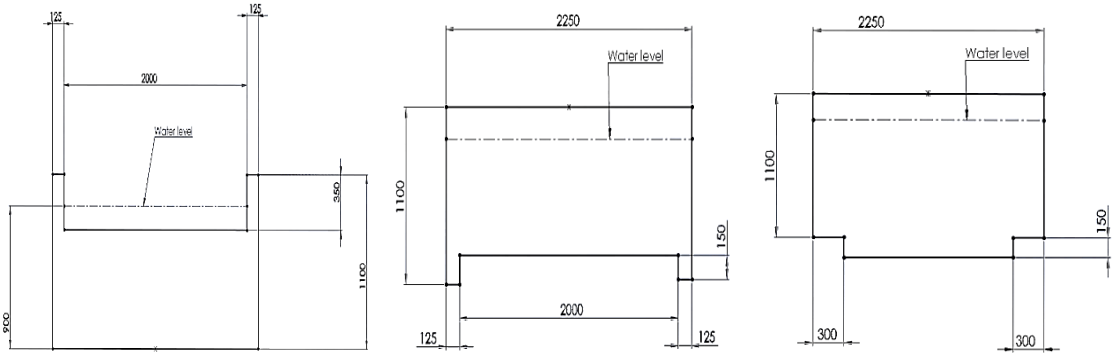

Figure 3-12: Baffles design

3.5.2 ARM system design

A schematic layout of the system is shown in Figure 3.13. The system consists of the following:

- An 8.1m^3 capacity **storage tank** placed upfront of the trial was used to collect wastewater from the humus tank and feed both systems with **untreated wastewater** via 110V pumps as shown in Figure 3.14 (a).
- **An Etatron (MIA series) diagram pump** was used to pass a controlled flow rate of 2m3/d from the storage tank to the trial.
- **The first process unit is a saturated vertical flow (SVF) aerated wetland containing forced bed aeration (FBA™).** This was fabricated from a 1m^3 Intermediate Bulk Container

(IBC) that was filled with approx. 800mm of 10-15mm angular limestone gravel media. It was planted with *Phragmites Australis* at a density of 8 reeds/m^2. The reeds were well established prior to the start of the trial. **A Hiblow (HP100) diaphragm air blower** was connected to an airline running vertically down through the media and to a dripline containing 300mm centre emitters at the base of the IBC through which 100 l/min of air was delivered. The purpose of the FBA™ was to remove BOD_5/NH_4 to prevent formation of biomass on the reactive media which would reduce the media surface area available for precipitation as shown in Figure 3.14 (b).

- A **collection/ holding tank** fabricated from a $1m^3$ IBC was positioned upstream of the SVF aerated wetland to receive treated wastewater from the aerated wetland and to transfer it forward to the columns containing reactive media 1 and 2 as shown in Figure 3.14 (c).
- From the collection/ holding tank, flow is split into four columns with effluent drawn through foot valves set 50mm above the base and passed forward onto the columns using Etatron D.S series solenoid pumps at controlled flow rates of 80 l/d (column 1 and 3) and 200 l/d (column 2 and 4). Water level loggers are positioned in the collection/holding tank to highlight periods of no flow (low levels) from the collection/ holding tank to the columns as shown in Figure 3.14 (d).
- Flows are dosed at the pre-calibrated flow and loading rate onto a set of 4 600mm columns via 12mm UPVC trickle bars. Columns 1 and 2 are filled with media 1 and columns 3 and 4 are filled with media 2. Each of the four columns had a 50mm deep layer of 10-14mm natural crystalline high purity calcium carbonate ($CaCO^3$) limestone installed on the surface of the reactive media. Effluent flows vertically down through each of the four columns via gravity before entering a second set of 4 columns in series. The second set of columns contained no media.
- A **final collection tank** to receive the wastewater from the columns and the Cardiff system and transfer it to the works reedbed via a submersible pump operating on a float switch as shown in Figure 3.14 (e).

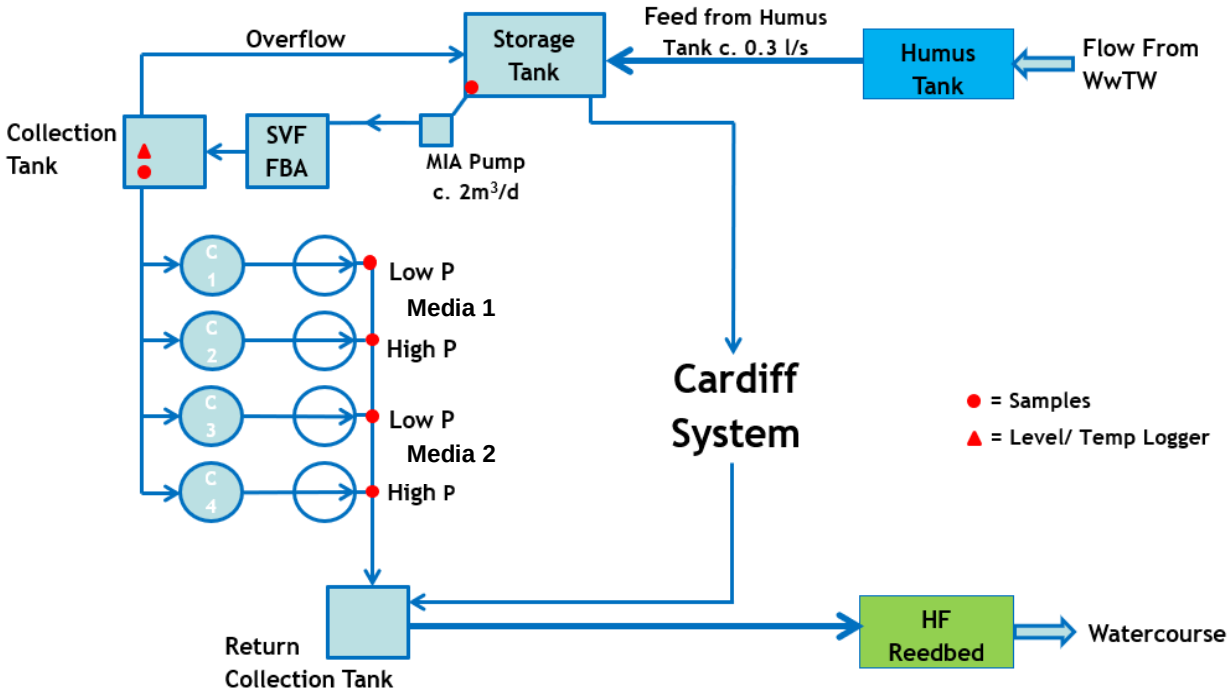

Figure 3- 12: Schematic layout of the apatite system

(a) Holding tank (b) Reed bed (c) Collection IBC

(d) Column series (e) Final collection tank

Figure 3- 13: System Stages during experimentation. (a) Holding tank (b) Reed bed (c) Collection IBC (d) Column series (e) Final collection tank.

3.6 Field sampling methods

The following section describes the methods used in the filed part of this study in monitoring of the P removal trial.

3.6.1 Determinations of temperature, pH, electrical conductivity and dissolved oxygen

Temperature, pH, electrical conductivity and dissolved oxygen where determined using a Hanna Instruments HI-991003. Props were calibrated at each site visit using manufacturer's calibration

procedure set out in the operator manual. The meters were kept stored in their original cases and care was taken to ensure the probs were kept in wet in manufacturer's storage solution when not in use. Measurements were recorded once the reading had settled. Accuracy was stated as ± 0.1 ppm in the manufacturer's guidelines, and this was taken as absolute.

3.6.2 Field determination of alkalinity and acidity

Alkalinity was determined using a HACH Alkalinity test kit. In this, Hach 16900 digital titrator using a 1.600 N sulfuric acid cartridge and bromocresol green methyl red indicator powder pillows were used. Titrations were conducted to a light violet -pink end point and alkalinity was read directly from the titrator counter in mg/l as $CaCO_3$. Prior to measurement it was made sure that any air bubbles were removed from the delivery tube and any excess acid was removed with deionised water before the counter was reset. Acidity was determined using a HACH Acidity test kit. In this, Hach 16900 digital titrator using a sodium hydroxide digital titrator 1.600 N cartridge Phenolphthalein indicator powder pillows were used.

3.6.3 Filtration and sample preservation

Water samples were taken for metals analysis in Cardiff University's CLEER facility using ICP-OES. When filtration is indicated samples were filtered in the field using Whatman 0.45 µm cellulose nitrate membrane filters. Samples were preserved for ICP-OES analysis of metals with 1 mL of 10 % HNO_3 per approximately 20 ml of sample to a pH less than 2.

3.6.4 Cation and anion analysis

Inductively Coupled Plasma Optical Emission Spectrometry (ICP-OES) (See section 3.3.5) was used to detect and quantify cationic metal concentrations. The instrument used was a Perkin Elmer Optima 2100 DV in conjunction with an AS90 plus autosampler and WinLab 32 software. This analysis was carried out for the unfiltered and filtered samples to determine the total and dissolved concentrations of Ca, P, Mg, Na, K, Fe, Mn, Zn and S respectively. In each case the analysis was calibrated against a set of three commercial standards used to construct a calibration curve covering the detection range for the expected concentration of each required element. These standards, and an analytical control of deionised water acidified with 2% (v/v) HNO3, were analysed after every ten samples to identify any analytical drift. If there was ≥10% error in the analysis of the standards the tests of that element were rejected, and the analysis redone. Each sample run also included a duplicate sample. As with the standards, if the duplicate sample returned measurements in excess of 10% error the sample run was rerun. For anion analysis

unacidified filtered samples were taken for the determination of SO_4, Cl, F and NO_3. The instrument used was ICS-2000 Ion Chromatography System. Samples were loaded into a Dionex® AS40 automated sampler. Analysis of samples was against a set of standards. The first place in the automated sampler is for the blank then the standards from the lowest concentration to the highest then the samples. Samples with of range concentrations were diluted with deionised water and analysed. Chromeleon software used to interpret the results.

3.7 Chapter summary

This chapter has described the material and methods used for the experimental side of this thesis. Firstly, the material was described in terms of source and preparation, the laboratory system equipment then listed with detailed operational procedure. The methods of water samples analysis were outlined. The methods of precipitate characterisation were explained. The detailed design and operation procedure of Cardiff university and ARM Ltd field trials were described. Finally, the measurements methods carried out in the field were expained.

Chapter 4: Experimental and theoretical investigation of P removal by calcite

4.1 Introduction

This chapter presents the results of the first part of this study, focuses on the laboratory data obtained from running the proposed process. The specific objectives of this chapter are: (1) to determine the behaviour of limestone dissolution during carbonation stage, (2) to determine the effect of degassing CO_2 on encoraging calcium carbonate/phosphate precipitation, (3) to determine the removed P concentration during process stages. All experiments included in this chapter were carried out in triplicate and all replicates were with less than 10% of each other. The Chapter is split into the following sections:

Section 4.2: Preliminary test – presenting the results of the characterisation tests on the crushed limestone and calcite precipitate including total carbon, total digest particle size distribution XRD, ESEM and the results of running the process to determine the working parameters.

Section 4.3: Lab experiments – presenting and discussing the results of running the lab process under the working parameters identified in the previous section with different phosphorus concentrations.

Section 4.4: PHREEQC – The PHREEQCI software was used to predict calcium and phosphate species and saturation index.

Section 4.5: CO_2 optimisation – Presenting and discussing the results of alternatives to reduce CO_2 consumption. This includes alternatives related to the design of the system and others like using acid dosage instead of CO_2 and using a mixture of limestone with gypsum.

Section 4.5: Chapter summary and conclusions

4.2 Preliminary tests

4.2.1 Characterisation of the material used:

The material used in this study was limestone rocks of 2-5mm particle size. Characterisation tests were performed on this material after crushing (see section 3.2.3.1 chapter 3) and the same tests were performed on the precipitate resulting from running the process with limestone and water without phosphorus.

4.2.1.1 Total digest and total carbon

The chemical composition of limestone powder was determined using Inductively Coupled Plasma Optical Emission Spectrometry (ICP-OES). This was carried out through the digestion of the sample (see section 3.3.5 chapter 3). The fully digested sample was analysed for the presence of the following elements (calcium, silicon, magnesium iron, aluminium and phosphorus) as shown in Table 4.1. Total carbon analysis was performed to determine the carbon content in the precipitate using a Leco SC-144DR furnace (see section 3.4.2 chapter 3). Carbonate content in limestone powder was 59.94% and in calcite precipitate was 59.91% giving limestone and $CaCO_3$ precipitate a purity of 96% based on stoichiometry.

Table 4- 1: Results of the total digest for the limestone powder and calcite precipitate (%)

Element	Percentage weight content (%) Limestone powder	Calcite precipitate
Ca	35.1	35.7
Si	0.68	0.53
Mg	0.06	0.02
Fe	0.1	0.01
Al	0.24	0.0
P	0.03	0.01

4.2.1.2 Particle size distribution

A sample of the collected $CaCO_3$ precipitate was tested with the Malvern mastersizer (see section 3.4.8 chapter 3), the results of which are displayed in Figure 4.1. The particles had a D_{10} of 12.2 µm and D_{90} of 46.1 µm. One peak is visible from the profile located at 30 µm. The D_{50} value of the precipitate is 27.6 µm.

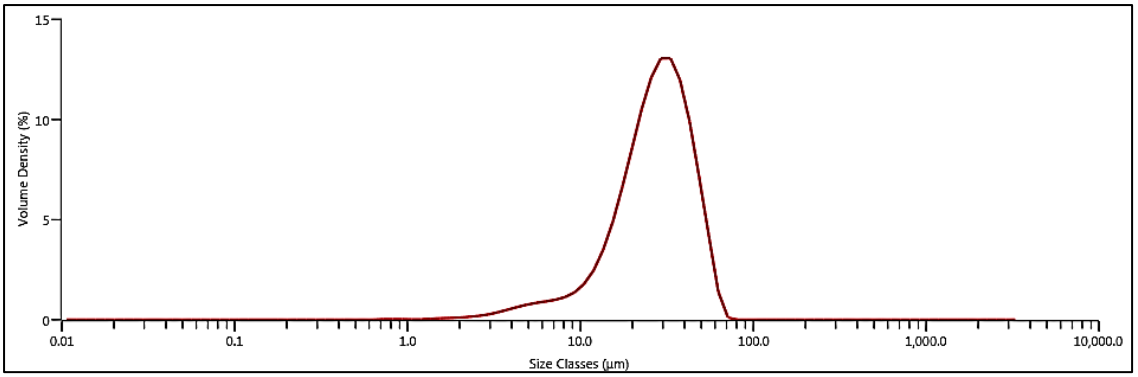

Figure 4- 1: Malvern Mastersizer particle size distribution analysis of $CaCO_3$ precipitate

4.2.1.3 Mineral composition

The limestone used in the experiments was characterized by X-ray diffraction (XRD) to detect the main components. Figure 4.2 (a, b) represent the XRD spectra of the ground limestone and the precipitate respectively. In each case the XRD are displayed as plots of total counts against goniometric angle °2Theta (°2θ). Both limestone powder and precipitate obtained from running the process without phosphorus show peaks at 26.5, 34.0, 36.5, 42.0, 46.0, 50.5, 55.5, 57.0, 68.0, 73.0, 77.0, 78.0, 84.0 and 88 °2θ. The x-ray patterns indicated that the dominant mineral in both samples was calcite with well crystalline phase. This demonstrates the similarity in mineral composition between the original material and the precipitate out of it.

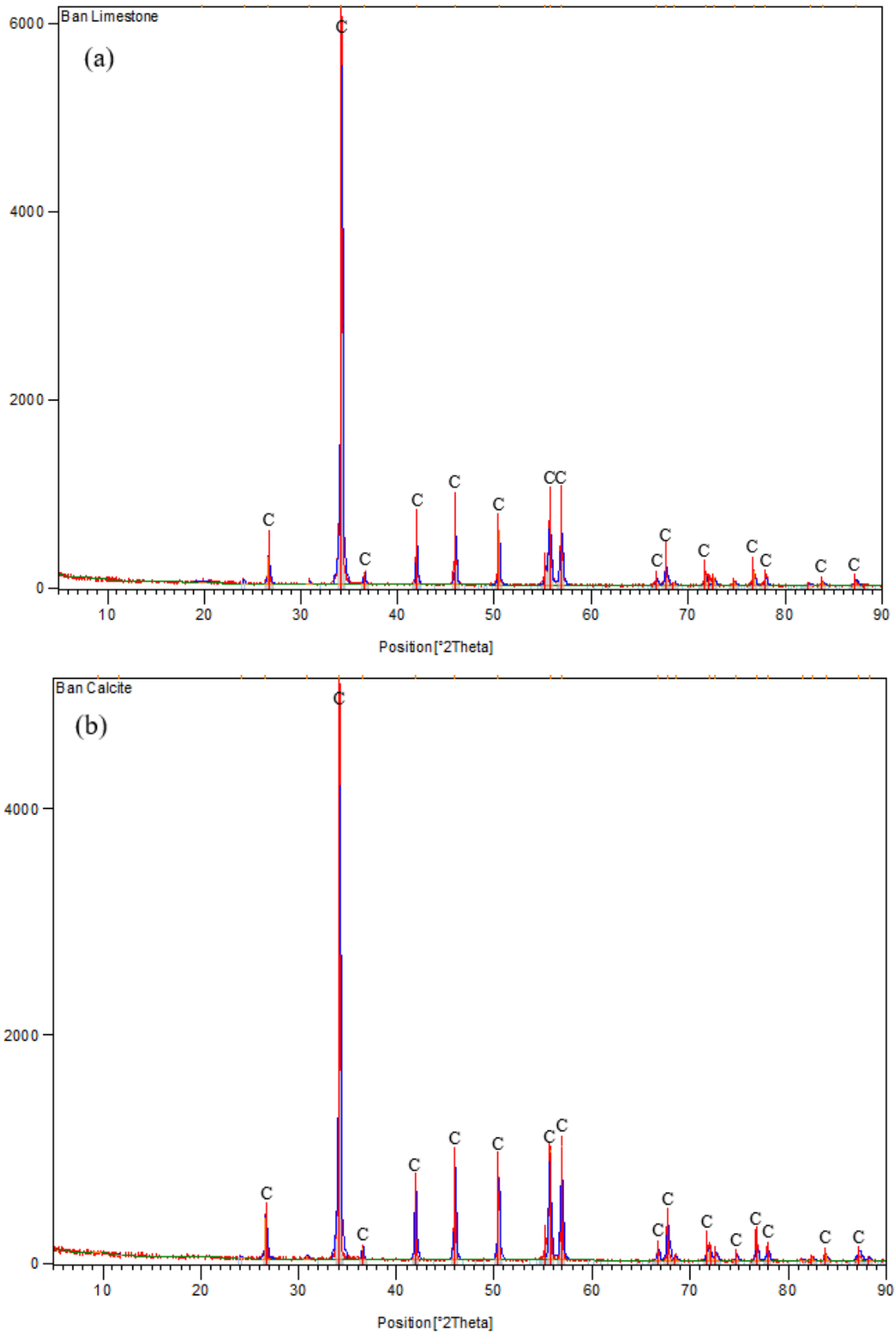

Figure 4- 2: X-ray diffraction chart of (a) crushed limestone (b) calcite precipitate

4.2.1.4 ESEM

Figures 4.3 and 4.4 show Scanning Electron Microscopy (ESEM) images of the crushed limestone and calcite precipitate. Clear crystalline structure can be identified from the images for both samples which is consistent with the interpretation of the XRD graphs in section 4.2.1.4 suggesting this is a crystalline calcite. The ESEM results have also indicated that the limestone used in this study and the calcite precipitate obtained from the system have the Ca content of 34.41% and 35.1% respectively, which compares well with the data from the total digestion and demonstrates the similarity in Ca content. There is a large size range with individual particulates from calcite precipitate of < 2.5 µm in diameter to particulates of > 23.4 µm.

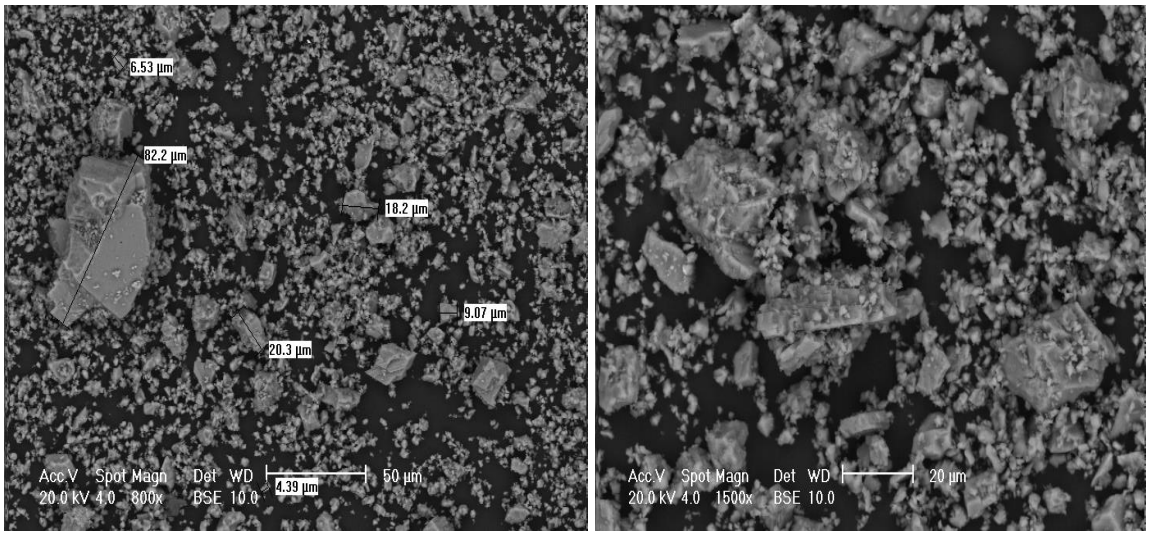

Figure 4- 3: SEM image of the original limestone showing crystalline structure

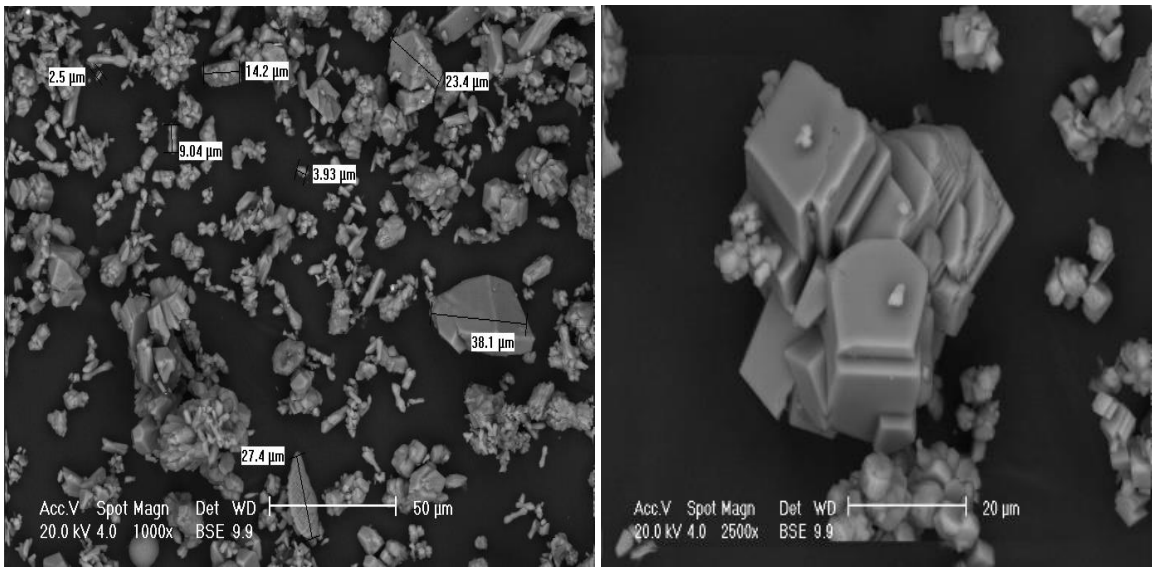

Figure 4- 4: SEM image of the precipitated calcite from running the experiment showing crystalline structure

4.2.2 Preliminary tests

In this section a series of tests were carried out on the laboratory system to determine the operational parameters involved in the experimentation i.e. CO_2 and air flow rates and contact time.

4.2.2.1 Tests of CO_2 flow rate

The aim behind using CO_2 is to dissolve calcite and generate a solution with high enough concentration of dissolved calcium ions (Ca^{2+}) to permit the required phosphate removal at the following stages. This will enable the precipitation to occur later in the process. For that reason, the first experiment was carried out to determine the Ca concentration resulted from using 3 different flow rates of CO_2 100, 500 and 750 ml/min for 40 min contact time. Experiments were carried out on batches 1, 2 and 3 on 1L of deionised water and 1Kg of limestone using CO_2 flow rates of 100 ml/min, 500 ml/min and 750 ml/min respectively. Table 4.2 shows the experimental conditions of each batch.

Table 4- 2: Experimental conditions for the carbonation stage of batches 1, 2 and 3 (1L of water and 1kg of limestone)

Batch Number	CO_2 Flow Rate (l/min)	Limestone Bed Depth (mm)	Chip Size (mm)	Type of Wastewater
1	0.1	70	2-5	DI
2	0.5	70	2-5	DI
3	0.75	70	2-5	DI

As it mentioned in the literature chapter that for the process to work effectively, a significant amount of calcium carbonate must be dissolved in the water. Initial investigations focused on production of solutions contains high concentration of calcium via the carbonation process. Experimentation was carried out for 5, 10, 15, 20, 25, 30 and 40 min for each CO_2 flow rate respectively, in order to determine the required CO_2 flow rate and time of carbonation stage. Samples were removed and filtered at the appropriate times and analysed with Inductively Coupled Plasma Optical Emission Spectrometry (ICP-OES) (Section 3.3.5 chapter 3). The variation of calcium concentration with time is presented in Figure 4.5. The elapsed time is plotted on the x-axis and the corresponding calcium concentration upon the y-axis.

It can be seen from Figure 4.5 Ca concentration is affected by CO_2 flow rate through the residence time that the water spends in contact with limestone, the Ca concentration in solution increased relative to the length of carbonation and the CO_2 flow rate. These results are in accordance with

equation (4.1) below which describes the reaction of $CaCO_3$ in water, in the presence of CO_2.

$$CaCO_{3(S)} + H_2O_{(l)} + CO_{2(g)} = Ca^{2+}_{(aq)} + 2HCO^{3-} \quad (4.1)$$

CO_2 and water form H_2CO3, which is in equilibrium with $HCO_3^-$and hydrogen ions H^+. A change in the concentration of the reactants on either side of the equation affects the subsequent direction of the reaction. The increase in CO_2 will result in increased carbonic acid formation which leads to an increase in both HCO_3^- and H^+. it can be seen that the Ca^{+2} concentration increases with increasing CO_2 .The final concentration after 40 minutes was 109.6 mg/l for the 0.1 l/min CO_2 flow rate, 203.7 mg/l for 0.5 l/min CO_2 flow rate and 341.6 mg/l for 0.75 l/min CO_2 flow rate respectively. The relevant key findings were that a higher flow rate of CO_2 reduce the time required for calcite to dissolve. Ca concentration by flow rate of 0.75 l/min for 40 min was close to the equilibrium concentration of calcium, which at 22°C, was suggested to be 400 mg/l (Stumm and Morgan 1996).

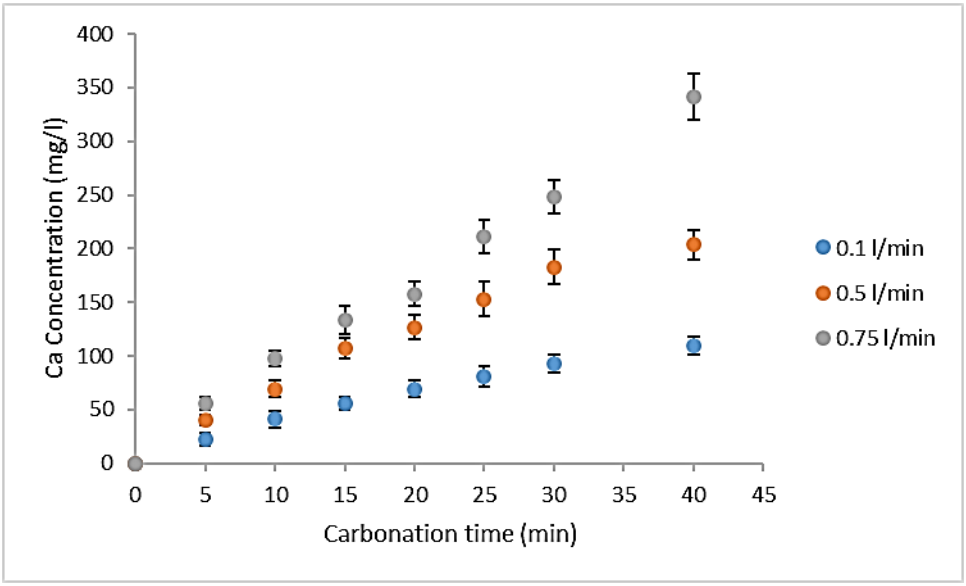

Figure 4- 5: Variation in calcium concentration for batch 1, 2 and 3 over different course of CO_2, each point represents a mean value of three replicates.

4.2.2.2 Experiment parameters

Under (section 3.2.3.2 chapter 3) a detailed description of the developed procedure is presented. Four sets of initial experiments were carried out sequentially to optimise the final operational conditions, 2 mg/l was used as an initial P concentration as the tertiary treatment needs to remove the last few mg/l of P. Seven batches of different carbonation intervals were examined. Table 4.3 shows the first set of the conditions. Selecting a lower CO_2 flow rate 0.1 l/min in the first set to minimise the CO_2 consumption as the most expensive part in the process.

Table 4- 3: First set of operational conditions

Carbonation Stage		Aeration Stage		Settlement Stage
CO_2 Flow Rate (l/min)	**Time (min)**	**Air Flow Rate (l/min)**	**Time (min)**	**Time (hr)**
0.1	5-40	0.5	10-60	1

It can be seen from Figure 4.6 (a) that the maximum Ca concentration of 102.8 mg/l was obtained by running the carbonation stage for 40 min. There was almost no decrease in Ca concentration during aeration stage for all the time intervals and P concentration fluctuated around the initial value as shown in Figure 4.6 (d, e) showing no reduction in P concentration during this stage. As shown in Figure 4.6 (g, h). The same trend was observed for Ca and P concentrations during settlement stage as shown in Figure 4.6 (e, f). Figure 4.6 (c, f and i) show the changes in pH over the experiment stages respectively. The pH value dropped to around 5.5 during carbonation stage as a result of carbonic acid formation as shown in Figure 4.6(c)then it increased to maximum of 6.5 due to the degassing of CO_2 for all aeration intervals during aeration stage as shown in Figure 4.6(f). During settlement stage there was no change in the pH as shown in Figure 4.6(i). These results showing that the applied conditions are not sufficient to remove P from solution. The Ca concentration from the carbonation stage was to low and the aeration stage showing that the 0.5 l/min air flow rate is not enough to encourage precipitation during aeration stage and 1 hr of settlement stage.

As the first set of experiment parameters did not show any P removal, another set of parameters was applied as shown in table 4.4 By changing the CO_2 flow rate to 0.5 l/min instead of 0.1 l/min for 5,10,15,20,25,30 and 40 min and the air flow rate to 1 l/min instead of 0.5 l/min, the Ca concentration increased to 204.8 mg/l for the 40 min during carbonation stage as shown in Figure 4.7 (a) and a slight decrease in Ca concentration was observed during aeration stage and this decrease was proportional with the initial Ca concentration at the beginning of this stage as shown in Figure 4.7 (d). P concentration in this stage fluctuated around the initial value showing no decrease in the aeration stage as shown in Figure 4.7 (e). Applying one hour of settlement did not reduce the concentration for both Ca and P concentrations as shown in Figure 4.7 (g, h). Figure 4.7 (c, f and i) show the changes in pH over the experiment stages respectively. The pH value dropped to around 5.5 during carbonation stage as shown in Figure 4.7(c) then it increased to 6.9 during aeration stage Figure 4.6(f). During settlement stage there was no change in the pH as shown in Figure 4.7(i).

Table 4- 4: Second set of operational conditions

Carbonation Stage		Aeration Stage		Precipitation Stage
CO_2 Flow Rate (l/min)	Time (min)	Air Flow Rate (l/min)	Time (min)	Time (hr)
0.5	5-40	1	10-60	1

As the second set of experiment parameters did not show any P removal, another set of parameters was applied as shown in table 4.5 By changing the CO_2 flow rate to 0.75 l/min instead of 0.5 l/min for 5,10,15,20,25,30 and 40 min, and keeping the air flow rate at 1 l/min to see if the increase in Ca concentration is sufficient to precipitate P and a 6 hours of settlement time was applied instead of 1hr. It can be seen from Figure 4.8 (a) that the Ca concentration increased to 328.6 mg/l for the 40 min carbonation. Applying the same air flow rate of 1 l/min a decrease in Ca concentration was observed and this decrease was proportional with the initial Ca concentration at the beginning of this stage as shown in Figure 4.8 (d). P concentration in this stage was fluctuated around the initial value showing no decrease in the aeration stage as shown in Figure 4.8 (e). By increasing the precipitation time to 6 hours no decrease in both concentrations was observed in this stage as shown in Figure 4.8 (g, h). Figure 4.8 (c, f and i) show the changes in pH over the experiment stages respectively. The pH value dropped to around 5.5 during carbonation stage as shown in Figure 4.8 (c) then it increased to 6.9 during aeration stage Figure 4.8 (f). During settlement stage there was no change in the pH Figure 4.8(i). These results showing that the applied conditions are not sufficient to remove P from solution. The decrease in Ca concentration caused by applying 1 l/min aeration and 6 hr of settlement time did not lead to precipitation of P from solution.

Table 4- 5: Third set of the operational conditions

Carbonation Stage		Aeration Stage		Settlement Stage
CO_2 Flow Rate (l/min)	Time (min)	Air Flow Rate (l/min)	Time (min)	Time (hr)
0.75	5-40	1	10-60	6

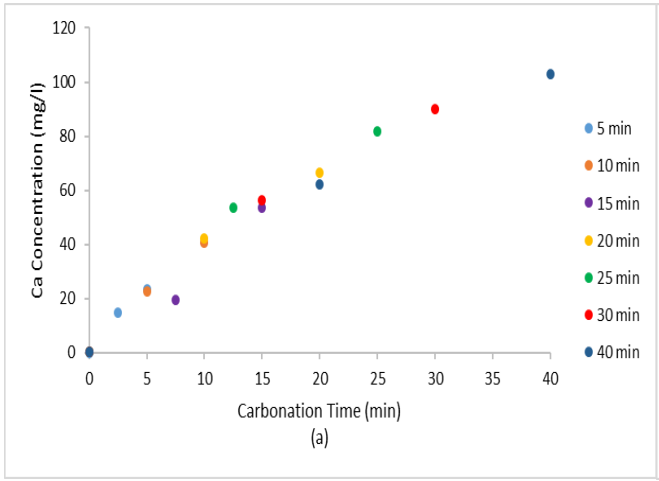
Ca Concentration (mg/l)
Carbonation Time (min)
(a)
5 min
10 min
15 min
20 min
25 min
30 min
40 min

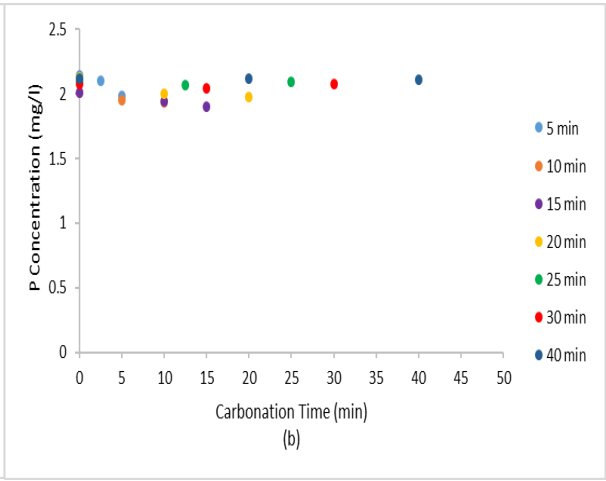
P Concentration (mg/l)
Carbonation Time (min)
(b)
5 min
10 min
15 min
20 min
25 min
30 min
40 min

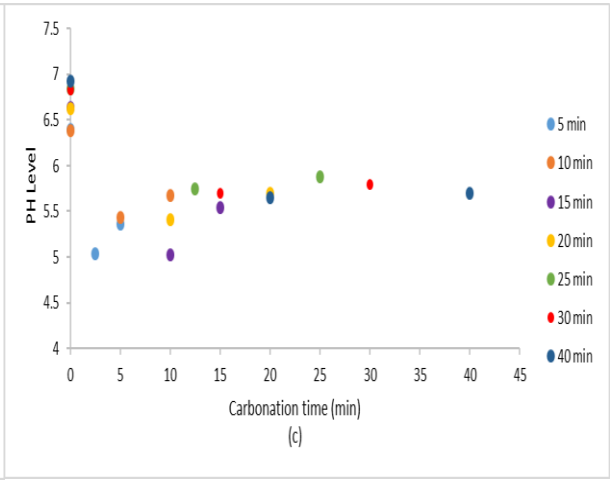
PH Level
Carbonation time (min)
(c)
5 min
10 min
15 min
20 min
25 min
30 min
40 min

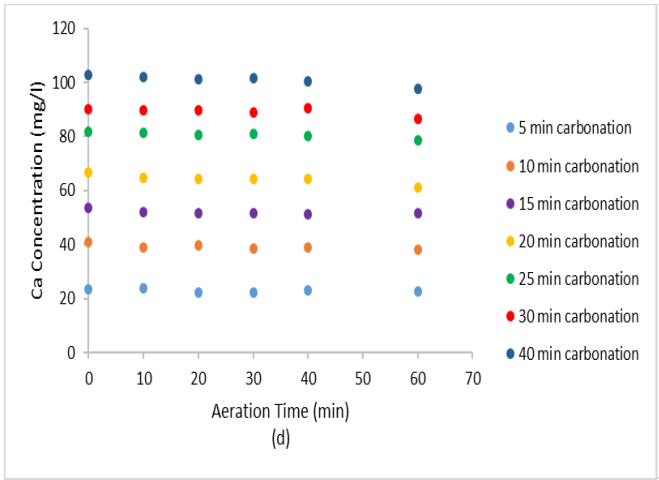
Ca Concentration (mg/l)
Aeration Time (min)
(d)
5 min carbonation
10 min carbonation
15 min carbonation
20 min carbonation
25 min carbonation
30 min carbonation
40 min carbonation

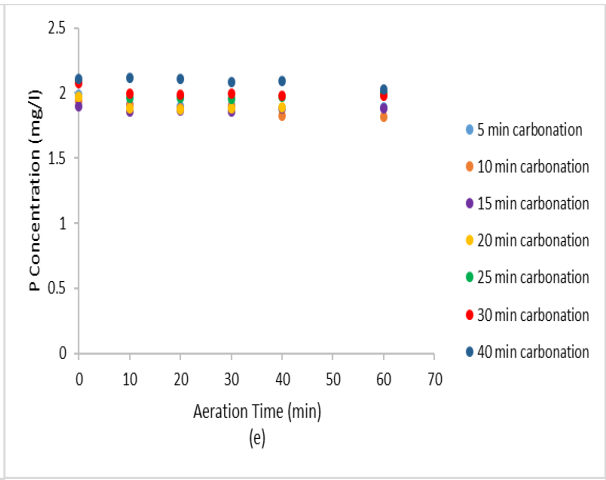
P Concentration (mg/l)
Aeration Time (min)
(e)
5 min carbonation
10 min carbonation
15 min carbonation
20 min carbonation
25 min carbonation
30 min carbonation
40 min carbonation

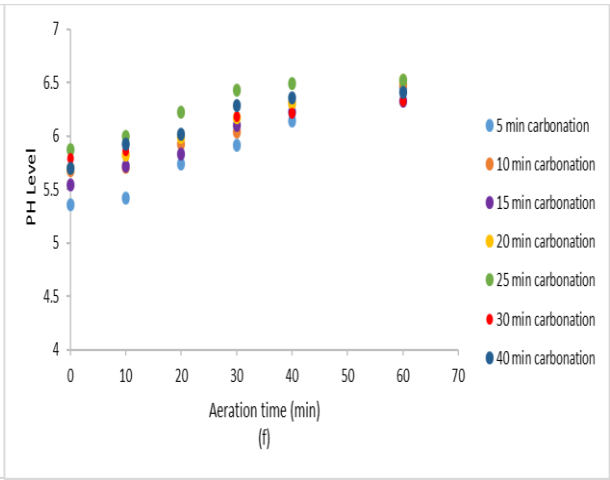
PH Level
Aeration time (min)
(f)
5 min carbonation
10 min carbonation
15 min carbonation
20 min carbonation
25 min carbonation
30 min carbonation
40 min carbonation

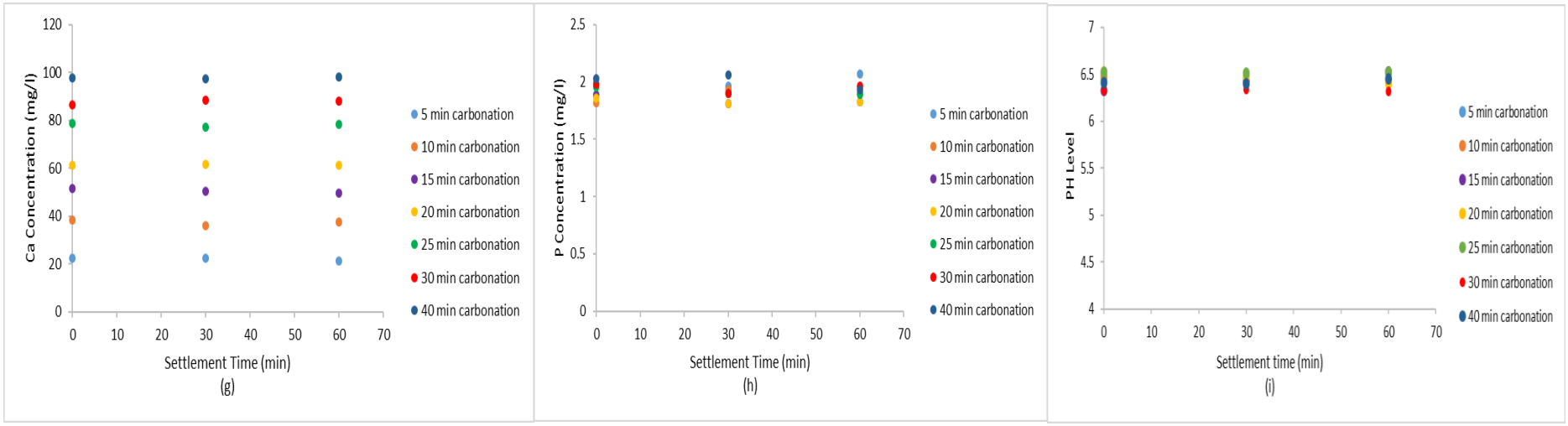

Figure 4- 6: (a-i) Ca, P and pH during the experiment stages. Legends in carbonation stage figures (a,b,c) represent the carbonation time. Legends in figures (d,e,f,g,h and i) represent the Ca, P and pH during aeartion and settlement stages of batches subjected to the 5,10,15,20,25,30 and 40 min carbonation. All data presented in these figures are under the operatinal conditions included in table 4.3

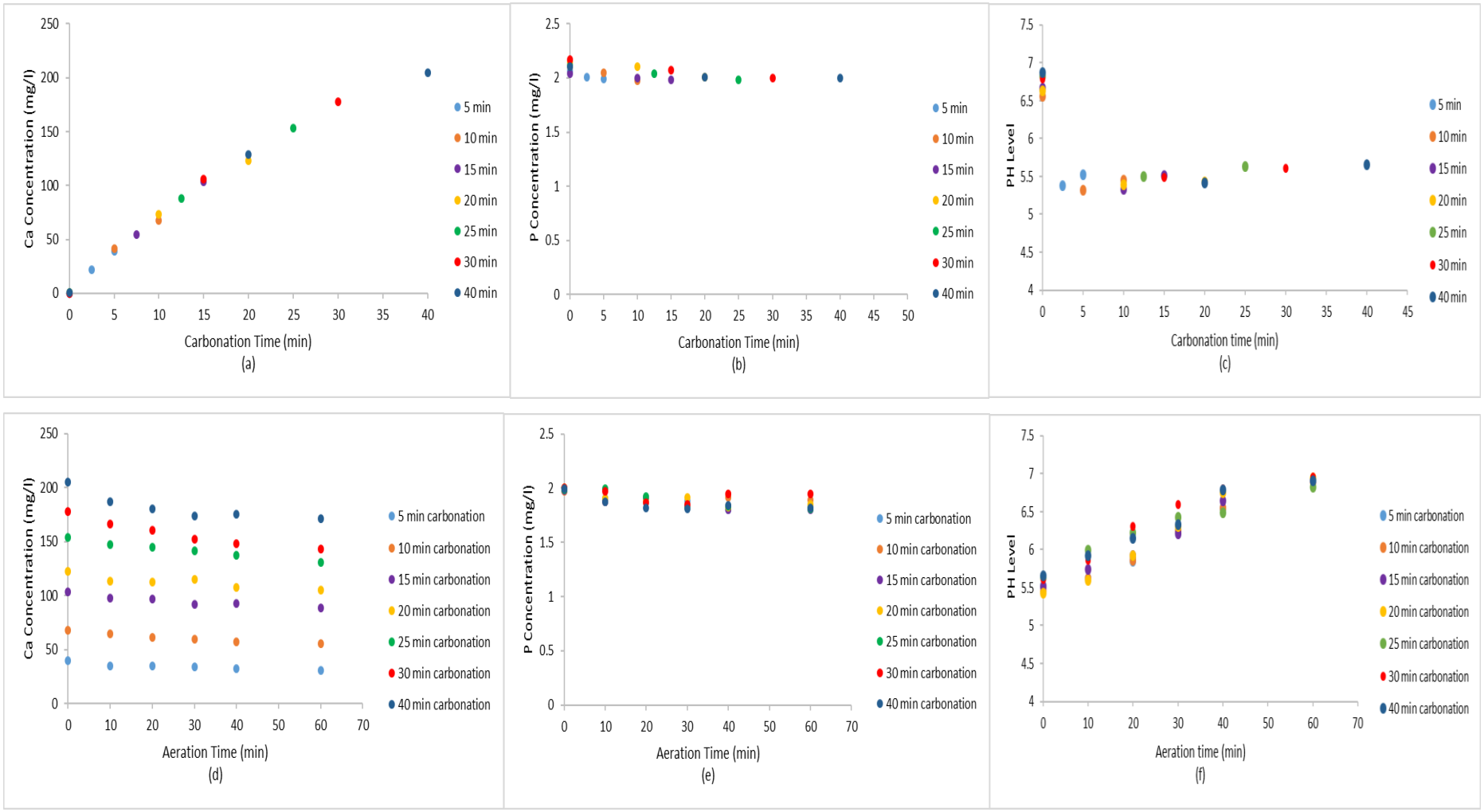
Ca Concentration (mg/l)
Carbonation Time (min)
(a)
5 min
10 min
15 min
20 min
25 min
30 min
40 min
P Concentration (mg/l)
Carbonation Time (min)
(b)
PH Level
Carbonation time (min)
(c)
Ca Concentration (mg/l)
Aeration Time (min)
(d)
5 min carbonation
10 min carbonation
15 min carbonation
20 min carbonation
25 min carbonation
30 min carbonation
40 min carbonation
P Concentration (mg/l)
Aeration Time (min)
(e)
PH Level
Aeration time (min)
(f)

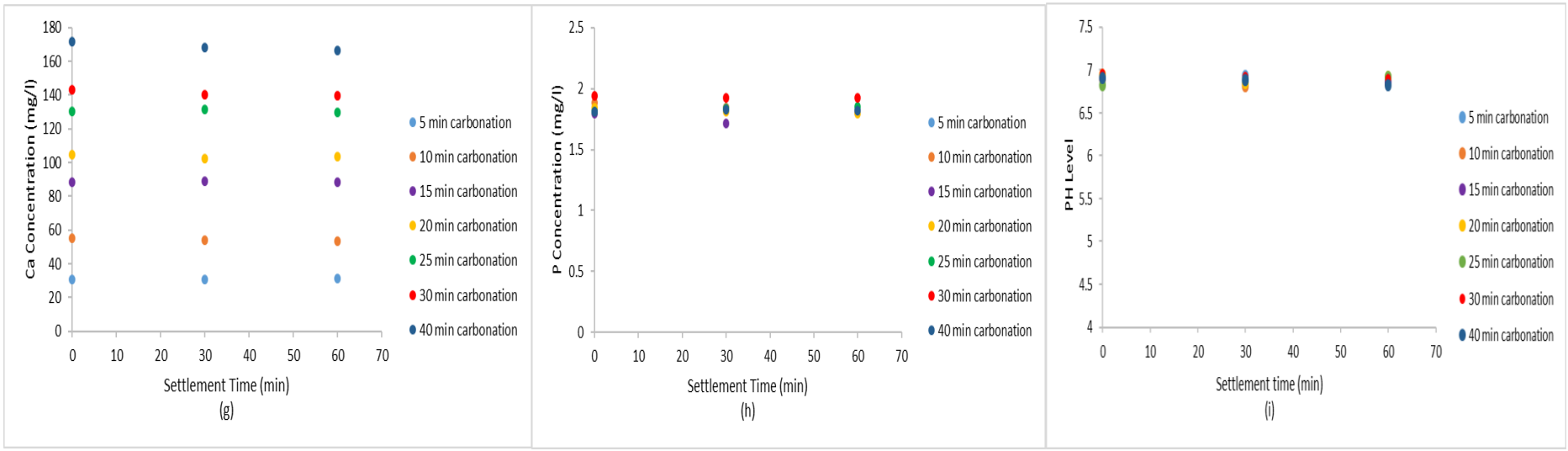

Figure 4- 7: (a-i) Ca, P and pH during the experiment stages. Legends in carbonation stage figures (a,b,c) represent the carbonation time. Legends in figures (d,e,f,g,h and i) represent the Ca, P and pH during aeartion and settlement stages of batches subjected to the 5,10,15,20,25,30 and 40 min carbonation. All date presented in these figures are under the operatinal conditions included in table 4.4

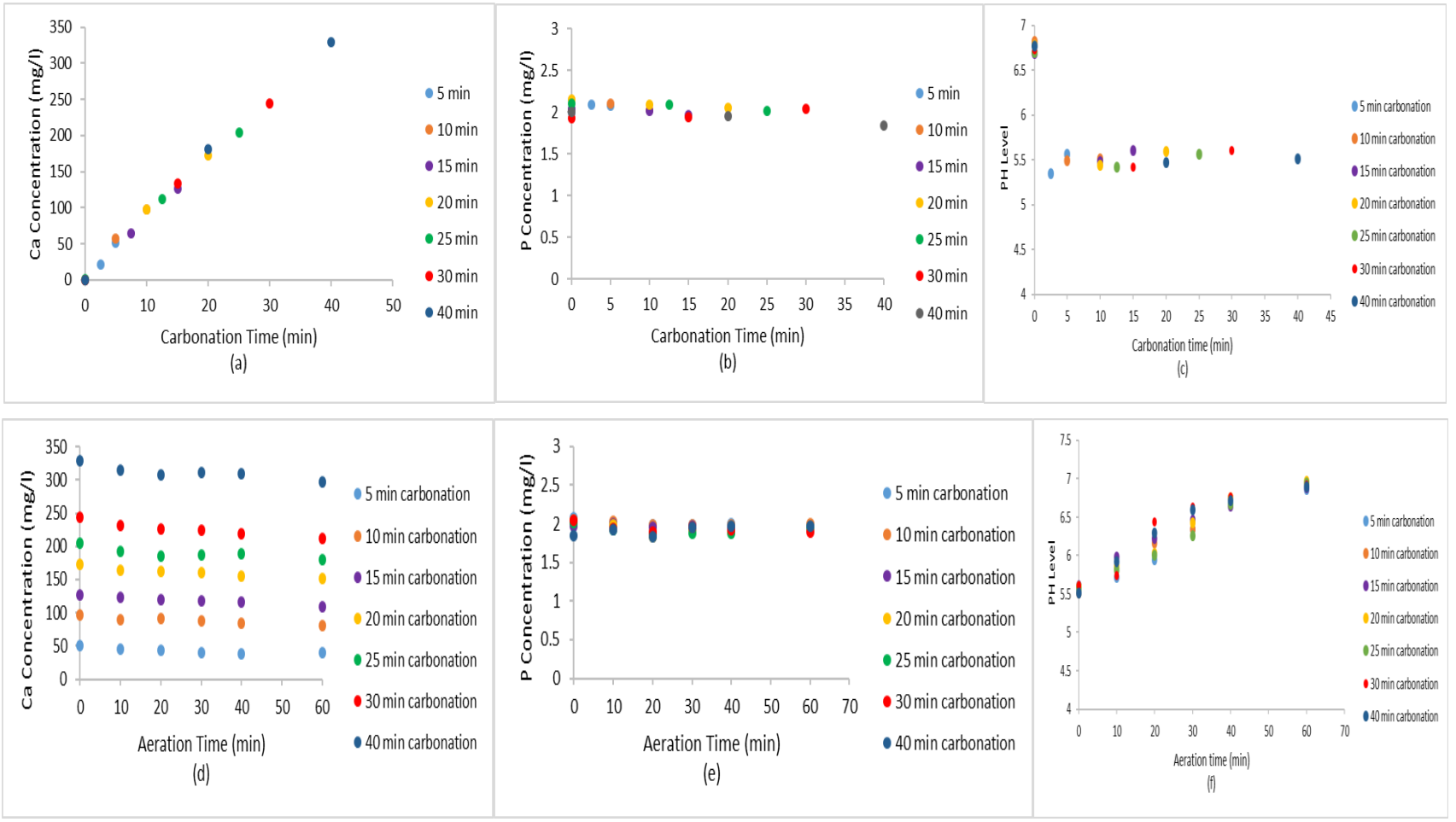
Ca Concentration (mg/l)
Carbonation Time (min)
(a)
5 min
10 min
15 min
20 min
25 min
30 min
40 min
P Concentration (mg/l)
Carbonation Time (min)
(b)
PH Level
Carbonation time (min)
(c)
5 min carbonation
10 min carbonation
15 min carbonation
20 min carbonation
25 min carbonation
30 min carbonation
40 min carbonation
Ca Concentration (mg/l)
Aeration Time (min)
(d)
P Concentration (mg/l)
Aeration Time (min)
(e)
PH Level
Aeration time (min)
(f)

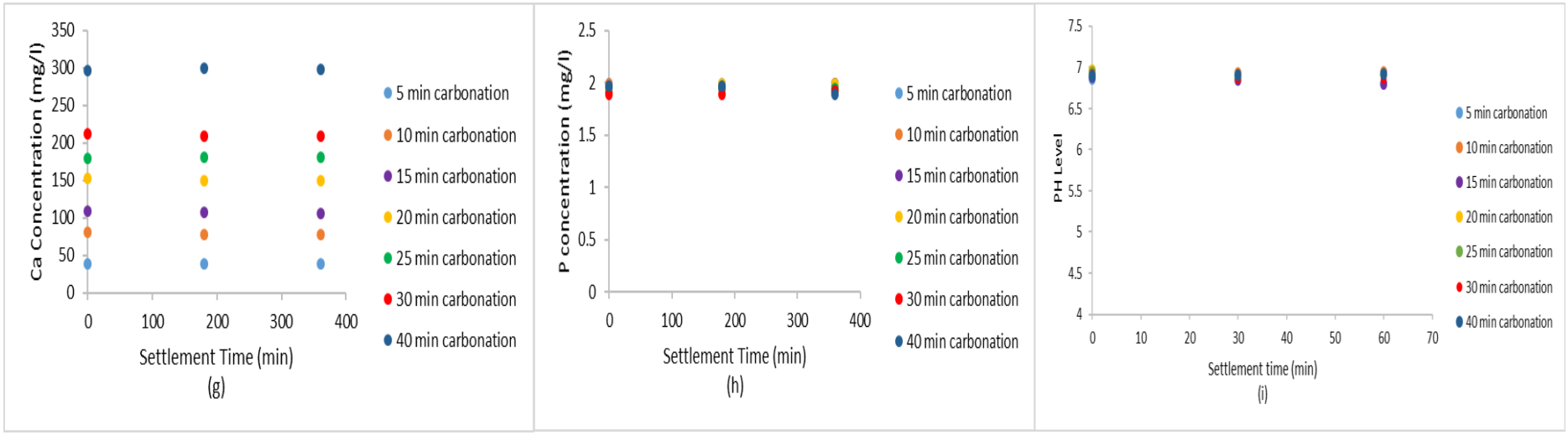

Figure 4- 8: (a-i) Ca, P and pH during the experiment stages. Legends in carbonation stage figures (a,b,c) represent the carbonation time. Legends in figures (d,e,f,g,h and i) represent the Ca, P and pH during aeartion and settlement stages of batches subjected to the 5,10,15,20,25,30 and 40 min carbonation. All date presented in these figures are under the operatinal conditions included in table 4.5

As the third set of experiment parameters did not show any P removal, another set of parameters was applied as shown in Table 4.6. By fixing the CO_2 flow rate to 0.75 l/min for 40 min in the carbonation stage, the Ca concentration was 331.2 mg/l. By increasing the air flow rate to 2 l/min instead of 1 l/min the Ca concentration in the aeration stage dropped from 331.2 to 238.2 mg/l. P concentration in this stage dropped from 2.26 mg/l to 0.58 mg/l as shown in Figure 4.9 (a). Figure 4.9 (b) show the changes in pH over the experimentation time, it can be seen that when pH increased to 7.7 the drop in Ca and P concentration occurred. There was no decrease in Ca concentration and a slight increase in P concentration was observed during settlement stage as shown in Figure 4.9 (a).

Table 4- 6: Fourth set of the experiment parameters

Carbonation Stage		**Aeration Stage**		**Settlement Stage**
CO_2 Flow Rate (l/min)	**Time (min)**	**Air Flow Rate (l/min)**	**Time (min)**	**Time (hr)**
0.75	40	2	60	6

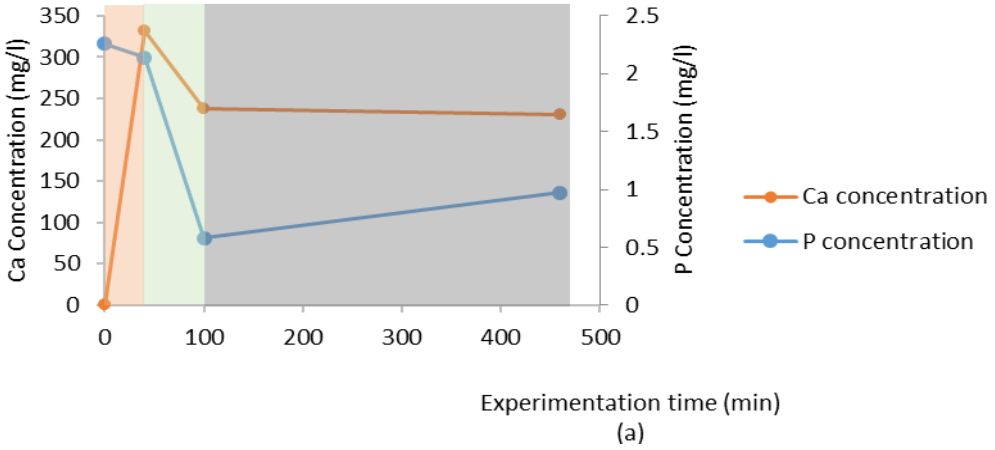

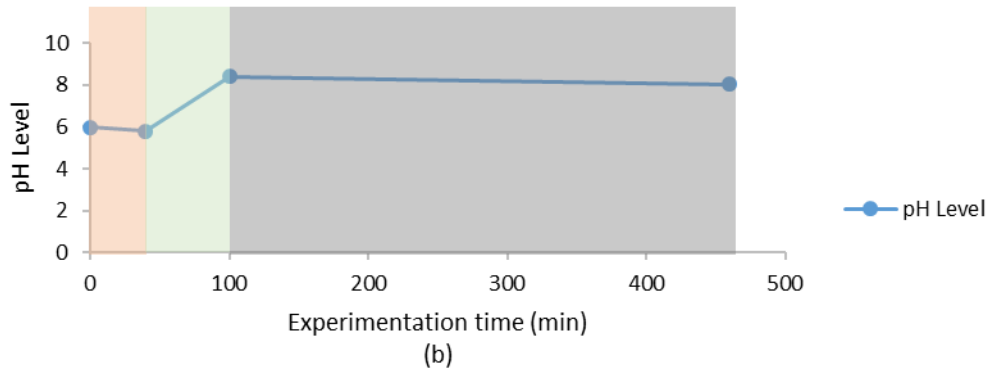

Figure 4- 9: (a,b) Ca, P and pH during the experiment stages. Carbonation stage represented by the pink zone, aeration stage representd by the blue zone and precipitation stgae represnted by the purpule zone.

The stoichiometry of the Ca and P reaction is presented in equation (4.2) the active precipitating agent is calcium ion, which combines with orthophosphate ions to form calcium phosphate.

$$3Ca^{2+} + 2PO_4^{3-} = Ca_3(PO_4)_2 \quad (4.2)$$

In reality, precipitation of phosphorus with calcium is a more complex process, involving coprecipitation with calcium carbonate. This makes stoichiometric (based on chemistry of the reaction) calculations approximate. Equation 4.2 indicates that it will take 3 moles of calcium ion to react with 2 moles of phosphate, to form 1 mole of calcium phosphate and thus a 3:2 mole ratio of Ca:P is required for this reaction. Because the molecular weight of calcium is 40 and the molecular weight of phosphorus is 31, the weight ratio of Ca:P in Equation 4.2 is 1.94:1, as shown in the following calculation:

(120 g Ca/1 mol Ca) / (62 g P /1 mol P) = 1.94/1 or 1.94:1

This indicates that precipitation occurs when the Ca concentration is equal to/ greater than the stoichiometric amount. From the previous initial experimentation, it can be concluded that 0.75 l/min of CO_2 is required to bring enough Ca ions into solution in 40 min. pH is very important and limiting parameter when it reached to 7.7 the precipitate occurred, and P removed and that happened when 2 l/min air applied during aeration stage. The behaviour of Ca and P ions during settlement stage were not clear and for that reason a longer settlement time was applied for the following experimentation sets.

4.3 Laboratory system and Experimental plan

The experimental parameters adopted in this section were based on the outcome of the preliminary tests included in section 4.2.2.2. and presented in table 4.7. In order to ensure the process is working for wide range of P concentration, solutions of 2, 10, 20 and 100 mg/l were prepared using deionised water and tap water (which is reflective of what goes down the sink/ toilet) to show the effect of other ions presented in tap water in inhibiting or encouraging the P removal. Real wastewater samples were also running through the process. Applying 2 l/min of air for 60 min in the aeration time was critical so in this section 7-time intervals 10,15,20,25,30,40 and 60min of aeration stage were examined. As it mentioned at the end of the previous section that Ca and P concentration during settlement time needed more study, the settlement stage in this section was extended to 48 hr. The levels of Ca, P and pH within the collected samples were measured. The laboratory plan for the experimental work been carried out in this section is summarised in Figure 4.10.

Table 4- 7: Final set of the operational conditions for 1L of P solution

Carbonation Stage		**Aeration Stage**		**Settlement Stage**
CO_2 Flow Rate (l/min)	**Time (min)**	**Air Flow Rate (l/min)**	**Time (min)**	**Time (hr)**
0.75	40	2	10-60	48

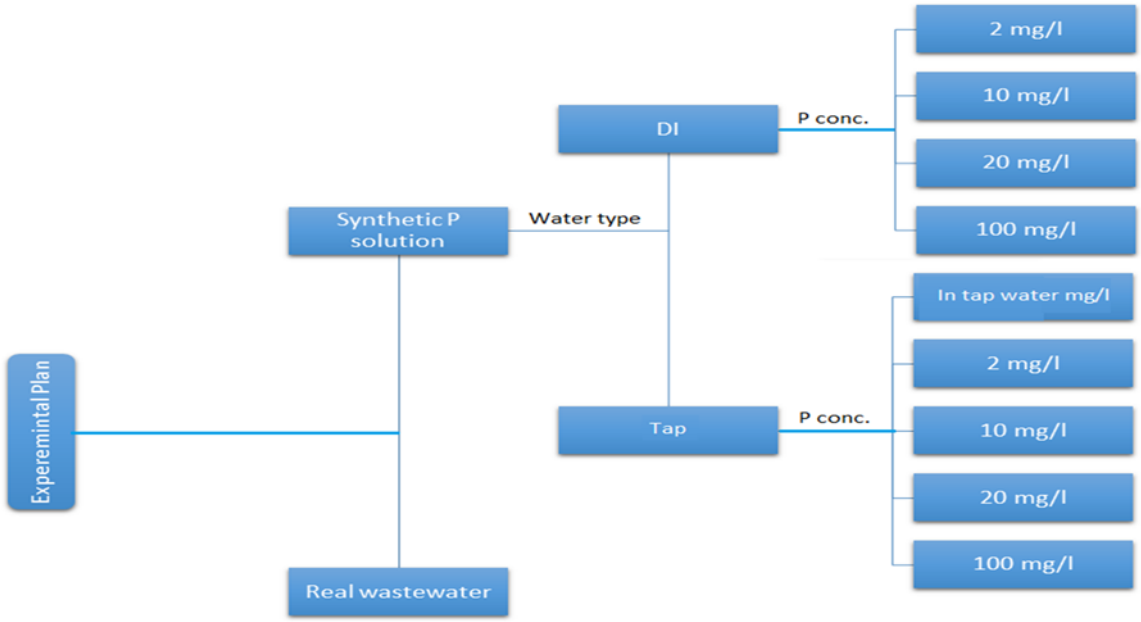

Figure 4- 10 Experimental lab plan showing water type and P concentration used.

4.3.1 Results of tests performed on P solutions using deionised water

In order to present the kinetics of removal, batch experiments were carried out on the prepared solutions. Seven aeration intervals 10, 15, 20, 25, 30, 40 and 60 min were examined during the aeration stage. Samples from each batch were collected to determine the concentration of phosphate and calcium in each batch. All batches were subjected to 0.75 l/min CO_2 for 40 minutes, 2 l/min air for 10,15,20,25,30,40 and 60 min and 48 hours settlement. The only experimental variance between these seven tests for each P concentration was the period that each batch was aerated for. In each figure, each vertical row of data points represents one experiment (in triplicate), the blue points represent the initial concentrations, the red points represent the concentration after carbonation, the coloured points represent the concentration after aeration, the green and purple points represent the concentration after 24 and 48 hr respectively.

4.3.1.1 Initial P concentration of 2 mg/l

Figure 4.11 (a) shows the changes in Ca concentration during the three stages of the process. The initial Ca concentration ranged between 0.94 and 5.3 mg/l for the seven runs. It can be seen that after 40 minute of carbonation, Ca concentration increased to between 336.2 and 345.6 mg/l, this range of Ca concentration is in agreement with the result in Figure 4.9 where the Ca concentration increased to 331.2 mg/l after 40 min carbonation. Figure 4.11 (b) shows the changes in Ca concentration during the three stages of the process. At the end of aeration stage, Ca concentration decreased to 310.8 mg/l for 10 min aeration and 238.9 mg/l for 60 min aeration, this range indicating that by increasing the aeration time the Ca decreased and the final concentration after 60 min aeration 238.9 mg/l is close to that in Figure 4.9 where the Ca concentration decreased to 238.2 mg/l after 60 min aeration. Further reduction in Ca concentration occurred in the first 24 hr of settlement, this decrease continued for the second 24 hr. The lowest Ca concentration of 186.6 mg/l at the end of the process was by a 15min aeration and 48 hr settlement.

From Figure 4.11 (b) it can be seen that during carbonation stage there was a small decrease in P concentration. At the end of aeration stage P concentration decreased to 1.5 mg/l for 10 minutes aeration followed by further decrease during the first 24 hour of precipitation to 0.837 mg/l and P concentration achieved after 48 hour was 0.763 mg/l while for the 15, 20, 25, 30, 40 and 60 min aeration the main decrease in concentration was during aeration stage followed by small drop in the precipitation stage. P concentration after 60 min aeration was 0.49 mg/l which is in agreement with the results from Figure 4.9 where the P concentration decreased to 0.58 mg/l

after 60 min aeration for the same initial P concentration. The 0.32 mg/l was the lowest P concentration for 60 min aeration and 48 hr precipitation.

Figure 4.11 (c) shows the variation of initial pH with final pH, the initial pH ranged between 6.4 and 6.5, the first change in pH occurred during carbonation stage, the pH dropped to approximately 5.5 for all batches and this was due to the formation of carbonic acid. During the aeration stage the pH increased due to CO_2 degassing. The pH values increased with increasing the aeration time, the pH readings ranged between 7.7 for 10 min aeration and 8.736 for 60 min. There was a decrease in pH during the first 24 hour of settlement followed by slight increase during the second 24 hours settlement for all batches.

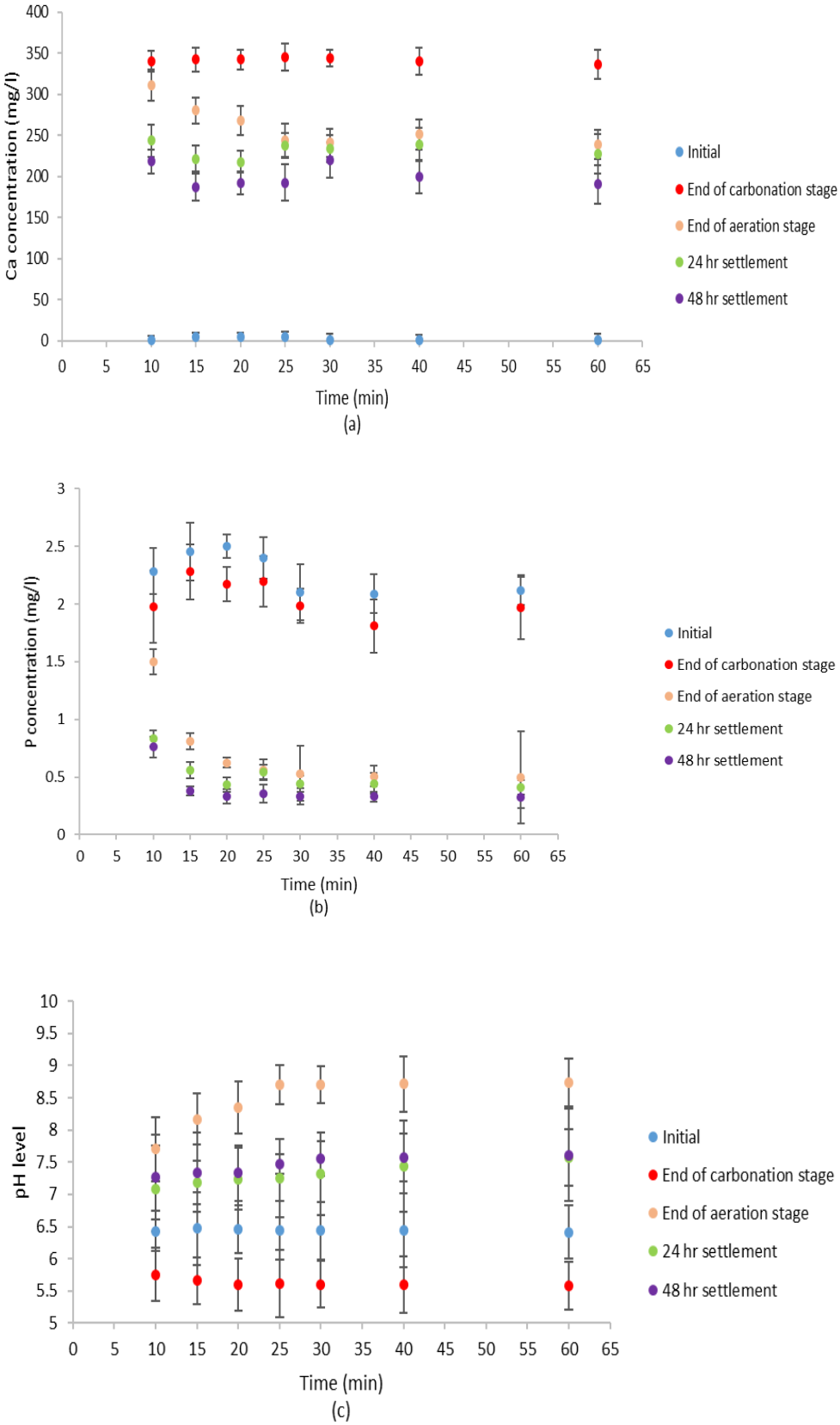

Figure 4- 11 Variation of (a) Ca concentration, (b) P concentration and (c) pH level during carbonation, aeration and settlement stages. Experiment conditions: Carbonation with 0.75 l/min for 40 min, Aeration with 2 l/min for either 10,15,20,25,30,40 and 60 min, settlement for 48 hr. Each vertical row of data points represents one experiment (in triplicate). The x-axis represents aeration time. Deionised water solutions. Initial P Concentration of 2mg/l.

4.3.1.2 Initial P concentration of 10 mg/l

From Figure 4.12(a), it can be seen that the Ca concentrations after 40 min carbonation ranged between 319.7 and 329.3 mg/l at the end of carbonation stage. At the end of aeration stage, the Ca concentration decreased to between 274.3 mg/l for 10 min aeration and 228.2 mg/l for 60 min aeration. The main decrease in Ca concentration was found to occur during this stage for all batches. Further reduction in Ca concentrations occurred during the 48hr settlement. The lowest Ca concentration of 198.2 mg/l was by 25min aeration and 48 hr settlement.

From Figure 4.12(b) it can be seen that the main decrease in P concentration occurred during the aeration stage for all batches except the 40 and 60 min aeration. The P concentration decreased to between 2.26 mg/l for 10 min aeration and 1.62 mg/l for 25 min. The lowest P concentration of 1.18 mg/l was 40 min aeration and 48 hr settlement.

From figure 4.12(c) it can be seen that the pH values at the end of aeration time ranged between 7.8 for 30 min aeration and 8.2 for 40 min aeration. The pH readings after the 24 and 48 hr were close.

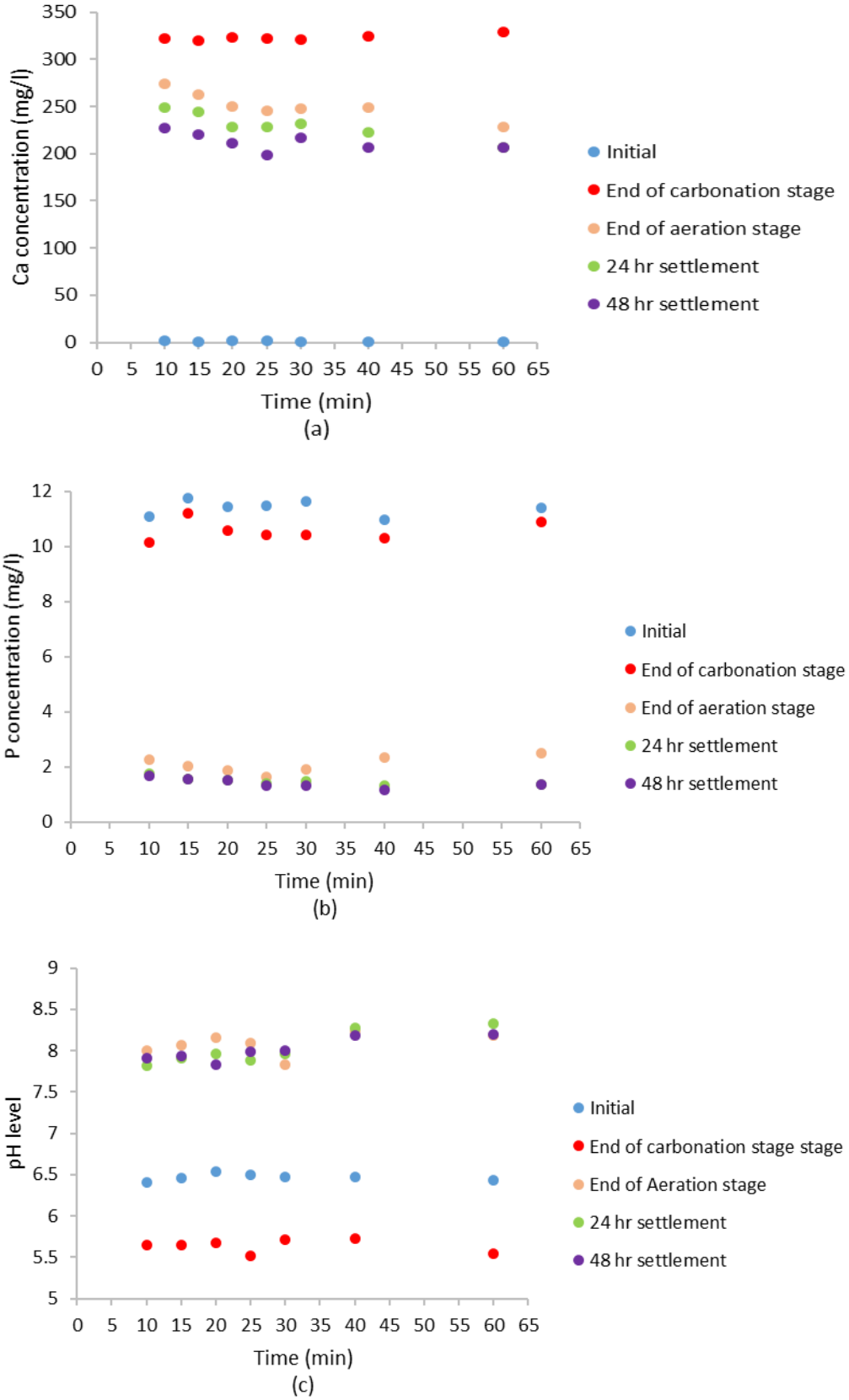

Figure 4- 12: Variation of (a) Ca concentration, (b) P concentration and (c) pH level during carbonation, aeration and settlement stages. Experiment conditions: Carbonation with 0.75 l/min for 40 min, Aeration with 2 l/min for either 10,15,20,25,30,40 and 60 min, settlement for 48 hr. Each vertical row of data points represents one experiment (in triplicate). The x-axis represents aeration time. Deionised water solutions. Initial P Concentration of 10mg/l.

4.3.1.3 Initial P Concentration of 20 mg/l

From Figure 4.13 (a), it can be seen that the Ca concentrations after 40 min carbonation ranged between 310.7 and 322.3 mg/l at the end of carbonation stage. The main decrease in Ca concentration occurred during the aeration stage, Ca concentration decreased with the increase in the aeration time, to between 254.5 mg/l for 10 min aeration and 200 mg/l for 60 min aeration. Further reduction in Ca concentrations occurred during the 48 hr of settlement for all batches. The lowest Ca concentration of 166.3 mg/l by 60 min aeration and 48 hr settlement.

From Figure 4.13 (b) it can be seen that the main decrease in P concentration occurred during the aeration stage for all batches, this decrease ranged between 3.71 mg/l for 10 min aeration and 1.16 mg/l for 30 min aeration. Further decrease in P concentration occurred during the first 24 hr of settlement followed by additional decrease in the second 24 hr of settlement for all batches except the batch of 20 min aeration there was no further decrease in P concentration. The lowest P concentration of 0.81mg/l by 30 min aeration and 48 hr settlement.

From figure 4.13 (c) it can be seen that the pH values ranged between 8.4 for 10 min aeration and 8.7 for 30 min aeration. The pH readings after the 24 and 48 hr were close.

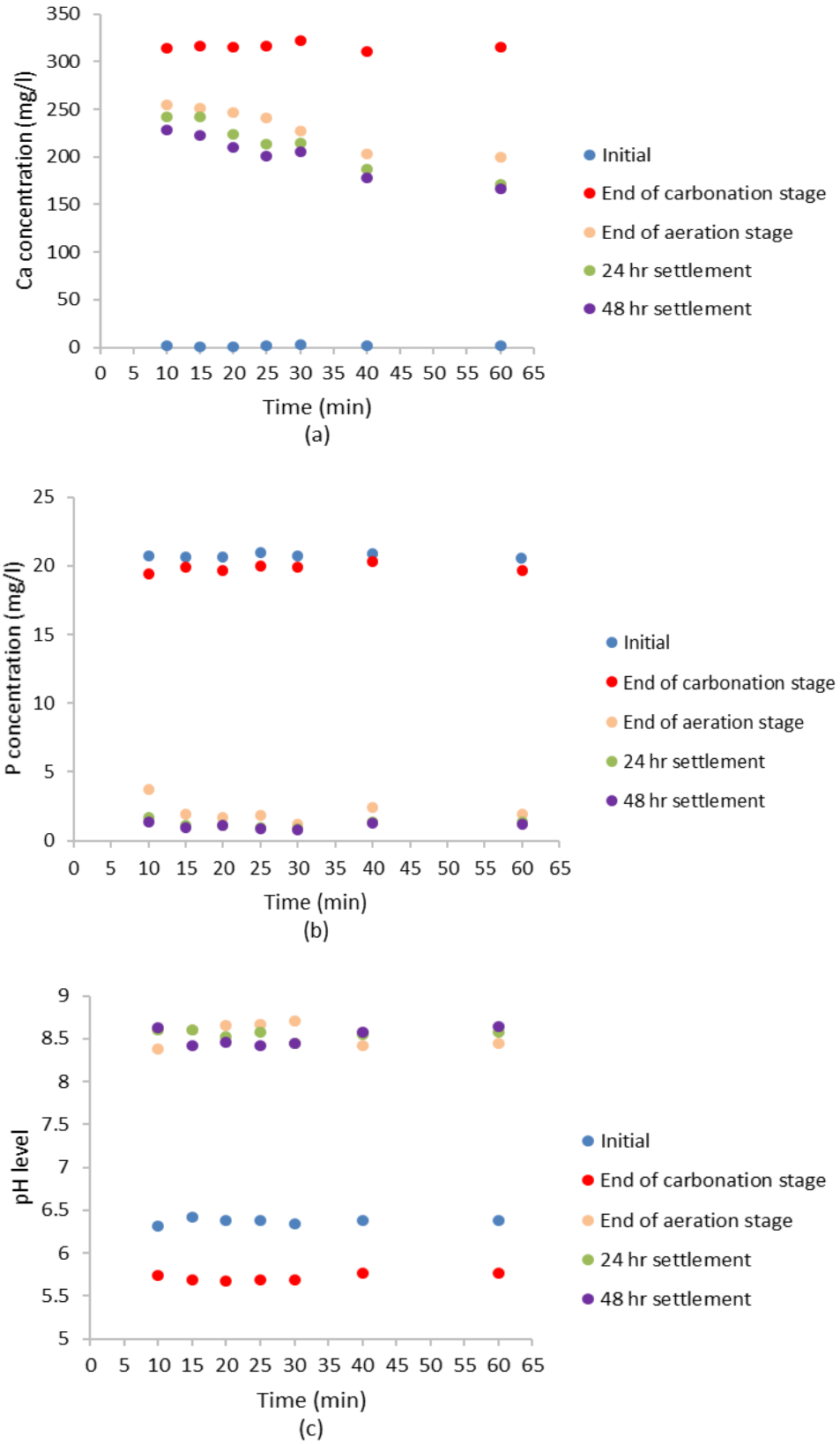

Figure 4- 13: Variation of (a) Ca concentration, (b) P concentration and (c) pH level during carbonation, aeration and settlement stages. Experiment conditions: Carbonation with 0.75 l/min for 40 min, Aeration with 2 l/min for either 10,15,20,25,30,40 and 60 min, settlement for 48 hr. Each vertical row of data points represents one experiment (in triplicate). The x-axis represents aeration time. Deionised water solutions. Initial P Concentration of 20mg/l.

4.3.1.4 Initial P concentration of 100 mg/l

From Figure 4.14 (a), it can be seen that the Ca concentrations after 40 min carbonation ranged between 264.5 and 280.3 mg/l at the end of carbonation stage, the main decrease in Ca concentration occurred during the aeration stage where Ca concentration decreased to between 132.0 for 10 min aeration and 89.2 mg/l for 40 min aeration. Further reduction in Ca concentrations occurred during the first 24 hr of settlement and continued during the second 24 hr for all batches. The lowest Ca concentration of 69.2 mg/l by 25 min aeration and 48 hr settlement

From Figure 4.14 (b) it can be seen that the main decrease in P concentration occurred during the aeration stage for all batches, P concentration decreased to between 37.1 mg/l for 10 min aeration and 12.3 mg/l for 40 min aeration. Further decrease in P concentration occurred during the first 24 hr of settlement followed by additional decrease in the second 24 hr of settlement for all batches except the batches of 25 and 30 min aeration when there was no change in P concentration. The lowest P concentration of 5.2 mg/l by 60 min aeration and 48 hr settlement.

From figure 4.14 (c) it can be seen that the pH values during aeration stage ranged between 7.5 for 20 min aeration and 8.1 for 60 min aeration pH readings after the 24 and 48 hr were close.

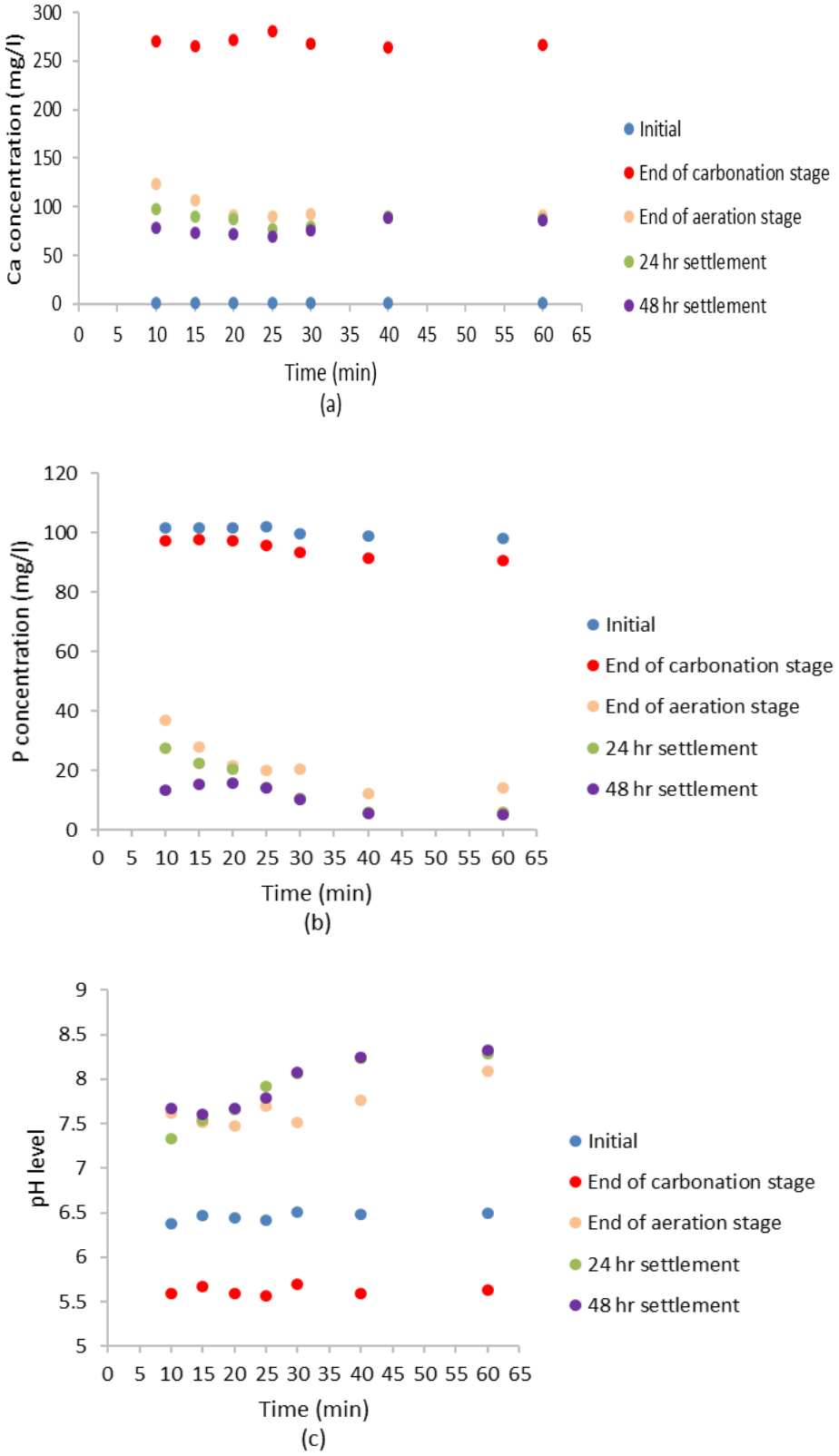

Figure 4- 14 Variation of (a) Ca concentration, (b) P concentration and (c) pH level during carbonation, aeration and settlement stages. Experiment conditions: Carbonation with 0.75 l/min for 40 min, Aeration with 2 l/min for either 10,15,20,25,30,40 and 60 min, settlement for 48 hr. Each vertical row of data points represents one experiment (in triplicate). The x-axis represents aeration time. Deionised water solutions. Initial P Concentration of 100mg/l.

4.3.2 Results of tests performed on P solutions using tap water

To examine the effect of other ions on removal of P sets of experiments were carried out on P solution using tap water and 2, 10, 20 and 100 mg/l of stock solution of 1000 mg/l concentration. The levels of phosphate and calcium within the collected samples were measured. All batches were subjected to 0.75 l/min CO_2 for 40 minutes, 2 l/min air and 48 hours of precipitation, the only experimental variance between these seven tests for each P concentration was the period that each batch was aerated for. The chemistry of tap water for a single batch presented in table 4.8.

Table 4- 8: Anions and cations concentration in Cardiff tap water

Anions/ Cations	**Ca**	**P**	**Mg**	**Na**	**K**	**Cl**	**SO_4**	**F**
Concentration mg/l	34.74	1.0	4.47	15.86	1.52	15.58	24.69	0.44

4.3.2.1 Concentration of P presented in Tap water

The results presented in this section are obtained from running the laboratory system with solution of tap water without any add P. From Figure 4.15 (a), it can be seen that the Ca concentrations after 40 min carbonation ranged between 300.1 and 317.5 mg/l at the end of carbonation stage. During the aeration stage the Ca concentration decreased with the increase in the aeration time, Ca concentration ranged between 307.0 mg/l for the 10 min aeration and 190.8 mg/l for 60 min aeration. Further reduction in Ca concentrations occurred during the 48 hr of settlement. The lowest Ca concentration of 175.6 mg/l by 60 min aeration and 48 hr settlement. From Figure 4.15 (b) it can be seen that P concentration decreased for all batches during aeration stage. P concentration ranged between 1.17 mg/l for 10 min aeration and 0.62 mg/l for 60 min aeration. The 0.472 mg/l was the lowest P concentration by 25 min aeration and 48 hr settlement. From Figure 4.15 (c) shows the variation of initial pH with final pH, the initial pH ranged between 7.02 and 7.11. During the aeration stage the pH of the batches of 10, 15, 20 and 25 increased more than those of 30, 40 and 60 min aeration. The pH values for batches of 10, 15, 20 and 25 decreased during the 48 hr of settlement and the lowest pH reading was 7.2 for the batch of 25 min aeration while pH of batches of 30, 40 and 60 min aeration increased after the 48 hour of settlement.

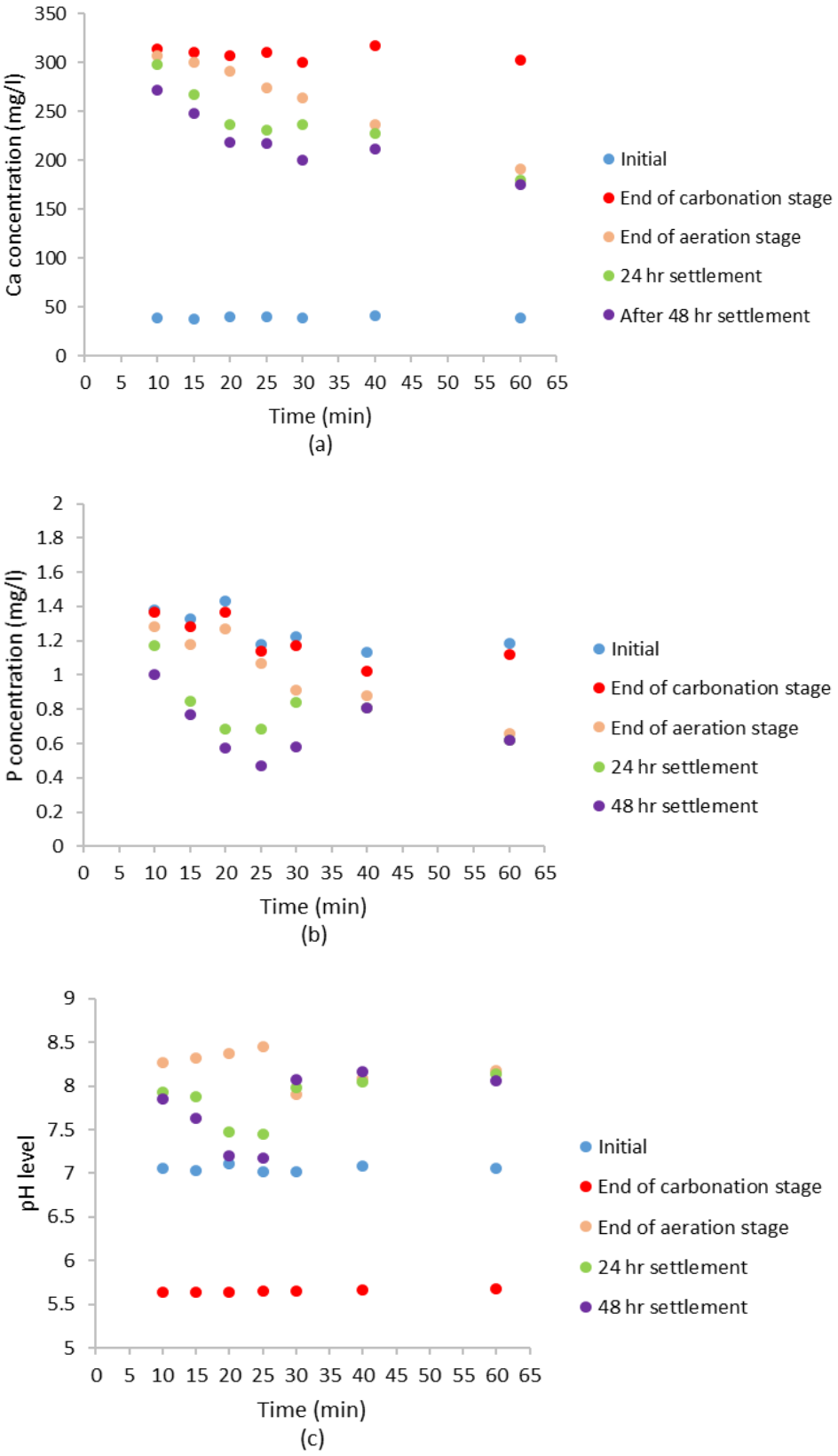

Figure 4- 15: Variation of (a) Ca concentration, (b) P concentration and (c) pH level during carbonation, aeration and settlement stages. Experiment conditions: Carbonation with 0.75 l/min for 40 min, Aeration with 2 l/min for either 10,15,20,25,30,40 and 60 min, settlement for 48 hr. Each vertical row of data points represents one experiment (in triplicate). The x-axis represents aeration time. Tap water solutions. Tap water P concentration

4.3.2.2 Initial P concentration of 2 mg/l + P in tap water

From Figure 4.16 (a), it can be seen that the Ca concentrations after 40 min carbonation ranged between 293.8 and 307.7 mg/l at the end of carbonation stage. The Ca concentration decreased with the increase in the aeration time, Ca concentration ranged between 272.4 mg/l for 10 min aeration and 228.4 mg/l for the 60 min aeration. Further reduction in Ca concentrations occurred during the 48 hr of settlement. The lowest Ca concentration of 110.5 mg/l by 25 min aeration and 48 hr settlement.

From Figure 4.16 (b) it can be seen that the main decrease in P concentration occurred during the aeration stage, the decrease in P concentration increased by increasing the aeration time this can be seen through batches of 10, 15, 20, 25 and 30 then P concentration started to increase after 40 min aeration and 60 min aeration. All batches showed further decrease in concentration after 24 hr, this decrease in concentration continued for the second 24 hr of settlement except for the 25 min aeration batch which showed a slight increase to 1.07mg/l. The 0.7 mg/l was the lowest P concentration by 20 min aeration and 48 hr settlement.

From Figure 4.16 (c) shows the variation of initial pH with final pH. During aeration stage the highest pH value of 8.49 by the 30 min aeration. During the settlement stage pH values were close except the pH of 40 min aeration batch there was an increase in the pH during the second 24 hr of settlement.

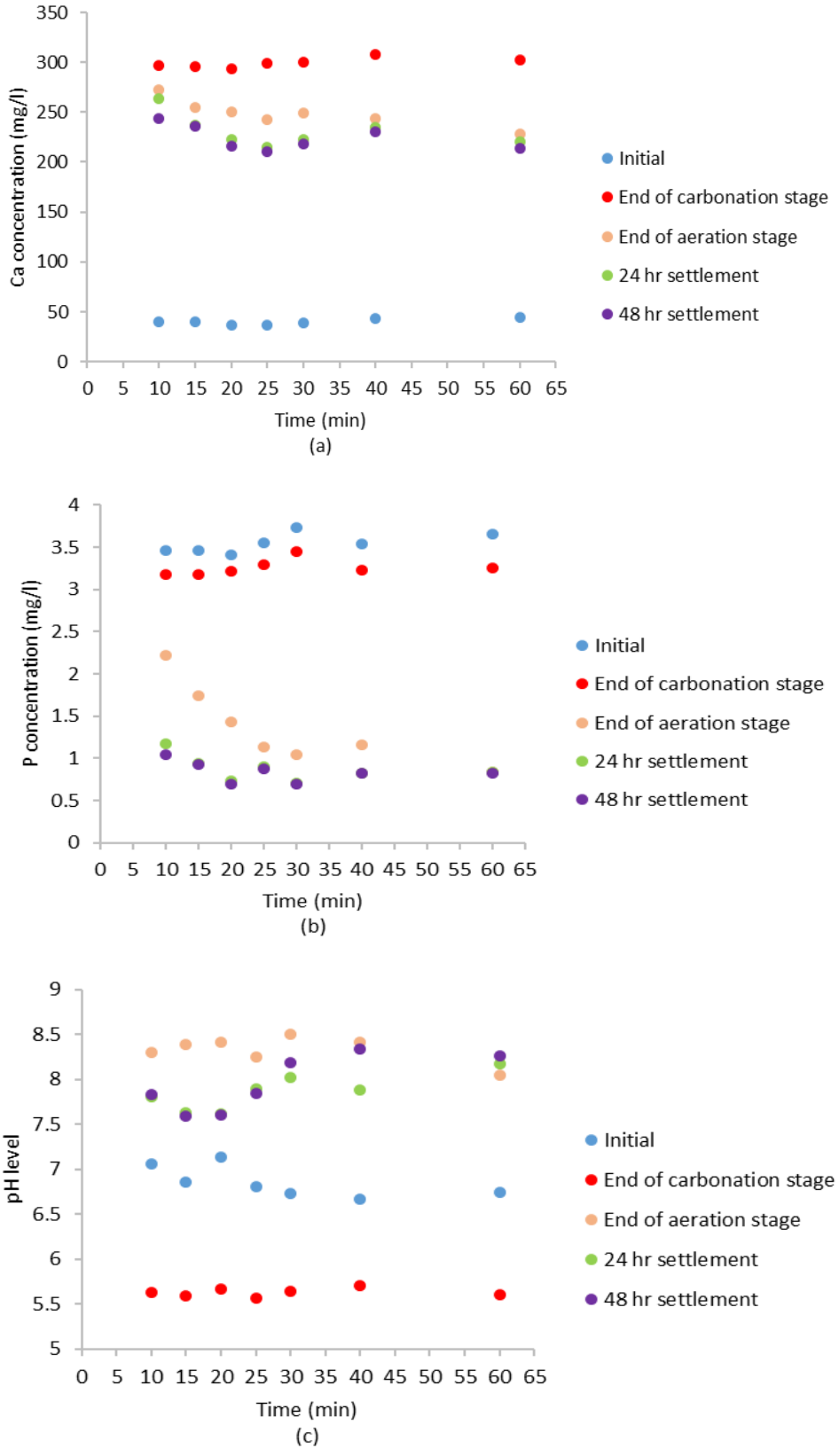

Figure 4- 16: Variation of (a) Ca concentration, (b) P concentration and (c) pH level during carbonation, aeration and settlement stages. Experiment conditions: Carbonation with 0.75 l/min for 40 min, Aeration with 2 l/min for either 10,15,20,25,30,40 and 60 min, settlement for 48 hr. Each vertical row of data points represents one experiment (in triplicate). The x-axis represents aeration time. Tap water solutions. Initial P concentration of 2mg/l + P in tap water

4.3.2.3 Initial P concentration of 10 mg/l + P in tap water

From Figure 4.17 (a), it can be seen that the Ca concentrations after 40 min carbonation ranged between 244.6 and 257.1mg/l at the end of carbonation stage. The Ca concentration decreased with increasing the time during aeration stage, Ca concentration ranged between 288.2 mg/l for 10 min aeration and 188.6 mg/l for the 60 min aeration. Further reduction in Ca concentrations occurred during the 48 hr of settlement. The lowest Ca concentration of 175.9 mg/l by 40 min aeration and 48 hr settlement.

From Figure 4.17 (b) it can be seen that the main decrease in P concentration occurred during the aeration stage, the decrease in P concentration increased by increasing the aeration time except the batches of 30 and 40 min aeration where the concentration increased, the decrease in P concentration in this stage ranged between 3.798 mg/l for 10 min aeration and 1.637 mg/l for by 25 min aeration. All batches showed further decrease in concentration after 24 and the concentration increased after the48 hour of settlement for 10, 15, 20, 25, and 30 while the concentration decreased for the 40 min aeration and remain constant for the 60 min aeration. The 1.174 mg/l was the lowest P concentration by 15 min aeration and 48 hr settlement.

From Figure 4.17 (c) it can be seen that during aeration stage pH values ranged between 8.11 and 8.47. The pH of batches 10 and 15 increased in first 24 hour of settlement and decreased in second 24 hour of the settlement stage while there was a decrease in pH reading for the other batches during the first 24 hour followed by further decrease in the second 24 hr of settlement.

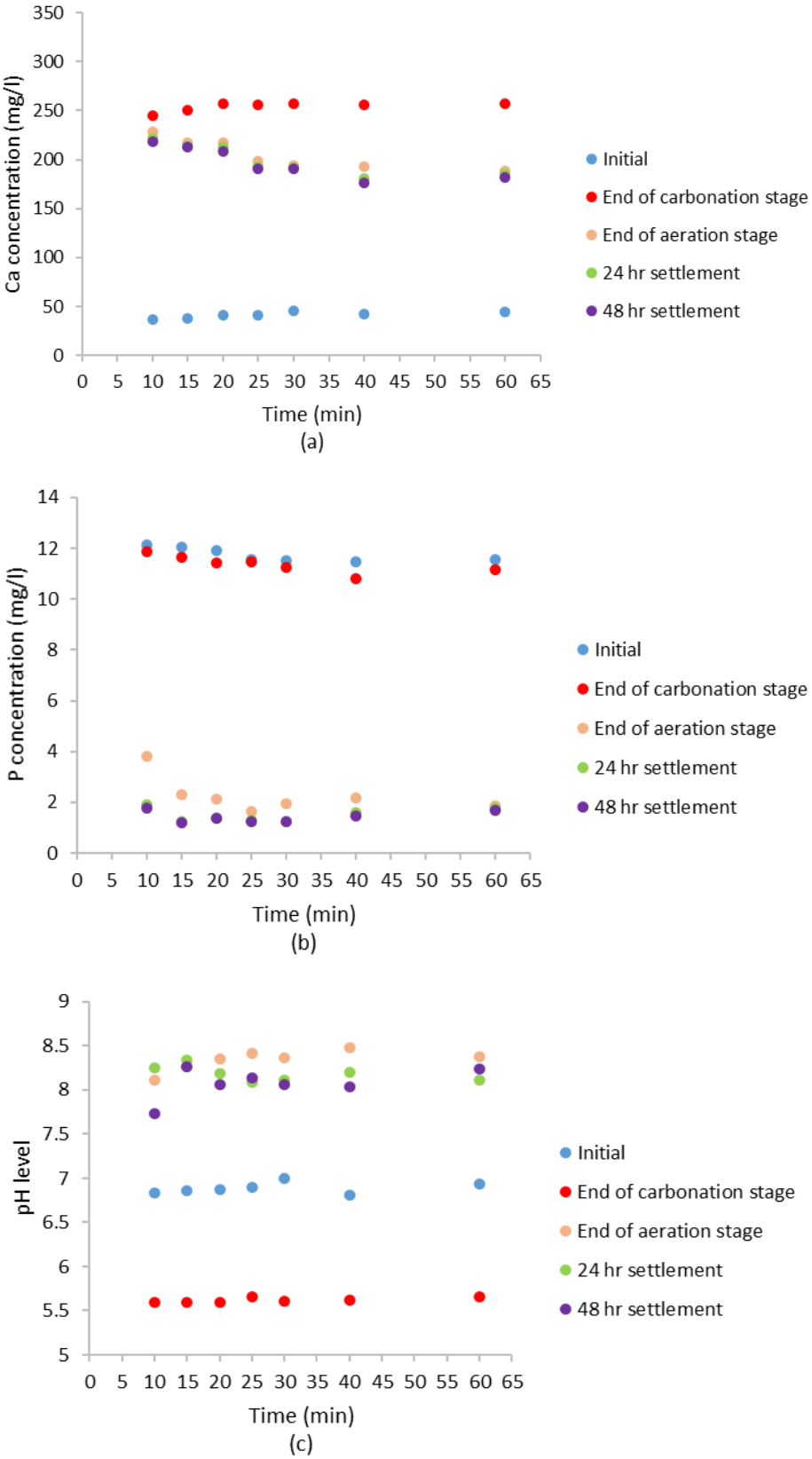

Figure 4- 17: Variation of (a) Ca concentration, (b) P concentration and (c) pH level during carbonation, aeration and settlement stages. Experiment conditions: Carbonation with 0.75 l/min for 40 min, Aeration with 2 l/min for either 10,15,20,25,30,40 and 60 min, settlement for 48 hr. Each vertical row of data points represents one experiment (in triplicate). The x-axis represents aeration time. Tap water solutions. Initial P concentration of 10mg/l + P in tap water

4.3.2.4 Initial P concentration of 20 mg/l + initial tap water

From Figure 4.18 (a), it can be seen that the Ca concentrations after 40 min carbonation ranged between 234.1 and 242.4mg/l at the end of carbonation stage. During aeration stage the Ca concentration decreased with increasing the time of aeration, Ca concentration ranged between 198.8 mg/l for 10 min aeration and 167.1 mg/l for the 60 min aeration. Slight decrease in Ca concentrations occurred during the 48 hr of settlement. The lowest Ca concentration of 155.6 mg/l by 60 min aeration and 48 hr settlement.

From Figure 4.18 (b) it can be seen that the main decrease in P concentration occurred during the aeration stage, the decrease in P concentration increased by increasing the aeration time except for batch of 30 min aeration when the concentration increased, P concentration in this stage ranged between 6.80 mg/l for 10 min aeration and 1.45 mg/l for 40 min aeration. All batches showed further decrease in concentration after 48 hr of settlement. The 1.35 mg/l was the lowest P concentration by 40 min aeration and 48 hour settlement.

From Figure 4.18 (c) during aeration stage pH values ranged between 8.02 and 8.48. All batches showed decrease in pH values during the settlement stage except batches of 40 and 60 min aeration showed an increase in the pH level.

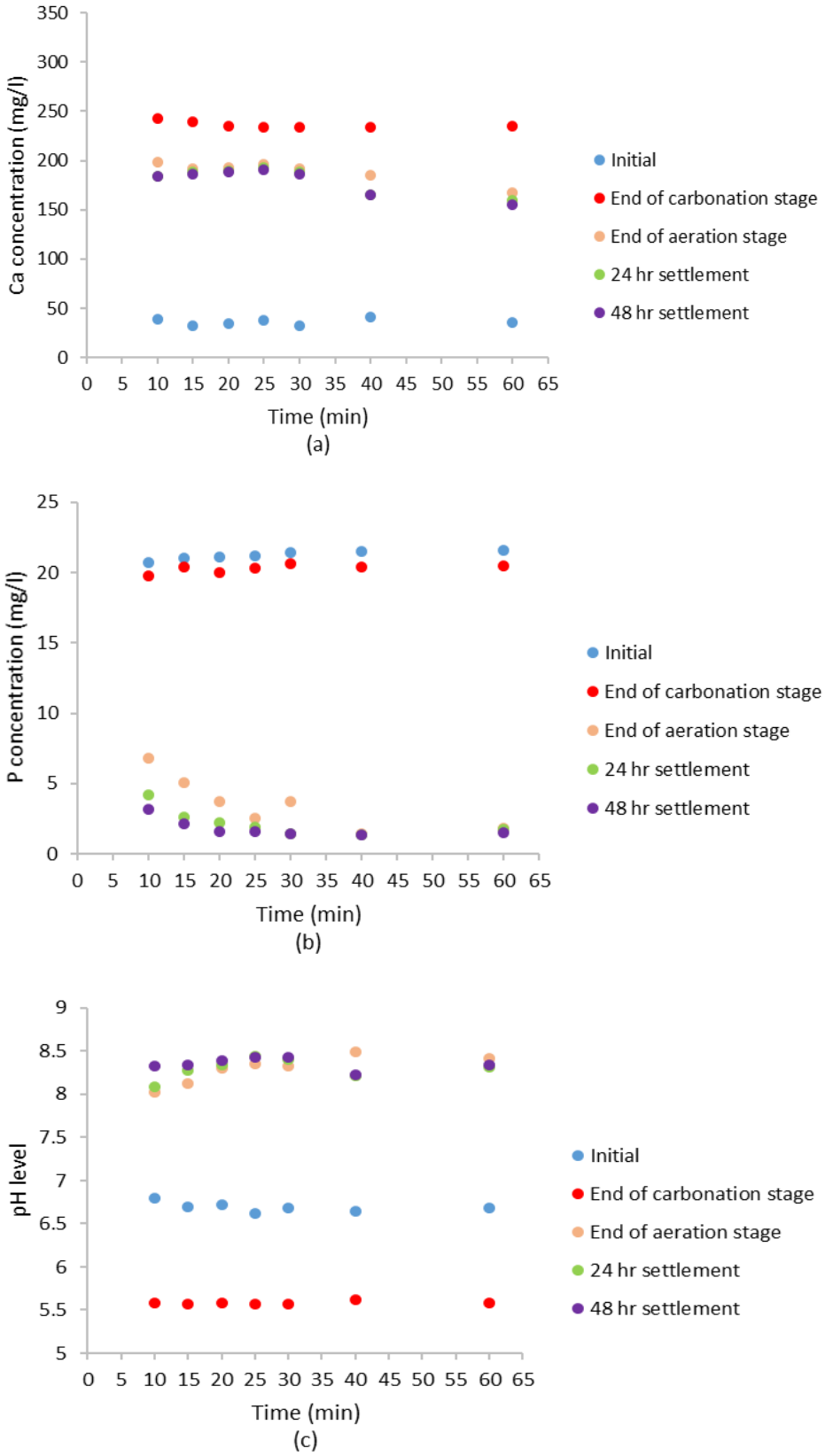

Figure 4- 18: Variation of (a) Ca concentration, (b) P concentration and (c) pH level during carbonation, aeration and settlement stages. Experiment conditions: Carbonation with 0.75 l/min for 40 min, Aeration with 2 l/min for either 10,15,20,25,30,40 and 60 min, settlement for 48 hr. Each vertical row of data points represents one experiment (in triplicate). The x-axis represents aeration time. Tap water solutions. Initial P concentration of 20mg/l + P in tap water

4.3.2.5 Initial P concentration of 100 mg/l + initial tap water

From Figure 4.19 (a), it can be seen that the Ca concentrations after 40 min carbonation ranged between 211.7 and 206.2 mg/l at the end of carbonation stage. During aeration stage the Ca concentration decreased with increasing the time of aeration except the batches of 25 and 30 min aeration, Ca concentration in this stage raged between 105.7 mg/l for 10 min aeration and 51 mg/l for 60 min aeration. Further reduction in Ca concentrations occurred during the 48 hr of settlement. The lowest Ca concentration was 32 mg/l by 20 min aeration and min settlement.

From Figure 4.19 (b) it can be seen that the main decrease in P concentration occurred during the aeration stage, the decrease in P concentration increased by increasing the aeration time, P concentration in this stage ranged between 56.2 mg/l for 10 min aeration and 30.2 mg/l for 60 min aeration. All batches showed further decrease in concentration after 48 hr of settlement. The 24.3 mg/l was the lowest P concentration by 60 min aeration and 48 hr settlement.

From Figure 4.19 (c) during aeration stage it can be seen that the pH values ranged between 7.5 and 7.76. All batches showed decrease in pH values during the first 24 hr settlement except batches of 40 and 60 min aeration showed an increase in the pH level. During the second 24 hour a decrease in pH occurred in all batches.

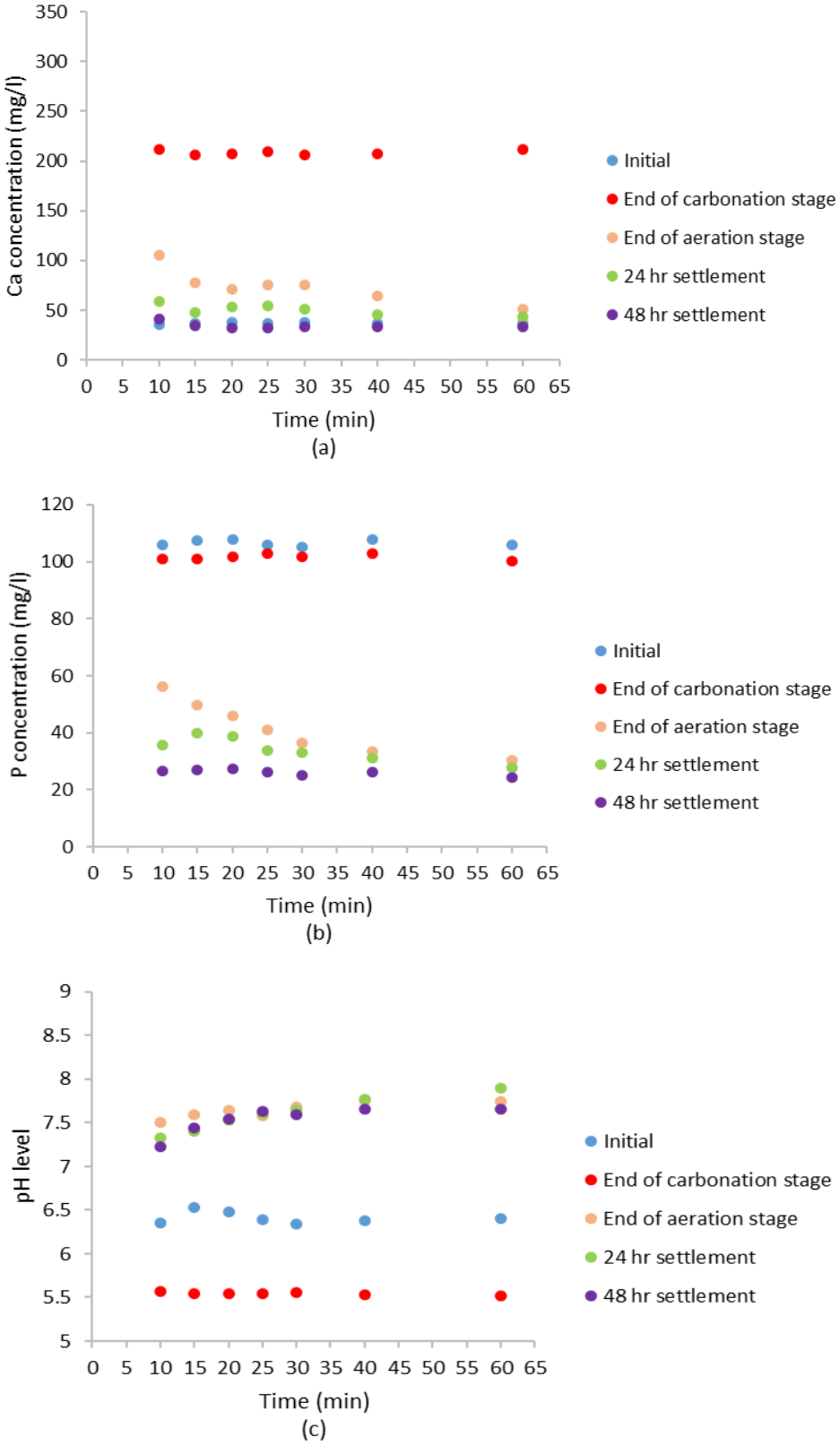

Figure 4- 19: Variation of (a) Ca concentration, (b) P concentration and (c) pH level during carbonation, aeration and settlement stages. Experiment conditions: Carbonation with 0.75 l/min for 40 min, Aeration with 2 l/min for either 10,15,20,25,30,40 and 60 min, settlement for 48 hr. Each vertical row of data points represents one experiment (in triplicate). The x-axis represents aeration time. Tap water solutions. Initial P concentration of 100mg/l + P in tap water

4.3.3 Results of Tests Performed on Real Wastewater

The results presented in this section are obtained from running the laboratory system with real wastewater from West Bonvilstone treatment work. Wastewater collected from the site at 3 different dates on 17/6/2017, 13/12/2017 and 6/4/2018. It is important to highlight the fact that the initial P concentration was varied on the above dates. TP concentration (8.8,1.4 and 5.6) mg/l while PO_4-P (6.2, 1.1 and 4.0) mg/l respectively. The levels of phosphate and calcium within the collected samples were measured. The results of running the 3 samples in the lab system is presented in Figure 4.20 (a-l). All batches were subjected to 0.75 l/min CO_2 for 40 minutes, 2 l/min air and 48 hours of precipitation, the only experimental variance between these seven tests for each P concentration was the period that each batch was aerated for. Table 4.9 present the chemistry of wastewater sample collected from West Bonvilstone treatment work.

Table 4- 9: Anions and cations concentration in West Bonvilston Wastewater

Anions/ Cations	Ca	P	Mg	Na	K	Cl	SO_4	F	NO_3	Date
Concentration mg/l	67.5	8.8	8.7	55.8	17.5	49.9	38.9	1.0	54.1	17/6/2017
Concentration mg/l	56.4	1.4	7.3	51.7	13.4	40.1	33.5	2.4	38.9	13/12/2017
Concentration mg/l	42.8	5.6	8.8	48.7	14.4	48.8	40.2	1.7	46.1	4/6/2018

Figure 4.20(a-d) represent the results for the first real wastewater sample collected on the 17/6/2017. From Figure 4.20 (a), it can be seen that the Ca concentrations after 40 min carbonation ranged between 240.2 and 255.4 mg/l the end of carbonation stage. Ca concentration in the aeration stage ranged between 230.9 mg/l for 10 min aeration and 217.2 mg/l for 25 min aeration. Further reduction in Ca concentrations occurred during the 48 hr of settlement. The lowest Ca concentration was 205.6 mg/l by 25 min aeration and 48 hr settlement. From Figure 4.20 (b) it can be seen that the main decrease in P concentration occurred during the aeration stage, the decrease in P concentration increased by increasing the aeration time for all batches except the batch of 25 min aeration when the concentration increased to 2.23 mg/l, P concentration in this stage ranged between 4.04 mg/l for 10 min aeration and 1.92mg/l for 40 min aeration. All batches showed further decrease in concentration after 48 hr of settlement. The 1.3 mg/l was the lowest P concentration by 40 min aeration and 48 hr settlement.

From Figure 4.20 (c) it can be seen that the main decrease in PO_4-P concentration occurred during the aeration stage, the decrease in OP concentration increased by increasing the aeration time. OP concentration in this stage ranged between 2.9 mg/l for 10 min aeration and 1.42 mg/l for 60

min aeration. All batches showed further decrease in concentration after 48 hr of settlement. The 1.18 mg/l was the lowest PO_4-P concentration by 40 min aeration and 48 hr settlement.

From Figure 4.20 (d) during aeration stage it can be seen that the pH values ranged between 8.025 and 8.27. All batches showed decrease in pH values during the first 24 hr settlement except batches of 60 min aeration showed a slight increase in the pH level. During the second 24 hr a decrease in pH occurred in all batches.

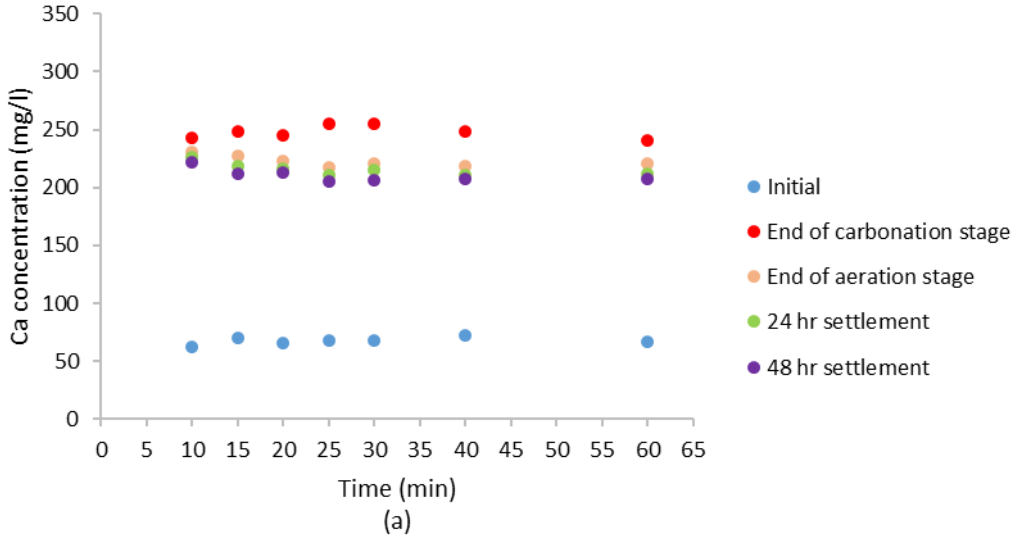

(a)

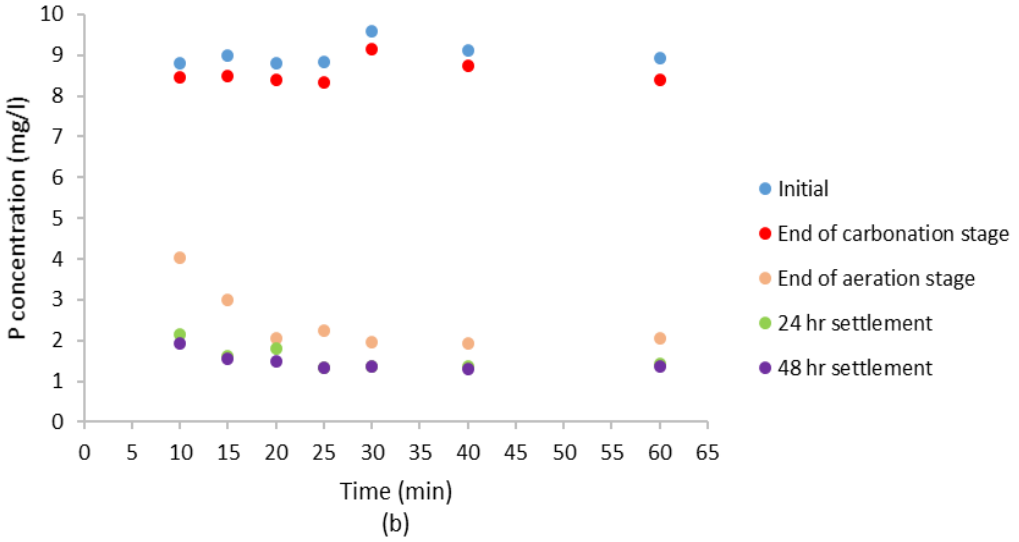

(b)

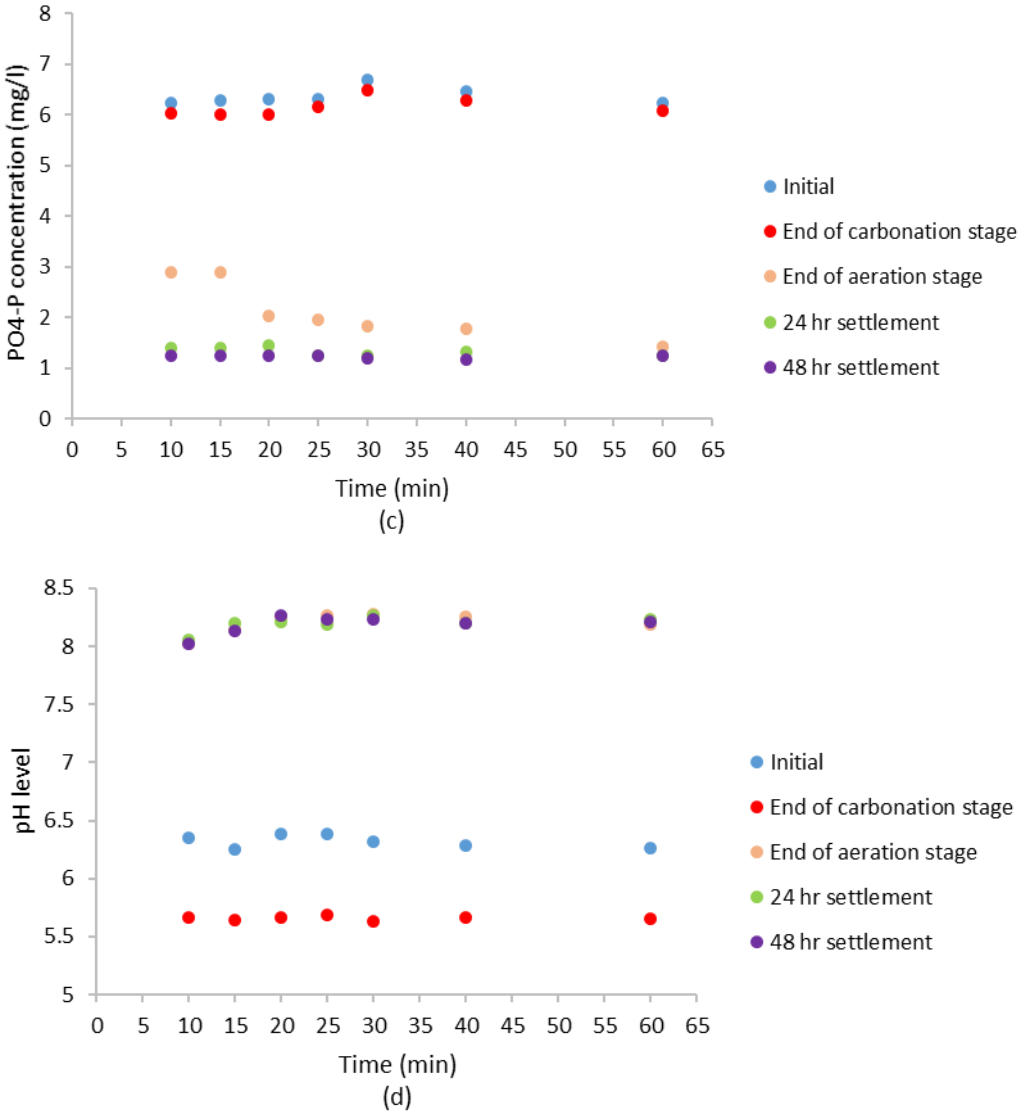

Figure 4- 20 Variation of (a) Ca concentration, (b) P concentration, (c) PO_4-P concentration and (d) pH level during carbonation, aeration and settlement stages. Experiment conditions: Carbonation with 0.75 l/min for 40 min, Aeration with 2 l/min for either 10,15,20,25,30,40 and 60 min, settlement for 48 hr. Each vertical row of data points represents one experiment (in triplicate). The x-axis represents aeration time. Wastewater sample 17/6/2017

Figure 4.21 (a-d) represent the results for the second real wastewater sample collected on the 13/12/2017.From Figure 4.21 (a) it can be seen that the Ca concentrations after 40 min carbonation ranged between 274.4 and 281.4 mg/l the end of carbonation stage. Ca concentration in the aeration stage ranged between 215.1 mg/l for 30 min aeration and 239.1 mg/l for 25 min aeration. Further reduction in Ca concentrations occurred during the 48 hr of settlement. The lowest Ca concentration was 196.0 mg/l by 30 min aeration and 48 hr settlement. From Figure 4.21 (b) it can be seen that the main decrease in P concentration occurred during the aeration stage, the decrease in P concentration increased by increasing the aeration time for all batches. P concentration in this stage ranged between 1.19 mg/l for 10 min aeration and 0.911

mg/l for 40 min aeration. All batches showed further decrease in concentration after 48 hr of settlement. The 0.65 mg/l was the lowest P concentration by 40 min aeration and 48 hr settlement. From Figure 4.21 (c) it can be seen that the main decrease in PO_4-P concentration occurred during the aeration stage, the decrease in PO_4-P concentration increased by increasing the aeration time. PO_4-P concentration in this stage ranged between 0.88 mg/l for 10 min aeration and 0.65 mg/l for 40 min aeration. All batches showed further decrease in concentration after 48 hr of settlement. The 0.56 mg/l was the lowest P concentration by 40 min aeration and 48 hr settlement. From Figure 4.21 (d) during aeration stage it can be seen that the pH values ranged between 7.48 and 7.61. All batches showed decrease in pH values during the first and second 24 hr settlement.

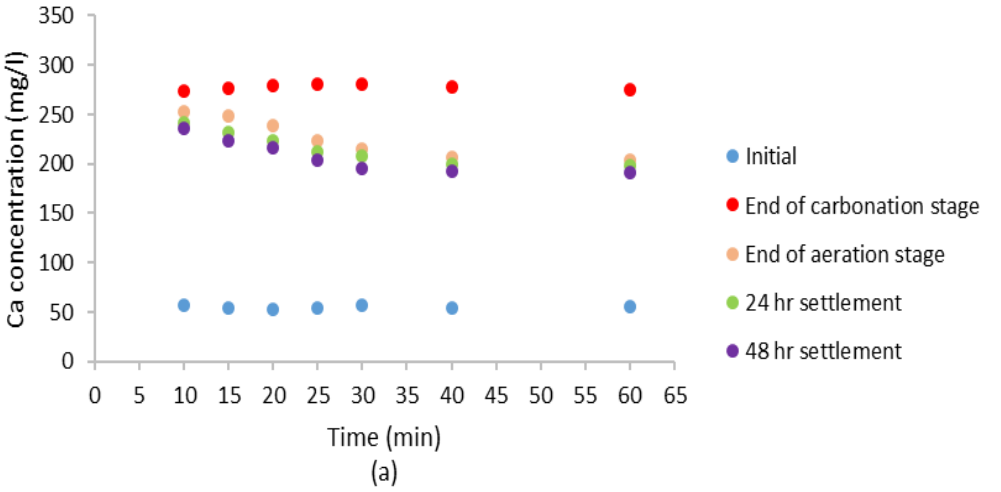

(a)

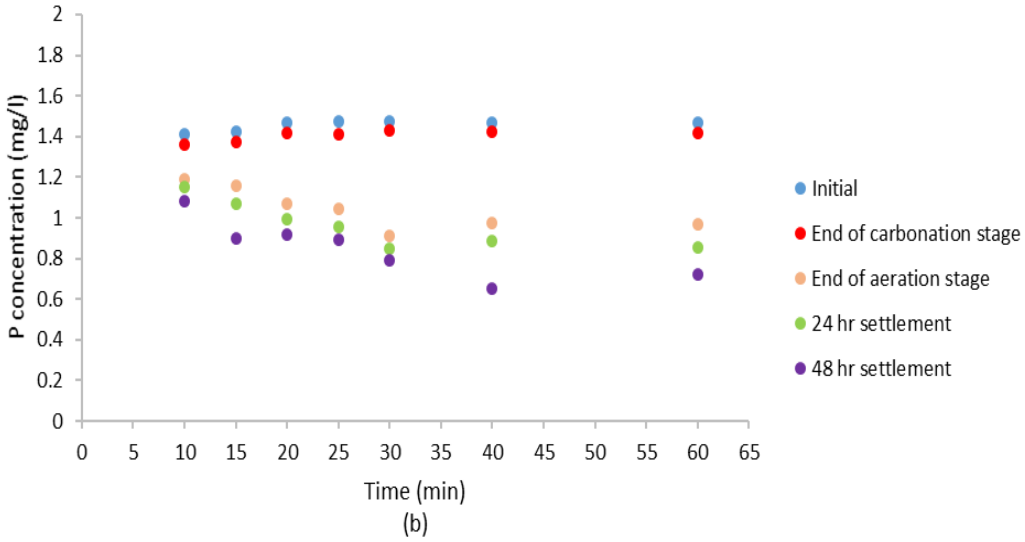

(b)

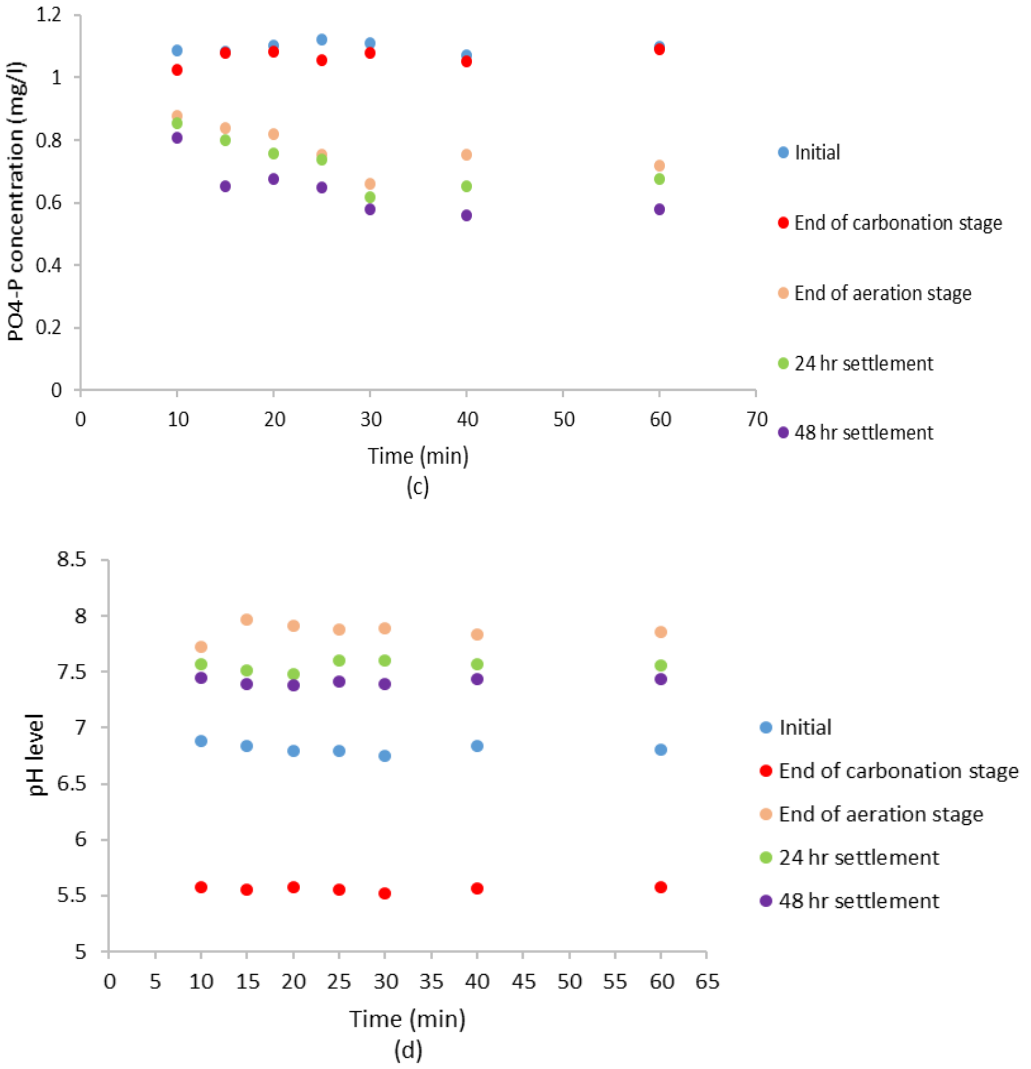

Figure 4- 21: Variation of (a) Ca concentration, (b) P concentration, (c) PO_4-P concentration and (d) pH level during carbonation, aeration and settlement stages. Experiment conditions: Carbonation with 0.75 l/min for 40 min, Aeration with 2 l/min for either 10,15,20,25,30,40 and 60 min, settlement for 48 hr. Each vertical row of data points represents one experiment (in triplicate). The x-axis represents aeration time. Wastewater sample 13/12/2017

The experimentation on the third sample was by applying 40 min carbonation and 40 min aeration as it showed the maximum decrease in P concentration and 48 hr settlement. Figure 4.22(a-d) represent the results for the third real wastewater sample collected on the 6/4/2018.From Figure 4.22(a) it can be seen that the Ca concentrations after 40 min carbonation was 261.9 mg/l. Ca concentration at the end of 40 min aeration 229.5 mg/l for 25 min aeration. P concentration in this stage dropped to 1.34 mg/l. PO_4-P concentration in this stage dropped to 0.95 mg/l after aeration. From Figure 4.22(b) pH dropped to 5.75 after carbonation and raised to 7.6 after aeration. Figure 4.22(c) shows further reduction in Ca concentrations occurred during settlement stage; Ca dropped to 217.1 mg/l the end of first 24 hr of settlement. P concentration in this stage dropped to 1.04 mg/l. The lowest Ca concentration was 208.4 mg/l at the end of second 24 hr

settlement. The 0.74 mg/l was the lowest PO_4-P concentration at the end of settlement. pH decreased during settlement stage to 7.2 as shown in Figure 4.22(d).

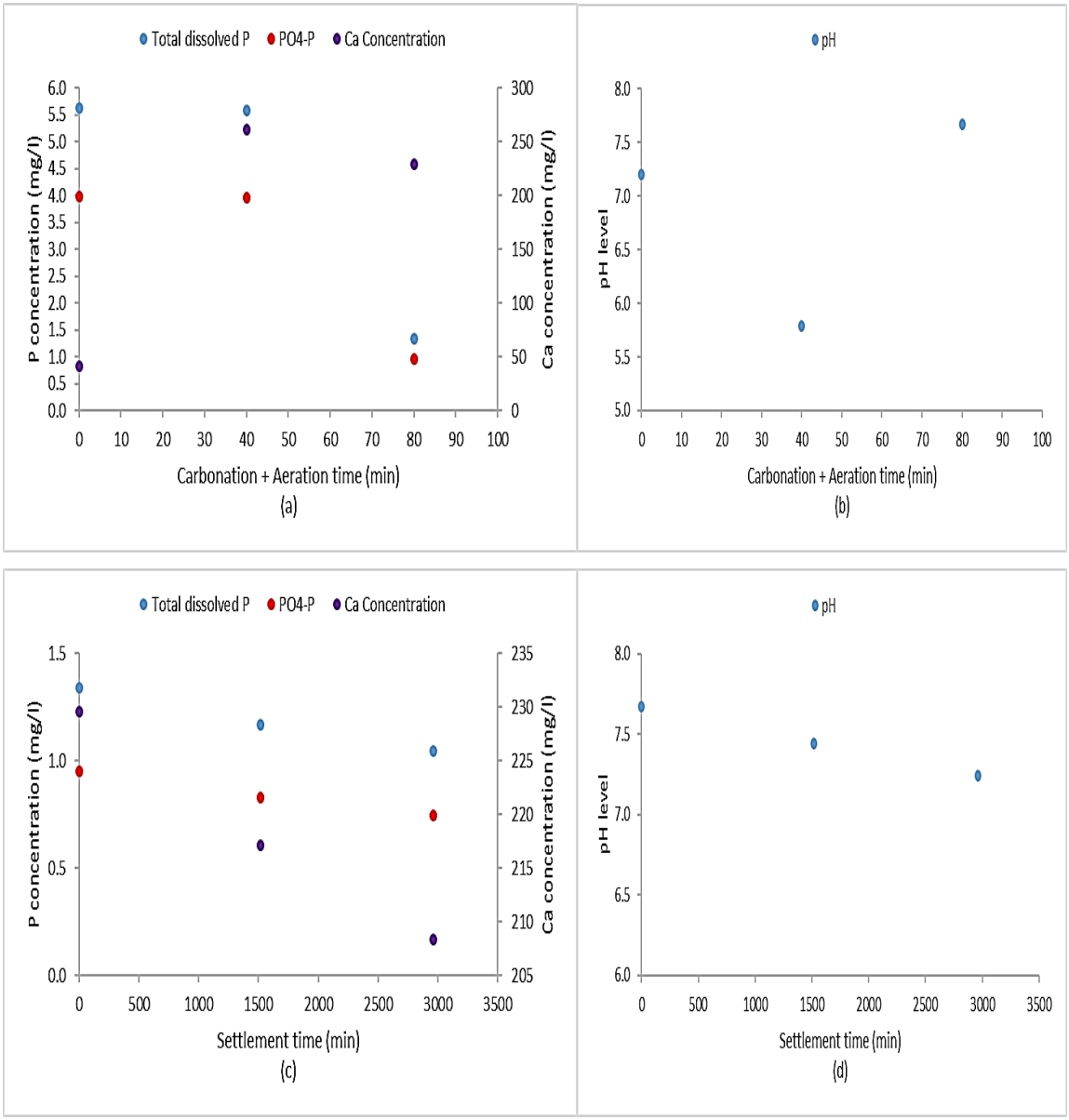

Figure 4- 22: Variation of (a) P, PO_4-P and Ca concentration during carbonation and aeration stage, (b) pH during carbonation and aeration stage, (c) P, PO_4-P and Ca concentration during settlement stage (d) pH during settlement stages. Experiment conditions: Carbonation with 0.75 l/min for 40 min, Aeration with 2 l/min for 40min, settlement for 48 hr. The y-axis represents aeration time. Wastewater sample 6/4/2018

4.4 Discussion

This section summarises and discusses the results presented in section 4.3 examines the trends to show the relationships and the effects of all the contributing parameters on the removing process. Emphasising on the parameters for field trial.

4.4.1 Effect of initial phosphorus concentration on calcium dissolution during carbonation stage

Figure 4.23 shows the variation of calcium dissolution during carbonation stage with initial phosphorus concentration. Data demonstrates that calcite dissolution was clearly retarded by dissolved phosphorus at acidic pH. In carbonation stage the pH dropped to around 5.5 due to carbonic acid formation as a result of injecting CO_2 in solution as shown in the equation (4.3).

$$CO_2 + H_2O \rightleftharpoons H_2CO_3 \rightleftharpoons H^+ + HCO^{3-} \quad (4.3)$$

The decrease in calcium concentration by increasing the initial phosphorus concentration can show the kinetic effect of phosphorus alone in deionised water solutions and phosphorus with other oxyanions in tap water. A similar observation was made by Montes-Hernandez et al. (2009) and the result of Alkattan et al. (2002) study illustrated that aqueous phosphate, which is also known to be a strong calcite dissolution inhibitor at neutral to basic pH, was found to also strongly inhibit calcite dissolution at acidic conditions. Jonasson et al. (1996) results suggest that the interaction of phosphate with calcite involves dissolution of the surface of the calcite, and reprecipitation of the corresponding calcium phosphonate. The selective nucleation of calcium phosphonate along surface steps, suggests that this may be an important aspect of the mechanism by which phosphonates inhibit calcite crystal growth. However, the degree of inhibition on calcite dissolution due to the presence of aqueous phosphate is likely not sufficient to significantly affect most natural processes and the inhibition was attributed to aqueous phosphate adsorption as calcite surfaces have been noted to be extremely favourable adsorption sites for aqueous phosphate (Berner and Morse 1974; Alkattan et al. 2002). The same trend was outlined in real wastewater solutions when the phosphorus concentration was 1.4 mg/l and calcium concentration was 274.4 mg/l after carbonation. For other real wastewater solution when the initial phosphorus concentration was 5.6 mg/l the calcium concentration was 261.4 mg/l after carbonation. For other real wastewater solution when the initial phosphorus concentration was 8.8 mg/l the calcium concentration was 243 mg/l after carbonation.

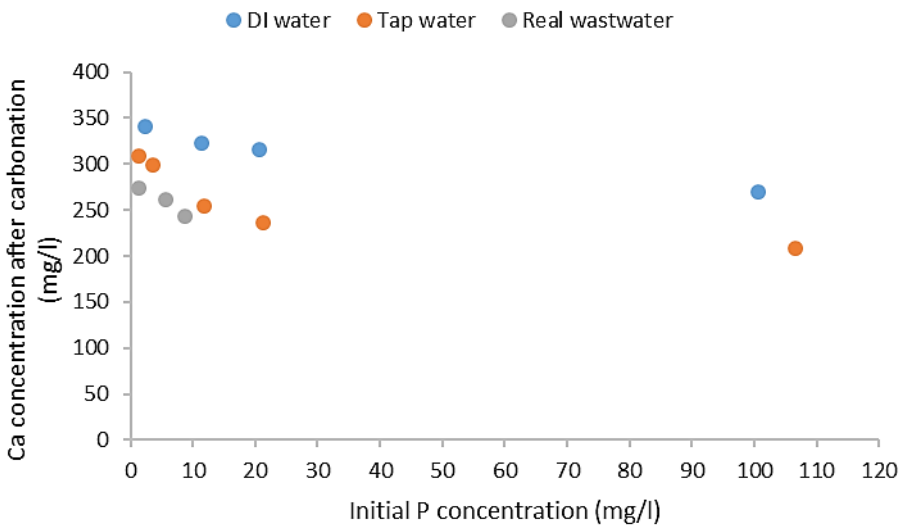

Figure 4- 23: Effect of initial P concentration on calcite dissolution during carbonation stage. 40 min carbonation time and 0.75l/min CO_2 flow rate.

4.4.2 Ca and P removed during aeration stage

Figures 4.24, 4.25 and 4.26 show the changes in P, Ca and pH for DI, tap and real wastewater solutions for all aeration times 10,15,20,25,30,40 and 60 min when 2 l/min air flow rate were applied during aeration stage. The pH of all solutions increased during this stage with less increase in pH for solutions with high initial P concentration of 100.66 and 106.59 mg/l in both DI and tap water. This increase in pH indicating the degassing of CO_2 from solution by aeration. The concentrations of Ca and P were decreased with the rise in pH. This decrease in concentration was caused by the precipitation of Ca and P. The same observation was outlined in a study of enhancing the P removal from swine water by aeration using 1.1 l/hr, the pH increased from 7 to 8.5 after 3 hr. The experiments were carried out with a cylinder of 21 cm in diameter and 105cm high. Thirty litters of swine wastewater was poured into the cylinder and aerated continuously using a diffuser for 3h (Suzuki et al. 2002). It can be seen from the previous results in section 4.3 that the removal occurring mainly during aeration stage. By comparing the results from DI water solutions with tap water solutions and real wastewater to summarise the key comparative data it can be seen that by applying different aeration intervals, the removed P concentration for each initial concentration was close in DI water solutions while the removed P concentration increased with increasing aeration time to 40 min for tap water solution and the same trend was outlined in real wastewater solutions. Increasing aeration time to 60 min seems to have no significant effect on increasing the removal of P. The same observation was outlined for Ca concentration. Nassef (2012) found that an increase in Ca concentration increases the removal of phosphorous at high pH values (8.5-10). This is ascribed to the fact that the higher the concentration of Ca the higher the ability of Ca ions to form the complex with phosphate and precipitate it in the solution

at high pH. This agrees with the results presented in Figure 4.24 (a and b) that the removal of P increased with Ca concentration. On the other hand the pH range obtained during aeration between 7.5- 8.7 was lower than that found by Nassef (2012) for all initial P concentrations.

it can be seen that the P and Ca concentrations removed in this stage from tap water solution is lower than that from DI water solutions and pH recorded was slightly lower than that for the DI solutions. This might be because the effect of other elements available in tap water such as Mg which was found in the composition analysis of tap water in Table 4.8 in concentration of 4.47 mg/l this might inhibit the formation of calcium phosphate by competing with phosphate ions and forming calcium magnesium precipitate or enabling the formation of more soluble amorphous calcium phosphate phase that precipitate slowly (House et al. 1986; Cao et al. 2007). In addition, the presence of SO_4 in concentration of 24.69 mg/l might prevent the formation of calcium phosphate although sulfate can promote calcite to dissolve, high concentrations of sulfate compete with phosphate forming calcium sulfate (Liu et al. 2012) the same trend was observed in the real wastewater solutions when the Mg concentration was found to be 8.7 mg/l and sulfate concentration 38.9 mg/l. Dissolved phosphate also inhibits the crystal growth of calcite and, this depends on the initial inhibitor concentration and the surface density of phosphate controls the potential forming of a nucleus on a certain step, may stop growth completely (House, 1987; House, 1990). The crystal growth of calcite can be also inhibited by organic ligands presented in wastewater by adsorption of these organic compounds on the calcite surface and blocking of crystal growth sites (Stabel, 1986) . The presence of carbonates might reduce or inhibits hydroxyapatite (calcium phosphate) formation (Battistoni et al. 1997; Cao and Harris 2008). Karunanithi et al. (2015) found that at pH 8 phosphate precipitation was significantly lessened by carbonate and the corresponding precipitation efficiency also decreased due to the formation of ion pairs between carbonate and calcium, thereby diminishing the free calcium concentrations. The same study also found that at pH greater than 9 the effect of carbonate on the precipitation of phosphate was very small. This indicates that carbonate may decrease P precipitation in the current study as the pH level was less than 9 in all experiments. Figure 4.24(c) and 4.25 (c) showed that pH of solution with an initial P concentration of 100.66 and 106.59 mg/l is around 7.5 which is in agreement with a study of Liu et al. (2012) examining solutions with high phosphate concentrations and pH in ranging from 4 to 12 showed that the highest phosphate removal efficiency was obtained in the pH range of 7 to 8, and the efficiency decreased with increasing pH. The effect of pH on phosphate removal can be attributed to changes in the surface sites or speciation of phosphorus in the solution as well as the dissolution of calcite (Liu et al. 2012). In this study, the phosphate removal was not significantly changed with increasing pH of

solution within the obtained range 7.3 – 8.7. This may be explained by considering such competing effects as a decrease in the dissolved Ca^{2+} concentrations and an increase of PO_4^{3-} species from hydrolysis products of phosphate with increasing pH (Karaca et al. 2006).

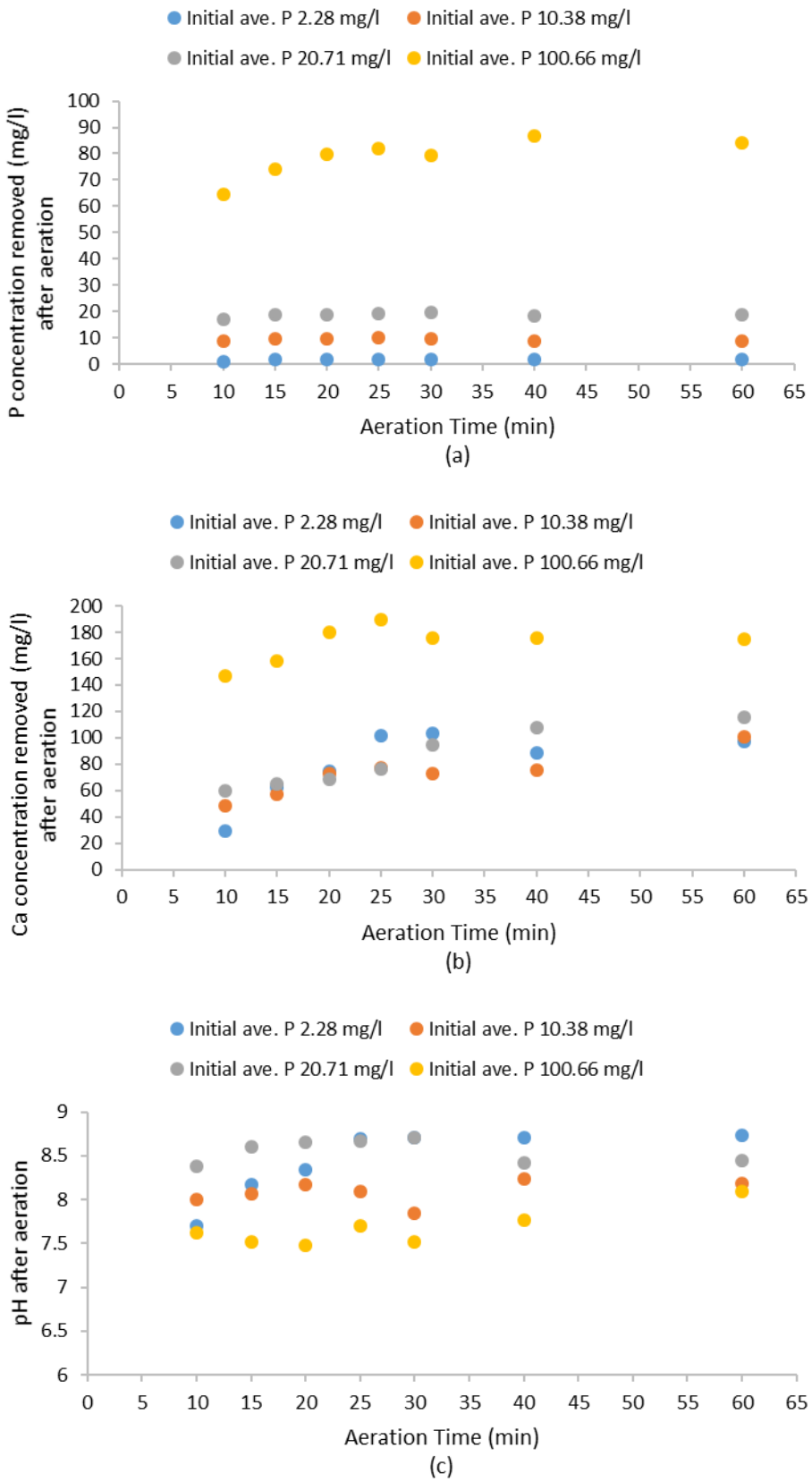

Figure 4- 24: (a) removed P concentration (b) removed Ca concentration (c) pH during aeration stage of either (10,15,20,25,30,40 and 60) min. DI water P solution. (Note: these are not time series data, each data point represents a single experiment in triplicate)

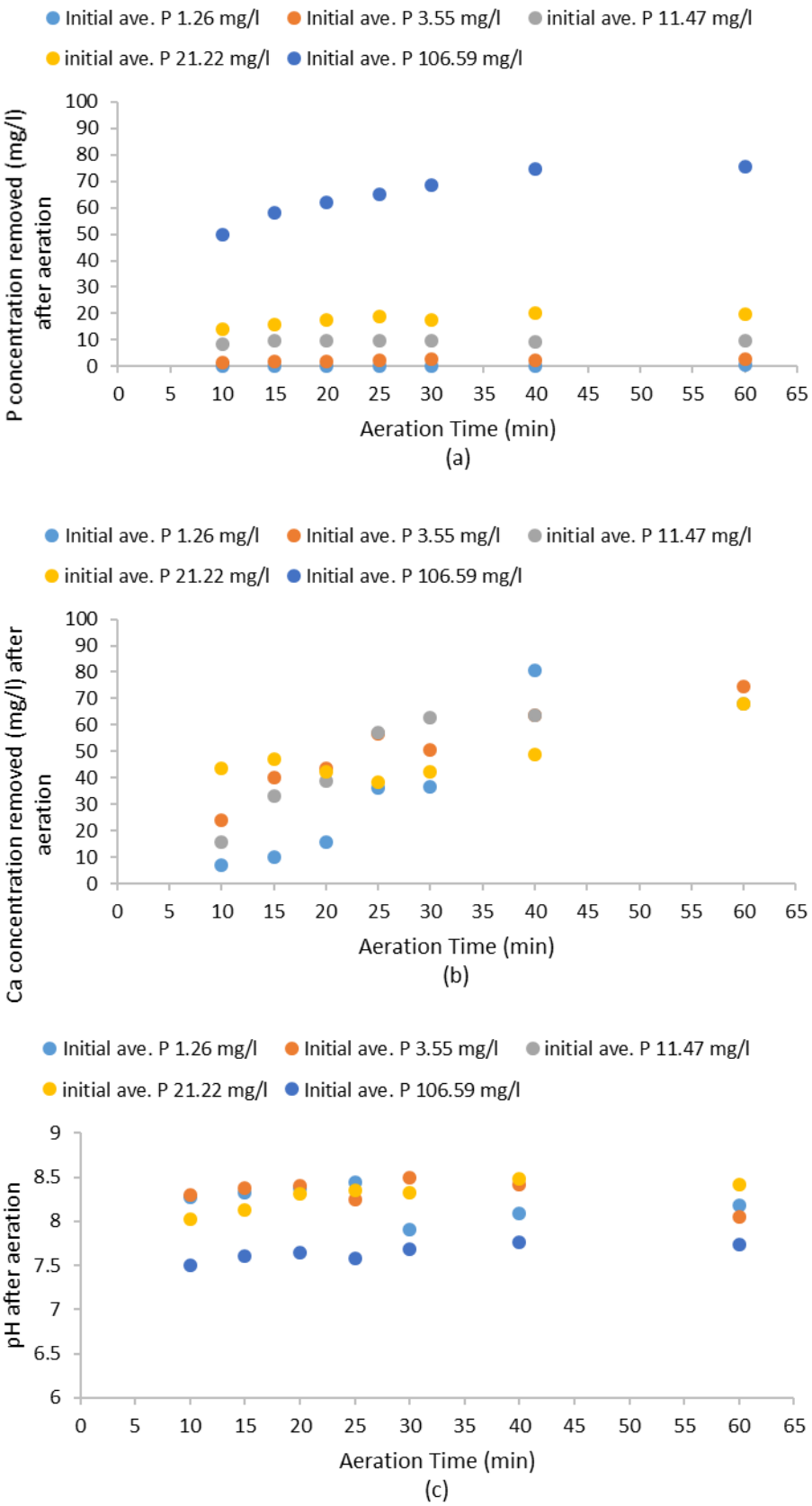

Figure 4- 25: (a) removed P concentration (b) removed Ca concentration (c) pH during aeration stage of either (10,15,20,25,30,40 and 60) min. Tap water P solution. (Note: these are not time series data, each data point represents a single experiment in triplicate)

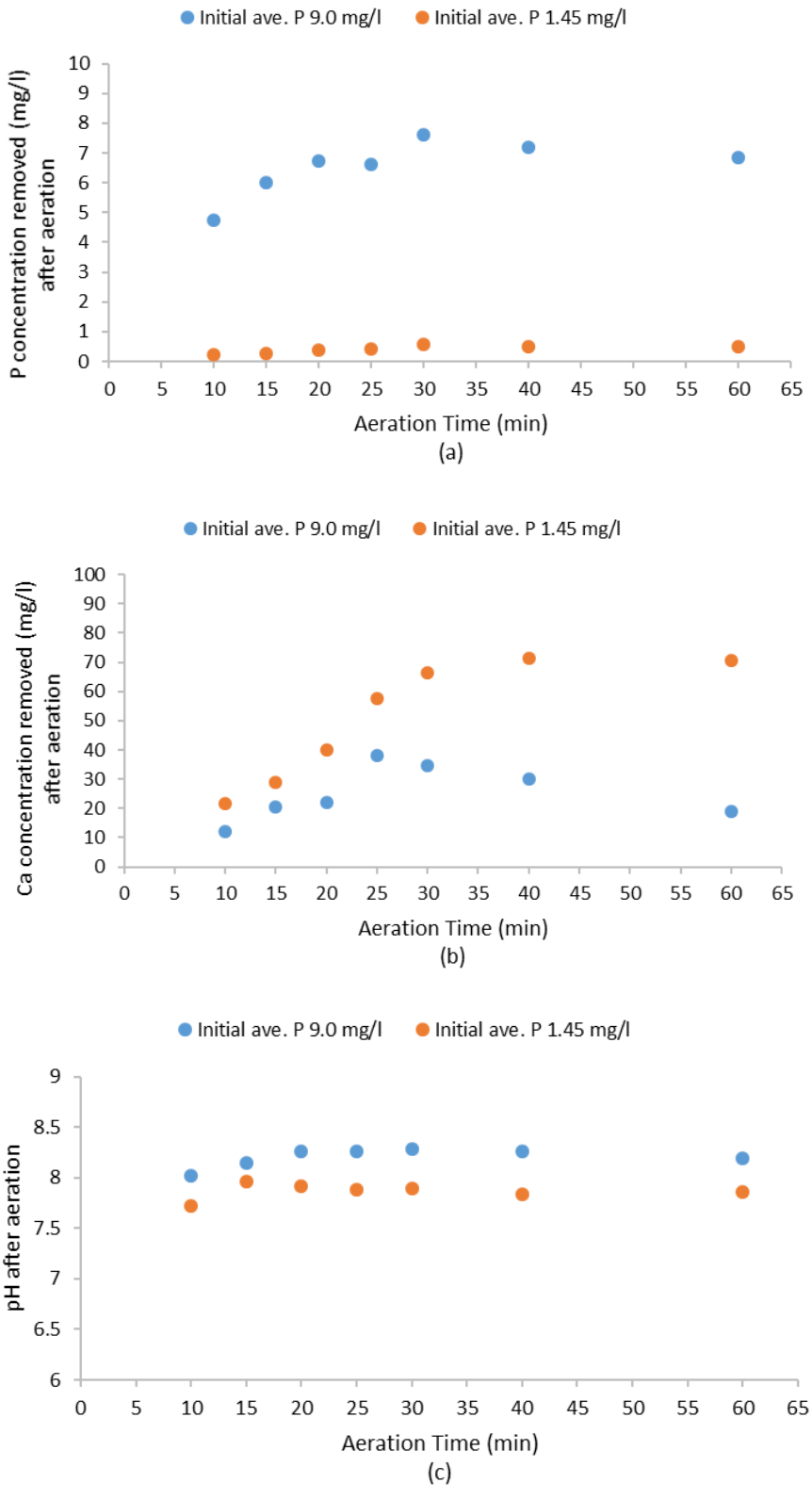

Figure 4- 26: (a) removed P concentration (b) removed Ca concentration (c) pH during aeration stage of either (10,15,20,25,30,40 and 60) min. Real wastewater solution. (Note: these are not time series data, each data point represents a single experiment in triplicate)

4.4.3 Ca and P removed during settlement stage

The previous results in section 4.3 showed that there is further removal occurring during settlement stage. Figures 4.27, 4.28, 4.29, 4.30, 4.31 and 4.32 show the removed P and Ca concentrations during settlement stage for all batches that were subjected to aeration times of either 10, 15, 20, 25, 30, 40 and 60 min for DI, tap and real wastewater solutions respectively. Results included in these figures are not time series data, each data point represents a single experiment in triplicate. It can be seen that the removal in the settlement stage is lower than the removal in the aeration stage although there is sufficient Ca concentration in solution. That low removal in the settlement stage can be attributed to the lower phosphate activity in solution as a result of P precipitation (Sø et al. 2011). The same trend was observed in tap water solutions and in real wastewater solutions as shown in Figures 4.29, 4.30,4.31 and 4.32 respectively. it also observed that during this stage the removed Ca concentration decreased with increasing the initial P concentration in DI water solutions as shown in Figures 4.27(b) and 4.28(b) were deionised water used in preparing solutions indicating that higher P concentrations in solution lead to lower Ca precipitation rates because P acted as an inhibitor for Ca precipitation (Sindelar et al. 2015) while this was not the case when tap water used in solutions preparation indicating the effect of the presence of other ions in tap water which compete with phosphate ions to form other components as shown in Figures 4.29(b) and 4.30(b). There is an inverse correlation between the removal of P and Ca during the first 24 hr and the removal during the second 24 hr of settlement and that can be attributed to the fact of calcium phosphate formation depends on the pH during the removal process and on the concentration of calcium and phosphate in the solution (Heleen J. Danen-Louwerse 1995). As pH increases to more basic values calcium phosphate becomes increasingly insoluble. In contrast, as the pH approaches the acidic regime, calcium phosphate becomes increasingly soluble. The final Ca concentrations remaining in all P solutions are far in excess comparing with expected solubility limits of HAP (see section 2.3.3 figure 2.2 chapter 2) in pH range between 7 to 8 indicating the possibility of further HAP precipitation (Koutsoukos 1995).

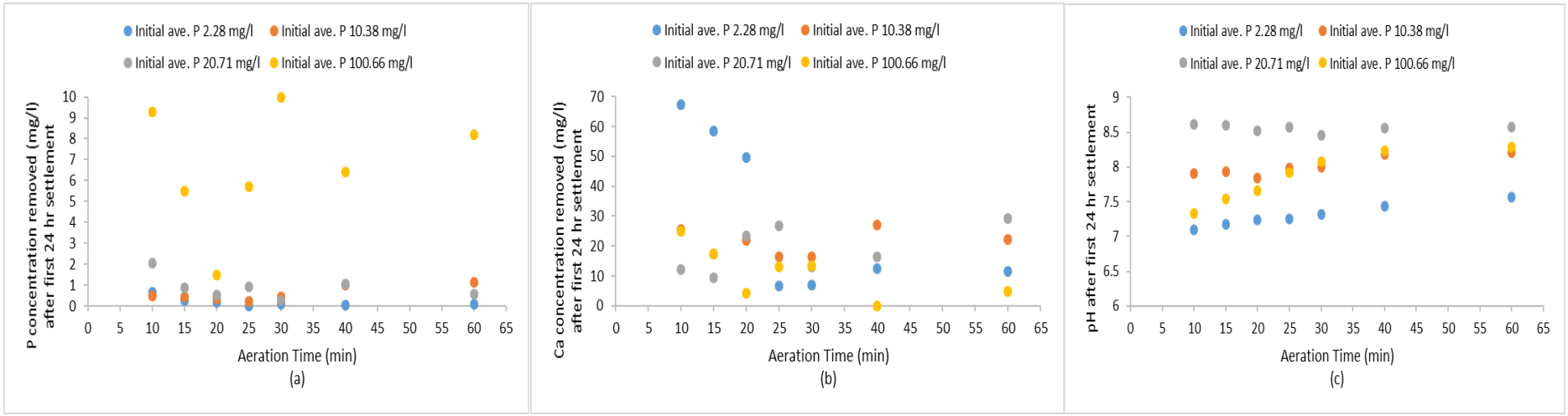

Figure 4- 27: (a) removed P concentration (b) removed Ca concentration (c) pH during first 24 hr settlement stage. DI water P solution.

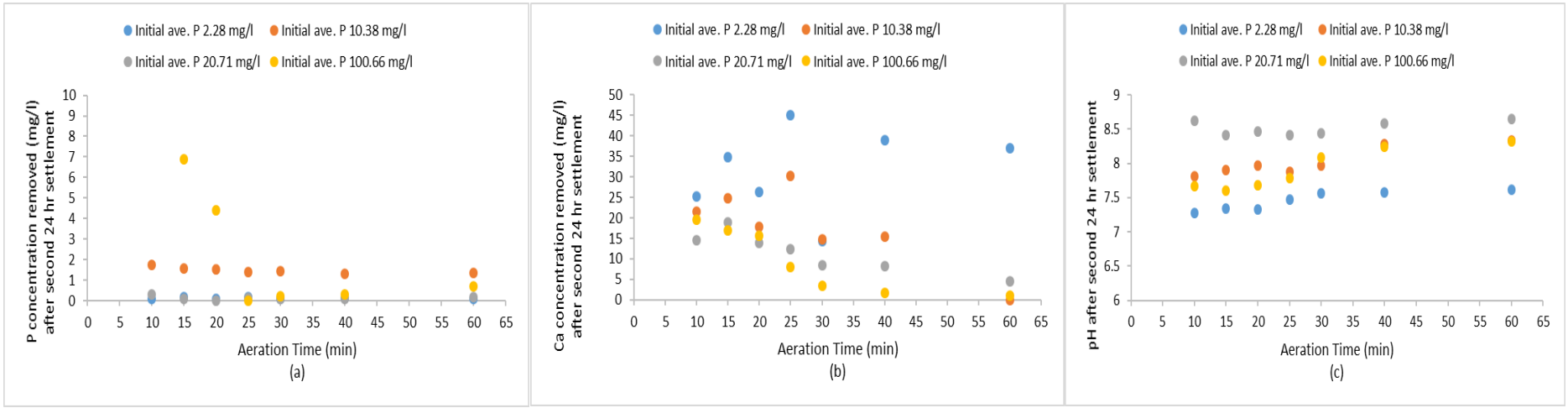

Figure 4- 28: (a) removed P concentration (b) removed Ca concentration (c) pH during second 24 hr settlement stage. DI water P solution.

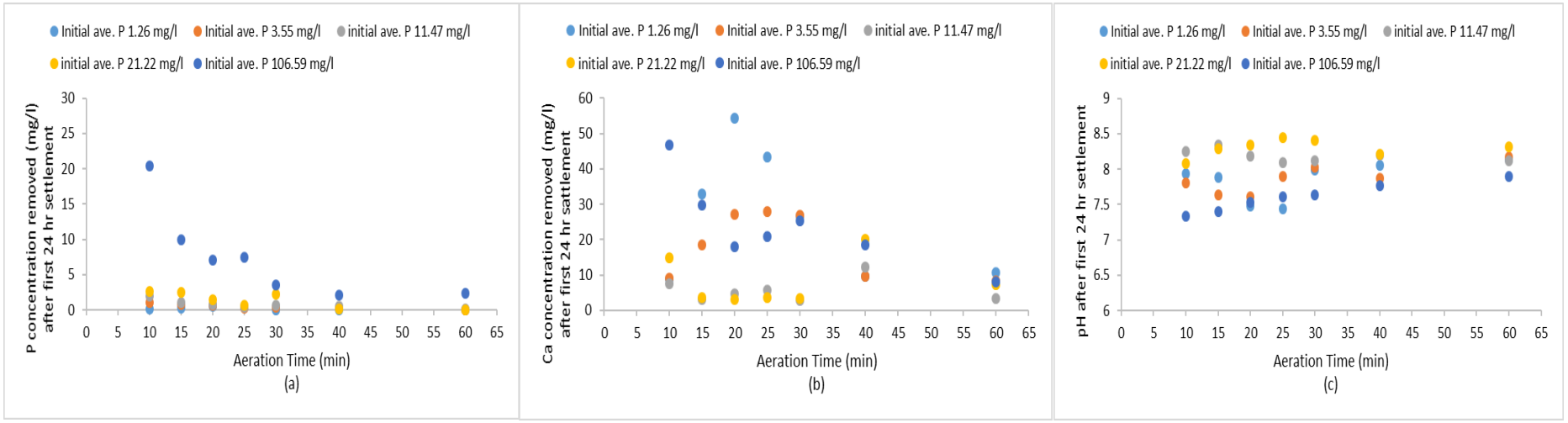

Figure 4- 29 (a) removed P concentration (b) removed Ca concentration (c) pH during first 24 hr settlement stage. Tap water P solution.

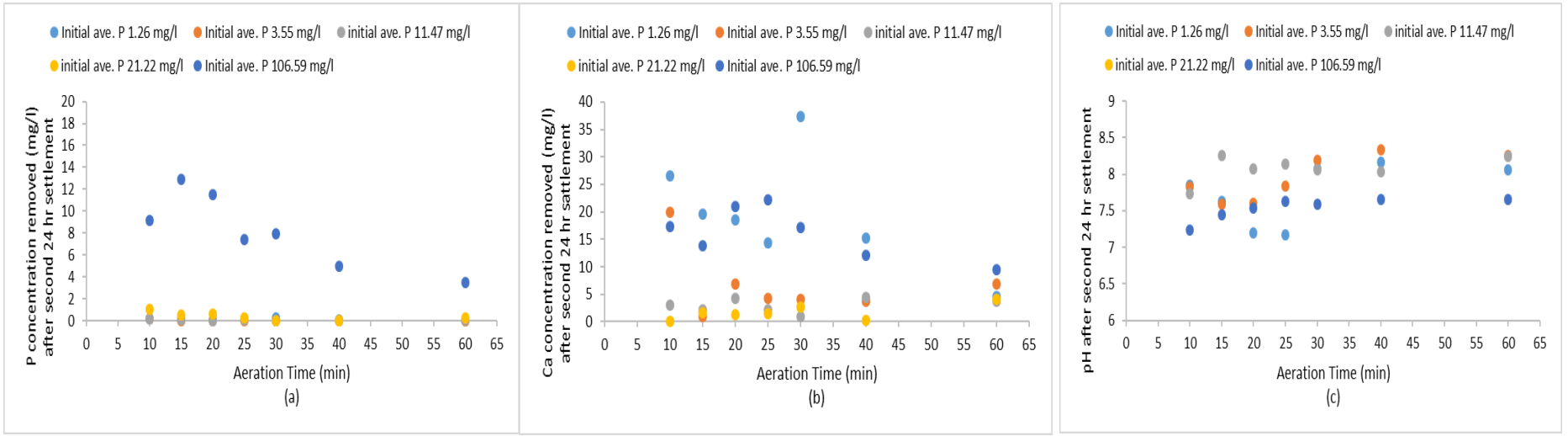

Figure 4- 30: (a) removed P concentration (b) removed Ca concentration (c) pH during second 24 hr settlement stage. Tap water P solution.

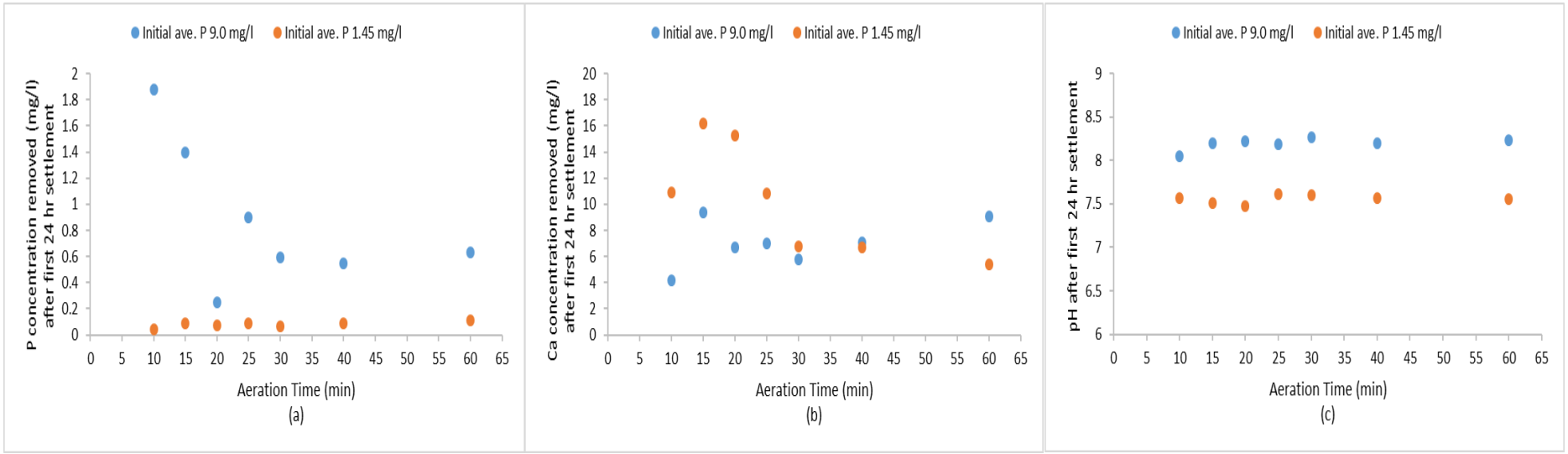

Figure 4- 31: (a) removed P concentration (b) removed Ca concentration (c) pH during first 24 hr settlement stage. Real wastewater solution

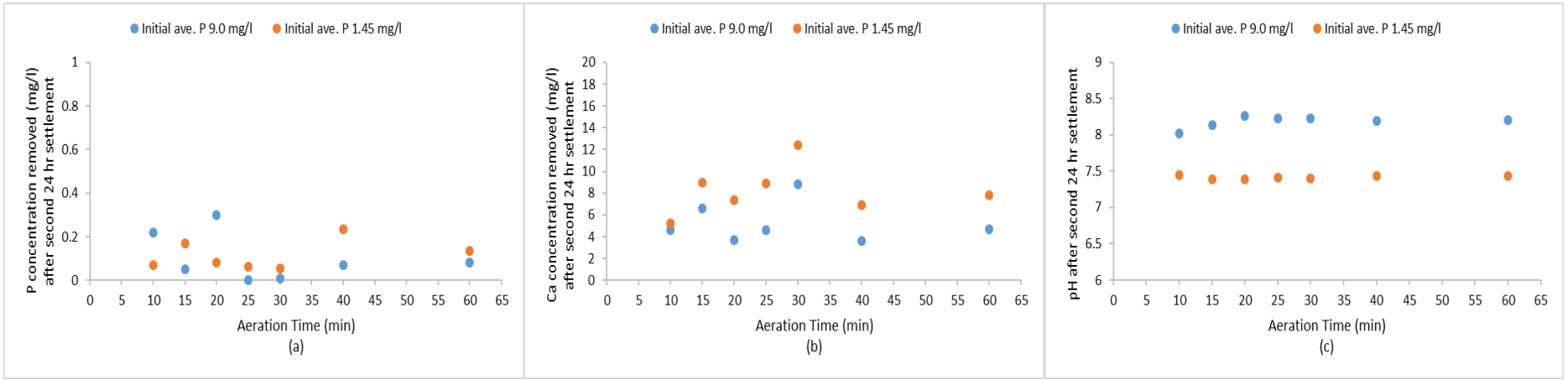

Figure 4- 32: (a) removed P concentration (b) removed Ca concentration (c) pH during second 24 hr settlement stage. Real wastewater solution

4.5 PHREEQCI

The software PHREEQCI was used to predict likely precipitates and to predict the variation of their saturation indices with pH and the species in the solution for a range of conditions related to the lab system tests presented in this chapter. The chosen concentrations and conditions were inputted into the program which then calculates the molality of species and the saturation indices of predicted precipitates. Data was inputted for the concentrations of phosphorus, calcium, and carbonate ions, the pH and temperature were also defined.

4.5.1 SI variation with pH

Saturation indices are a measure of the thermodynamic driving force for a reaction. However, they cannot predict the occurrence of a particular reaction as there may be kinetic constraints. where a positive value indicates that the solution is supersaturated and a negative value indicates undersaturation (Plant and House 2002). In this section SI was calculated to determine whether the solution will precipitate calcium carbonate/phosphate or not through the stages of the process. All tests upon P removal by calcite carried out in support of this thesis have shown that pH is an important factor in the removal of phosphorus through calcium phosphate precipitation. The program was operated with five initial influent concentrations of phosphorus 1.26, 3.55, 11.74, 21.22 and 106.59 mg/l, were used so as to allow some appreciation of the importance of both pH and initial phosphorus concentration. The pH values tested were the values that recorded at the end of each stage of the process and presented on table 4.10. PHREEQCI predicted three precipitates namely Calcite ($CaCO_3$) this is represented as CAL in Figure 4.33, hydroxyapatite ($Ca_5(PO_4)_3OH$) represented as HAP and aragonite ($CaCO_3$) represented as ARG.

Table 4- 10: Ave. pH values for each stage used in PHREEQCI for phosphorus concentrations of (1.26, 3.55, 11.74, 21.22 and 106.59 mg/l)

Stage	Ave.pH
Initial	6.4
Carbonation	5.5
Aeration	8.4
24 hr Settlement	7.6
48 hr Settlement	7.4

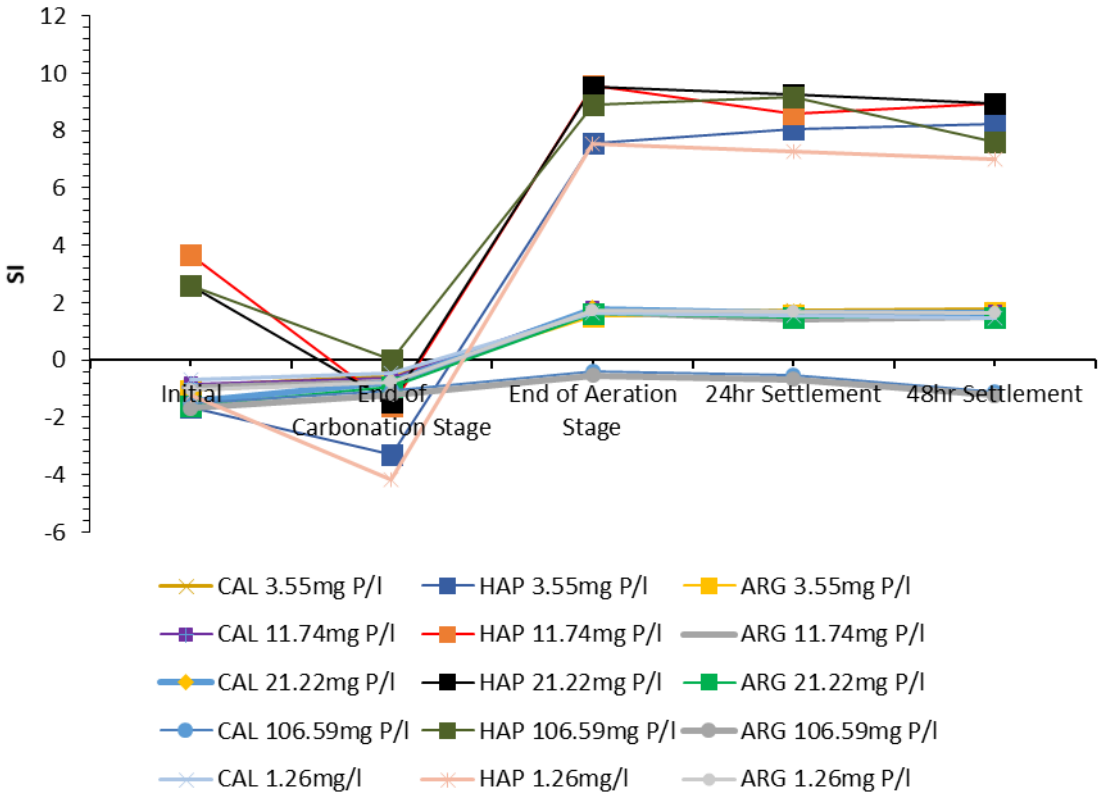

Figure 4- 33: Variation of SI with pH and initial phosphorus concentration for calcite (CAL) hydroxyapatite (HAP) and aragonite (ARG). For the runs of 40 min carbonation, 40 min aeration, 24 and 48 hr settlement

At a pH of 6 and below the SI of HAP at low phosphorus concentrations 1.26 and 3.55 were negative indicating unsaturated phase while at initial P concentrations 11.74, 21.22 and 106.59 HAP was saturated as the pH was within the acidic regime whereas all phases of calcium phosphate becomes increasingly soluble (Vanderesse et al. 2011). The prediction of HAP as a likely precipitate backs up the theory presented earlier in Chapter 2 of this thesis and in agreement with the results presented in section 4.4.3 suggesting that the increase in pH to more basic values resulted in calcium phosphate becomes increasingly insoluble and precipitate. In contrast, as the pH approaches the acidic regime, calcium phosphate becomes increasingly soluble. Many studies on the use of calcium containing materials to remove phosphorus predicted HAP as a final product such as Chen et al. (2007) and Kim et al. (2006). The SIs of both aragonite and calcite remain negative during carbonation stage indicating that calcite never saturated in the initial stage at all initial P concentrations, this is also in agreement with the results presented in section 4.3 suggesting no precipitation during carbonation stage. The SIs of both aragonite and calcite becoming positive after a pH of 6 showing a positive correlation between pH and SI for calcite and indicating saturation with respect to calcite. These predictions are in agreement with the results in section 4.4.2 and 4.4.3 suggesting that the decrease in Ca concentration during aeration and settlement stages is due to precipitation of calcium carbonate/phosphate. The difference in SI for

HAP due to change in pH can be seen to be much more dramatic than the change in SI for calcite, therefore for the situations studied here, pH is the more important factor. It can be seen that at high initial P concentration of 106.59 calcite and aragonite never saturated through the whole process and this is in agreement with the earlier finding presented in section 4.4.1 of increasing initial P concentration inhibits calcite dissolution.

4.5.2 Speciation

PHREEQCI was also used to predict what species are likely to be found in solution. pH has been shown to have an important effect on the SI of HAP and so its effect on the species present was also determined. The species present at a pH between 7.3 and 8.7 were determined, these roughly equating to the lower and upper pH limits found experimentally. All other variables were fixed. Figure 4.34 presents the predicted species present in terms of their concentrations (mg/l). for the tap water solutions. Only predicted species containing calcium or phosphorus are shown. The first column in each stage represent the species concentration for 3.55 mg P/l, the second column represent the species for the 11.71 mg P/l, the third column represent the 21.22 mg P/l and the forth column represent the species for 106.59 mg P/l. It can be seen that Ca^{+2} is the dominant species for the different concentrations and for all stages followed by $CaHCO^{3+}$and $CaCO_3$. Whereas $CaHPO_4$, H_2PO_4 and HPO_4^{-2} were found in the speciation of the 100.66 mg P/l. $CaPO_4$ and HPO_4^{-2} were found in very small amount in solutions of 11.71 and 21.22 mg P/l. the predicted species within the mentioned pH range in agreement with the distribution of phosphate species reported in Chapter 2 Figure 2-3 where it is possible to find $H_2PO_4^-$ and HPO_4^{2-} in the acidic or slightly base medium and PO_4^{3-} species becomes significant and exceeds that of HPO_4^{2-} in the basic medium and acts as a source of anions. it can be seen that the main precipitate is calcite in solutions at low P concentration and calcite with calcium phosphate in solutions of high P concentration. These results agree with XRD, total carbon and total digest results.

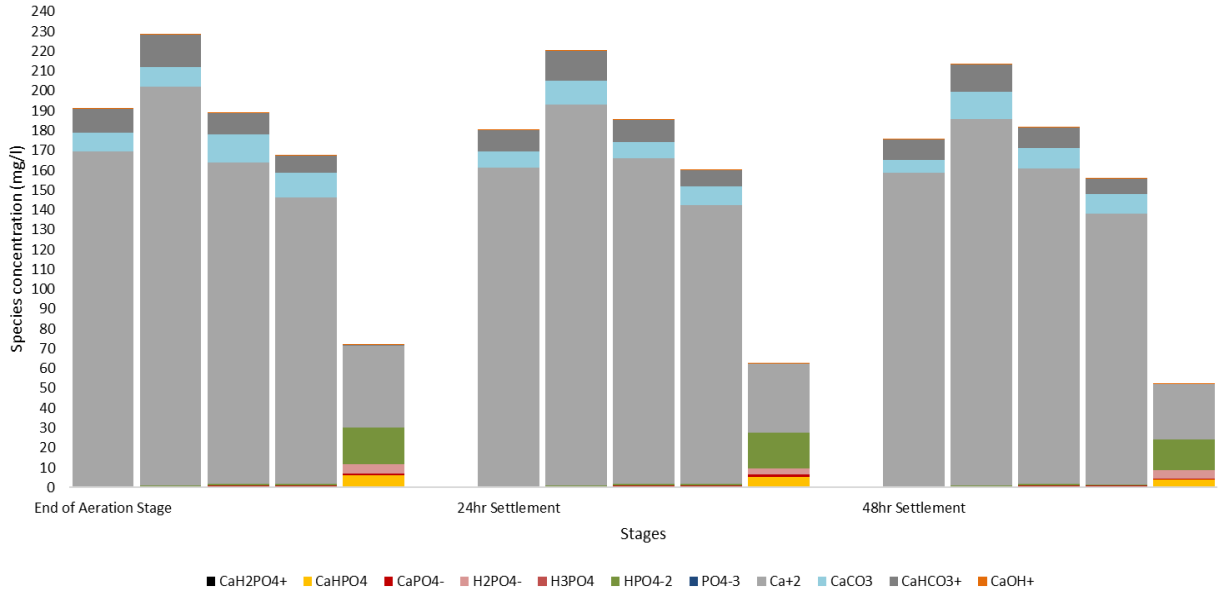

Figure 4- 34: PHREEQCI predicted calcium and phosphorus species. For the runs of 40 min carbonation, 40 min aeration, 24 and 48 hr settlement

4.6 CO_2 optimisation

This section investigates the alternatives to reduce or replace the carbon dioxide used previously to dissolve limestone as a most expensive part in the process.

4.6.1 Unsaturated and saturated carbonation stage

This section examines the calcite dissolution and the opportunity of getting the same or close calcium concentration to what was obtained from the previous system by changing the carbonation stage from an open column with limestone fully saturated with water as described in Chapter 3 section 3.2.1 to closed column with water circulating through the limestone. Calcium carbonate solubility is strongly influenced by the presence and availability of CO_2. When CO_2 is present, the solubility of calcium carbonate and thus the concentration of Ca^{2+}, will vary with changes in the P_{CO2}. as shown in the equation (4.4).

$$CaCO_3(s)+CO_2(g)+H_2O=Ca^{2+}+2\ HCO_3^- \quad (4.4)$$

Applying only 100 ml/min CO_2 flow rate for 1 hr and three circulation speeds of 100, 200 and 400 revolutions per minute (rpm) were used to circulate 1L of water through the limestone column. Figure 4.35(a) presents the effect of using unsaturated calcite column on Ca concentration using deionised water only. It is clear to see that by changing the carbonation stage to closed and unsaturated it is possible to get a Ca concentration of 201.1 mg/l within 40 min and 254.3 mg/l within 60 min of carbonation by using 100 ml/min CO_2 flow rate. While a Ca concentration of 250 mg/l obtained previously by running the carbonation stage using 750 ml/min of CO_2 for 30 min in the open saturated column. The increase in Ca concentration in the closed unsaturated system

may attributed to the availability of CO_2 and the contact between calcite and water. whereas a study on calcite dissolution in the ternary system $CaCO_3$ - H_2O - CO_2 by Buhmann and Dreybrodt (1985) have shown that for thin water film as they occur on rock surface exposed to rain fall, the dissolution rate depend on the thickness of the water film. It also can be seen that by applying slow circulation speed of 100 rpm resulted in higher Ca concentration of 201.1 mg/l whereas the concentration was 194.4 mg/l and 177.7 mg/l for the 200 and 400 rpm respectively after 40 min and that might be due to the increased thickness of the water film occurred on the calcite surface as a results of increasing the speed. Figure 4.35(b) show the change in pH values for the three speeds during carbonation stage. The pH trend was the same for the three speeds, a drop in pH value after 5 min of carbonation due to the formation of carbonic acid was observed followed by a gradual increase to the end of carbonation stage. The drop in pH value of the 400 rpm was less than of the 100 and 200 rpm indicating that high speed inversely correlated with pH and Ca concentration. Figure 4.36 presents the Ca concentration obtained by running the carbonation stage for 60 min with 100 ml/min in a closed saturated column. The results showed that after 40 min of carbonation, Ca concentration was 150.9 mg/l which is less than the concentration in the closed unsaturated column. This concentration increased to 224 mg/l after 20 min. Same pH trend was observed in the closed saturated system. The fundamental relationship between Ca concentration and P_{CO2} as described by Segnit et al. (1962) showing that under 1 atm P_{CO2} the Ca concentration will be 263 mg/l with pH of 5.98 and the results obtained in this section is in line with that fact.

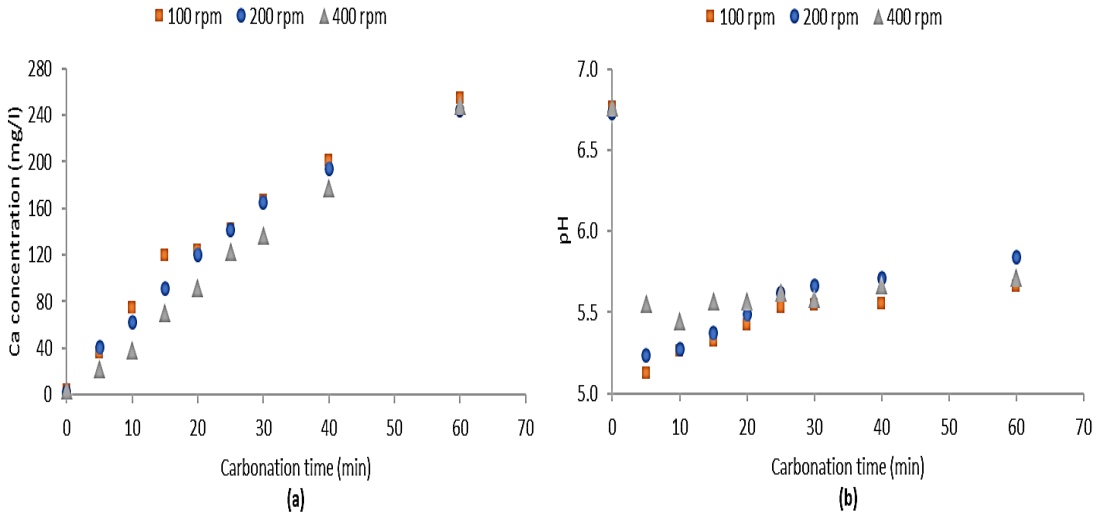

Figure 4- 35: (a) Ca concentration obtained by running the carbonation stage for 60 min with 100 ml/min CO_2 flow rate in a closed unsaturated column using 1 kg of limestone (b) shows the change in pH values

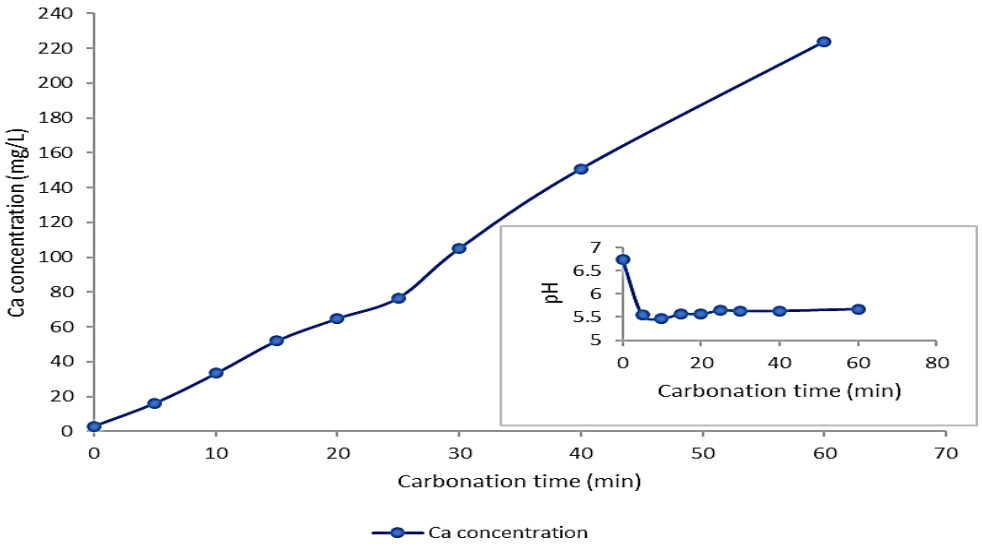

Figure 4- 36: Ca concentration obtained by running the carbonation stage for 60 min with 100 ml/min CO_2 flow rate in a closed saturated column

4.6.2 Acid usage instead of CO_2 gas

As mentioned in the literature chapter that limestone is not very soluble and do not dissolve very quickly. Earlier in this chapter, CO_2 was used to dissolve limestone. In the following test series, hydrochloric acid was added to deionised water with the intent of generating CO_2 and solubilising Ca. By adding acid, hydrogen ions H^+ will be added which will react with the carbonate to form hydrogen carbonate HCO_3^- ions, which are very soluble in water, and the limestone will dissolve. Or, if there is more acid, two hydrogen ions will react with a carbonate to form carbonic acid $H_2CO_3^-$ which will decompose to form carbon dioxide CO_2 which eventually bubbles off into the atmosphere, and water H_2O. Limestone can be dissolved according to the following mechanisms:

$$CaCO_3 + H^+ = Ca^{2+} + HCO_3^- \quad (4.5)$$

$$CaCO_3 + H_2O + CO_2 = Ca^{2+} = 2HCO_3^- \quad (4.6)$$

$$CaCO_3 + H_2O = Ca^{2+} + HCO_3^- + OH^- \quad (4.7)$$

Under certain conditions of pH and CO_2 pressure, one or another of these mechanisms may be dominant. At low pH, the acid dissolution mechanism is known to be the most rapid of the three mechanisms for limestone dissolution (Plummer et al. 1978). Three different doses of HCl (5 ml of 1%, 25 ml of 1% and 10 ml of 10%) were used for 48 hr contact time with 1kg of limestone in 1 litre of DI water, Ca concentration and pH values were measured. Figure 4.37 show the Ca concentration and pH as a function of contact time. Concentrations of Ca^{2+} increased considerably in the treated water. For the first dose of 5 ml of 1%, the Ca concentration was 15.5 mg/l after 5 min then increased to 27.2 mg/l after 2 hr then increased to 64.3 mg/l after 24 hr, the final concentration was 71.5 mg/l after 48 hr. By increase the volume to 25 ml, Ca concentration was 57.3 mg/l after 5 min, increased to 82.4 mg/l after 2 hr, 114.8 mg/l after 24 hr and 121.4 mg/l

after 48 hr. Whereas the concentration raised to 370.7 mg/l after 5 min then increased to 512 mg/l after 2 hr of adding (10 ml of 10%) HCl. After 24 hr Ca concentration increased to 656.4 mg/l and reached to 732.8 mg/l after 48 hr. The pH results show the instant drop in pH value due to the acid addition for all solutions. This decrease in pH were followed by gradual increase. pH values for the three solutions were 7.2, 6.9 and 7.2 respectively at the end of 48 hr.

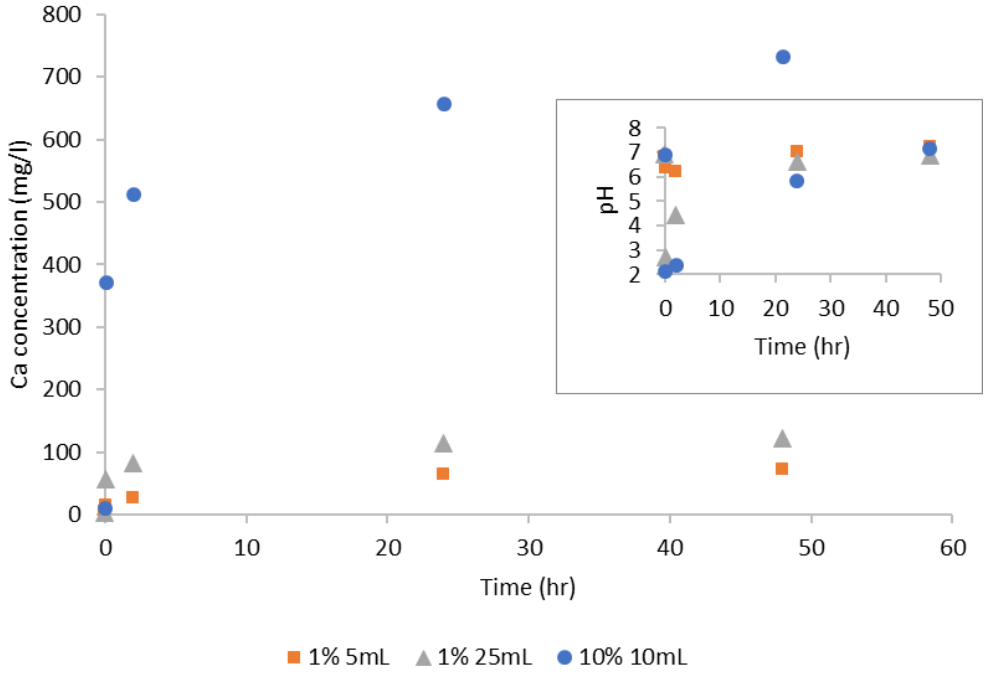

Figure 4- 37: Ca concentration and pH as a function of contact time with different HCl dose

The following batch test were carried out by adding HCl to a synthetic wastewater solution of 2 and 10 mg/l P concentration and run the aeration stage followed by settlement stage 5 and 10 ml of 10 % HCl were used for 48 hr contact time with acid. 30 min of aeration and 48 hr of precipitation. P, Ca concentrations and pH values were measured. Figure 4.38 (a, b and c) present the results of P concentration during the three stages respectively. As shown in Figure 4.38(a) There was no noticeable decrease in P concentration during the acid addition stage for initial P of 2 mg/l for both 5 and 10 ml of 10% of acid. Whereas there was a decrease in the concentration of 10 mg/l to 7.2 and 7.3 mg/l for 10 and 5 ml respectively. During aeration stage, P concentration decreased from 1.96 to 1.66mg /L for the solution of 2 mg/l P initial concentration and 10 ml acid and from 1.9 to 1.67mg/l for solution of 5 ml. Whereas for solutions of 10 mg/l initial P concentration and 10 ml acid, the concentration dropped from 7.2 to 1.7 mg/l and from 7.2 to 3.5 mg/l for 5 ml acid after 30 min aeration as shown in figure 4.38(b). During settlement, the concentration for the solutions of 2 mg P/l and 10 ml acid dropped from 1.66 to 1.2 mg/l and from 1.67 to 1.5 mg/l for 5 ml acid. Concentration for the solutions of 10 mg P/l and 10 ml acid dropped from 1.66 to 1.4 mg/l and from 1.66 to 2.1 mg/l for 5 ml acid as shown in figure 4.38(c).

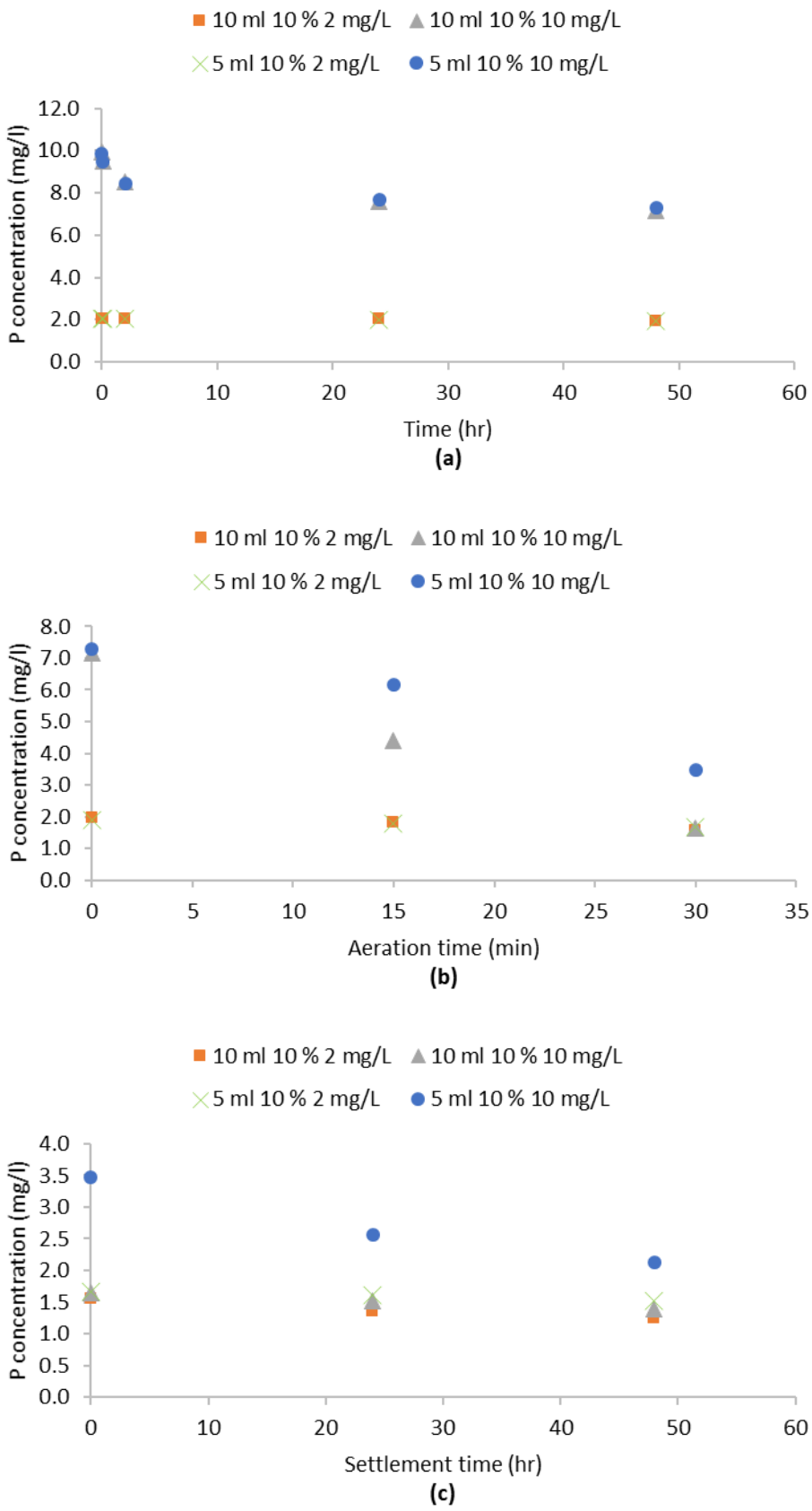

Figure 4- 38: P concentration during the three stages (a) contact with acid (b) aeration (c) settlement

Figure 4.39(a, b and c) present the results of Ca concentration during the three stages respectively. During acid addition stage there was a rapid increase in Ca concentration during the 48hr contact time. Solutions of 2 mg/l with 10 ml acid and 10 mg/l with 10 ml acid showed the highest Ca concentration of 555.7 and 511.3 mg/l respectively. Whereas the Ca concentration for solutions of 2 mg/l with 5 ml acid and 10 mg/l with 5 ml acid was 319.1 and 298.4 mg/l respectively as shown in figure 4.39(a). During aeration stage, Ca concentration dropped from 555.7 to 413.8 mg/l and from 511.3 to 315.8 mg/l in solutions of 2 mg/l with 10ml acid and 10 mg/l with 10 ml acid respectively. Whereas there was small decrease in Ca concentration from 319.1 to 295.6 mg/l in solution of 2 mg/l with 5 ml acid and from 298.4 to 274.6 mg/l in solution of 10 mg/l with 5 ml acid as shown in figure 4.39(b). During settlement stage, Ca concentration dropped from 413.8 to 238 mg/l in solutions of 2 mg/l with 10ml acid and from 315.8 to 248.5 mg/l in solutions of 10 mg/l with 10 ml acid. Ca concentration decreased from 295.6 to 269.6 mg/l in solution of 2 mg/l with 5 ml acid and from 274.6 to 252.9 mg/l in solution of 10 mg/l with 5 ml acid as shown in figure 4.39(c).

Figure 4.40(a, b and c) present the results of pH during the three stages respectively. An instant drop in pH value was observed for all solution followed by gradual increase over the contact time with acid. Increase in pH values for solutions of 10 mg/l initial concentration with 5 and 10 ml acid were close and showed higher pH than those of 2 mg/l initial P concentration as shown in Figure 4.40(a). This increase in pH values continued over the 30 min aeration time. pH values for solutions of 2 and 10 mg/l with 10 ml acid were close and higher than those of 5 ml acid as shown in Figure 4.40(b). During settlement time a decrease in pH values has been observed for all solutions as shown in Figure 4.40(c).

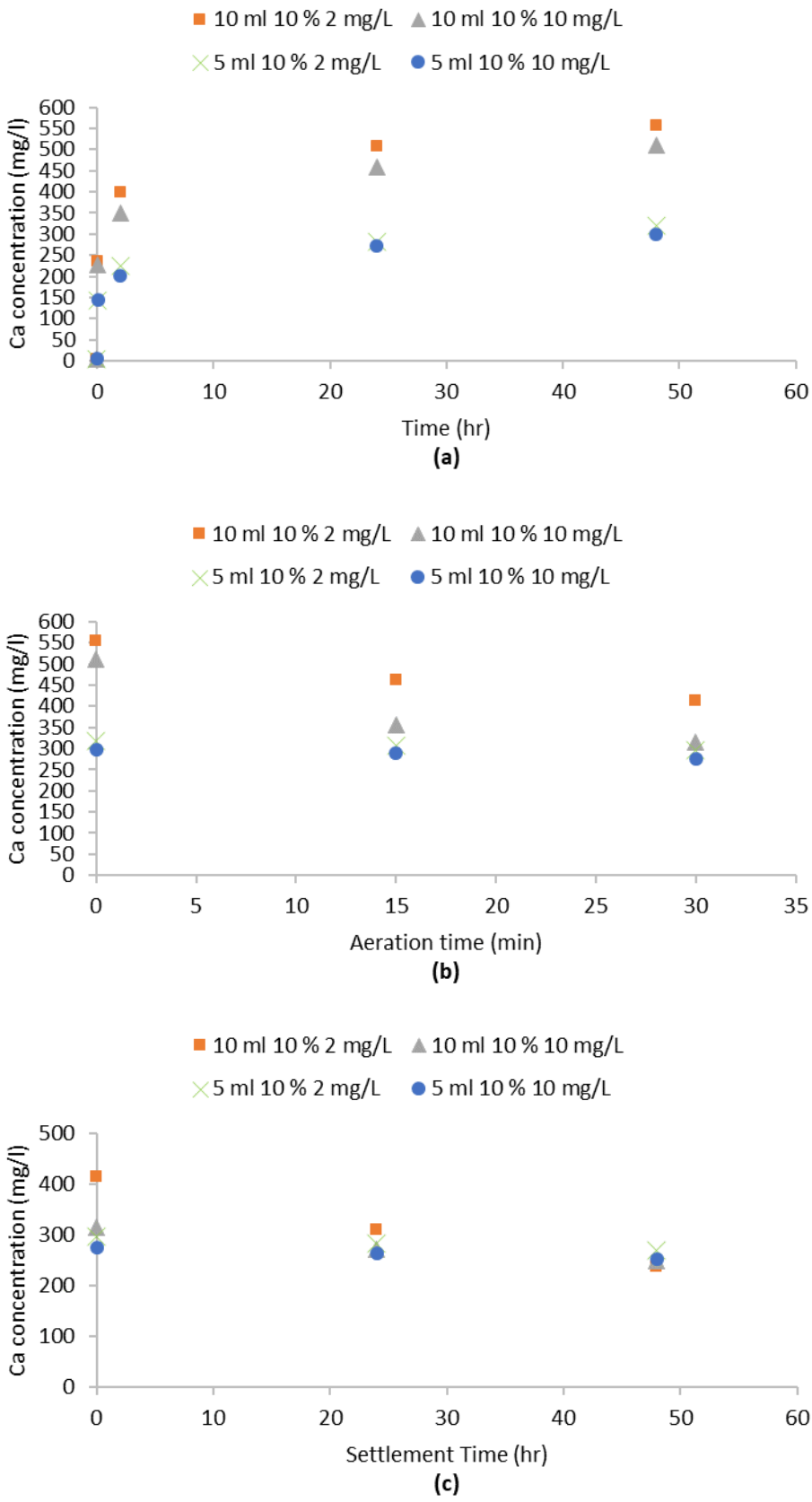

Figure 4- 39: Ca concentration during the three stages (a) contact with acid (b) aeration (c) precipitation

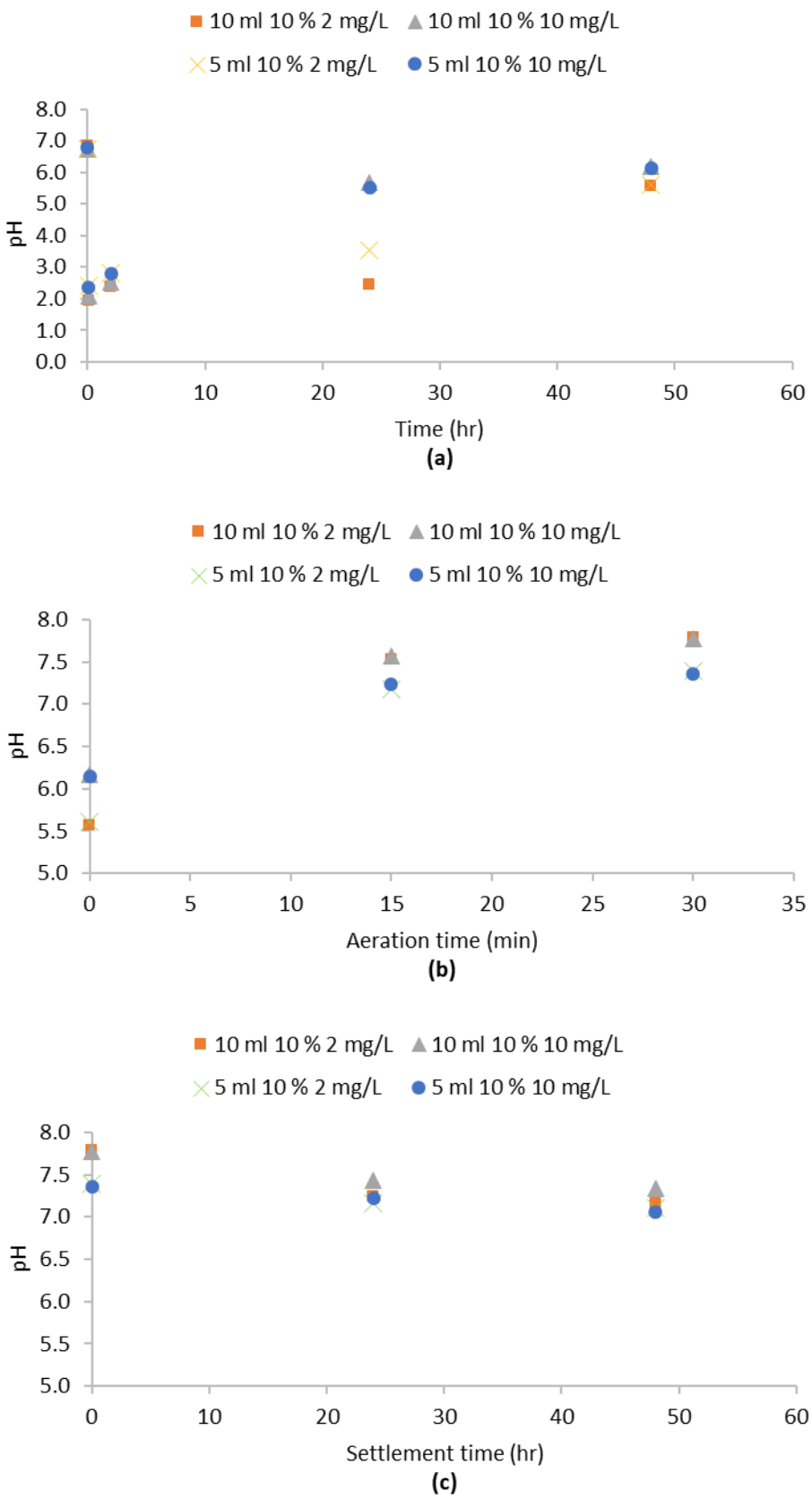

Figure 4- 40: pH during the three stages (a) contact with acid (b) aeration (c) precipitation

Figure 4.41 show the pH dependent solubility behaviour of calcium phosphates (Vanderesse et al. 2011). As pH increases to more basic values calcium phosphate becomes increasingly insoluble. In contrast, as the pH approaches the acidic regime, calcium phosphate becomes increasingly soluble. All phases of calcium phosphate become increasingly soluble below pH 6. The solubility of HAP at pH 7 to 8 is between 3.1 and 0.31 mg/l as seen in Figure 4.38 .From Figure 4.37(c) the final pH range for all solutions were 7.1 to 7.8 during settlement stage and the final P concentration in this stage ranged from 1.24 to 1.52 mg/l for all solution except the solution of 10mg/l initial P concentration and 5ml of 10% HCl the final concentration was 2.13 mg/l. these results are in line with the expected solubility of HAP.

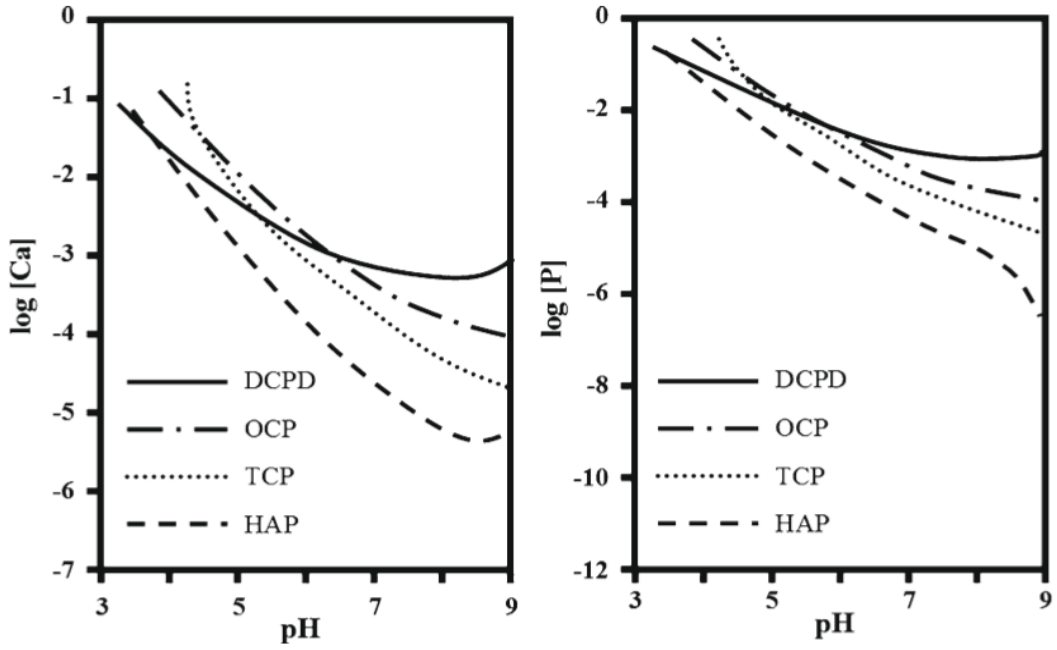

Figure 4- 41: pH dependent solubility behaviour of calcium phosphates. (Vanderesse et al. 2011)

4.6.3 Limestone with gypsum

Previous research indicates that the solubility of gypsum rock in 100 g water is greater than 200 mg at room temperature, while the solubility of limestone is just 12 mg (Liu et al., 2017; Ma et al., 2016; Wu et al., 2017).The solubility of gypsum rock is relatively high, so it readily dissolves under a range of external conditions following the equation below:

$$CaSO_4(s) + 2H_2O \rightleftharpoons CaSO_4 \cdot 2H_2O(s) \rightleftharpoons Ca^{2+} + SO_4^{2-} + 2H_2O \quad (4.8)$$

In comparison to gypsum rock, the dissolution of limestone is restricted to certain environmental conditions and depends on CO_2 and acid strength as illustrated in the following equations (Hong et al. 2018):

$$CaCO_3(s) \rightleftharpoons Ca^{2+} + CO_3^{2-} \quad (4.9)$$

$$CaCO_3(s) + CO_2 + H_2O \rightleftharpoons Ca^{2+} + 2HCO_3^- \quad (4.10)$$

$$CaCO_3(s) + 2H^+ \rightleftharpoons Ca^{2+} + CO_2 + H_2O \quad (4.11)$$

An experiment was carried out using the same lab system by replacing 500 gm of the limestone used previously with 500 gm of gypsum (2-5) mm particle size. The experimental conditions were as follows: 40 min carbonation, 40 min aeration and 48 hr settlement. The CO_2 flow rate was 100 ml/min. Initial P concentration of 10 mg/l was used. Figure 4.42(a) show the results of Ca concentration over the experiment time. It can be seen that after 40 min carbonation Ca concentration increased to 607.2 mg/l then decreased to 559.8 mg/l after 40 min aeration, this decrease continued during precipitation time to 520.8 mg/l. There was a small decrease in P concentration during carbonation stage from 10.3 to 9.38 mg/l. At the end of aeration stage P concentration dropped to 1.27 mg/l followed by further decrease to 0.69 mg/l at the end of settlement stage as shown in Figure 4.42(b). Figure 4.42(c) show pH changes during experiment. pH dropped from 6.85 to 5.16 during carbonation then increased to 6.78 during aeration, this increase in pH value continued to 7.42 during the first 24 hr settlement followed by slight decrease in the second 24 hr to 7.22. It can be seen that Ca concentration obtained by running the system with 100 ml/min CO_2 flow rate using 500 mg of gypsum with 500 mg of limestone is almost double the concentration when only limestone was used and at 750 ml/min CO_2 flow rate under the same conditions and P concentration. It should be noted that the greater solubility of $CaSO_4$ means that the number of molecules that are precipitated out when brought past the saturation point will be significantly higher than found with $CaCO_3$ under lower pH. The similar solution mechanisms with the high solubility of gypsum mean that $CaSO_4$ should have a similar reaction to changes in P_{CO2}. The decrease in Ca concentration during aeration and settlement stages indicated that the precipitation reaction works with calcium sulphate as well. The recorded drop in P concentration can suggest that calcium sulphate could be very effective at removing phosphates from wastewater when they are present in high concentrations.

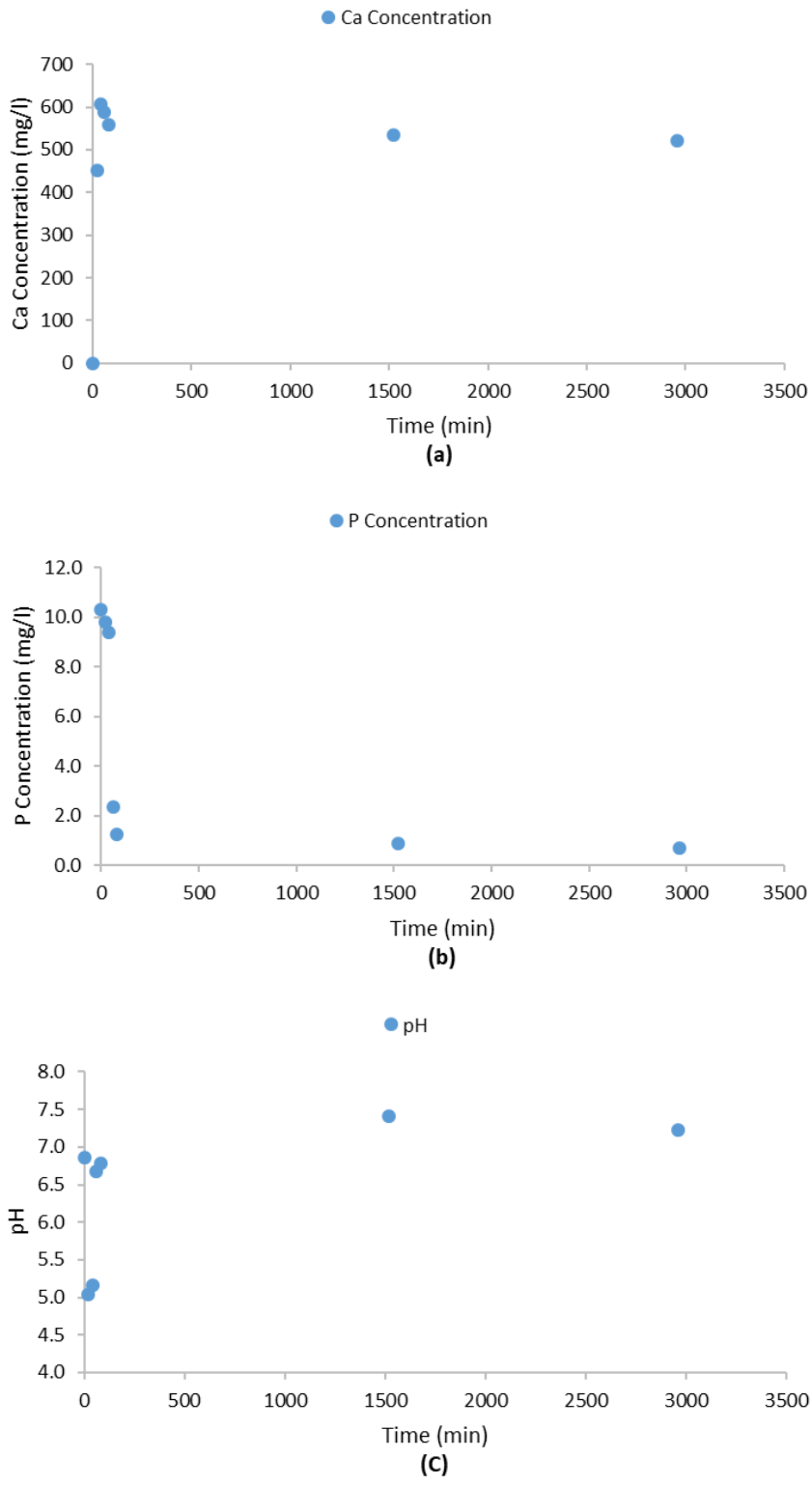

Figure 4- 42: Shows the changes in (a) Ca concentration (b) P concentration (c) pH Over the experiment time

4.7 Chapter Summary

This chapter has presented the data for running the process to remove phosphorus. It is possible to draw the following conclusions:

1. Different CO_2 flow rates were tested to optimize the parameters for the pilot plant. The results clearly showed that $CaCO_3$ dissolution increased by increasing the volumetric CO_2 flow rate and the duration.
2. XRD analysis showed that the precipitate formed from running the proposed system with limestone and water in the absence of P to be calcite
3. A technique of removing phosphorus from wastewater was tested in this chapter. In all test runs phosphorus concentration was reduced, indicating that the carbonation process works as a treatment process to remove phosphate from solution.
4. All the tests showed a definitive and quantitative link between calcium and phosphate concentrations in the solution. Based on the carbonation precipitation theory, it is expected to see a drop in dissolved calcium concentration alongside a reduction in phosphorus concentration after aeration. Sampling after aeration back this theory up.
5. P removal during aeration stage varied with aeration time. Most runs showed maximum removal between 25 and 40 min. Lowest P concentration left in solution was 0.6 mg/l.
6. The major removal of P was found to occur during aeration stage. However, a decrease in P concentration along with Ca concentration during settlement stage indicating further removal of P.
7. In most of the test runs, the final effluent had calcium concentrations far in excess of the initial concentration. These high calcium levels give the potential for further precipitation and phosphorus removal.
8. It was confirmed that aeration is effective for elevating the pH of all solutions and for the precipitation of P by degassing CO_2.
9. Removal of CO_2 by aeration, resulting in the precipitation of calcium carbonate and calcium phosphate.
10. Calcite dissolution was clearly retarded by dissolved phosphorus concentrations and water composition.
11. Under the operating conditions of the limestone reactor, the CO_2 flow rate of 0.75 ml/min sets the maximum Ca concentration that can be achieved, in accordance with the equilibrium Ca concentration. However, because of the limited time available in the system, equilibrium is not reached.
12. The mass of P removal increased with increasing the initial phosphate concentrations

13. PHREEQCI modelling has demonstrated that all solutions of 1.26, 3.55, 11.71,21.22 and 106.59 mg P/l are unsaturated with respect to the carbonate mineral phases calcite and aragonite upon equilibration with atmospheric CO_2. SI of HAP at low phosphorus concentrations 1.26 and 3.55 were negative indicating unsaturated phase while at initial P concentrations 11.74, 21.22 and 106.59 HAP was saturated.
14. Changing the carbonation column to closed unsaturated with 100 rpm circulation speed at 100 ml/min CO_2 increased the Ca concentration to 201.0 mg/l after 40 min carbonation. Ca concentration recorded in this case was greater than that in the open saturated column when 750 ml/min of CO_2 was used. Using HCl instead of CO_2 to dissolve limestone was effective in increasing the dissolved Ca ions in solution and reducing P concentration. The effectiveness of using gypsum as a replacement reaction was gratifying. This is a very low energy consuming were only 100 ml/min of CO_2 were applied and cheap material that could easily be utilised, the resulting solution has a very high concentration of dissolved Ca.

Chapter 5: Precipitate characterisation and removal Mechanisms and laboratory experimentation on apatite

5.1 Introduction

Chapter 5 presents the results of precipitate full characterisation. Further to this, an investigation on the dominant removal mechanisms in which two concentrations of P were used. This chapter also include full characterisation of the two apatite media and their removal mechanism investigation. All experiments included in this chapter were carried out in triplicate. The chapter is split into the following sections:

Section 5.2: Precipitate characterisation – presenting and discussing the results of the precipitates mineral and geochemical characterisation tests including XRD, Total carbon, total digest ESEM and FEG-SEM

Section 5.3: Removal mechanism – Presenting and discussing the results of adsorption experiment, sequential extraction of synthetic and real wastewater precipitate and zeta potential charge of calcite

Section 5.4: Apatite – Presenting and discussing both media characterisation and removal mechanisms

Section 5.5: Chapter summary and conclusions.

5.2 Precipitate Characterisation

5.2.1 X-ray diffraction results

The precipitate was collected from the laboratory system (see section 4.3 chapter 4). The first group of samples was the precipitate collected from running P solution using deionised water in preparation and P concentration of (2,10,20 and 100) mg/l Figure 5.1 (a-d). The second group was the precipitate collected from running P solution using tap water in preparation and P concentration of (In tap water P concentration, 2,10,20 and 100) mg/l Figure 5.2 (a-e). The third XRD analysis was carried out on the precipitate produced from running a real wastewater sample Figure 5.3. The experimental conditions for the collected precipitates were: 40 min carbonation, 60 min aeration, and 48 hr settlement. In each case, the XRD analysis is displayed as plots of total counts against goniometric angle °2 Theta (°2θ). According to ion activity product calculation of different calcium phosphate phases, several calcium phosphate may be formed, including amorphous calcium phosphates (ACP), octacalcium phosphate (OCP, $Ca_4H(PO_4)_3 \cdot 2.5H_2O$),

tricalcium phosphate (TCP, $Ca_3(PO_4)_2$) and hydroxyapatite (HAP, $Ca_5H(PO_4)_3OH$), depending on the pH and the composition of calcium and phosphate ($H_2PO_4^-$ or HPO_4^{2-}) of the solution. Calcium phosphate precipitation depends on the formation of stable nuclei after which crystal growth takes place, and on the degree of supersaturation. The state of supersaturation is generally developed by increasing calcium, OH^- and phosphate concentrations in the solution. High total Ca^{2+} concentration and high pH are normally required for the precipitation of calcium. Abbona and Baronnet (1996) reported that ACP and octacalcium (OCP) could not be formed in an alkali solution having a pH of above 8. Johansson and Gustafsson (2000) showed that hydroxyapatite(HAP) is the major form of calcium phosphate precipitates and is connected to strongly alkaline conditions (pH > 9) and large amounts of soluble Ca. In general, XRD patterns for the precipitate of 2, 10, 20 mg P/L showed apparent well-ordered particle distribution of Ca minerals within the precipitates this implies that most Ca precipitates are in the crystalline nature. Whereas the XRD results suggested that the precipitate during the removal of phosphate by calcite for the precipitate of 100 mg P/l was hydroxyapatite and calcium carbonate.

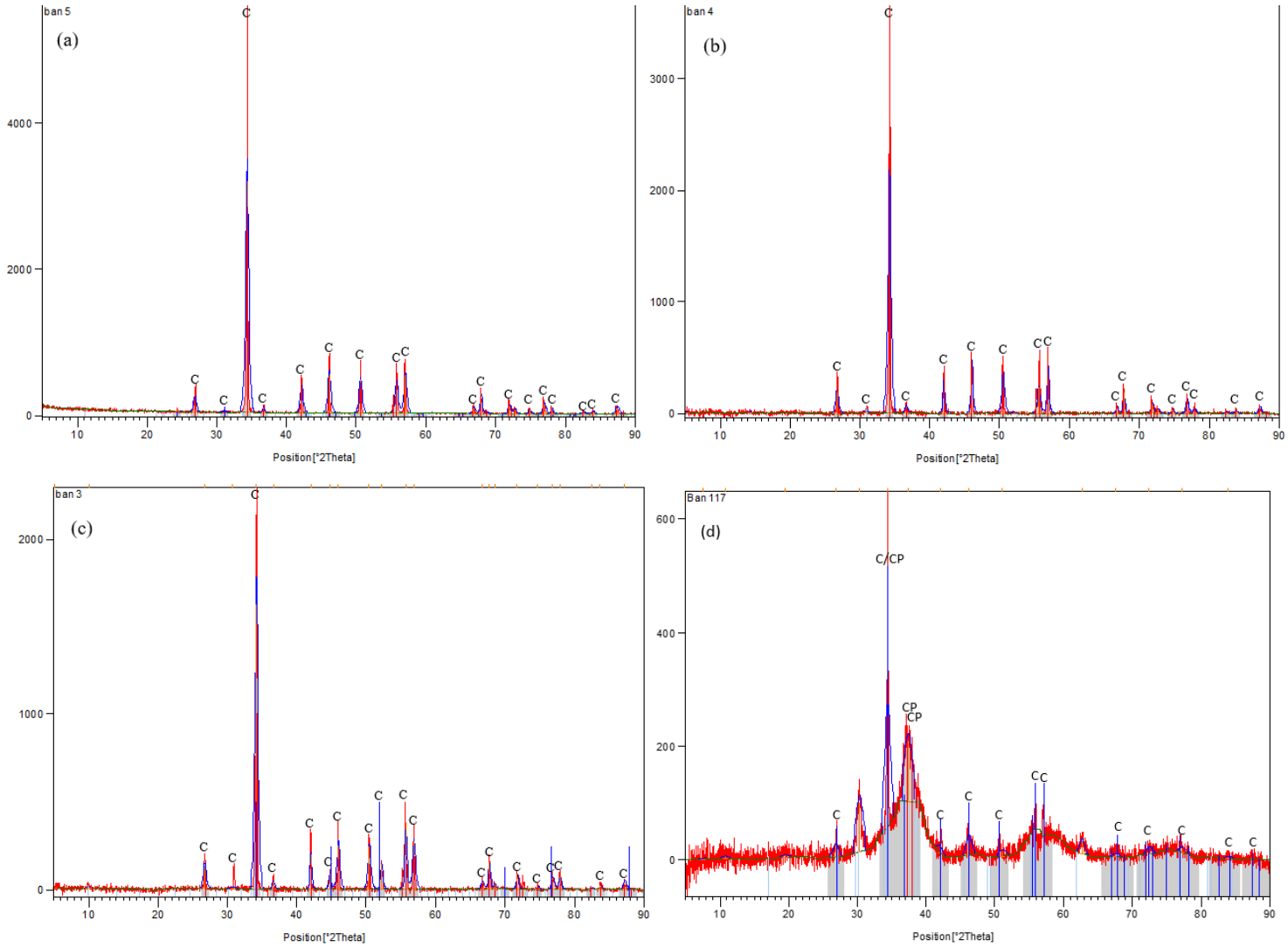

Figure 5- 1 (a-d) XRD trace determined for precipitates of 2.28,10.38,20.71and 100.66 mg P/L deionised water solutions

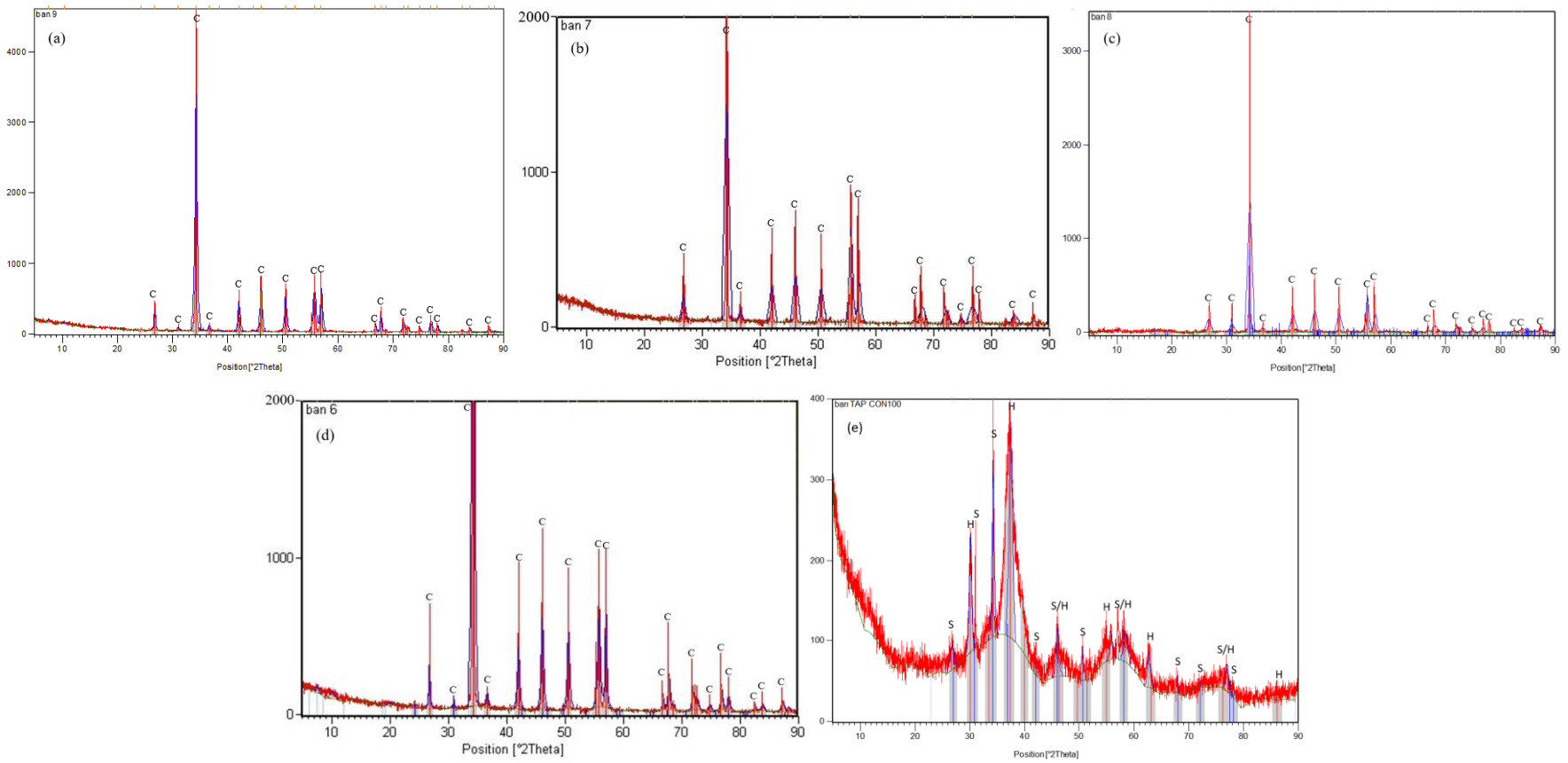

Figure 5- 2 (a-e) XRD trace determined for precipitates of 1.26,3.55,11.74, 21.22and 106.59 mg P/L Tap water solutions

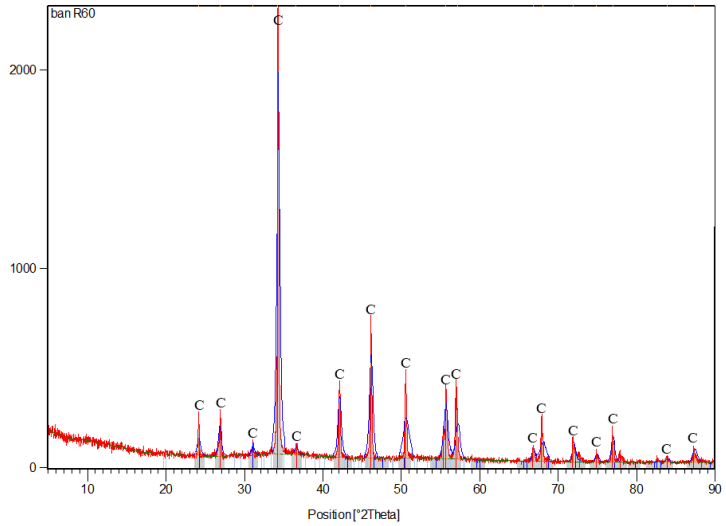

Figure 5- 3 XRD trace for real wastewater precipitate of TP 9mg/l

5.2.2 Total Carbon and Total Digest Results

The percentage content by weight for the all precipitate is included in table 5.1. The experimental conditions for the collected precipitates were: 40 min carbonation, 60 min aeration, and 48 hr settlement. In general precipitates of initial P concentration of 2,10,20 were found to contain 30-36 % calcium by weight and carbon content of 12-7.6% indicating that calcite is the main precipitant. Precipitates of 100 mg P/l were found to have less calcium content 23-26% and less carbon content not more than 2.7% indicating that hydroxyapatite is the precipitant in addition to calcite thus showing good agreement with XRD results. Various phosphorus content according to the initial concentrations were found in each sample. equation (5.1) describes the formation of calcite in the presence of carbonate and equation 5.2 shows the formation of calcium phosphate:

$$Ca^{2+} + HCO_3^- + OH^- \rightarrow CaCO_3 + H_2O \quad (5.1)$$

$$2PO_4^{3-} + 3Ca^{2+} \rightarrow 3Ca_3(PO_4)_2 \quad (5.2)$$

From equation 5.2 it can be seen that two phosphate ions replace three carbonate ions in order to form calcium phosphate. Ishikawa and Ichikuni (1981) suggested that the vacancy created as a result of orthophosphate substitution for carbonate ions in the calcite lattice structure is either filled with an alkali halide like OH^-, Cl^-, F^- and Br^- so the compound formed will be a variation of apatite i.e hydroxyapatite or the vacancy created filled with Ca^{2+} to form calcium carbonate again. Based on Ca and carbon content included in table 5.1 and from the molar mass of $CaCO_3$ (100 g/mol) with 12:40 of C: Ca and the molar mass of $CaPO_4$ (135 g/mol) with 31:40 of P: Ca and by assuming that all C content is in form of $CaCO_3$ the proportion of both components can be calculated.

Table 5- 1: Results of total digest and total carbon %

Water type	P concentration. mg/l	Elements (weight content %)						Carbon content %
		Ca	P	Mg	Si	Al	Fe	
Deionised water	2.28	33.93	0.423	0.068	1.432	0.19	0.233	11.8
	10.38	31.57	3.731	0.093	1.336	0.349	0.187	9.6
	20.74	30.44	7.015	0.062	0.92	0.276	0.122	8.2
	100.66	23.38	13.27	0.186	0.81	0.11	0.14	2.7
Tap water	1.26	35.48	0.111	0.065	0.196	0.109	0.114	12.0
	3.55	36.25	0.374	0.077	0.08	0.028	0.046	11.3
	11.71	33.89	2.314	0.113	0.174	0.104	0.152	10.7
	21.22	31.24	5.47	0.121	0.171	0.107	0.099	7.6
	106.59	26.46	12.07	0.287	0.074	0.033	0.042	2.0
Real wastewater	9	30.29	2.365	0.132	0.233	0.195	0.173	9.6

5.2.3 ESEM Results

ESEM images data were compared for the different precipitate samples. The first group was the precipitate collected from running P solution using deionised water in preparation and P concentration of (2,10,20 and 100) mg/l Figure 5.4, 5.5, 5.6 and 5.7. The second group was the precipitate collected from running P solution using tap water in preparation and P concentration of (In tap water P concentration, 2,10,20 and 100) mg/l Figure 5.8, 5.9, 5.10, 5.11 and 5.12. The third analysis was carried out on the precipitate produced from running a real wastewater sample Figure 5.13. The experimental conditions for the collected precipitates were: 40 min carbonation, 60 min aeration, and 48 hr settlement. The ESEM images shows that the precipitate has a crystalline appearance changed to amorphous phase with the increase in phosphorus concentration. By comparing the morphology of the precipitate resulted from DI, Tap and real wastewater, it can be seen that the foreign ions presented in tap water and real wastewater do not affect morphology of the precipitate. The ESEM images also correspond with the interpretation of the XRD graphs suggesting a crystalline phase for low P concentrations and an amorphous phase for the high concentration due to the formation of calcium phosphate precipitate. The spectrum data for these samples listed in table 5.2 show good correspondence with the results from ICP analysis for the element content. It is important to mention that carbon

was excluded from any quantification as most of the carbon signal is from the carbon coat rather than the sample.

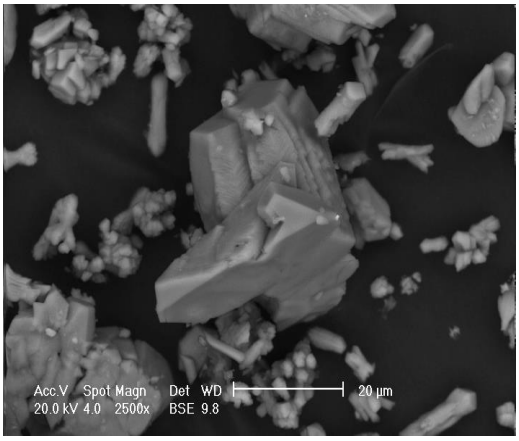

Figure 5- 4: SEM images for precipitates of 2.28 mg/l P, DI water solution showing the crystalline structure

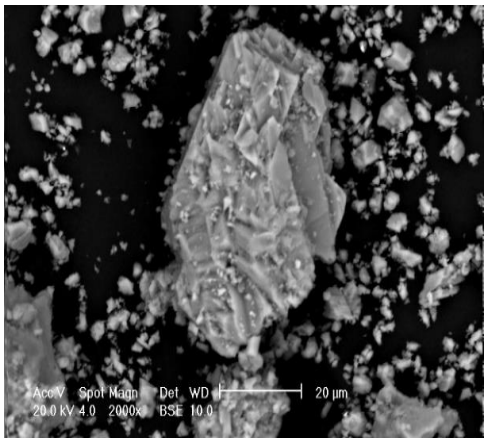

Figure 5- 5: SEM images for precipitates of 10.38mg/l P, DI water solution showing the crystalline structure

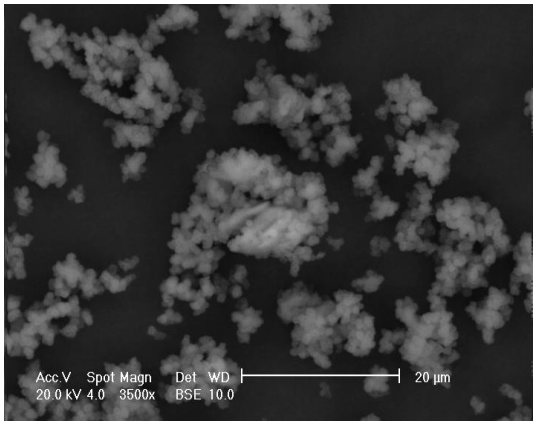

Figure 5- 6: SEM images for precipitates of 20.71mg/l P, DI water solution showing the crystalline structure

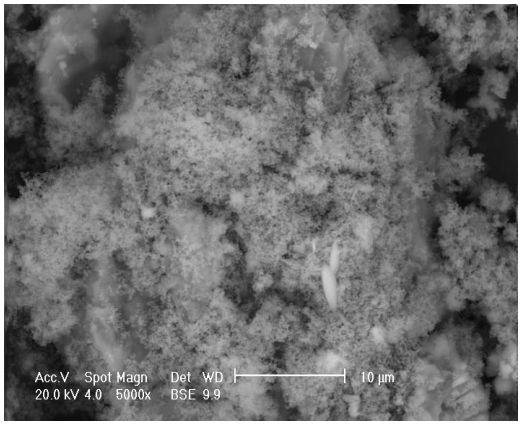

Figure 5- 7: SEM images for precipitates of 100.66mg/l P, DI water solution showing the amorphous structure

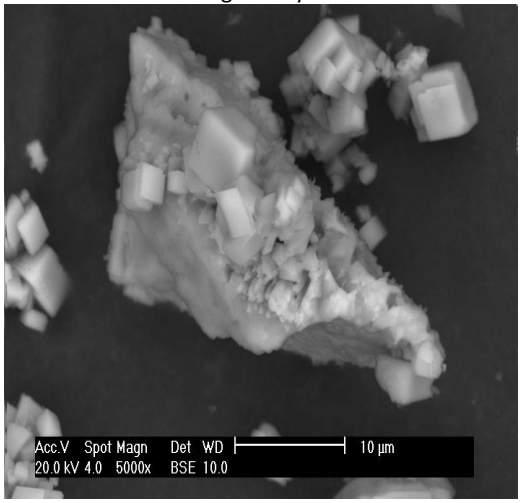

Figure 5- 8: SEM images for precipitates of 1.26mg/l P, tap water solution showing the crystalline structure

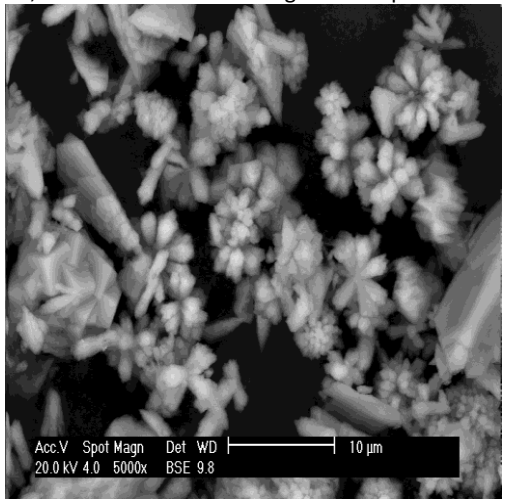

Figure 5- 9: SEM images for precipitates of 3.55 mg/l P, tap water solution showing the crystalline structure

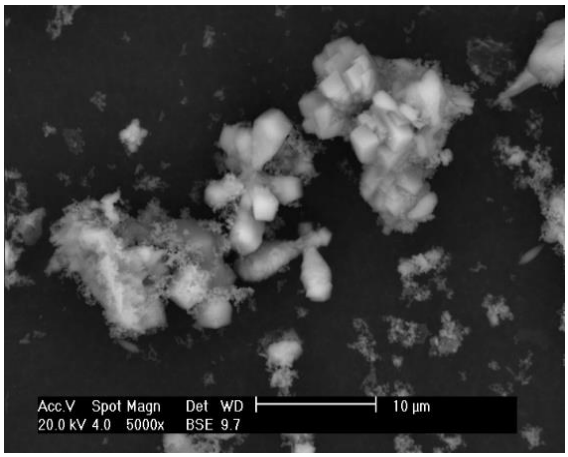

Figure 5- 10: SEM images for precipitates of 11.74 mg/l P, tap water solution showing the crystalline structure

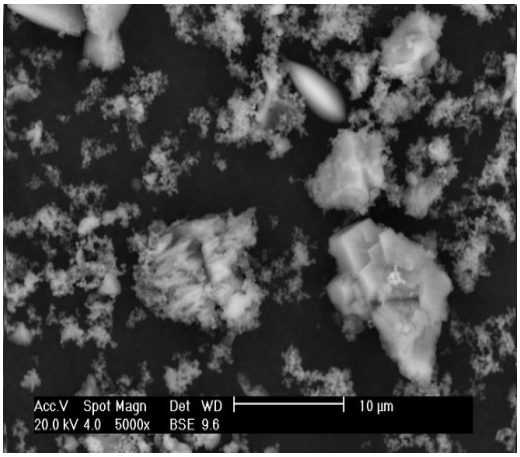

Figure 5- 11: SEM images for precipitates of 21.22 mg/l P, tap water solution showing the crystalline structure

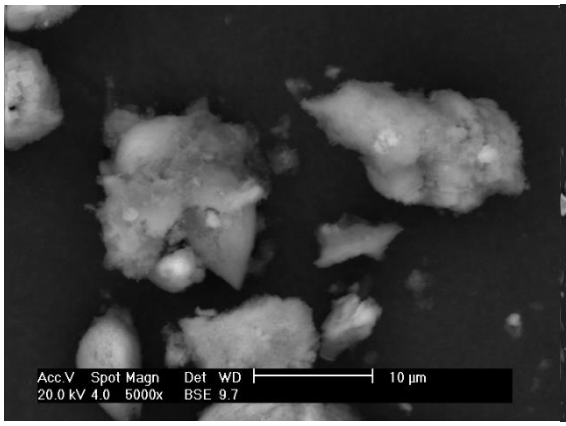

Figure 5- 12: SEM images for precipitates of 106.59 mg/l P, tap water solution showing the amorphous structure

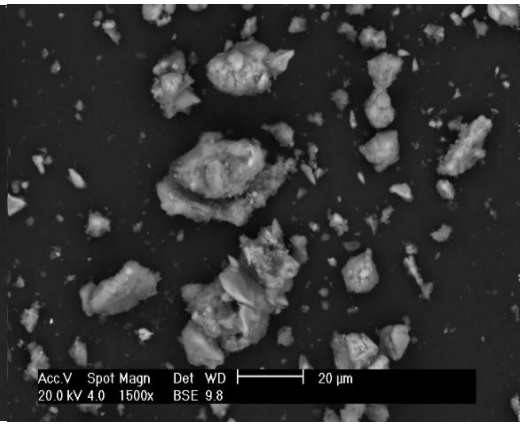

Figure 5- 13: SEM images for precipitates of real wastewater, showing the crystalline structure

Table 5- 2: Emission spectrum data from ESEM analysis of samples from figures 5.4 to 5.13

Sample description	Fig. ref.	Ca, wt % As CaO	P, wt %	O, wt %	Si,wt %	Mg,wt %	Total, wt %
Precipitate of 2 mg/l P and DI water	5.4	67.94	0.39	30.39	0.13	0.0	100.00
Precipitate of 10 mg/l P and DI water	5.5	66.91	2.05	30.52	0.28	0.0	100.00
Precipitate of 20 mg/l P and DI water	5.6	59.7	4.0	35.15	0.4	0.0	100.00
Precipitate of 100 mg/l P and DI water	5.7	36.76	21.6	40.68	0.95	0.0	100.00
Precipitate of tap water P solution	5.8	33.76	0.3	65.93	0.0	0.0	100.00
Precipitate of tap water P + 2mg/l P solution	5.9	31.66	0.29	68.05	0.0	0.0	100.00

Sample description	Fig. ref.	Ca, wt % As CaO	P, wt %	O, wt %	Si,wt %	Mg,wt %	Total, wt %
Precipitate of tap water P + 10mg/l P solution	5.10	52.52	0.31	46.91	0.25	0.0	100.00
Precipitate of tap water P + 20mg/l P solution	5.11	34.87	1.79	63.17	0.17	0.0	100.00
Precipitate of tap water P+100mg/l P solution	5.12	27.33	16.96	52.85	0.56	0.3	100.00
Precipitate of real wastewater sample	5.13	25.42	0.19	74.23	0.16	0.0	100.00

5.2.4 FEG- SEM Results

FEG-SEM analysis has carried out to show the elemental distribution with the precipitate. The first group was the precipitate collected from running P solution using deionised water in preparation and P concentration of (2,10,20 and 100) mg/l as shown in figures 5.14,5.15,5.16 and 5.17 respectively. The second group was the precipitate produced from running a P solution using tap water in preparation and P concentration of (In tap water P concentration, 2,10,20 and 100) mg/l as shown in figures 5.18,5.19,5.20,5.21 and 5.22 respectively. The third sample was the precipitate produced from running a real wastewater sample as shown in figure 5.23. The experimental conditions for the collected precipitates were: 40 min carbonation, 60 min aeration and 48 hr settlement. This analysis is clearly showing that P is present in the precipitate and distributed across the sample with calcium distributed uniformly over each sample indicating close association between Ca and P as there was no patches of P concentrated in one spot so the P coverage was uniform. At high P concentration, carbon presence was less suggesting that the precipitate is calcium phosphate while when carbon was concentrated more than phosphorus indicating calcium carbonate formation and this agrees with XRD, total carbon and total digest results. The results also showing that the presence of foreign ions in the tap water and wastewater did not affect P distribution within the precipitate.

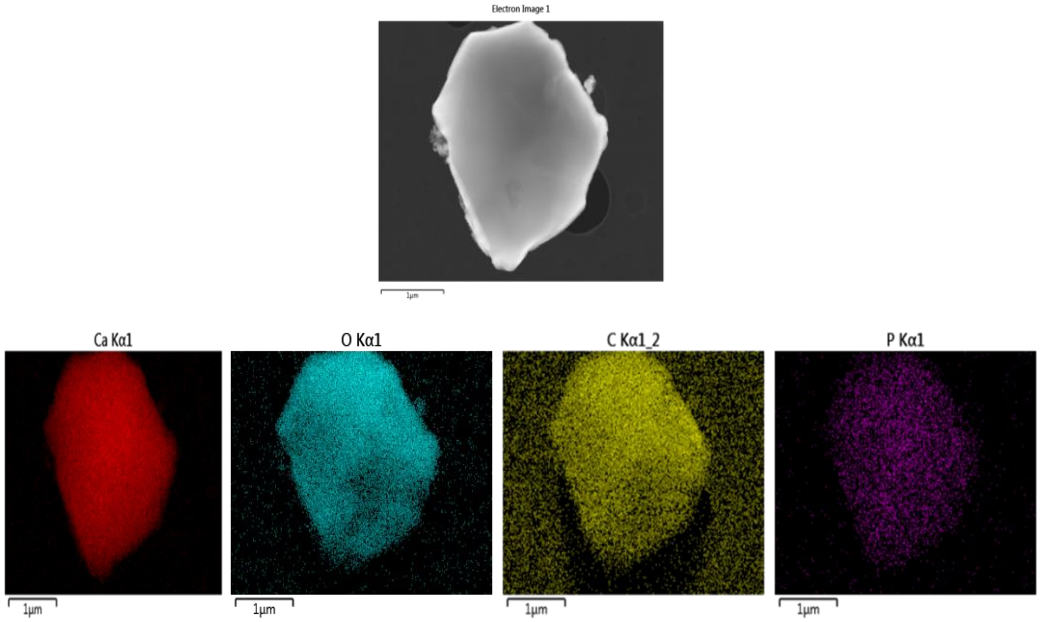

Figure 5- 14: FEG-SEM images showing elements distribution for 2.28 mg P/l precipitate. Deionised water solution

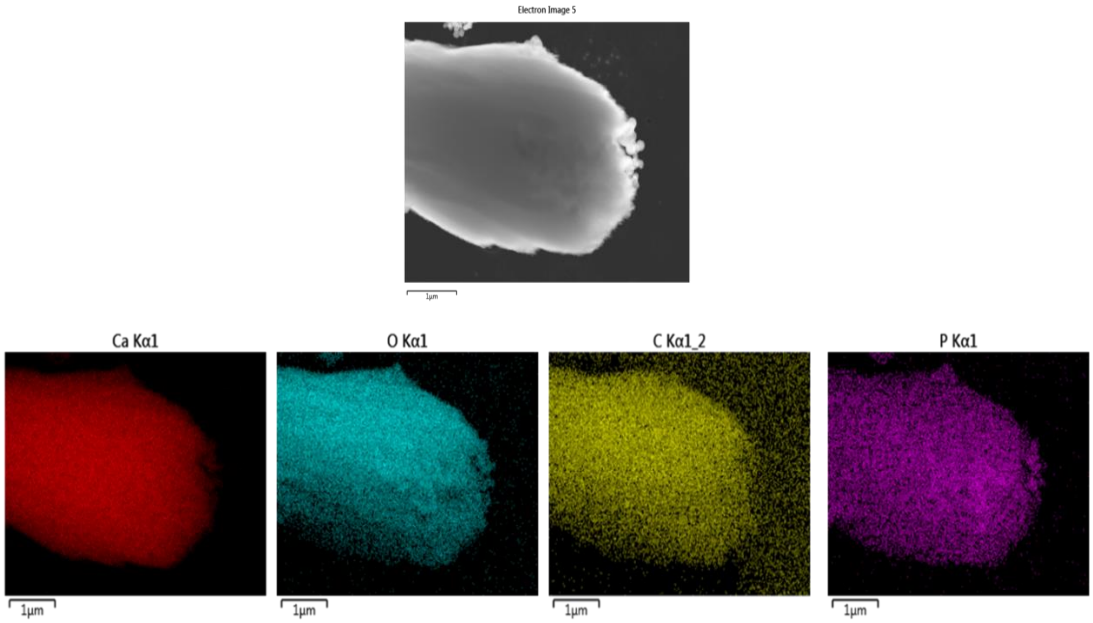

Figure 5- 15: FEG-SEM images showing elements distribution for 10.38 mg P/l precipitate. Deionised water solution

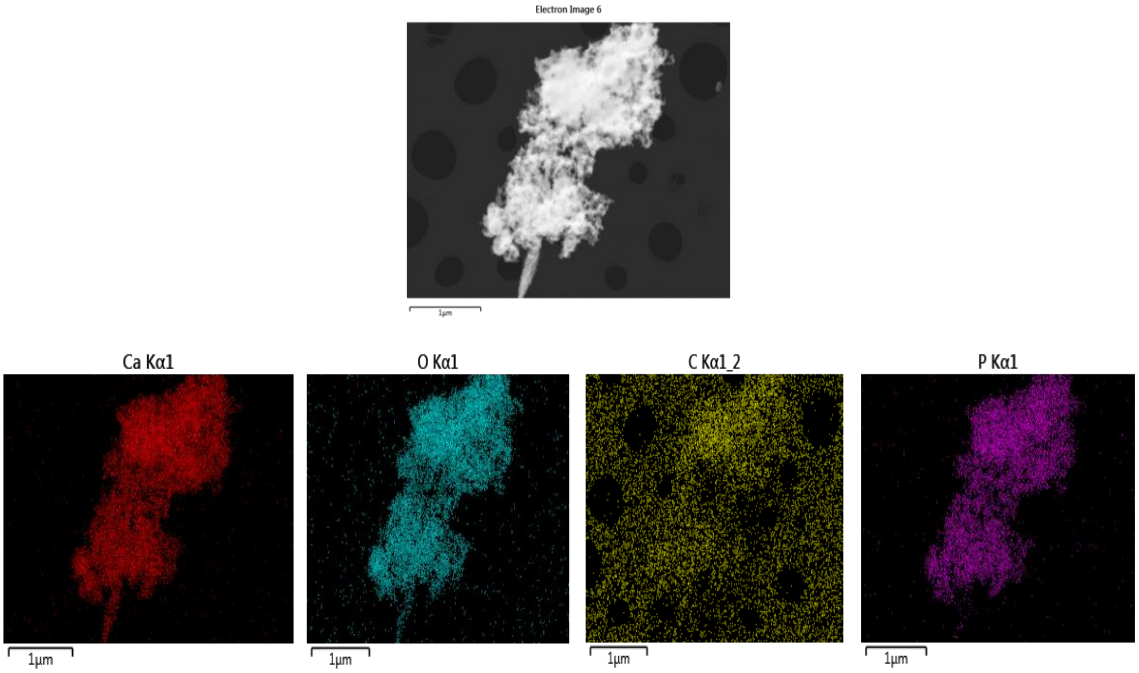

Figure 5- 16 FEG-SEM images showing elements distribution for 20.71 mg P/l precipitate. Deionised water solution

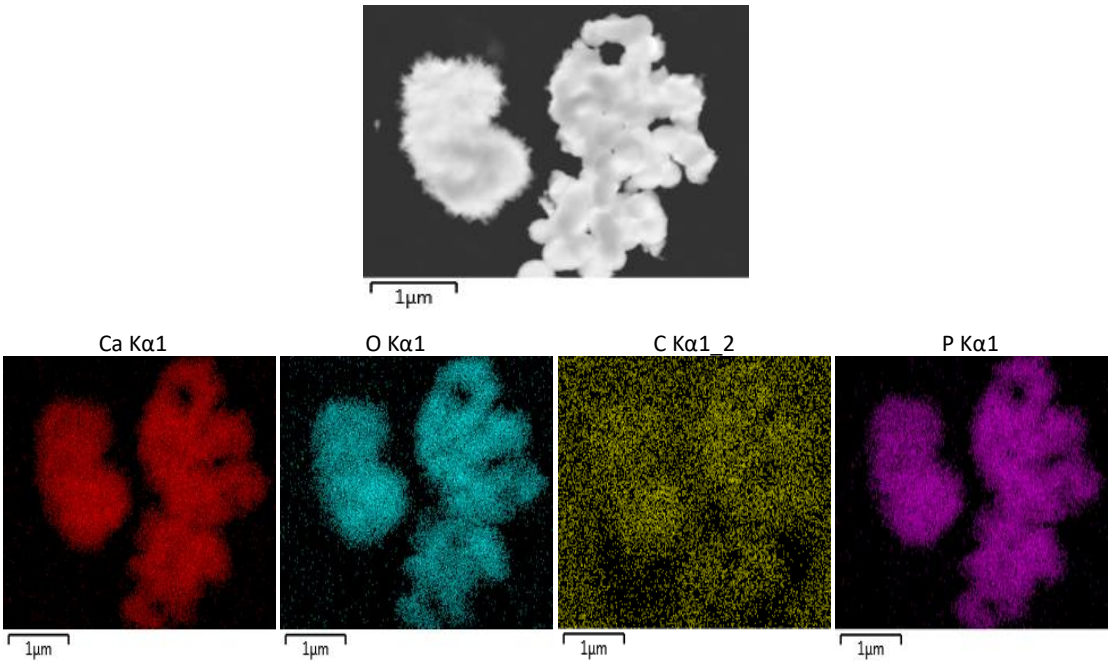

Figure 5- 17: FEG-SEM images showing elements distribution for 100.66 mg P/l precipitate. Deionised water solution

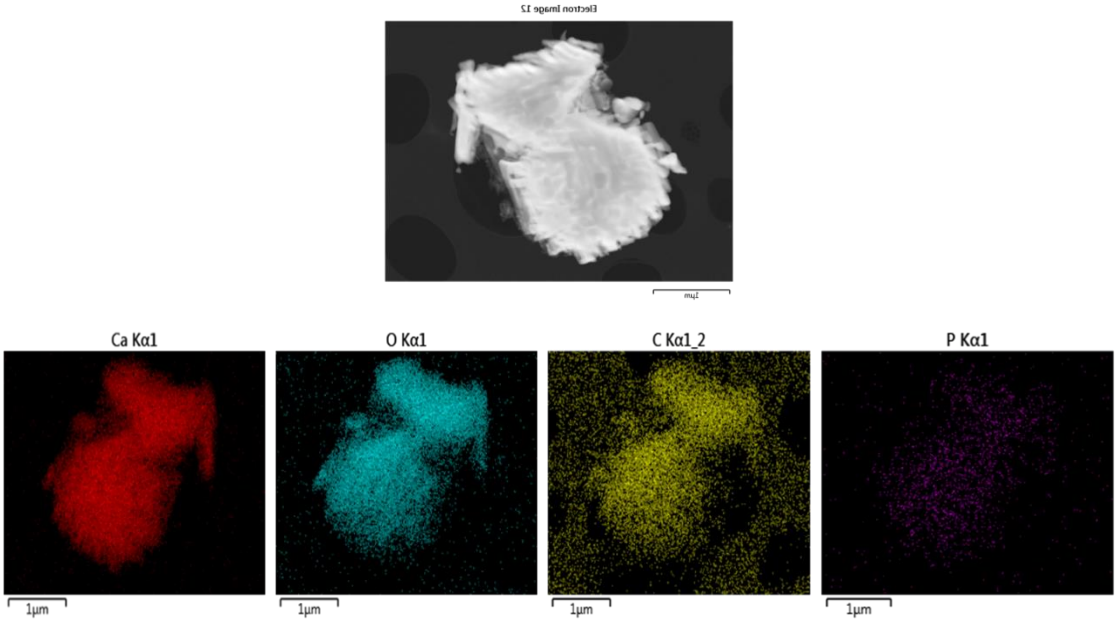

Figure 5- 18: FEG-SEM images showing elements distribution for 1.26 mg P/l precipitate. Tap water solution

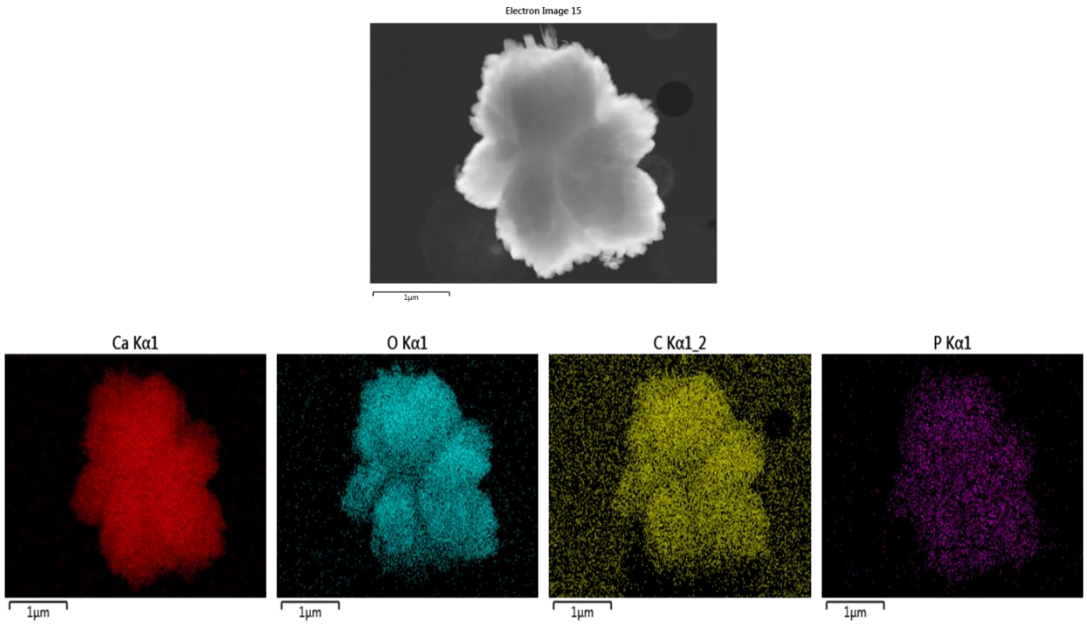

Figure 5- 19: FEG-SEM images showing elements distribution for 3.35 mg P/l precipitate. Tap water solution

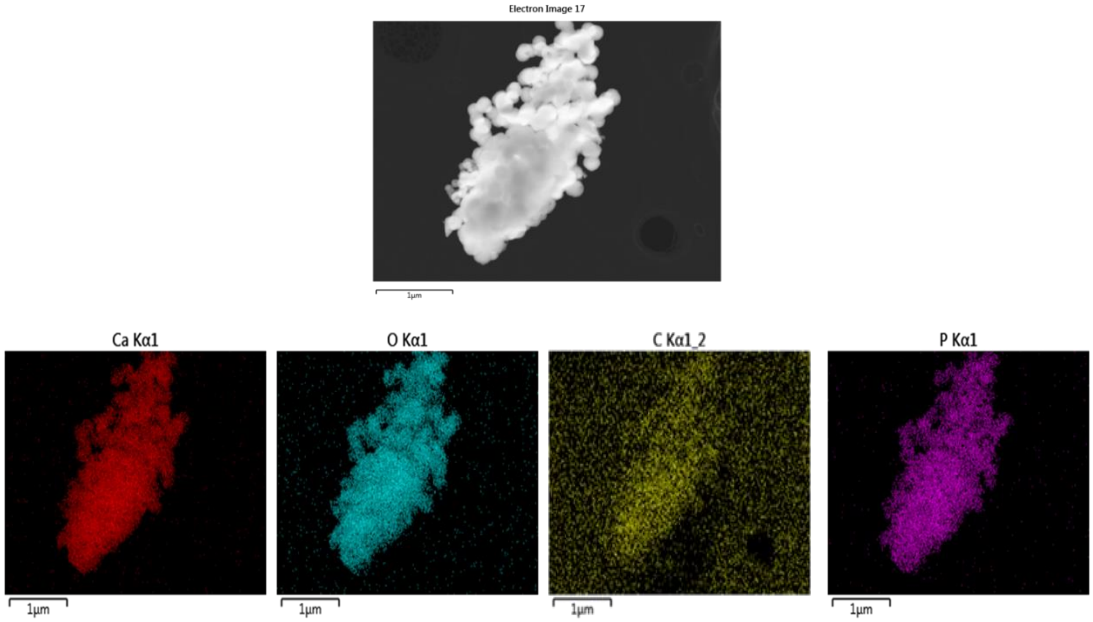

Figure 5- 20: FEG-SEM images showing elements distribution for 11.74 mg P/l precipitate. Tap water solution

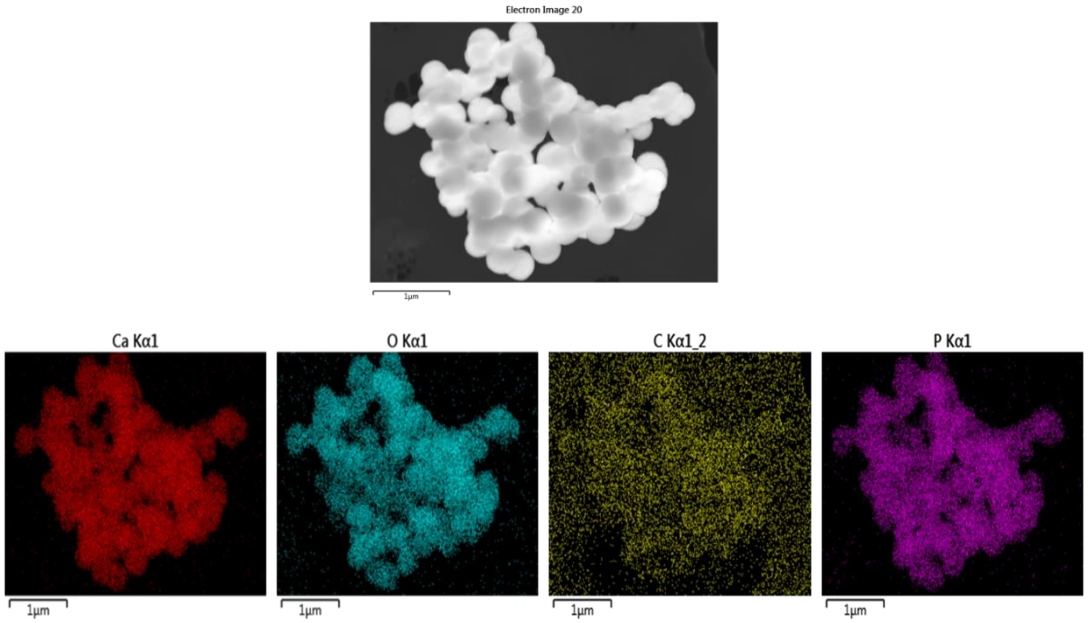

Figure 5- 21: FEG-SEM images showing elements distribution for 21.22 mg P/l precipitate. Tap water solution

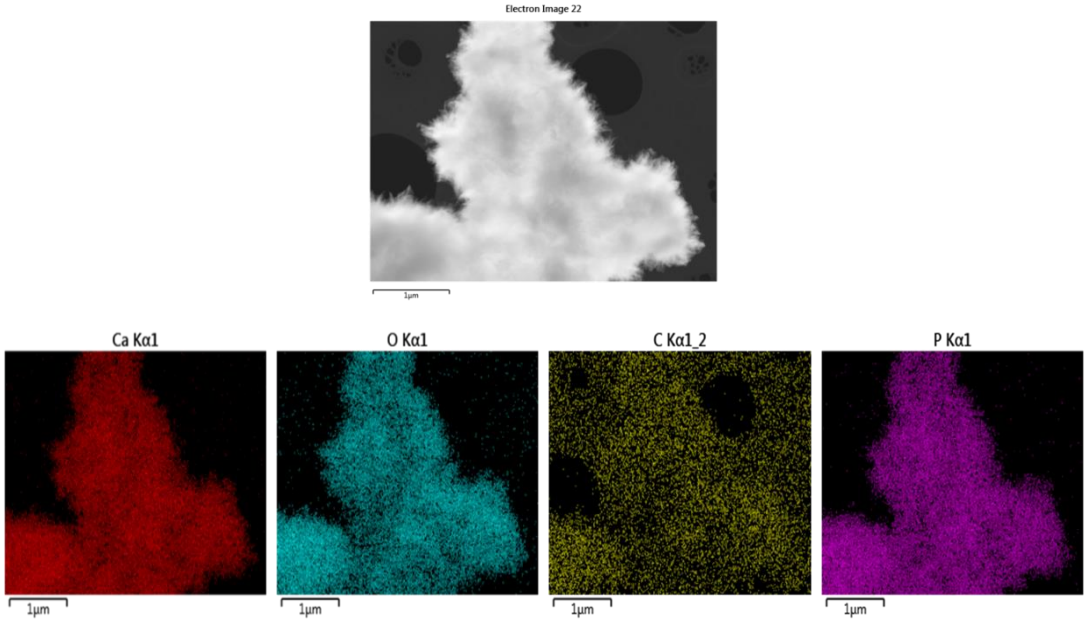

Figure 5- 22: FEG-SEM images showing elements distribution for 106.59 mg P/l precipitate. Tap water solution

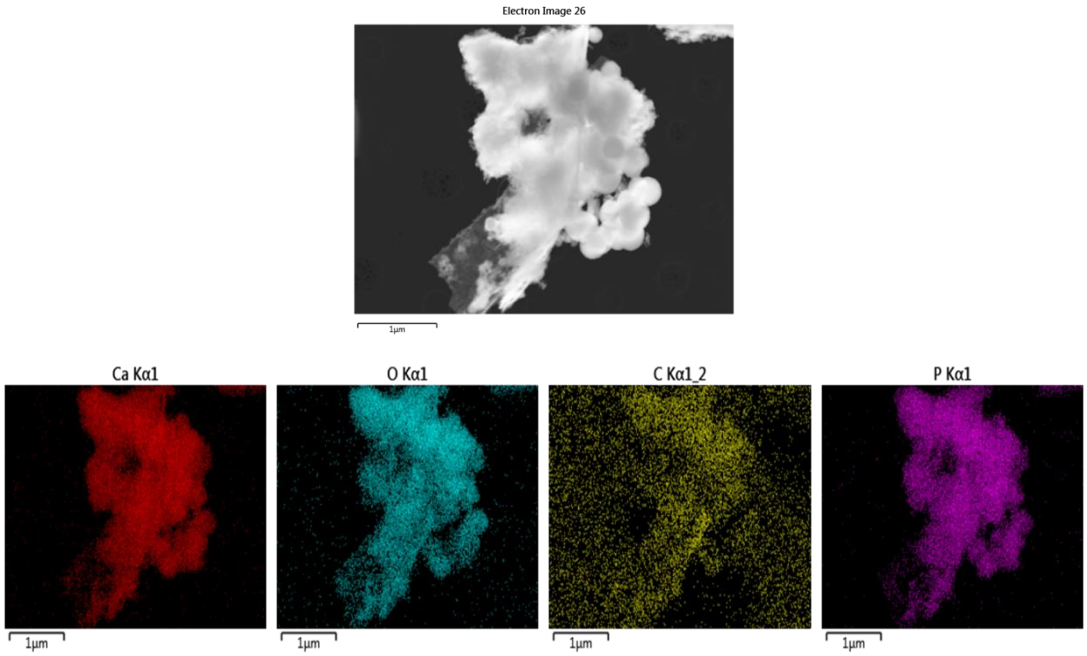

Figure 5- 23: FEG-SEM images showing elements distribution for 9.0 mg P/l precipitate. Real wastewater solution

5.3 Removal mechanism

The mechanism of removal of phosphate species on surface or onto the pores between the structure depends on different factors such as the solubility of the adsorbent in the aqueous medium, the chemical composition and the nature of phosphate species (Hanna et al. 2008). Sindelar et al. (2015), Song et al. (2006) and Wang et al. (2012b) have shown the following common features: the initial rapid uptake of phosphate onto calcite occurs through surface

adsorption, which is then followed by a slow transformation of amorphous calcium phosphate prior to nucleation or precipitation of calcium phosphate. Dove and Hochella (1993) both showed that P can be incorporated into active crystal growth sites. Liu et al. (2012) has proven that the reaction mechanisms of phosphate with calcite can be either adsorption at a low concentration, typically less than 4.64 mg/l or precipitation under high concentrations. The aim of this section is to work out a dominant mechanism of adsorption or precipitation using batch test by adjusting the initial PO_4^{3-} concentration, reaction time and pH.

5.3.1 Removal kinetics

The kinetics of phosphate removal by calcite precipitated by running the process with limestone and DI water are shown in Figure 5.24(a) and Figure 5.25(a) as a function of contact time. According to Figure 5.24(a) and 5.25(a) at initial P concentration of 2 mg/l and 10 mg/l respectively. Initially a plateau was observed indicating surface adsorption of P. The plateau lasted for 24 hr then followed by an abrupt drop. The duration of plateau signifies an induction time and the abrupt drop points may signify the change in the removal mechanism from adsorption to precipitation. The results from both figures showing that it took 24 hr to drop from 10 to 8 mg/l, while the P concentration of initial 2 mg/l dropped to only 1.88 mg/l during 24 hr for all initial pH levels. Sø et al. (2011) observed the sudden decrease in P concentration after 24 hr reaction time with initial concentration of 10 mg/l and this observation is in agreement with our result. Figure 5.24(b) presents the change in Ca concentration over the reaction time for initial P concentration of 2 mg/l. It can be seen that Ca concentration decreased with increasing pH value during the whole reaction time. The same trend has been observed for initial P concentration of 10 mg/l as shown in Figure 5.25(b). it should be noted that Ca concentrations for initial P concentration of 2 mg/l were higher than for the initial P concentration of 10mg/l for pH values of 8 and 9 indicating calcite dissolution was clearly retarded by dissolved phosphorus (Montes-Hernandez et al. 2009). Whereas for pH 7 Ca concentrations were lower for initial P concentration of 2 mg/l. Figure 5.24(c) presents the change in pH over the reaction time for 2 mg/l initial P concentration. It can be seen that at lower initial P concentrations and at initial pH of 7 and 9, pH value saw a slight increase during the first 24 hr and this increase fluctuated over the remaining time. At initial pH 8, pH value showed an obvious decrease within the first 6 hr and increased later. For 10 mg/l initial P concentration and at initial pH of 7 and 8, pH value saw a slight increase during the first 6 hr and this increase fluctuated over the remaining time. At initial pH 9, pH value showed an obvious decrease within the first 6 hr and increased after that as shown in Figure 5.25(c). For both initial concentration of 2 and 10 mg/l the increase in pH level after 24 hr may be attributed to the formation of hydroxyapatite indicating the precipitation as the dominant mechanism after 24 hr

contact time. In general, the results showed that Ca dissolution and P removal is comparatively higher in the slightly basic pH region of pH 7 and decreases for higher pH values of 8 and 9 for the initial P concentration of 2 and 10 mg/l. The same observation were made by Cowan et al. (1990) while House et al. (1986) reported the opposite. Mangwandi et al. (2014) found that the adsorption of phosphate is pH dependent and phosphate adsorption favoured acidic conditions. On the other hand Xu et al. (2014) reported the opposite when pH less than 8, phosphate at low concentration initially presented low sorption affinity on calcite and a significant decrease in the dissolved phosphate concentration due to increased precipitation on calcite mineral with increasing phosphate concentration. Sø et al. (2011) found that the adsorption of phosphate onto calcite is time dependent and adsorption only occurred in a short time less than 24 hr. Because precipitation is a continuation of surface complexation, it is expected that adsorption would dominate in the beginning of the process followed by precipitation. The transition between adsorption and precipitation is time dependant and can be linked to the concentration of the negative surface sites, as well as an increase in the calcite dissolution which promotes the formation of Ca-P compounds (Perassi and Borgnino 2014). By comparing Ca concentration at the end of experiment with the expected Ca concentration in equilibrium with HAP (figure 2.2 section 2.3.3 chpter 2) it can seen the Ca concentration inline with the expected concentration for the batches of 2 and 10 mg P/l at pH 7 and 8 while the Ca concentration of batches 2 and 10 mg P/l at ph 9 is higher that the expected concentration. It is well known that precipitated Ca-P phases in aqueous solutions mainly include dicalcium phosphate (DCPD), octacalcium phosphate (OCP) and hydroxyapatite (HAP). OCP and DCPD, however, have been regarded as precursors of HAP or the metastable phases of Ca-P because that they are kinetically favourable (Cao et al. 2007; Wang et al. 2012a). At the final pH levels ranged between 7.4 and 9.1, the dominant forms in solution were HPO_4^{2-}, $Ca^{2+}$and CO_3^{2} . The removal reactions can be described through the following reactions (Wang et al. 2012a). The first reaction occurs when pH is low and resulted in amorphous calcium phosphate formation which then transform to HAP. The second and third reaction resulted in the formation of HAP directly in higher pH range (Suzuki et al. 2002).

$$Ca^{2+} + HPO_4^{2-} = CaHPO_4 \quad (5.3)$$

$$10\ Ca^{2+} + 6PO_4^{3-} + 2OH^- = C_{10}(PO_4)_6(OH)_2 \quad (5.4)$$

$$10CaCO_3 + 2H^+ + 6HPO_4^{2-} + 2H_2O = Ca10(PO_4)_6(OH)_2 + 10HCO_3^- \quad (5.5)$$

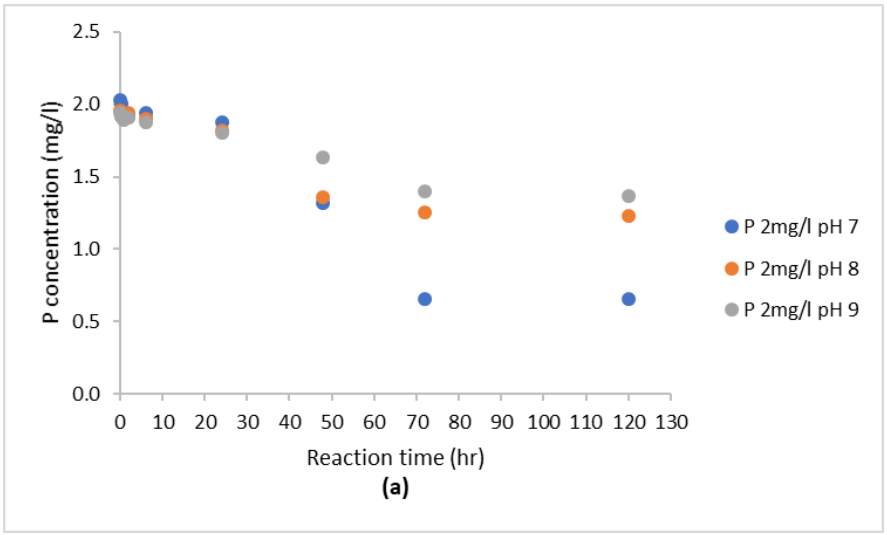

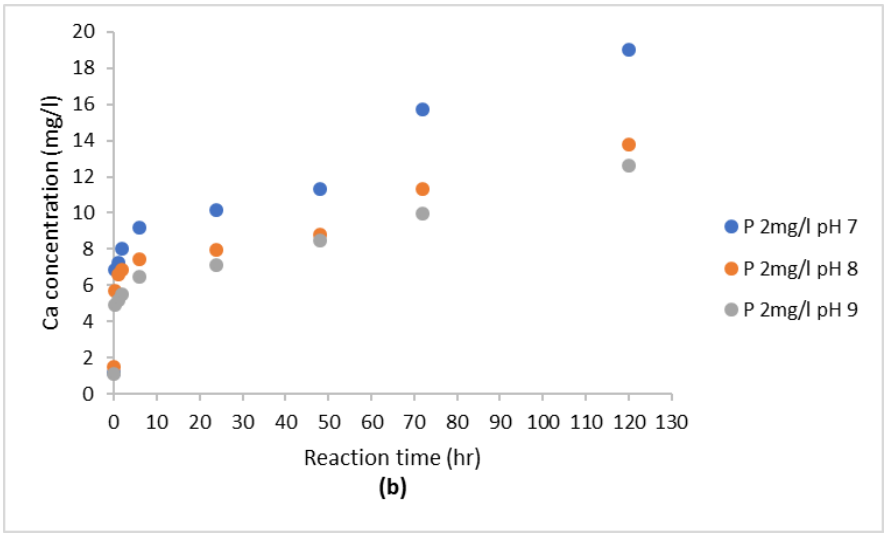

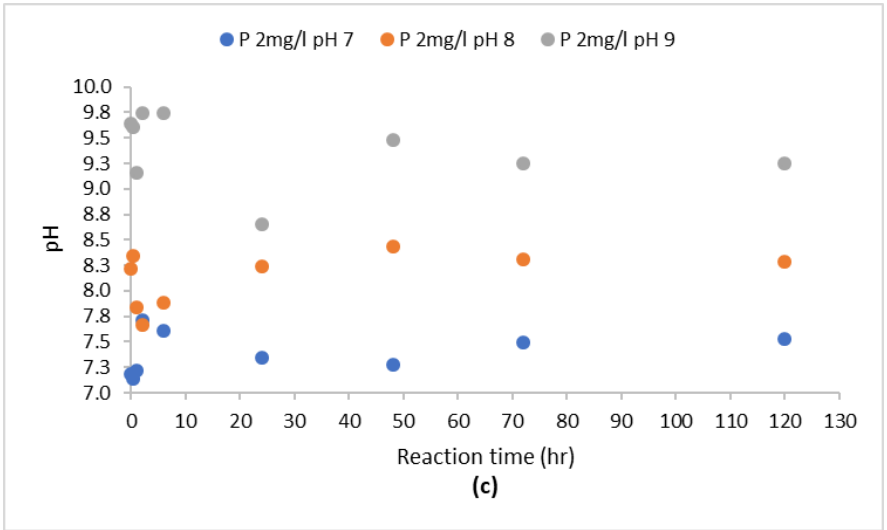

Figure 5- 24: (a) change in P concentration with time (b) change in Ca concentration with time (c) change in pH concentration with time. For initial 2mg/l P

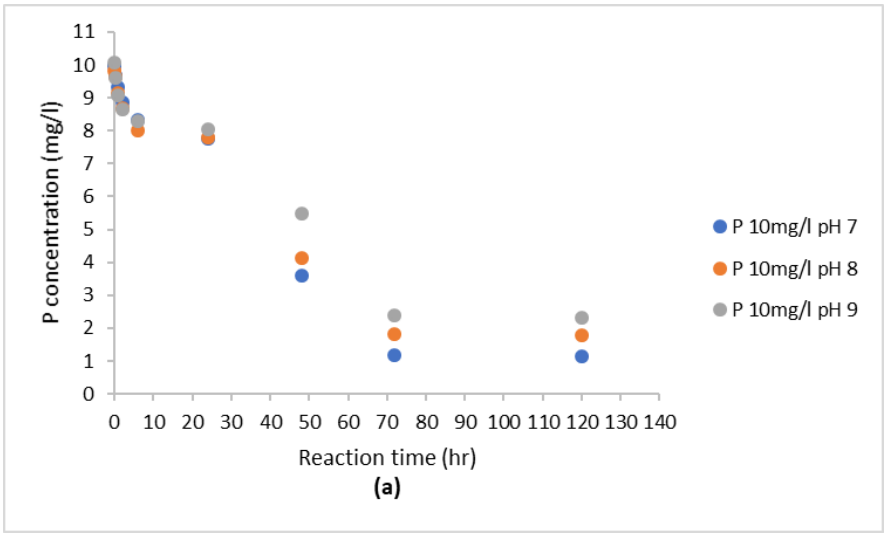

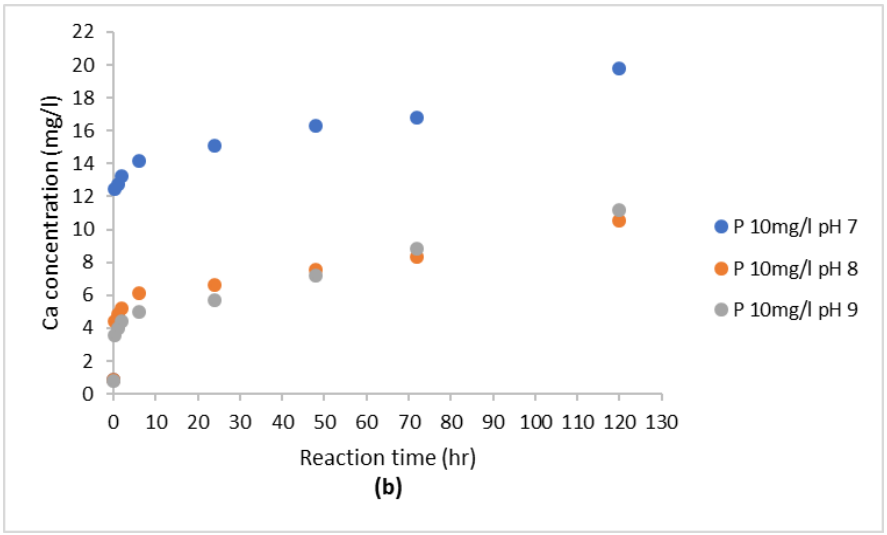

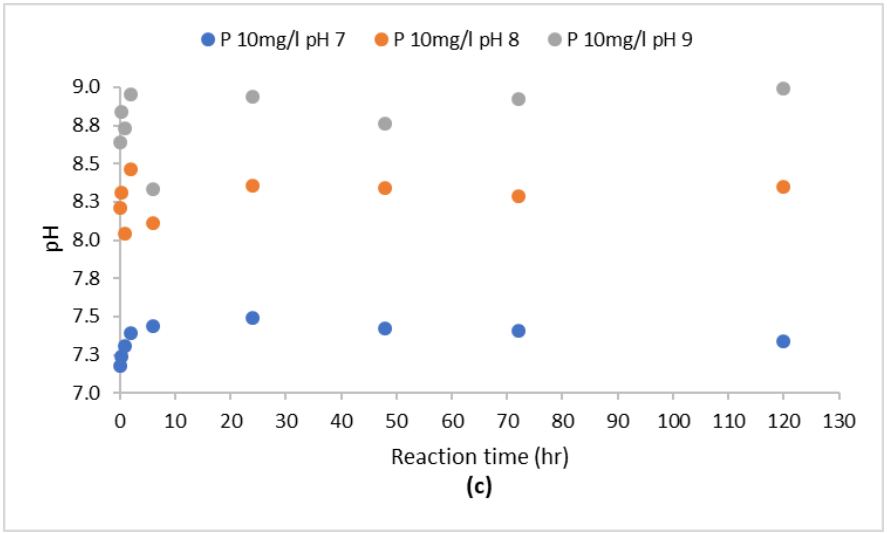

Figure 5- 25: (a) change in P concentration with time (b) change in Ca concentration with time (c) change in pH concentration with time. For initial 10mg/l P

Figure 5.26 (a and b) show the ESEM images for the 2 and 10 mg/l initial P concentration precipitate from the adsorption experiment. Corresponding EDX analyses for samples from Figure

5.26 (a and b) revealed the precence of O and Ca as the main elements for both initial concentrations with wt% of (60 and 39.4) respectivly for initial P concentration of 2 mg/l . While For initial P concentration of 10 mg/l, O and Ca content was (44.5 and 35.4) respectively. No phosphorus was detected for both samples. When SEM/EDX was found not to be sufficiently sensitive, X-ray photoelectron spectroscopy (XPS) was used to determine the presence or absence of phosphate at the calcite precipitate surface. The advantage of XPS is that the escape depth of the secondary electrons is shallow, and so is more likely to detect monolayer deposits. The XPS spectra for precipitate of the two concentrations of 2 and 10 mg/l clearly confirm that P was present onto the surface of calcite for both concentrations as shown in Figure 5.27 (a and b). The appearance of P in these figures represented by 2P peak. The XPS composition data confirmed that the amount of phosphonate on the surface of the calcite increased with increasing P concentration, P 0.72 % for the 2 mg/l and 1.82% for the 10 mg/l. Although, EDX did not show phosphorus on the surfaces of calcite exposed. That is, no particles or crystals were seen on the surfaces under SEM, so the layers would have to be less than the resolution of the SEM (1-10 nm). This is consistent with the results from adsorption test that the adsorbed layers are very thin.

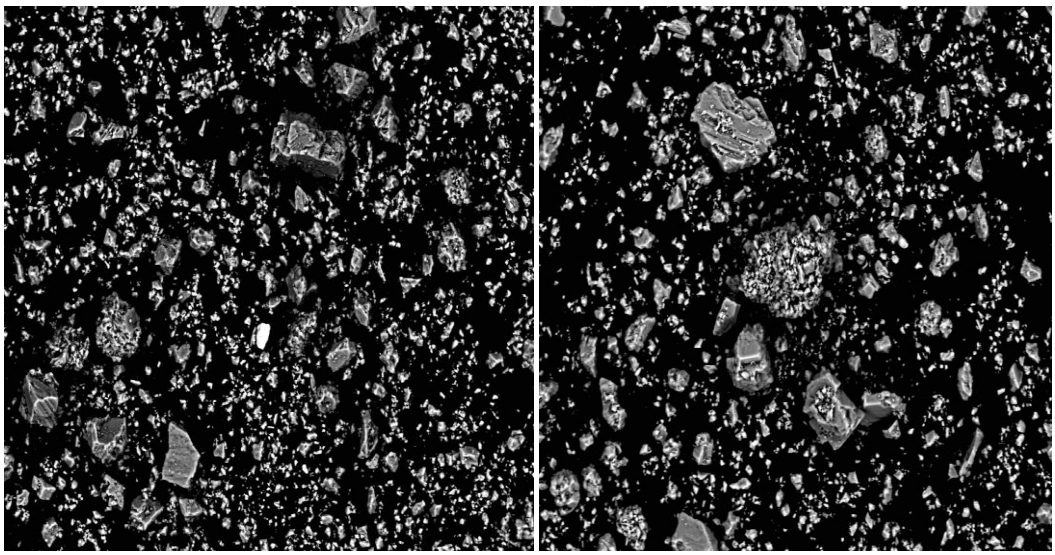

(a) (b)

Figure 5- 26: (a and b) ESEM images of the 2 and 10 mg/l initial P concentration in the adsorption experiment

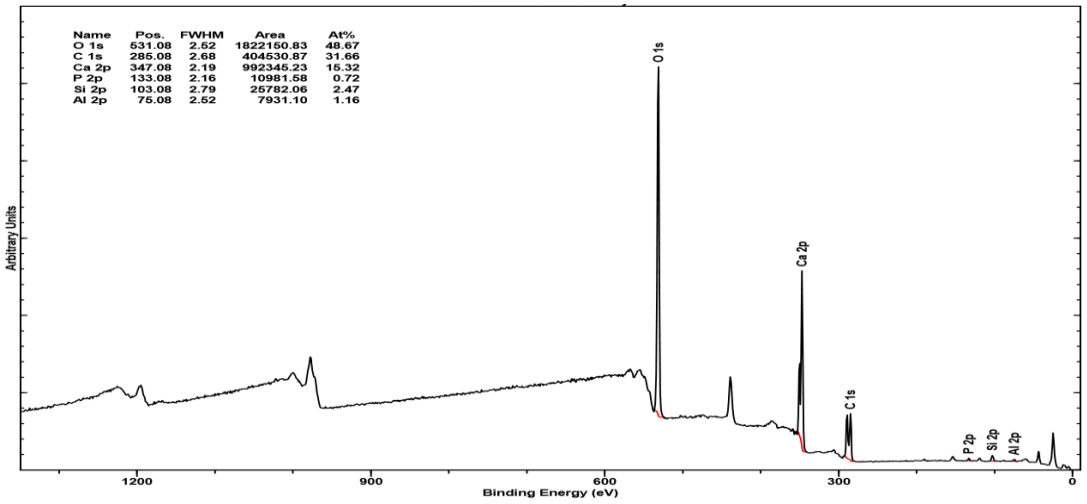

(a)

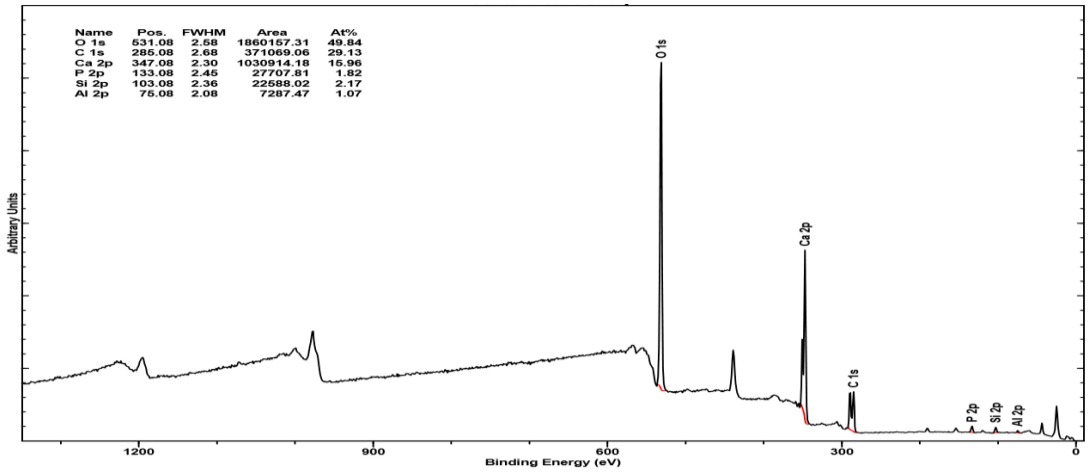

(b)

Figure 5- 27: (a and b) XPS showing elements distribution on the surface of 2 and 10 mg/l initial P concentration in the adsorption experiment

5.3.2 Zeta potential

The surface charge of calcite is considered as one of the main factors controlling adsorption/ precipitation in the calcite/water system. Zeta potential measurements of calcite in water were performed on three solutions. The first solution was calcite precipitate in DI water, the second was calcite precipitate in 2mg/l P solution and the third was calcite precipitate in 10mg/l P solution. The pH levels were 6,7,8,9,10,11 and 12. Zeta potential measurements of calcite in water showed that the calcite precipitate has a negative charge in the examined pH range and the pH_{PZC} was not within that examined range. On the other hand, Xu et al. (2014) reported the point of zero charge (PZC) of calcite occurs at about pH 9.2. When negatively charged ions of PO_4^{-3} were added to the solution, it is observed that the surface of calcite gained more negative charge and it increased by increasing P concentration as the presence of specific anions in solution can make the surface more negatively charged. Figure 5.28 showed the zeta potentials of calcite precipitate

and after adding P into solution. This can explain the results from the adsorption test, SEM and XPS analysis as the formation of outer surface complexes may not occur as calcite was negatively charged so the electrostatic interaction between the adsorbate represented by PO_4^{-3} and the adsorbent surface that could change the surface charge is minimum. Thus, it is clear that a specific precipitation rather than adsorption existed between the phosphate and calcite as a main removal mechanism. Same observation has been highlighted by Su et al. (2013); Huang et al. (2008). Karageorgiou et al. (2007) pointed out that the effects of pH on the removing of phosphates are essentially depending on the isoelectric point of the adsorbent surface. For calcite, from zeta-potential measurements it was found that the surface of calcite gained more negative charges as the pH increases.

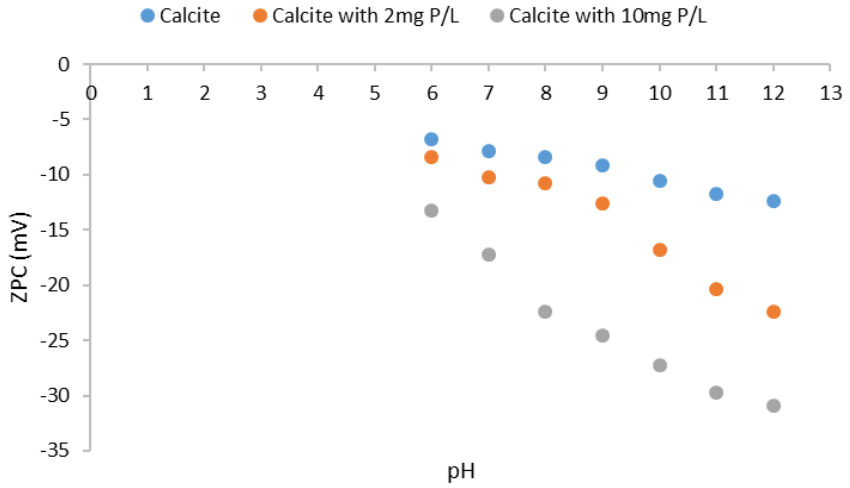

Figure 5- 28 Zeta Potential of calcite as a function of pH

5.3.3 Sequential extraction

The sequential analysis for the synthetic wastewater precipitate suggests that the majority of the phosphorus (79.8%) within the sample is located within the authigenic apatite plus $CaCO_3$- bound P plus biogenic apatite phase, while the remainder is broadly held within the exchangeable or loosely sorbed P phase (18.1%). Only minor quantities are located within the detrital apatite plus another inorganic P phase (2.1) as shown in Figure (5.29a). Figure (5.29b) shows the distribution of phosphorus throughout the sequential extraction phases applied to the precipitate collected from real wastewater sample through the lab system. The authigenic apatite plus $CaCO_3$ - bound P plus biogenic apatite phase is again prevalent with (72.2%) of phosphorus located within this phase. The remainder is held within the exchangeable or loosely sorbed P phase (12.7%). The most significant difference, compared with synthetic precipitate, is the increased proportion of phosphorus located within the detrital apatite plus another inorganic P phase (14%) phase. This suggests that most of the phosphate is present in calcium phosphate minerals.

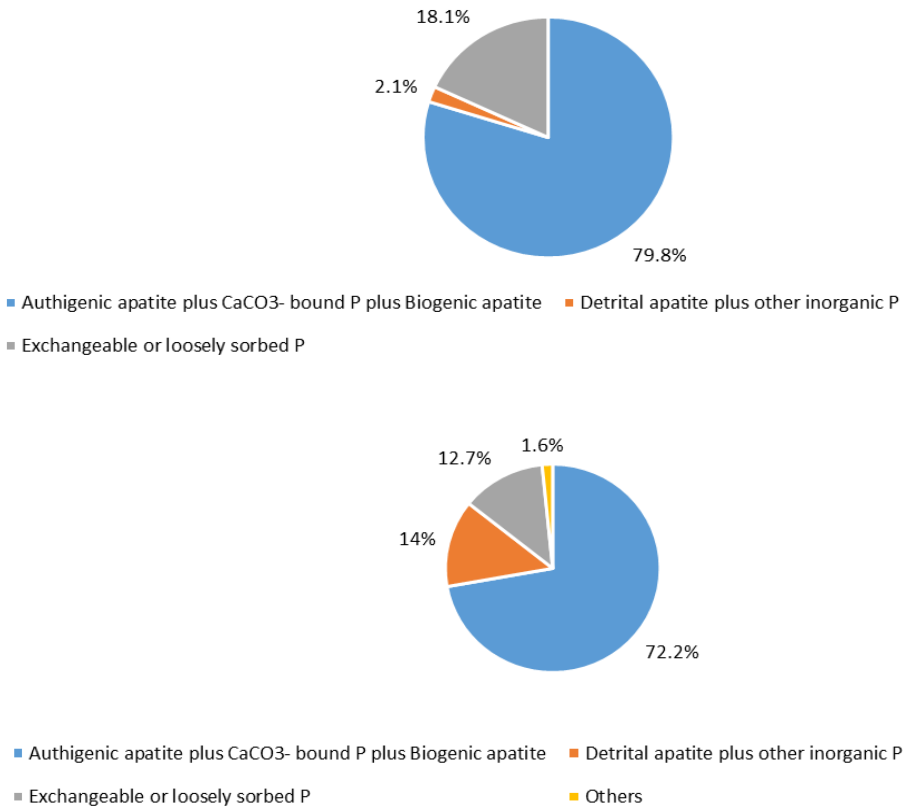

Figure 5- 29 shows the distribution of phosphorus throughout the sequential extraction phases applied to the precipitate collected from (a) synthetic solution precipitate (b) real wastewater precipitate

5.4 Laboratory Experiments with Apatite

This section provides a laboratory study on two types of apatite pellets which were used in the field trial.

5.4.1 Media Characterisation

The media used in this chapter were two types of apatite, as shown in Figure 5.30. The physical and chemical properties are listed in table 5.3 below.

Figure 5- 30: Media 1 and 2

Table 5- 3: Physical and chemical properties for both media

Properties	Media 1	Media 2
Colour	Light cream - Grey	Brown
Particle size (mm)	3-8	3-8
Odour	Odourless	Odourless
Physical state	Solid	Solid

The chemical composition of both media was determined using Inductively Coupled Plasma Optical Emission Spectrometry (ICP-OES). This was carried out through the digestion of the sample (as described in the material and methods chapter). The fully digested sample analysed for the presence of the following elements (calcium, silicon, magnesium iron, aluminium, phosphorus, sulphur, sodium, potassium, manganese, and zinc) as shown in table 5.4. The Ca and P content of Media 1, and 2 was close to the apatite used by (Molle et al. 2005; Bellier et al. 2006). Total carbon was performed to determine the carbon content using a Leco SC-144DR furnace (see section 3.4.2 chapter 3). Carbon content in media 1 and media 2 was 2.1% and 1.9 % respectively.

Table 5- 4: Results of total digest

Element	% in Media 1	% in Media 2
Ca	32.2	29.3
Si	7.5	2.4
Mg	0.4	0.6
Al	0.7	0.2
Fe	0.3	2.3
P	11.3	10.9
S	0.8	2.1
Na	0.6	0.9
K	0.2	0.2
Mn	0.009	0.007
Zn	0.02	0.01

Both media were characterized by the X-ray diffraction method to detect the main mineralogical components. Figure 5.31 (a, b) represents the x-ray diffraction of the grey and brown media respectively. The x-ray patterns indicated that the dominant mineral in media 1 was hydroxyapatite with a minor amount of silicon dioxide, and the dominant component in media 2 was fluorapatite with gypsum.

The morphology and appearance of the pellets produced was studied using a Scanning Electron Microscope (SEM). This analysis was carried out at the Cardiff University School of Earth and Ocean Science by the author with the assistance of a laboratory technician. Micrographs are presented of 50 µm. Both pellet sizes were found to have similar, rough surface. There are valleys in the pellets surface which will assist in the contact of the pellet with the water as shown in Figure 5.32 (a and b).

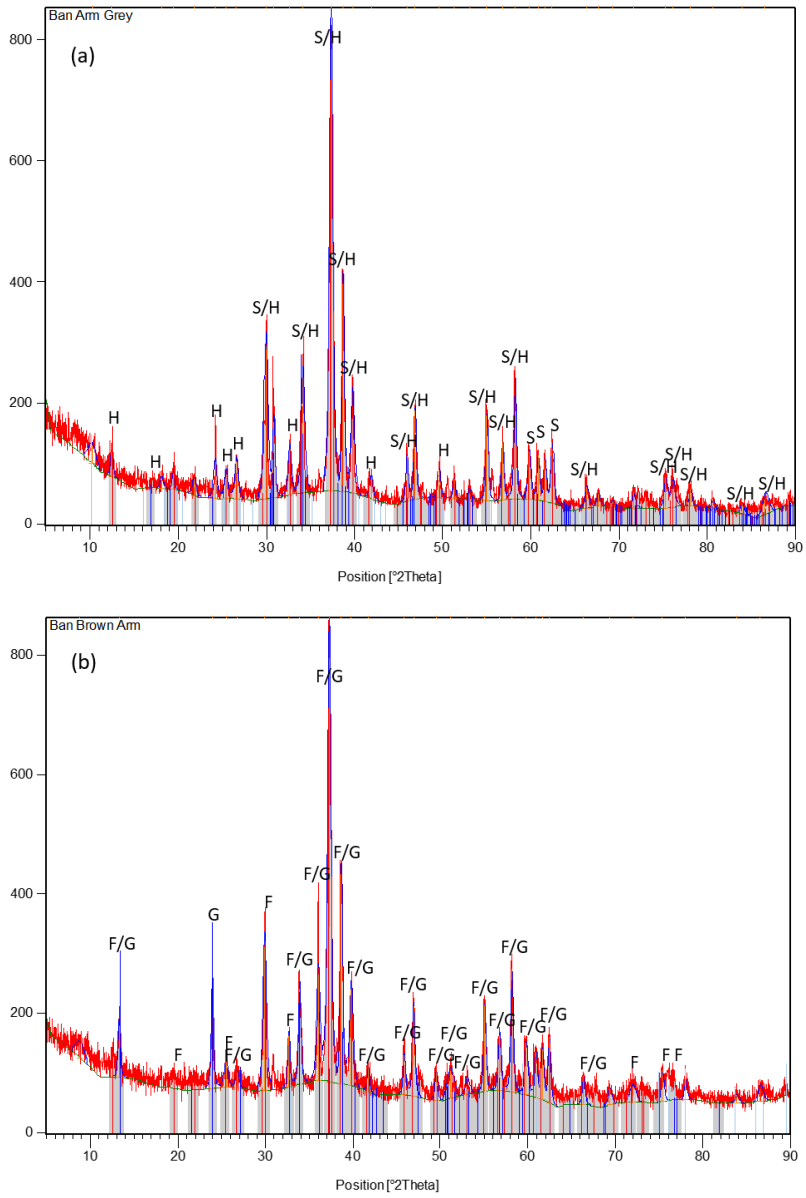

Figure 5- 31: XRD results (a) media 1 (b) media 2

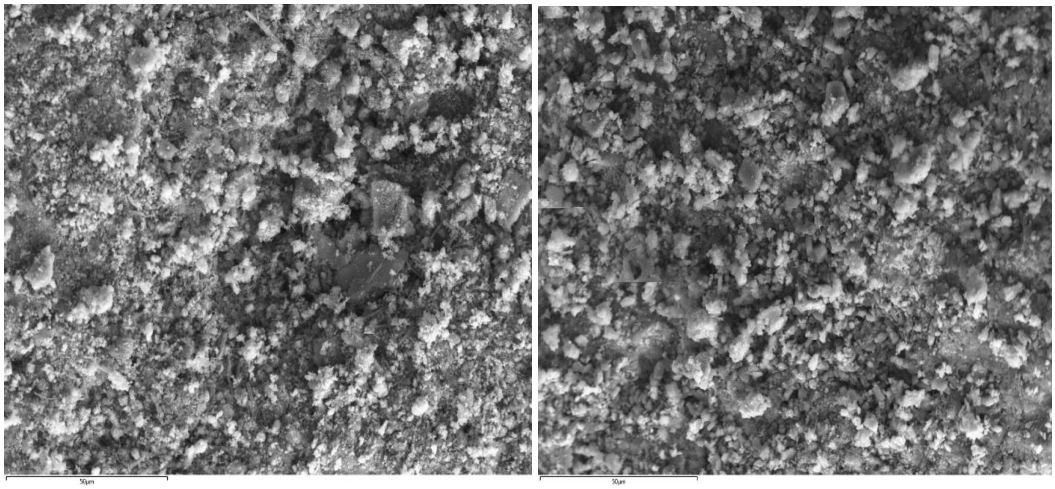

(a) (b)

Figure 5- 32: ESEM images for (a) media 1 (b) media 2

5.4.2 Removal Mechanism

To thoroughly understand the removal mechanism for both media, batch tests were conducted using 1 and 5 g of pellets of each media in 100 ml of tap water shaken for 168 hr. Table 5.5 present the working condition for each batch test. Artificial orthophosphate solutions were used throughout the adsorption tests. Initially, a stock solution of 100 ppm orthophosphate was prepared by dissolving a certain amount of chemically pure K_2HPO_4. An aliquot of the stock solution was mixed with a specific volume of water so that a phosphate solution was prepared at the desired experimental concentration of P concentration in tap water, 2 and 10 mg/l. pH value was the pH of tap water 6.7. After the set time had elapsed, 0.45 µm filters were used to filter the suspension, and the supernatants were analysed for Ca, and P. For 1 g of media 1, It was observed that Ca concentration slowly increased over the first 48 hr, the increase in the concentration continued to the end of the contact time. A small decrease in P concentration from the initial concentration observed during the first 24 of contact time, this decrease continued over the 120 hr. P concentration was 0.43 after 168 hr contact time as shown in Figure 5.33(a). pH values increased over the 1st 24 hr then decreased to almost the same initial value by the end of the contact time as shown in Figure 5.33(b). By increasing P concentration to 2 mg/l and 10 mg/l as shown in Figure 5.34(a, b) and 5.35(a, b) the same trend was observed regarding Ca, P and pH. It was observed that the final Ca concentration decreased by increasing the initial P concentration from 1.2 to 2 and then to 10 mg/l indicating the inverse relation between Ca dissolution and initial P concentration due to the effect of phosphorus in retarding the dissolution. pH did not show any significant change during the contact time for all P concentrations and that might be due to the acidic nature of the KH_2PO_4 used to create the stock solution that might neutralise the pH. By

increasing the amount of the media to 5 g, the same trend was observed in Ca and P with the 3 mg/l initial P concentrations as shown in Figure 5.36(a), 5.37(a) and 5.38(a). A noticeable increase in pH level was highlighted over the contact time as shown in Figure 5.36(b), 5.37(b) and 5.38(b). The increase in pH values might be attributed to the increase in the amount of the media. The same procedure was applied to Media 2, using the same P concentrations of 1.2, 2 and 10 mg/l the changes in P, Ca and pH values over the reaction time were as shown in Figures 5.39(a, b), 5.40(a, b) and 5.41(a, b). It was observed that by using only 1 g of this media the Ca concentration at the end of the contact time was between 300- 400 mg/l for the 3 mg/l initial P concentration. It was also noticed that there was a noticeable increase in pH level to around 9. By increasing the amount of media to 5 g, Ca concentration increased to around 500 mg/l by the end of the contact time for all P concentrations while the pH level was almost the same to that pH when 1 g of the media used as shown in Figure 5.42(a, b), 5.43(a, b) and 5.44(a, b).

Table 5- 5: Working conditions of the adsorption tests

Batch test number	P Concentration mg/l	Media type	Pellets dosage g	Figure number
1	1.2 (Tap water P concentration)	Media 1	1	5.33 (a and b)
2	2 + initial tap water P concentration	Media 1	1	5.34 (a and b)
3	10 + initial tap water P concentration	Media 1	1	5.35 (a and b)
4	1.2 (Tap water P concentration)	Media 1	5	5.36 (a and b)
5	2 + initial tap water P concentration	Media 1	5	5.37 (a and b)
6	10 + initial tap water P concentration	Media 1	5	5.38 (a and b)
7	1.2 (Tap water P concentration)	Media 2	1	5.39 (a and b)
8	2 + initial tap water P concentration	Media 2	1	5.40 (a and b)
9	10 + initial tap water P concentration	Media 2	1	5.41 (a and b)
10	1.2 (Tap water P concentration)	Media 2	5	5.42 (a and b)
11	2 + initial tap water P concentration	Media 2	5	5.43 (a and b)
12	10 + initial tap water P concentration	Media 2	5	5.44 (a and b)

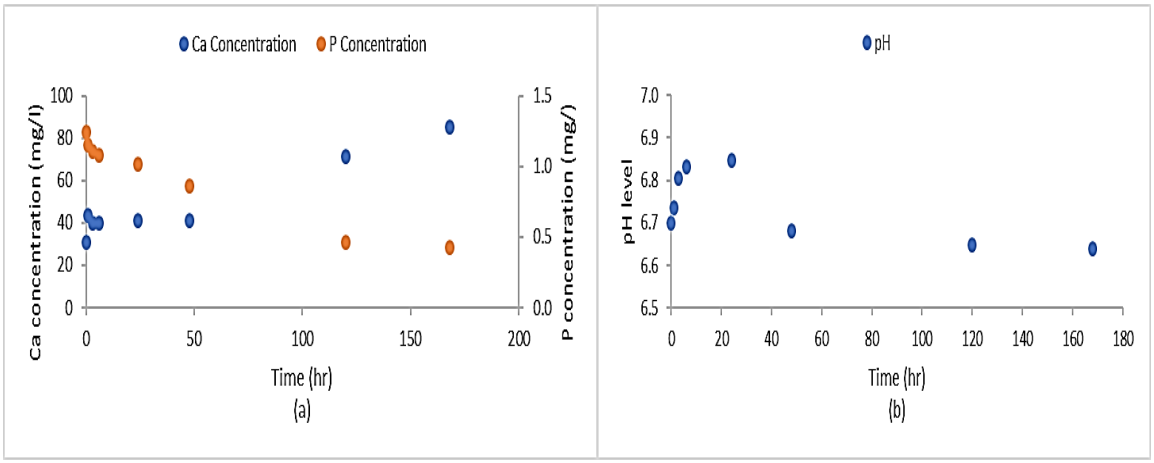

Figure 5- 33(a and b) changes in P, Ca and pH values over the reaction time. At P concentration 1.2 mg/l and 1g of Media 1

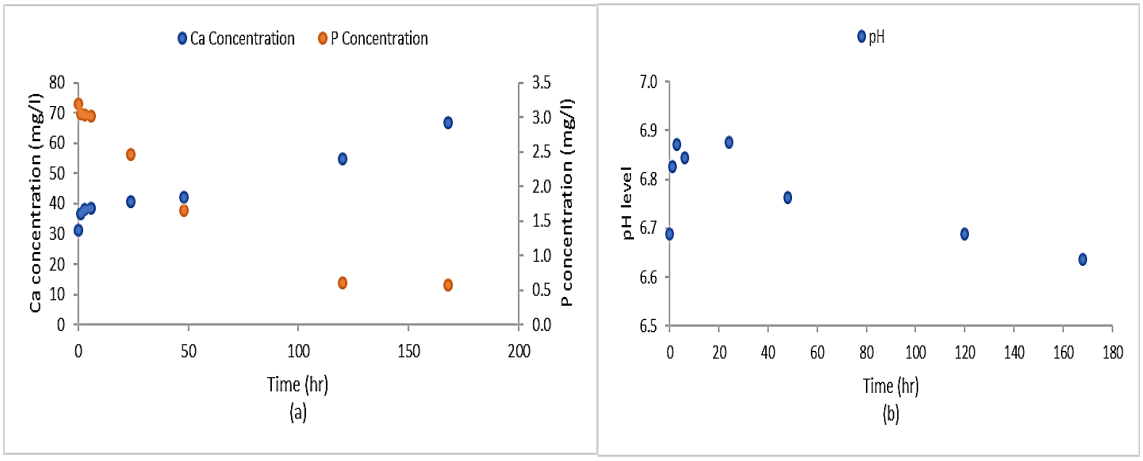

Figure 5- 34(a and b) changes in P, Ca and pH values over the reaction time. At P concentration 2mg/l and 1g of Media 1

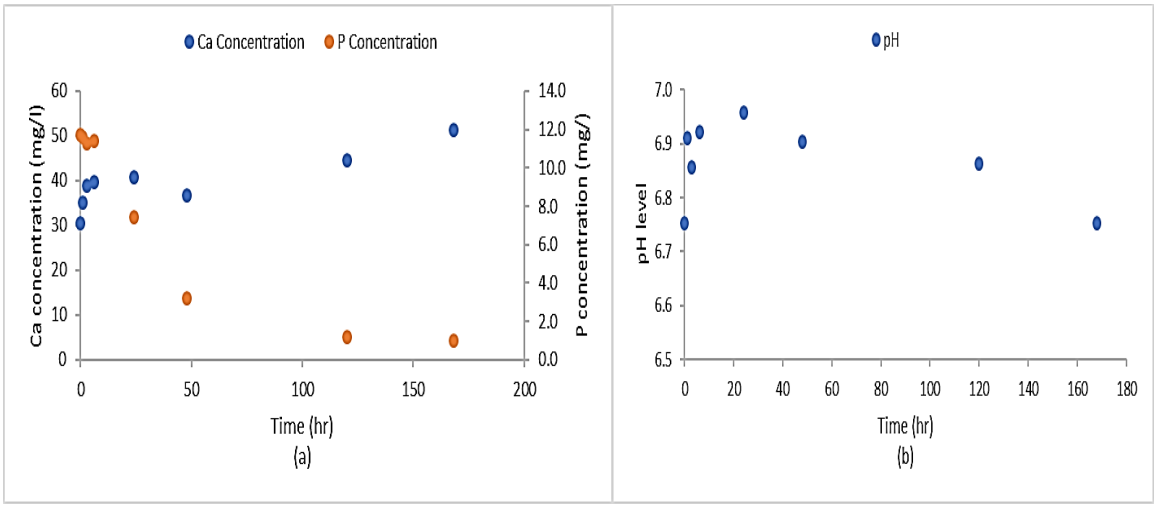

Figure 5- 35(a and b) changes in P, Ca, and pH values over the reaction time. At P concentration 10 mg/l and 1g of Media 1

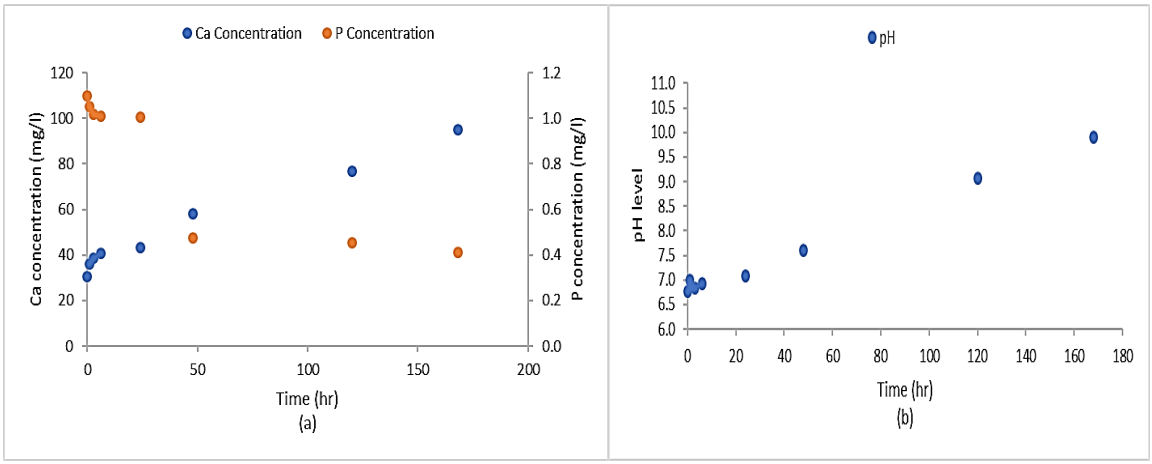

Figure 5- 36(a and b): changes in P, Ca and pH values over the reaction time. At P concentration 1.2 mg/l and 5g of Media 1

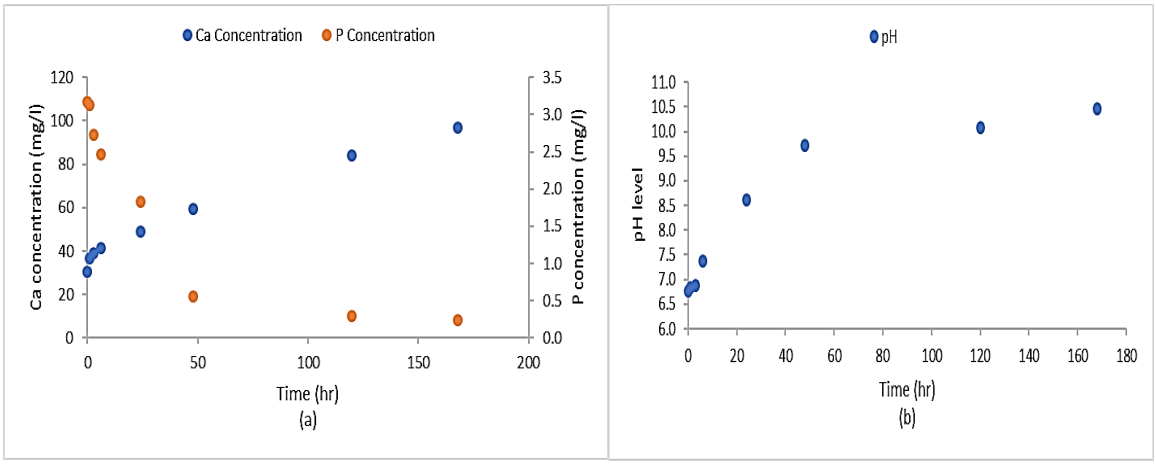

Figure 5- 37(a and b) changes in P, Ca and pH values over the reaction time. At P concentration 2mg/l and 5g of Media 1

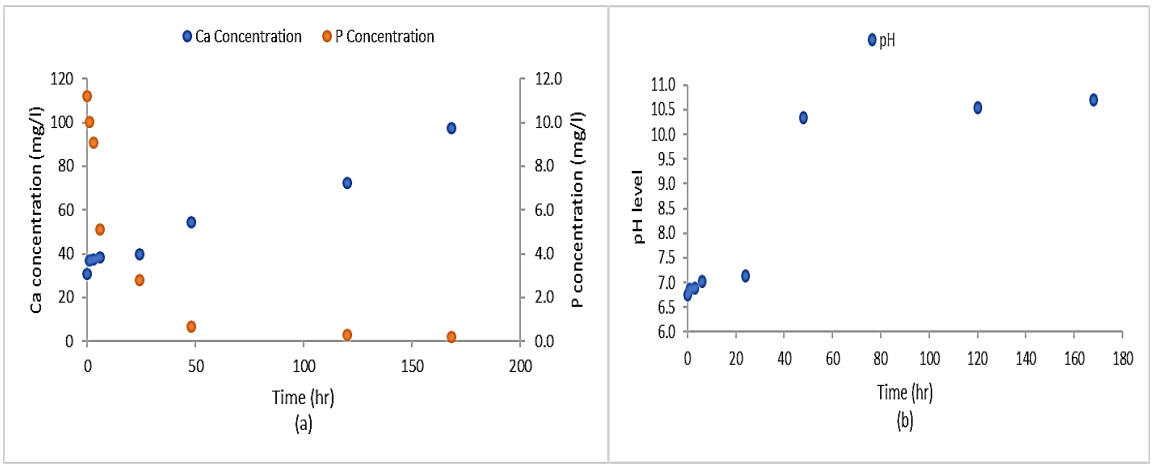

Figure 5- 38(a and b) changes in P, Ca, and pH values over the reaction time. At P concentration 10 mg/l and 5g of Media 1

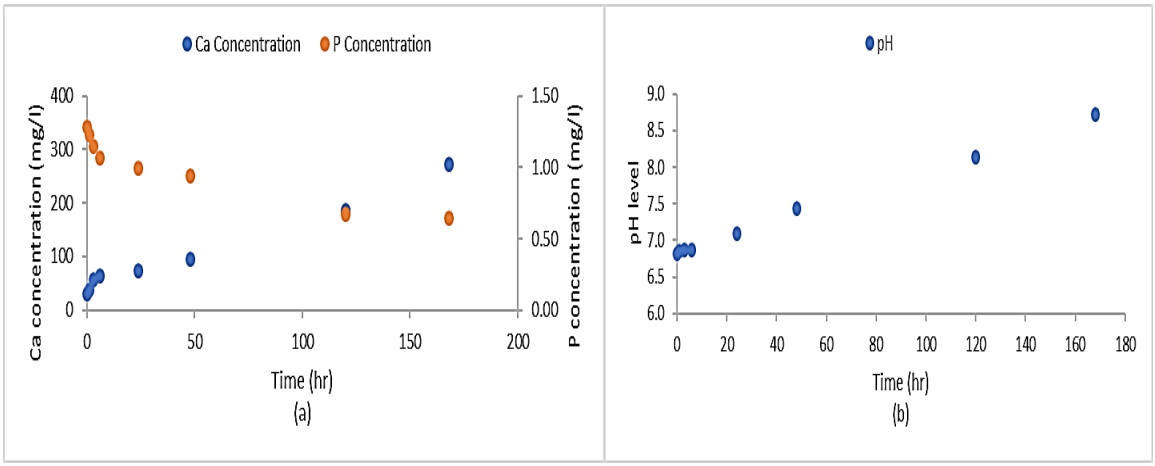

Figure 5- 39(a and b) changes in P, Ca and pH values over the reaction time. At P concentration 1.2 mg/l and 1g of Media 2

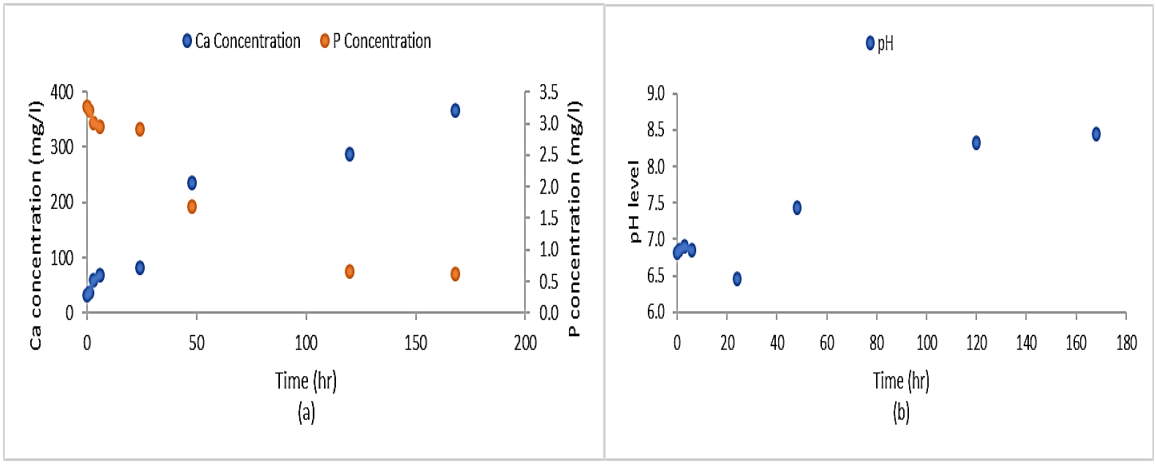

Figure 5- 40(a and b) changes in P, Ca and pH values over the reaction time. At P concentration 2 mg/l and 1g of Media 2

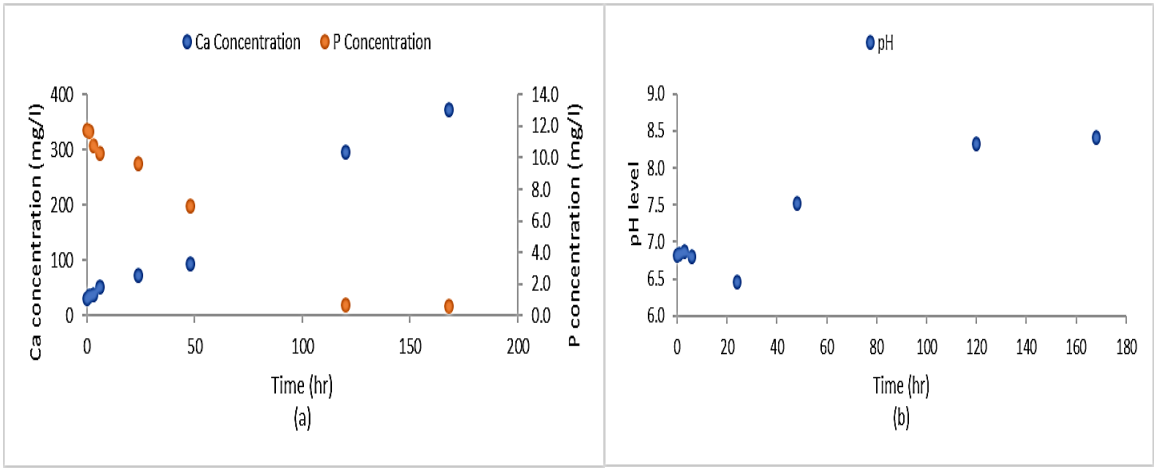

Figure 5- 41(a and b) changes in P, Ca and pH values over the reaction time. At P concentration 10 mg/l and 1g of Media 2

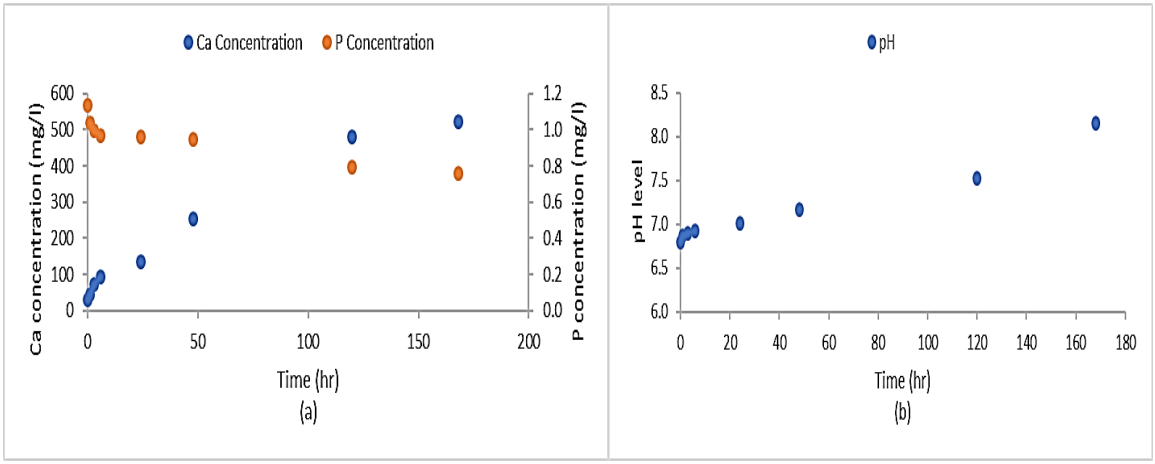

Figure 5- 42(a and b) changes in P, Ca and pH values over the reaction time. At P concentration 1.2 mg/l and 5g of Media 2

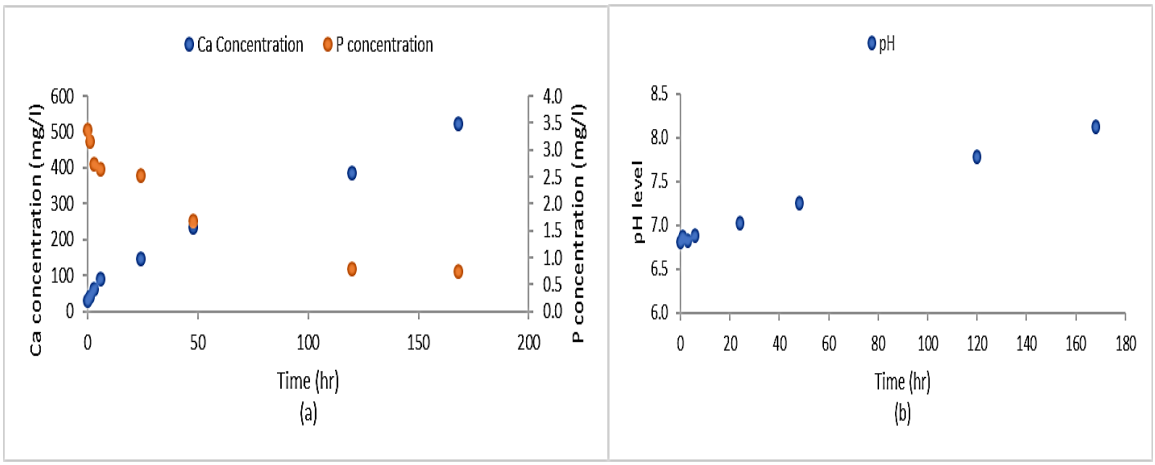

Figure 5- 43(a and b) changes in P, Ca and pH values over the reaction time. At P concentration 2 mg/l and 5g of Media 2

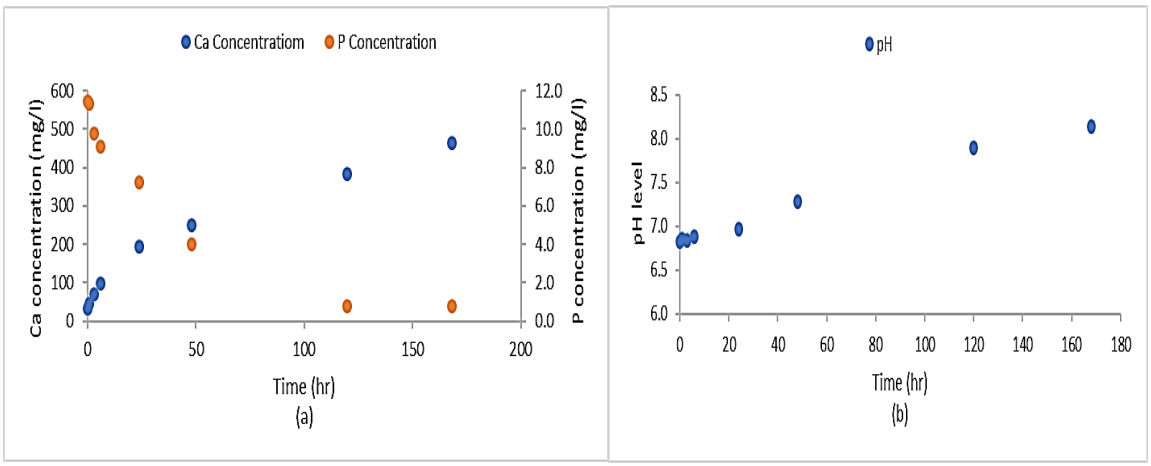

Figure 5- 44(a and b) changes in P, Ca and pH values over the reaction time. At P concentration 10 mg/l and 5g of Media 2

The final phosphorus concentration results are plotted against the corresponding initial concentrations in Figure 5.45. Although, Ca concentration and pH level of Media 2 were higher than Media 1 for the initial P concentration of 1.2 and 3.2 mg/l, it can be seen that pellets of media 1 remove slightly more phosphorus than media 2 pellets and that might suggest that the removal mechanism of P by media 1 was adsorption while precipitation was the removal mechanism by which P removed using media 2 for the initial P concentration of 1.2 and 2 mg/l when the dosage was 1 g. For the initial P concentration of 10 mg/l media 2 showed better removal for the same dosage. By increasing the dosage to 5 g for each media, it can be seen that media 1 remove more phosphorus than media 2 for all initial P concentrations. It should be noted that by increasing the dosage from 1 to 5 g, media 1 showed better removing of P and that increased with increasing the initial P concentration. While the increase in the amount of media 2 gave an opposite result with almost consistent final concentration of around of 0.62 mg/l for 1g and 0.75 mg/l for the 5g for all the initial P concentrations. These tests become more meaningful if the data are processed to provide the adsorption capacity at equilibrium (mg/g). This allows the phosphorus removed in terms of milligrams of phosphorus (as milligrams of total phosphorus removed per gram of pellets) to be plotted against the relevant equilibrium concentration, as shown in Figure 5.46 The mass of P adsorbed per mass of adsorbent (q) in mg/g was calculated using equation (5.6).

$$q = \frac{(C_o - C_e)}{m} V \qquad (5.6)$$

where C_o and C_e are the initial and equilibrium P concentrations, respectively in the solution (mg/l), V represents the volume of the solution (l), and m is the mass of the adsorbent (g).

In the range of equilibrium concentrations 0.22 – 1.0 mg/l both media are removing 0.01 - 1.1mg/g which were low compared to those found in the literature (2.7 – 4.8 mg P/l apatite) (Molle et al. 2005). Figure 5.47 shows the variation of final Ca concentration with initial phosphorus concentration. An increase in initial phosphorus concentration resulted in a decrease in Ca concentration released from media 1 when 1 g of that media were used indicating the retarded force to calcium dissolution by increasing P concentration. While the opposite was observed by using 1 g of media 2 were Ca concentration increased by increasing the initial P concentration. By Increasing the amount to 5 grams, Ca concentration released from media 1 was almost constant for all P concentration to around 96.8 mg/l, and the same trend was observed for media 2 were Ca concentration was around 523.6 mg/l except when P concentration was 10 mg/l the Ca concentration was 463.2 mg/l. It can be seen that Ca concentration released from media 2 was more than from media 1 and that is due to the gypsum content in media 2 as shown in the XRD analysis for that media. Figure 5.48 shows the variation of final pH with mass of p

removed. Best pH conditions are conflicting as a low pH would favour Ca dissolution and a high pH would favour HAP precipitation. All final pHs of Media 1 in the case of 1 g were below 9 which is the lower limit for calcium phosphate precipitation stated by Johansson and Gustafsson (2000). This could suggest adsorption to the available adsorption sites to be the dominant removal mechanism especially as the range of Ca concentration released from this media is above the minimum level of Ca recommended for Ca-P precipitation of 40 – 60 mg/l suggested by Jang and Kang (2002). The final pH of media 1 in the case of 5 g ranged from 9.9-10.7 suggesting the potential presence of a calcium phosphate precipitation mechanism especially with the increased level of calcium. The final pH for media 2 was 8.4 – 8.7 for the 1 g and 8.1 for the 5 g for all concentrations. Media 1 pellets resulting in a consistently higher final pH than media 2 pellets for the 5 grams dosage. This suggests a link between a higher range of final pHs and improved removal. Papers such as (Johansson and Gustafsson 2000) suggest that high pH is necessary for efficient calcium phosphate precipitation. In this experiment adsorption was seen to be the main removal mechanism involved.

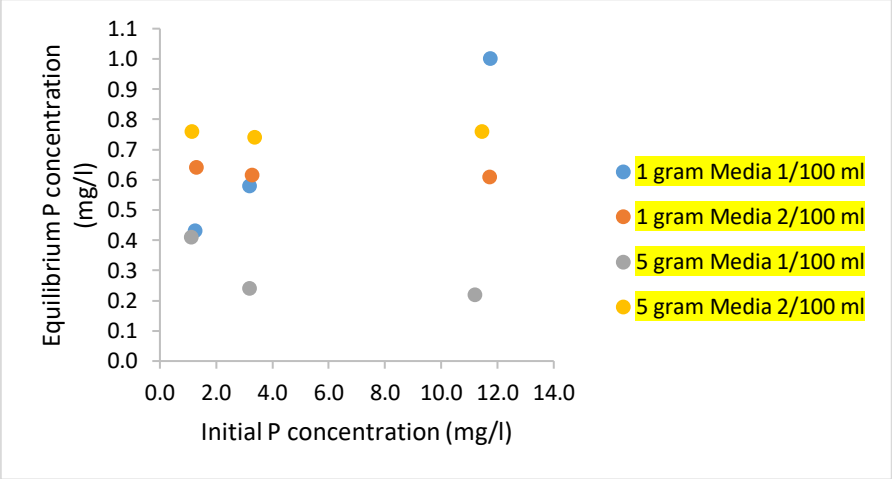

Figure 5- 45: Comparison between Media 1 and 2 performance. For initial P concentrations of 1.2, 2 and 10 mg/l. the

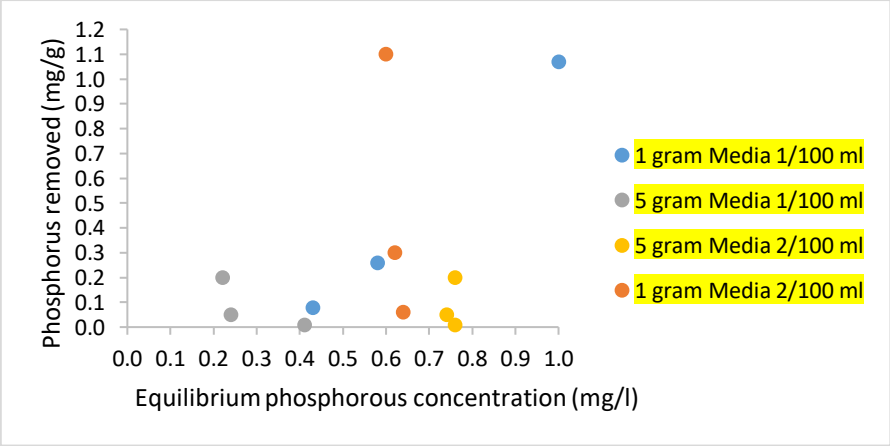

Figure 5- 46: Adsorption isotherm data for batch tests on the pellets of Media 1 and 2. For initial P concentrations of 1.2, 2 and 10 mg/l

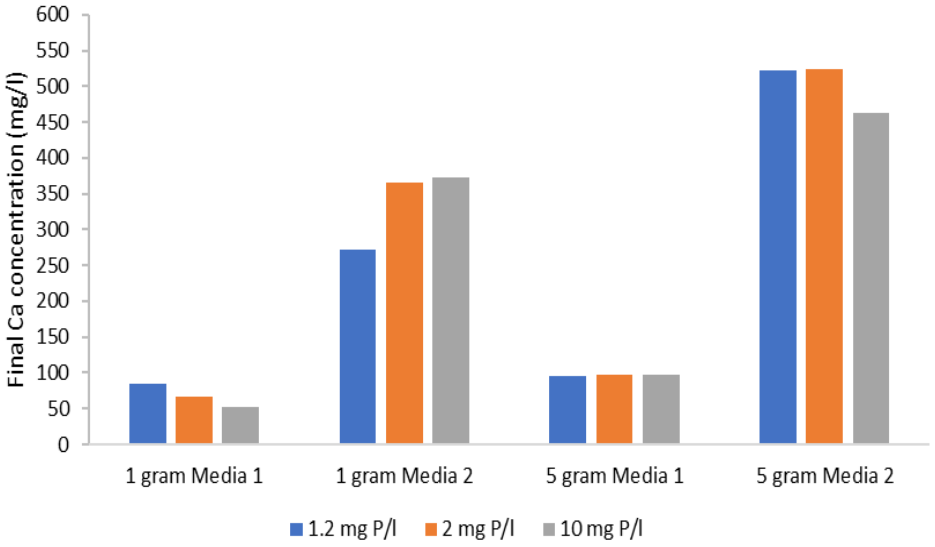

Figure 5- 47: Comparison of Ca concentration between Media 1 and 2. For initial P concentrations of 1.2, 2 and 10 mg/l

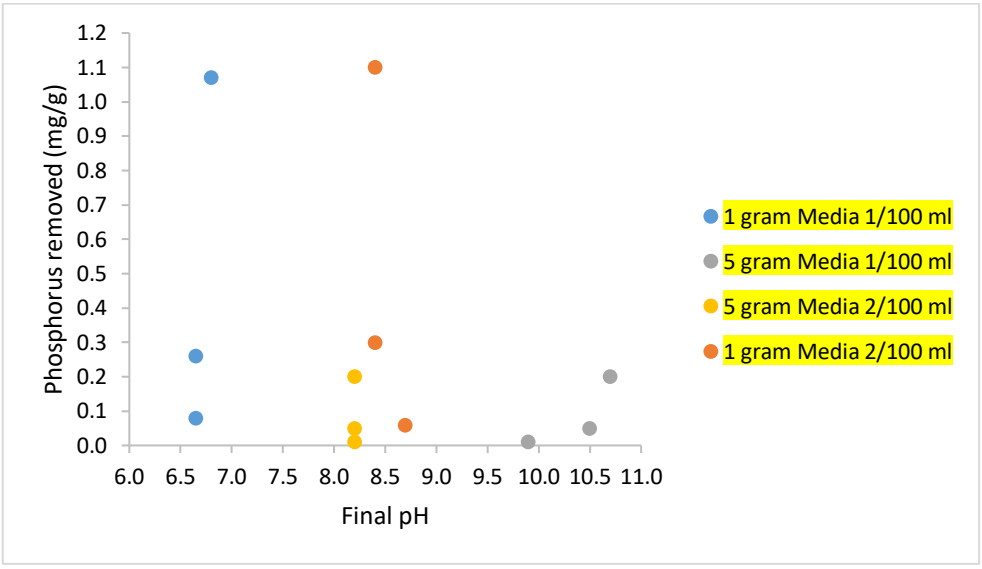

Figure 5- 48: Variation of final pH with phosphorus removed. For initial P concentrations of 1.2, 2 and 10 mg/l

5.5: Chapter summary and conclusions.

1. XRD analysis performed on precipitate samples taken from the bottom of the settlement beaker after the process had been completed proved that the calcium and phosphorus precipitation/sorption process was occurring and calcite is the dominant precipitate for the solutions of P ranged between (1-20mg/l) whereas hydroxyapatite and calcite are the precipitates with initial P concentration of 100 mg/l for both DI and tap water solutions. XRD results of a precipitate from real wastewater sample of an initial P concentration 9

mg/l indicated that the main precipitate was calcite. These findings were in line with total carbon and total digest results.

2. ESEM analysis showed that the morphology of the precipitate changes from crystalline to amorphous by increasing initial P concentration. This analysis also showed that the foreign ions presented in tap water and real wastewater do not affect the morphology of the precipitate.
3. FEG-SEM analysis clearly showed that P is present in the precipitate and distributed across the sample with calcium distributed uniformly over each sample indicated close association between Ca and P as there was no patches of P concentrated in one spot so the P coverage was uniform. The results also showing that the presence of foreign ions in the tap water and wastewater did not affect P distribution within the precipitate.
4. Adsorption tests with synthetic P solution of (1.2 mg/l and 10 mg/l) revealed that the dominant removal mechanism of phosphorus was by precipitation. Adsorption was at the beginning of the process. The adsorbed phosphorus was not detectable by EDX under SEM examination but could be detected by XPS indicating the formation of very thin layer on calcite surface. Zeta potential charge indicated that calcite surface has a negative charge over the examined pH rage increased with the addition of P, this is in agreement with the results from the adsorption test, SEM and XPS analysis suggesting precipitation as the main mechanism as the formation of outer surface complexes may not occur as calcite was negatively charged so the electrostatic interaction between the adsorbate represented by PO_4^{-3} and the adsorbent surface that could change the surface charge is minimum.
5. Sequential extraction experiment indicated that calcium phosphate is the main phase in both synthetic P solution and real wastewater sample and very little loosely sorbed phase.
6. XRD results indicated that the main mineral of media 1 was hydroxyapatite and fluorapatite was the dominant component of media 2.
7. ESEM analysis showed that media 1 and 2 were found to have similar, rough surface.
8. Media 1 and 2 adsorption tests indicated that adsorption is the dominant mechanism at low pH and Ca concentration with potential calcium phosphate precipitation when pH greater than 9 at high Ca concentration.

Chapter 6: P removal – Field trials results and discussion

6.1 Cardiff university field trial - results and discussion

This section presenting the results obtained by running Cardiff university field system trial at different operational parameters and a relevant discussion to the main finding is provided at the end of this section.

6.1.1 Inlet phosphorus concentration measured during the experimentation time

There was a variation in the Inlet flow of the total phosphorus concentration through the field trial period. The initial concentration ranged between 10.3 and 1.0 mg/l as shown in Figure.6.1. Sample dates are shown in table 6.1. The dissolved concentration was close to the total concentration. PO_4-P represents the major, but not the only form of phosphorus in the raw wastewater. The principal form of phosphorus that is removed by chemical precipitation is soluble orthophosphate ions. In this project limestone was used to remove phosphorus from wastewater in the form of orthophosphate (PO_4-P) as shown in the equation below, the presence of other forms might affect the removal by limestone.

$$3Ca^{2+} + 2PO_4^{3-} \rightleftharpoons 3Ca_3(PO_4)_{2\,(s)} \qquad (6.1)$$

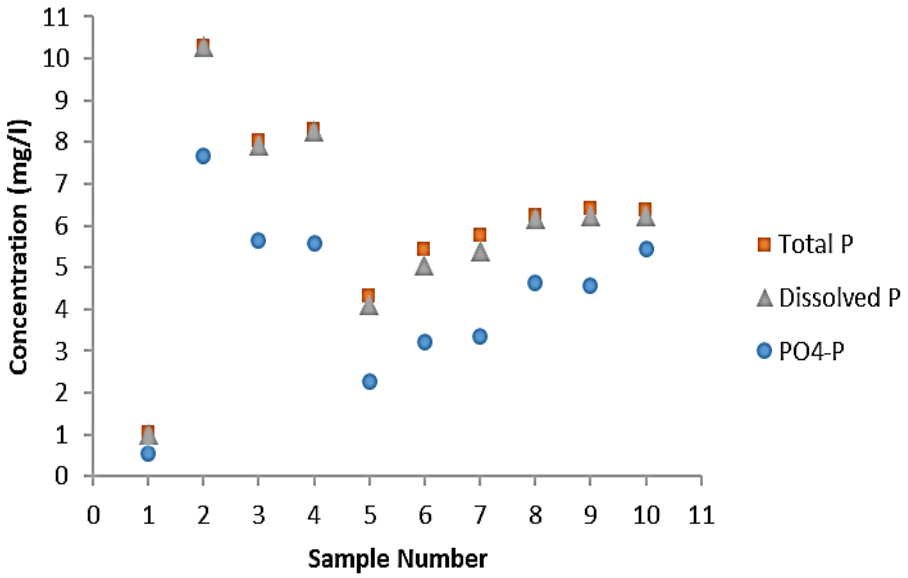

Figure 6- 1: P concentrations measured in the influent during experimentation. Dates of sampling presented in table 6.2

Table 6- 1: show the dates of sampling

Sample No.	1	2	3	4	5	6	7	8	9	10
Date	2/7/18	5/7/18	26/7/18	9/8/18	13/8/18	16/8/18	20/8/18	23/8/18	13/9/18	17/9/18

6.1.2 Calcium and Phosphorus concentrations measured through field system stages at inlet flow of 6 l/min

The first day of sampling was on 2/7/2018. The working parameters were set as shown in table 6.2. CO_2 flow rate was adjusted 6 l/min. The initial inlet wastewater flow rate was 6 l/min and the circulation flow rate through the limestone column was 12 l/min. It can be seen from Figure 6.2 that Ca concentration after 50 min carbonation increased due to the formation of carbonic acid, increasing acidity lead to drop in pH to 5.8 resulted in calcite dissolution and free Ca ions into solution. Alkalinity and conductivity increased accordingly. After approximately 20 min aeration there was a decrease in Ca concentration and an increase in pH as a result of CO_2 degassing. Acidity decreased while alkalinity and conductivity were almost the same as the carbonation stage. There was very small drop in Ca concentration after approximately 5 hr settlement while there was a decrease in alkalinity and acidity dropped to zero. The circulation flow was then adjusted to a 10 l/min instead of 12 l/min due to a leaking problem in the limestone cylinder because of the water pressure inside it was too high. By reducing the circulation flow to 10 l/min, the increase in Ca concentration after 50 min carbonation was less than that at 12 l/min the increase in acidity was also less than previously with pH dropped to the same previous level. A drop in the concentration was observed after aeration stage as expected due to the increase in pH. There was no decrease in Ca concentration after the 5 hr settlement. The circulation flow was then adjusted to 3 l/min instead of 10 l/min due to the leaking problem in the limestone cylinder. The increase in Ca concentration after carbonation was very small so as the acidity and the drop in pH was less than before as well indicating that the circulation flow was very low to achieve sufficient Ca concentration after carbonation. Due to the very low Ca concentration, the circulation flow adjusted to 7 l/min instead of 3 l/min. By increasing the circulation flow to 7 l/min, there was an increase in Ca concentration after 50 min carbonation due to the increased circulation flow but less that at 12 and 10 mg/l. The acidity increased to the same level as when the flow rate was 12 l/min, pH dropped to 5.8. By keeping the circulation flow rate adjusted on 7 l/min for the next two times, the same trend was observed in the three stages. Figure 6.3 show the changes in P concentration over the process stages and according to the changes in circulation flow and Ca concentrations. As previously mention in section 6.1.1 that the inlet P concentration was varide and ranged between 10.3 and 1.0 mg/l. only small decrease in P concentration was noticed after aeration stage when the initial P concentration was 10.3 by using 10 l/min circulation flow whereas there was almost no daecrease in other concentrations. Tables 6.3, 6.4, 6.5, 6.6, 6.7 and 6.8 listing some of the related parameters. Each table present the readings according to a certain working parameter.

Table 6- 2: Working parameters on site

Carbonation Stage			Aeration Stage	Settlement Stage	Date
Inlet Flow Rate (l/min)	Circulation Flow Rate (l/min)	Carbonation Time (min)	Time (min)	Time (hr)	DD/MM/YY
6	12	50	20	5	02/07/2018
6	10	50	20	5	05/07/2018
6	3	50	20	5	26/07/2018
6	7	50	20	5	09,13 and 16/08/2018

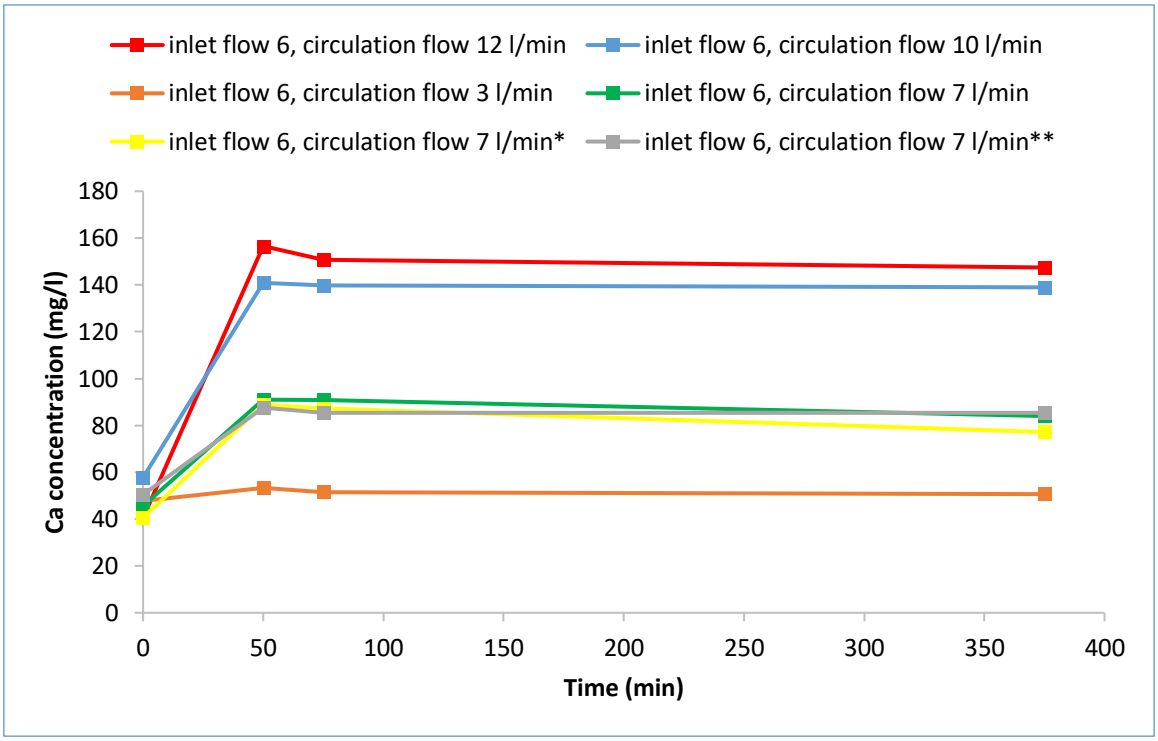

Figure 6- 2: Calcium concentration measured during field trial. At inlet flow 6 l\min and at different circulation flow rates. Trial conditions: Carbonation for 50 min, Aeration for 20 min, Settlement for 5 hr. Stars refer to number of times

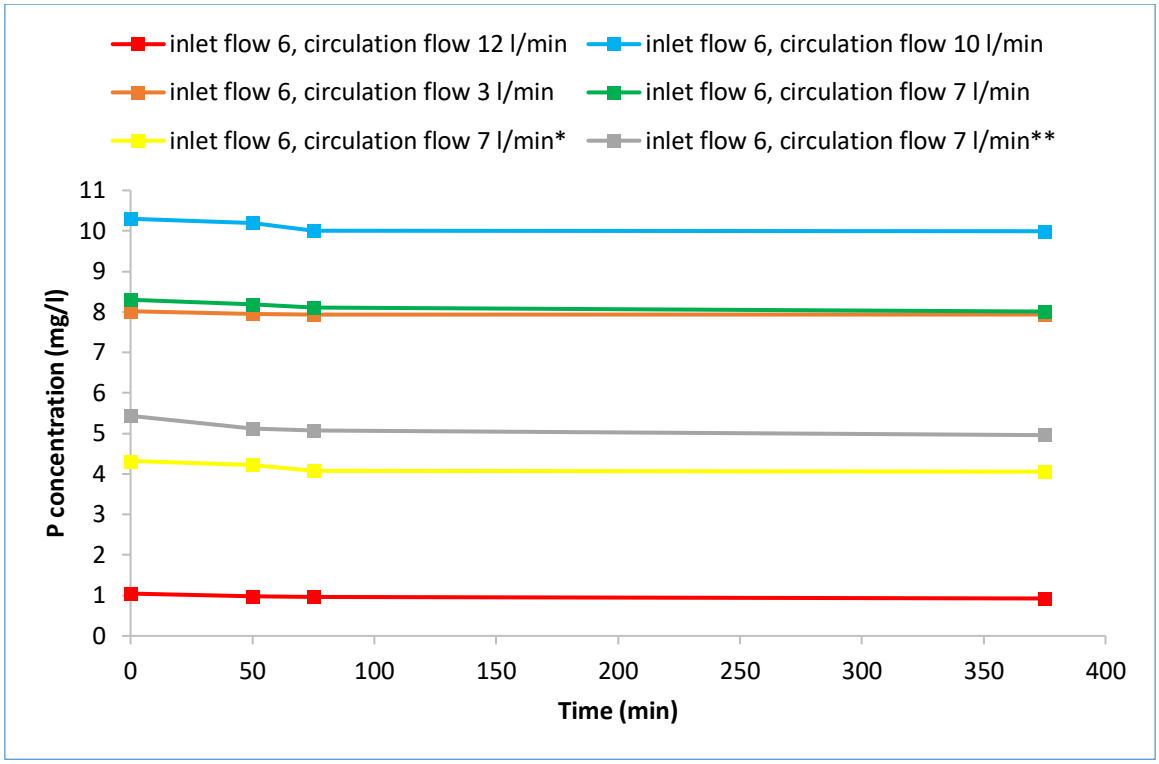

Figure 6- 3: Total phosphorus concentration measured during field trial. At inlet flow 6 l\min and at different circulation flow rates. Trial conditions: Carbonation for 50 min, Aeration for 20 min, Settlement for 5 hr. Stars refer to number of times

Table 6- 3: parameters measured during the field experimentation at 6 l/min inlet flow and 12 l/min circulation flow

System Stages	Sample point No.	TSS mg/l	Alkalinity mg/l as $CaCO_3$	Acidity g/l	DO (mg/l)	Temp °C	pH	Conductivity µScm^{-1}
Inlet Flow	1	52	89	0	10.3	20.9	8.5	497
After Carbonation	2	40	352	510	2.5	22.7	5.8	851
After Aeration	3	32	354	190	6.4	24	6.9	846
Outlet Flow	4	25	314	0	0.5	22.9	6.7	859

Table 6- 4: parameters measured during the field experimentation at 6 l/min inlet flow and 10 l/min circulation flow

System Stages	Sample point No.	TSS mg/l	Alkalinity mg/l as $CaCO_3$	Acidity g/l	DO (mg/l)	Temp °C	pH	Conductivity µScm^{-1}
Inlet Flow	1	44	57	50	6	21.7	7.1	882
After Carbonation	2	33	251	450	1.4	25.7	5.7	1074
After Aeration	3	24	255	190	6.6	23.4	6.7	1070
Outlet Flow	4	17	254	178	1.6	23.4	6	1110

Table 6- 5: parameters measured during the field experimentation at 6 l/min inlet flow and 3 l/min circulation flow

System Stages	Sample point No.	TSS mg/l	Alkalinity mg/l as $CaCO_3$	Acidity g/l	DO (mg/l)	Temp °C	pH	Conductivity μScm^{-1}
Inlet Flow	1	56	98	54	2.1	24.32	7.2	596
After Carbonation	2	40	152	85	3.4	24	6.6	625
After Aeration	3	33	155	66	4.6	22.8	6.7	625
Outlet Flow	4	22	148	49	1.6	25.5	6.7	704

Table 6- 6: parameters measured during the field experimentation at 6 l/min inlet flow and 7 l/min circulation flow

System Stages	Sample point No.	TSS mg/l	Alkalinity mg/l as $CaCO_3$	Acidity g/l	DO (mg/l)	Temp °C	pH	Conductivity μScm^{-1}
Inlet Flow	1	56	83	90	6.7	18.9	7.4	682
After Carbonation	2	43	170	565	2.8	21	5.8	733
After Aeration	3	31	195	194	5.6	22.3	6.7	693
Outlet Flow	4	21	185	185	2.2	19.7	6.8	652

Table 6- 7: parameters measured during the field experimentation at 6 l/min inlet flow and 7 l/min circulation flow

System Stages	Sample point No.	TSS mg/l	Alkalinity mg/l as $CaCO_3$	Acidity g/l	DO (mg/l)	Temp °C	pH	Conductivity μScm^{-1}
Inlet Flow	1	48	92	97	4.2	19	7.3	412
After Carbonation	2	34	160	640	1.2	20.5	5.8	547
After Aeration	3	25	200	246	5.5	19.5	6.3	544
Outlet Flow	4	18	165	168	1.3	17.9	6.5	600

Table 6- 8: parameters measured during the field experimentation at 6 l/min inlet flow and 7 l/min circulation flow

System Stages	Sample point No.	TSS mg/l	Alkalinity mg/l as $CaCO_3$	Acidity g/l	DO (mg/l)	Temp °C	pH	Conductivity μScm^{-1}
Inlet Flow	1	59	160	93	3.1	20.4	7.4	494
After Carbonation	2	41	215	463	0.8	22.2	5.8	602
After Aeration	3	34	234	188	5.2	21.5	6.6	638
Outlet Flow	4	24	205	160	5.6	19.6	6.3	508

6.1.3 Calcium and Phosphorus concentrations measured through field system stages at inlet flow of 3 l/min

According to the low calcium concentration and the low P removal obtained by running the system on 6 l/m inlet wastewater flow. It was decided to reduce the inlet flow to 3 l/min in order to increase the carbonation time toward increasing the Ca concentration. The new working parameters were set as shown in Table.6.9. CO_2 flow rate was adjusted 6 l/min same as previously. The circulation flow rate through the limestone column was 7 l/min. It can be seen from Figure 6.4 that Ca concentration after 95 min carbonation there was an increase in Ca to a maximum concentration which is higher than the concentration achieved by running the system with the same circulation flow and higher inlet flow, the acidity increased to the same level as previously at 6 l/min inlet flow, the same pH level was recorded. After 20 min aeration there was a small decrease in Ca concentration decreased and the same pH level recorded. By keeping the circulation flow rate adjusted on 7 l/min for the next time, the same trend was observed. Figure 6.5 show the changes in P concentration over the process stages. Only small decrease in P concentration was noticed after aeration stage when the initial P concentration was 5.8 whereas in the seconed time when the initial concentration was 6.2 a small drop in P concentration noticed after settlement stage. Tables 6.10 and 6.11 show the changes in all the related parameters after reducing the inlet flow to 3 l/min.

Table 6- 9: Working parameters on site

Carbonation Stage			**Aeration Stage**	**Settlement Stage**	**Date**
Inlet Flow Rate (l/min)	**Circulation Flow Rate (l/min)**	**Carbonation Time (min)**	**Time (min)**	**Time (hr)**	**DD/MM/YY**
3	7	95	20	9	20,23/08/2018

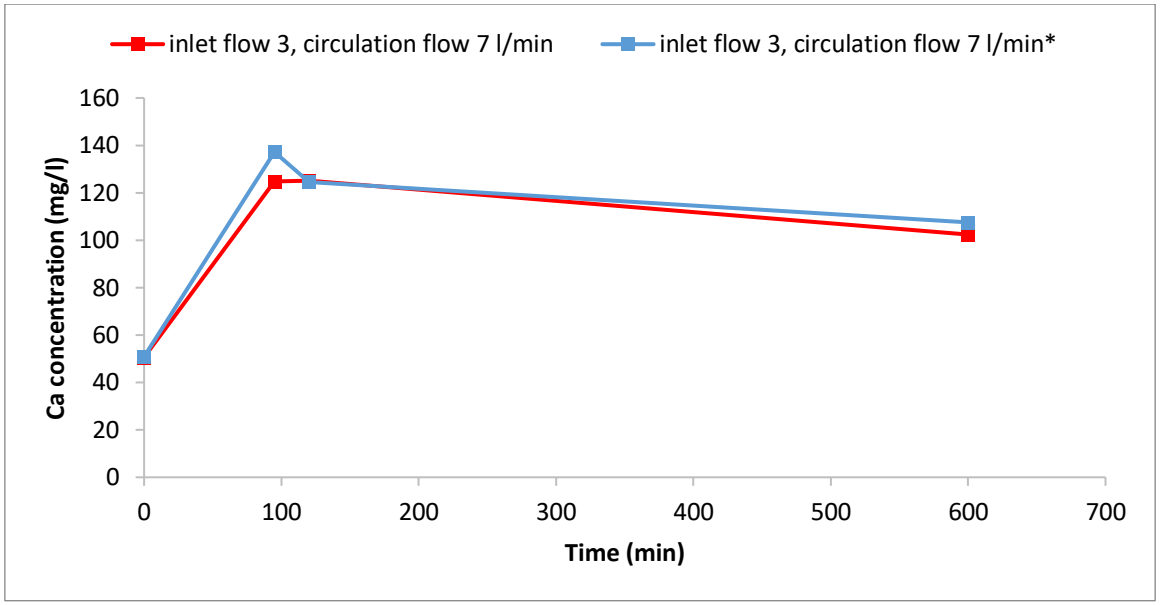

Figure 6- 4: Calcium concentration measured during field trial. At inlet flow 3 l\min. Trial conditions: Carbonation for 95 min, Aeration for 20 min, Settlement for 9 hr. Stars refer to number of times

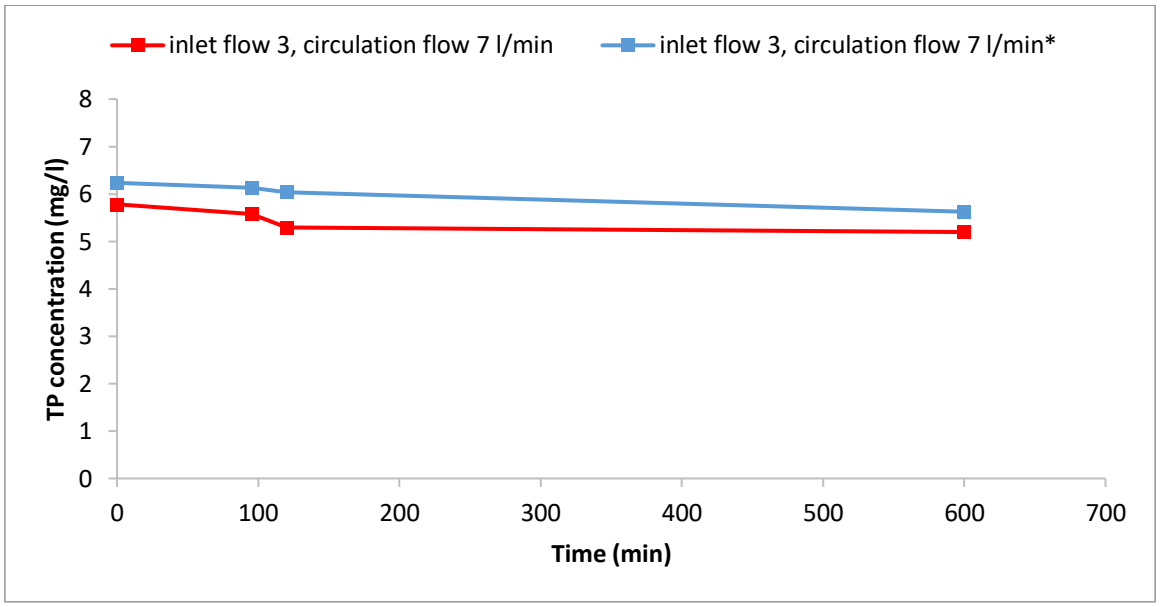

Figure 6- 5: Total phosphorus concentration measured during field trial. At inlet flow 3 l/min. Trial conditions: Carbonation for 95 min, Aeration for 20 min, Settlement for 9 hr. Stars refer to number of times

Table 6- 10: parameters measured during the field experimentation at 3 l/min inlet flow and 7 l/min circulation flow

System Stages	Sample point No.	TSS mg/l	Alkalinity mg/l as $CaCO_3$	Acidity g/l	DO (mg/l)	Temp °C	pH	Conductivity μScm^{-1}
Inlet Flow	1	51	129	79	5.2	19.2	7.3	506
After Carbonation	2	44	282	640	1.6	20.8	5.8	736
After Aeration	3	32	290	214	4.6	21.5	6.6	733
Outlet Flow	4	20	263	185	0.2	19.1	6.6	593

Table 6- 11: parameters measured during the field experimentation at 3 l/min inlet flow and 7 l/min circulation flow

System Stages	Sample point No.	TSS mg/l	Alkalinity mg/l as $CaCO_3$	Acidity g/l	DO (mg/l)	Temp °C	pH	Conductivity μScm^{-1}
Inlet Flow	1	35	144	59	3.6	21.5	7.3	526
After Carbonation	2	22	278	567	2.4	23	5.7	748
After Aeration	3	18	298	175	8	22.4	6.6	748
Outlet Flow	4	12	273	160	0.7	20.3	6.6	649

6.1.4 Calcium and Phosphorus concentrations measured through field system stages at inlet flow of 1 l/min

According to the low calcium concentration and the low P removal obtained by running the system on 3 l/min inlet wastewater flow. It was decided to reduce the inlet flow to 1 l/min in order to increase the carbonation time toward increasing the Ca concentration. The new working parameters were set as shown in Table 6.12 CO_2 flow rate was adjusted 6 l/min same as previously. The circulation flow rate through the limestone column was 7 l/min. It can be seen from Figure 6.6 that Ca concentration after 275 min carbonation increased to the same concentration when 12 l/min circulation and 6 l/min inlet flow were used with higher acidity recorded this time and the same drop in pH level. After 20 min aeration A drop in Ca concentration was observed due to the degassing effect followed by further drop during settlement stage. By keeping the circulation flow rate adjusted on 7 l/min for the next time, the same trend was observed. Figure 6.7 show the changes in P concentration over the process stages. It is clear to see that there was a noticeable drop in P concentration over the aeration and settlement stages for the two initial P concentration. Table 6.13 show the changes in all the related parameters after reducing the inlet flow to 1 l/min.

Table 6- 12: Working parameters on site

Carbonation Stage			Aeration Stage	Settlement Stage	Date
Inlet Flow Rate (l/min)	Circulation Flow Rate (l/min)	Carbonation Time (min)	Time (min)	Time (hr)	DD/MM/YY
1	7	275	20	16	13,17/09/2018

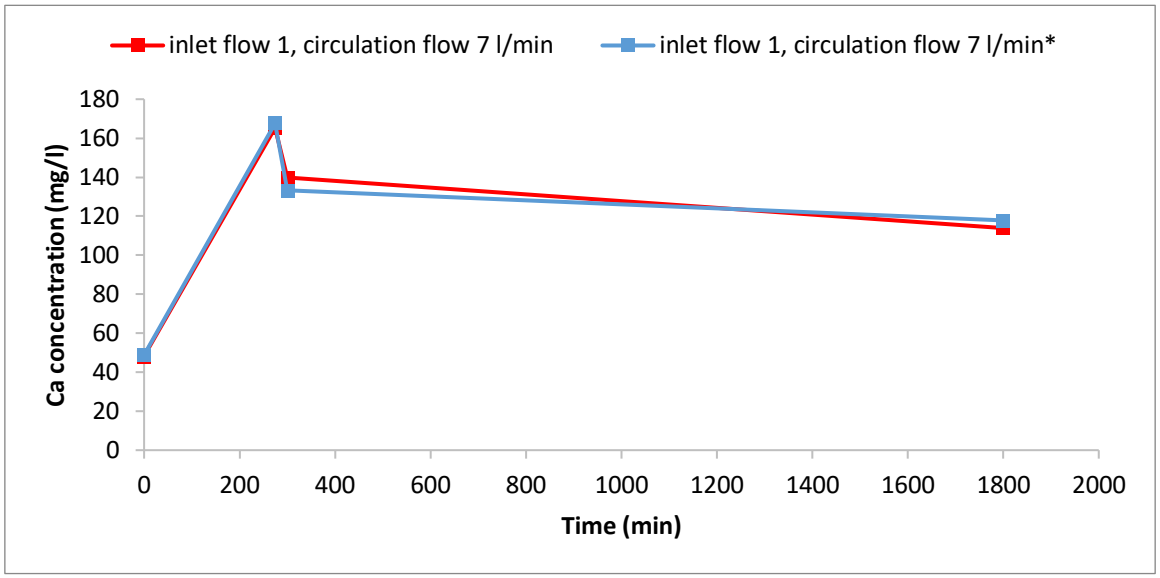

Figure 6- 6: Calcium concentration measured during field trial. At inlet flow 1 l\min and at 7 l/min circulation flow rate. Trial conditions: Carbonation for 275 min, Aeration for 20 min, Settlement for 16 hr. Stars refer to number of times

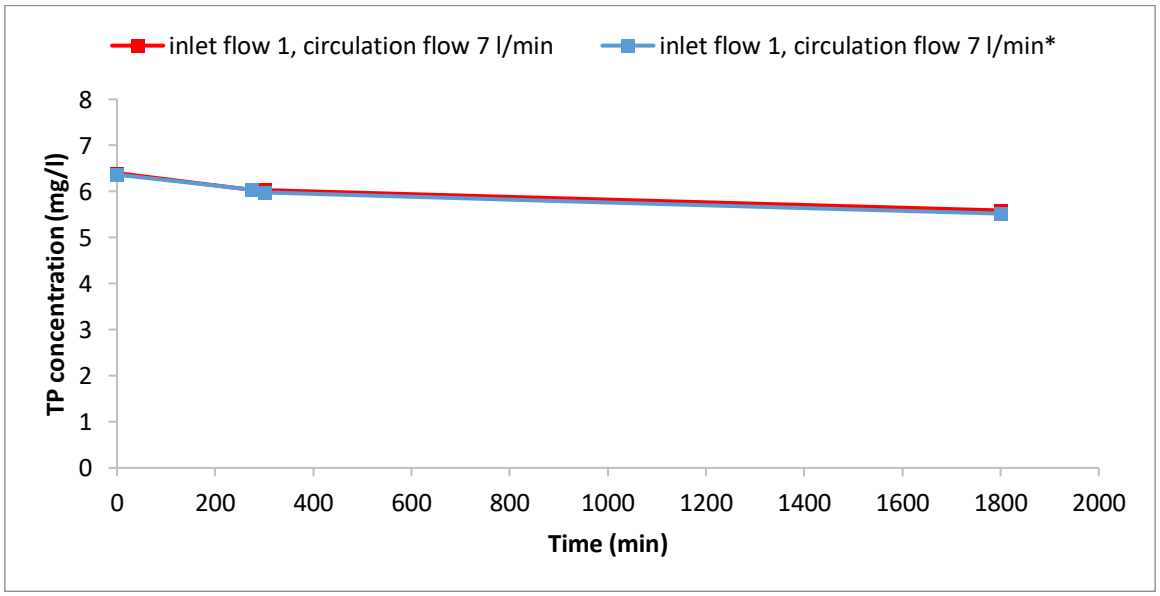

Figure 6- 7: Total phosphorus concentration measured during field trial. At inlet flow 1 l\min and at 7 l/min circulation flow rate. Trial conditions: Carbonation for 275 min, Aeration for 20 min, Settlement for 16 hr. Stars refer to number of times

Table 6- 13: parameters measured during the field experimentation at 1 l/min inlet flow and 7 l/min circulation flow

System Stages	Sample point No.	TSS mg/l	Alkalinity mg/l as $CaCO_3$	Acidity g/l	DO (mg/l)	Temp °C	pH	Conductivity μScm^{-1}
Inlet Flow	1	30	130	100	4.5	14.3	7.1	617
After Carbonation	2	17	380	800	1.8	17.7	5.8	825
After Aeration	3	13	389	335	6.5	19.1	6.6	787
Outlet Flow	4	8	317	210	0	22.2	7.1	276

6.1.5 Summary and discussion

As mentioned previously in the literature chapter that the aim of carbonation stage is to dissolve limestone and bring enough amount of Ca ions in solution as one of the dominant factors influencing calcium carbonate/phosphate precipitation (Dreybrodt, W. 1981; Zuddas and Mucci 1994) according to one or more of the following chemical reactions and processes responsible for the dissolution of calcite with respect to CO_2 (Langmuir 1997):

$$CaCO_3 + H^+ \leftrightarrow Ca^{2+} + HCO_3^- \quad (6.2)$$

$$CaCO_3 + H_2CO_3 \leftrightarrow Ca^{2+} + 2HCO_3^- \quad (6.3)$$

$$CaCO_3 + H_2O \leftrightarrow Ca^{2+} + HCO_3^- + OH^- \quad (6.4)$$

There was a positive correlation between calcite dissolution and circulation flow. It can be seen that calcite dissolution decrease significantly with decreasing the circulation flow rate and all the applied circulation flows of 12,10,7 and 3 l/min did not increase the Ca concentration to reach the concentration obtained from the laboratory experiments indicating that an increase in the time of this stage might improve the concentration at the same CO_2 flow rate. The drop in pH values during carbonation stage to a level of 5.8 indicating the formation of carbonic acid as a results of CO_2 injection. The pH level at this stage was close to the pH level obtained in the laboratory experiment. An increase in alkalinity in this stage was also noticed indicating calcite dissolution. The highest calcium concentration recorded during the field trial 156.6 mg/l was not sufficient to precipitate phosphate. Inskeep and Bloom (1985) and Zhang and Grattoni (1998) concluded in their studies that the CO_2 loss and pH are an important factor affecting precipitation. The aim of aeration stage was to degas the CO_2 and encourage precipitation by increasing the pH level to around 7.7 as obtained from the laboratory experiments. It can be seen that during aeration stage there was an increase in pH due to the CO_2 degassing, but it was not sufficient to promote precipitation and remove P. it is also clear to see that the wastewater was leaving the aeration stage with high Ca concentration. This suggests that the aeration that the wastewater was subjected to was insufficient. All the examined residence time in the settlement stage

indicated that more time is required for precipitation to occur under the same experiment conditions. The results presented in sections 6.1.2, 6.1.3 and 6.1.4 indicating that the Ca concentration obtained from carbonation stage was not high enough, pH level during aeration which was an important key factor identified during laboratory experiments was not elevated to the required level to promote precipitation comparing with the data obtained from the laboratory experiments.

6.2 ARM field trial - Results and discussion

6.2.1 Inlet and IBC phosphorus concentrations

Figure 6.8 shows the concentrations of total, dissolved, and ortho P in mg/l against time since sampling began. Values were recorded at the inlet and after the aerated reedbed (IBC). The inlet data shows an increase in TP concentration on 5/7/2018. Variation in the inlet concentrations is highest in the data after that with minimum and maximum values of 3.7 and 11.0 mg/l. With mean values decreasing from 5.1 mg/l at the inlet to 3.7 mg/l after the reedbed. The mean values of dissolved P decreased from 4.9 mg/l at the inlet to 3.6 mg/l after the reed bed. While the decrease in ortho P mean values was from 3.5 mg/l at the inlet to 2.7 mg/l after the reedbed. Sample dates are shown in table 6.14

Table 6- 14: Dates of sampling

Sample No.	**1**	**2**	**3**	**4**	**5**	**6**	**7**	**8**	**9**	**10**
Date	9/5/18	14/5/18	17/5/18	24/5/18	14/6/18	2/7/18	5/7/18	12/7/18	9/8/18	13/8/18
Sample No.	**11**	**12**	**13**	**14**	**15**	**16**	**17**	**18**	**19**	**20**
Date	16/8/18	20/8/18	23/8/18	28/8/18	30/8/18	3/9/18	10/9/18	13/9/18	17/9/18	24/9/18
Sample No.	**21**	**22**	**23**	**24**	**25**	**26**	**27**	**28**	**29**	
Date	1/10/18	4/10/18	8/10/18	11/10/18	15/10/18	18/10/18	22/10/18	25/10/18	29/10/18	

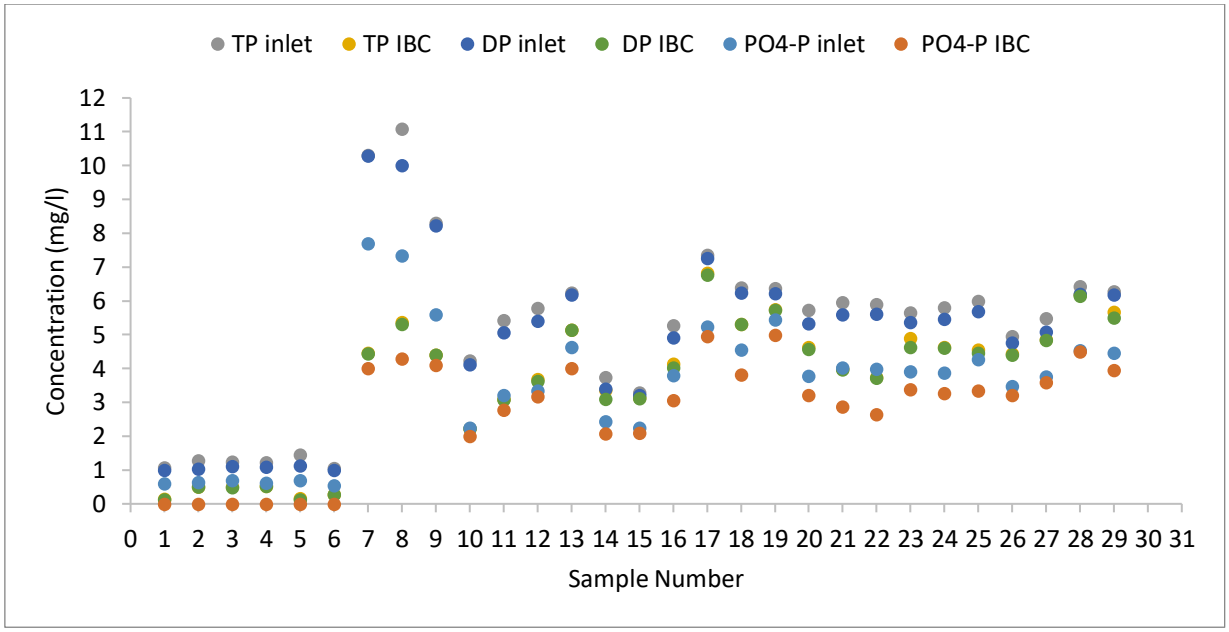

Figure 6- 8: P concentrations measured during experimentation from the inlet and IBC

6.2.2 Performance of each column in terms of media, concentration, pH and flow rate

Figure 6.9 shows the concentrations of total P in mg/l against time since sampling began. Values were recorded at the inlet, after the aerated reedbed and at the outlet of each column. The 1st and 2nd column (Media 1) with an average flow rate of 0.05 ml/min and 0.13 ml/min, respectively. The 3rd and 4th column (Media 2) with an average flow rate of 0.05 ml/min and 0.13 ml/min, respectively. It can be seen from these figures that all the inlet concentration values went to almost zero at the outlet of each column. Outlet total P concentrations are consistent with mean value decreased from 5.1 mg/l at the inlet to 0.1 mg/l at the outlet of each column. Figure 6.10 shows the pH values measured during the experimentation time for all system stages. The variation in the inlet pH is highest in the data from 9/5/2018 to 2/7/2018 with minimum and maximum values of 6.1 and 9.2. While the change in pH values was consistent from 5/7/2018 to 29/10/2018 with minimum and maximum values of 7.1 and 7.5. A slight increase in pH after the aerated reedbed with the mean inlet pH increased from 7.3 to 7.8. A significant increase in pH was noticed at the outlet of Column 1 and 2 (Media 1) with mean pH values of 11.6 and 11.3, respectively. While there was a small increase in pH for column 3 and 4 (Media 2) with mean pH values of 8.0 and 7.7 respectively. The minimum level of Ca recommended for Ca-P precipitation should be 40 – 60 mg/l (Jang and Kang 2002). The inlet Ca concentration showed an increase from 48.1mg/l to 143.5 and 87.1 mg/l in the 1st and 2nd column (Media 1) with average flow rate of 0.05 ml/min and 0.13 ml/min respectively and to 236.5 and 113.0 mg/l in the 3rd and 4th column (Media 2) with average flow rate of 0.05 ml/min and 0.13 ml/min respectively. This increase in Ca concentration led to an average pH increase from 7.8 to 11.6 and 11.3 in column 1 and 2

respectively, 8.0 in column 3 while the average value of pH in column 4 was 7.7. Bellier et al. (2006) highlighted the best pH conditions are conflicting as a low pH would favour Ca dissolution and a high pH would favour HAP precipitation.The final pHs of Media 1 in column 1 and 2 are above 9, which is the lower limit for calcium phosphate precipitation stated by (Johansson and Gustafsson 2000). This could explain the high performance of these pellets. However, the final pH of media 2 in column 3 and 4 are fluctuated around 9 as shown in Figure 6.18.

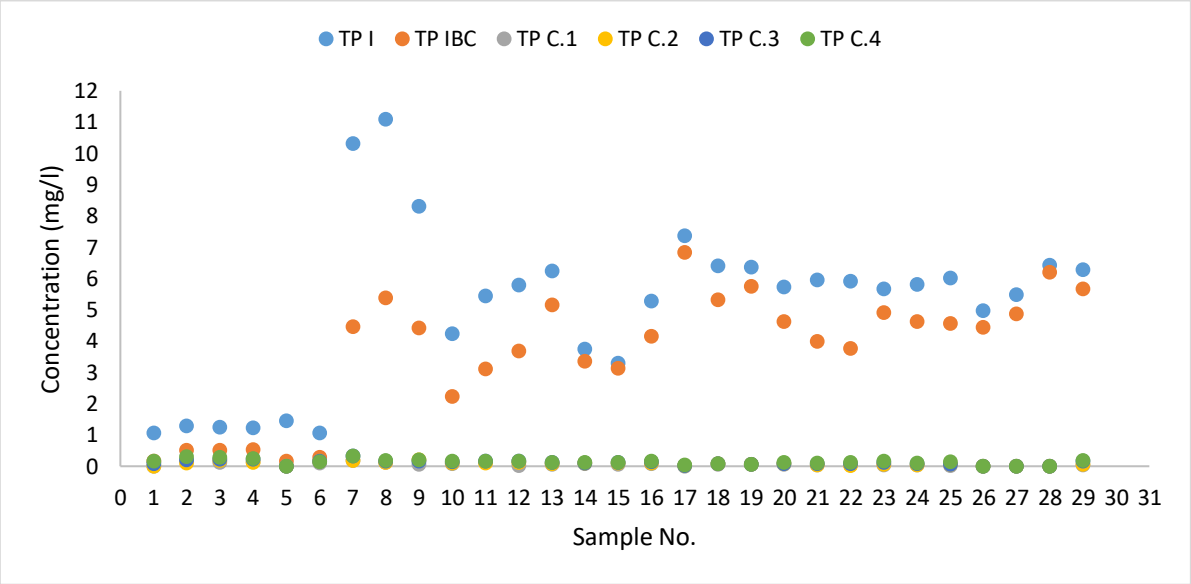

Figure 6- 9: Total phosphorus concentrations from the inlet, IBC (a) column 1 (b) column 2 (c) column 3 (d) column 4.

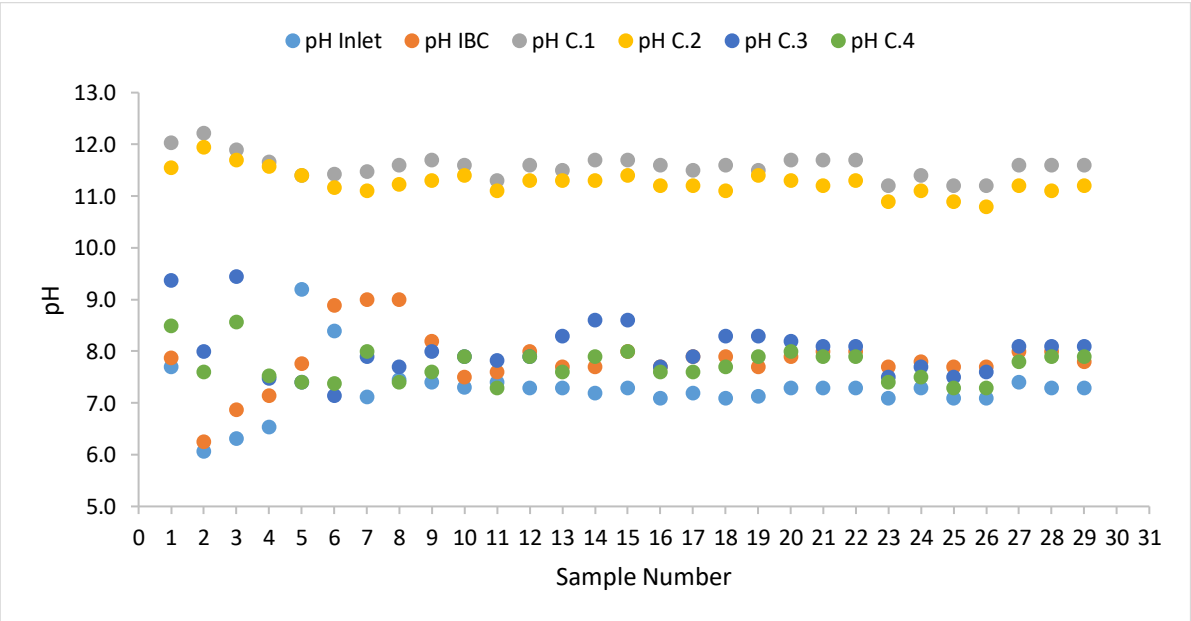

Figure 6- 10: pH reading from the system stages during experimentation

6.2.3 Media, concentration performance comparison

Figure 6.11 shows the concentration of total P for each column. It can be seen that the decrease in TP concentration for both media and for the two different flow rates was close. Although, Ca

concentration in Media 1 columns was less than in Media 2 columns. The performance of Media 1 in removing phosphate was slightly better over the examined period. The same observation was highlighted for the dissolved P while the results of ortho P showed the same trend for all columns, as shown in Figure 6.12 and 6.31 respectively.

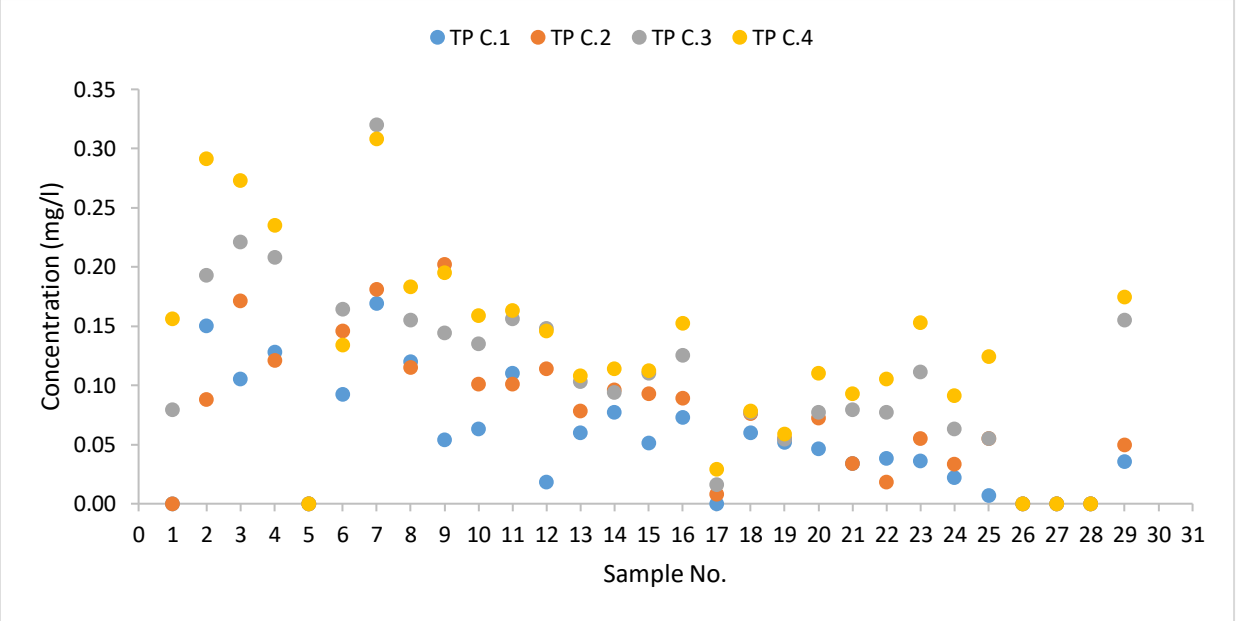

Figure 6- 11: Total phosphorus concentrations in the effluent from column 1, column 2, column 3 and column 4.

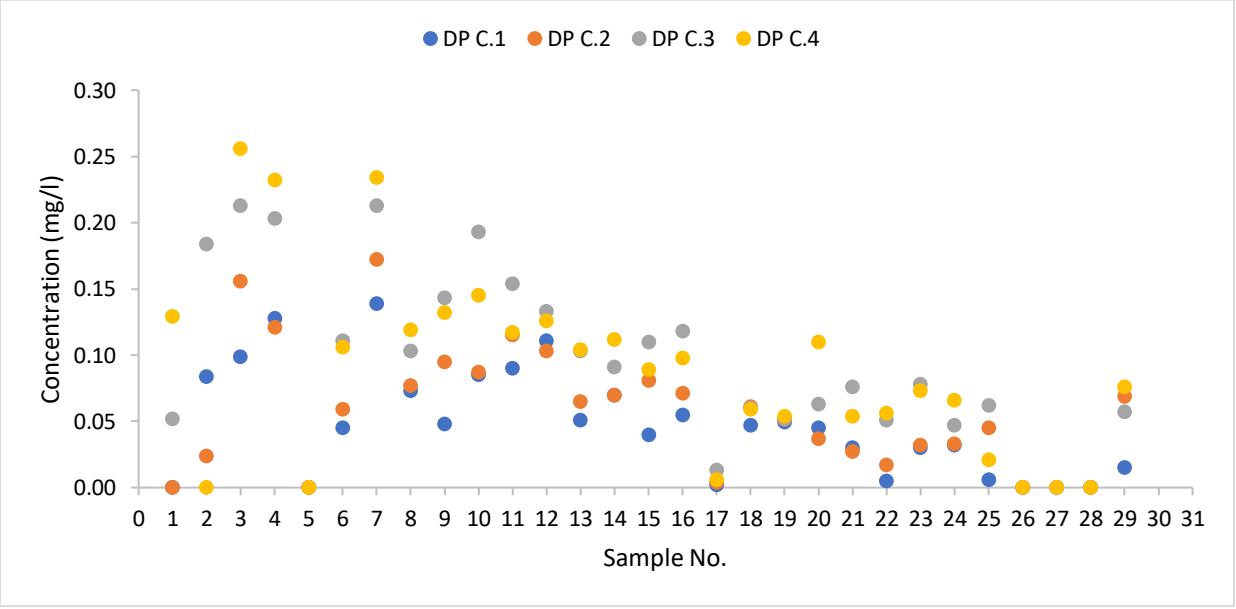

Figure 6- 12: Dissolved phosphorus concentrations in the effluent from column 1, column 2, column 3 and column 4.

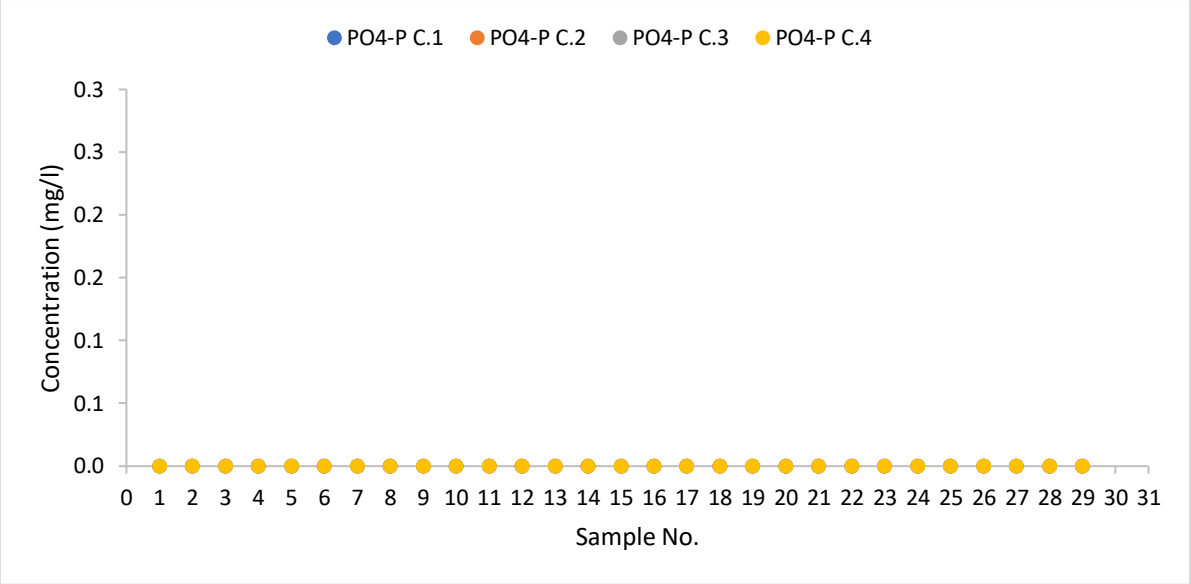

Figure 6- 13: PO_4-P concentrations in the effluent from column 1, column 2, column 3 and column 4.

Figure 6.14 (a, b) show the surface of both media after 173 days of use in the field trial, shows a clear difference in morphology between the used and the unused pellets (see figure 5.28, section 5.4.1, chapter 5). The virgin pellets were composed of smaller particles providing quite a rough surface as described in Chapter 5. Media 2 used pellets are showing much smoother surfaces that could well be as a result of calcium phosphates being precipitated onto the surface while there was no noticible difference between the virgin and the used pellets of Media 1. This may suggest that removal is limited by a decrease in kinetic reaction and not only by media saturation (Molle et al. 2005). In field trial, reactions were quite different due to different hydraulic conditions and contact time. this can be confirmed by the pH level, This may suggest that the removal mechanisim might be different than that in the batch tests. Same observation has been made by (Lee et al. 2005).

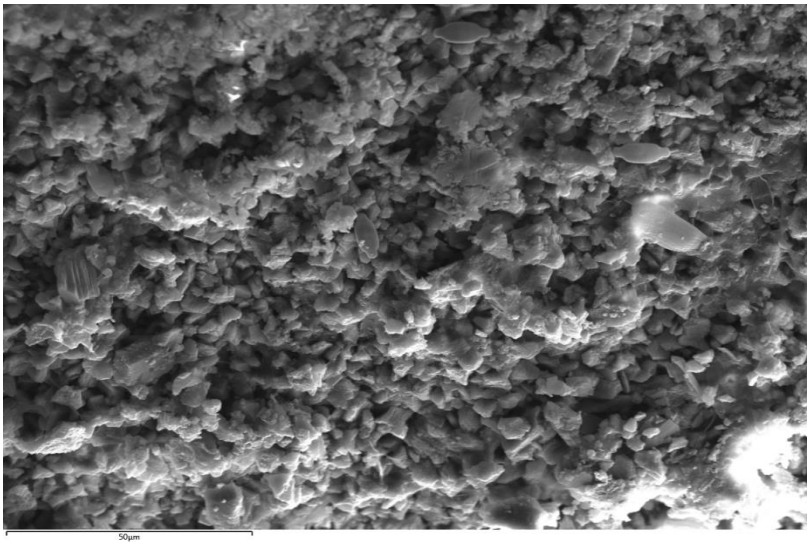

(a)

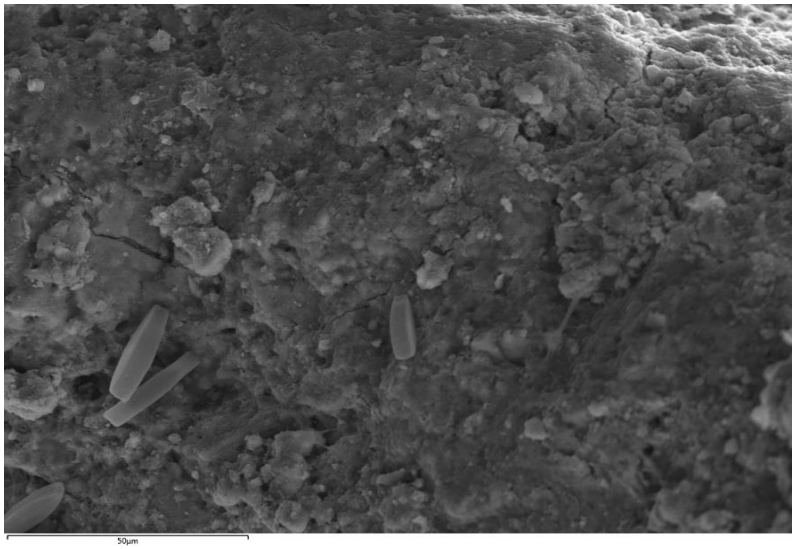

(b)

Figure 6- 14: ESEM images after 173 day for (a) Media 1 and (b) Media 2

To Calculate the cumulative P removed during the operation time the following equation was uesd:

Cumulative P removed (mg)= $(C_{in} - C_{out})*Q*t$

Where C_{in} and C_{out} is the removed P concentration mg/l measured during the operation time for P concentration of 10.04, Q is the flow rate (79.2 and 191.5 l/d) and t is the operation time (173 day). Cumulative P removed from each column is 137,02 and 331,295 mg respectivley. Comparing the previous calculations to the removal capacity calculated from the adsorption test showed that for both media, it is possible to remove 1.1 mg P for each gram of both media for initial P concentration of 10 mg/l by multiplying the removal capacity for each gram of media calculated from the laboratory experiment by the total amount of media in each column (330 kg), the maximum potential amount to be removed by each column of media is 363,000 mg indicating that by running the trial using 79.2 l/d flow rate, the media might last longer before get saturated than by using 191.5 l/d flow rate. Figure 6.15 and 6.16 (a, b) show P loading rate and P removal rate for the 4 columns at the 79.2 and 191.5 l/d flow rate respectively. it can be seen that the removal rate is higher when the flow rate is low and decrease with increasing flow rate.

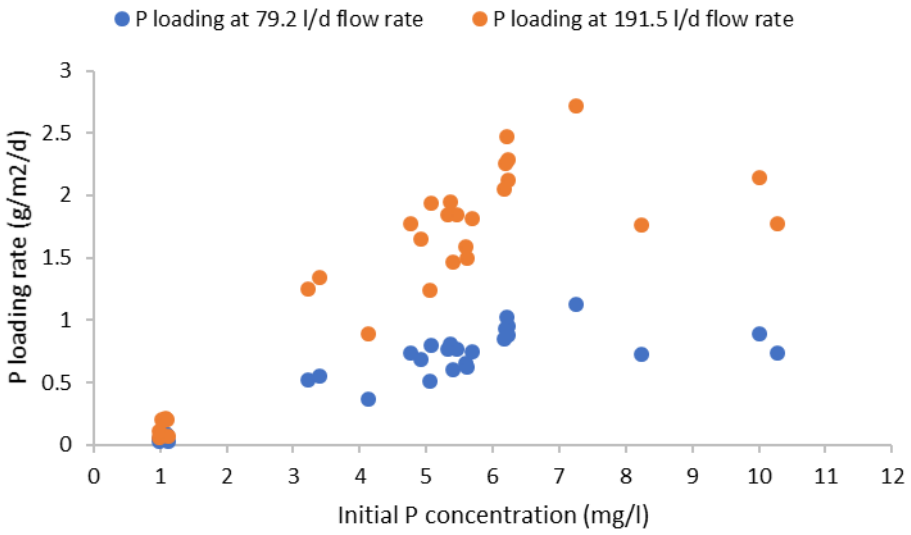

Figure 6- 15: P loading rate at 79.2 and 191.5 l/d during sampling period

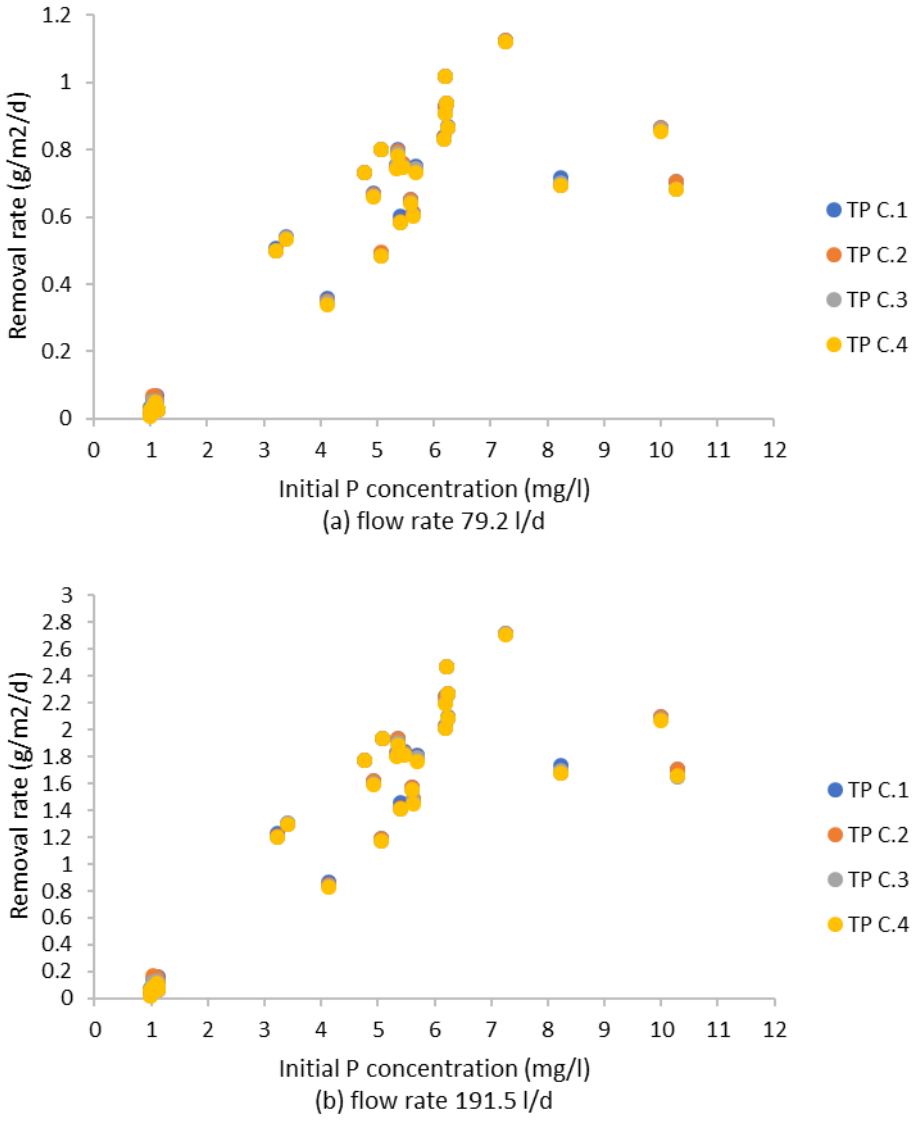

Figure 6- 16: Columns P removal rate at (a) 79.2 and (b) 191.5 l/d during sampling period

6.3 Chapter summary and conclusions

- **Cardiff University Trial**

  It is important to establish whether the system was working as intended as described in the methodology chapter. During the operation time of the carbonation treatment, there was a slight decrease in P concentration indicating that the carbonation process could work effectively with either prolonged residence times through the different stages of the process or implementing some changes within the system to enhance the performance. It was proven by the laboratory experimentation that the carbonation system was able to reduce P concentration to below 1 mg/l while it was established that the field system was not working as it had been seen to behave in the laboratory experimentation. the evolution of pH across the system is as anticipated (to varying degrees), the addition of CO_2 to the limestone reactor results in the effluent of that limestone reactor whith lower pH due to the presence of carbonic acid and that the system effluent pH is slightly higher than this because CO_2 degassed. A number of findings were made from analysing the results of the field trial and comparing it with the results obtained from the lab system:

1. In the limestone reactor and during carbonation stage, the expected trend of Ca concentration was in line with the proposed mechanism. However, the dissolved Ca was not reaching the same concentrations as observed in the laboratory. Maximum Ca concentration was obtained from running the trial at 6 l/min inlet flow, 12 l/min circulation flow and 6 l/min CO_2 flow rate for approximately 50 min was 156.5 mg/l. while the Ca concentration obtained from running real wastewater solutions through the laboratory system at CO_2 flow rate of 0.75 l/min for 40 min were 240-280 mg/l.
2. Circulation flow was an important parameter effecting the Ca dissolution in the carbonation stage. Maximum Ca concentration obtained from running the trial at 6 l/min inlet flow, 12 l/min circulation flow. By reducing the inlet flow rate to 1 l/min and circulation flow of 7 l/min it was possible to achieve the same Ca concentration of 6 l/min inlet flow and 12 l/min circulation flow.
3. Although the aeration using two aeration tanks and plastic media has shown that a significant reduction in P_{CO2}, was achieved by increasing the pH during this stage, pH didn't reach the required level > 7.3 as obtained during lab experimentation to encourage precipitation formation. Apply an air blower at the aeration stage to increase the CO_2 degassing could be beneficial to increase pH to levels closer to laboratory experiment and promote precipitation.

- **ARM LTD Trial**
    1. The field scale columns were efficient enough to reduce P-level to reach 0.0 mg P/l at flow rate of 72.9 and 191.5 l/d. A long-term stability of the process remains to be established under varying influent and operational conditions such as Ca availability, retention time and pH.
    2. The P removal of Media 1 is connected to strongly alkaline conditions (pH greater than 11) While the P removal of Media 2 is connected to (pH less than 9) and large amounts of soluble Ca.
    3. The change in morphology of media 1 before and after use examined by ESEM images confirmed the formation of crystalline hydroxyapatite.

Chapter 7: Conclusions and Recommendations

7.1 Conclusions

With reducing phosphate resources, tightening discharge limits and increasing treatment costs, it is clear to see that there is a need for the introduction of novel solution for removing phosphorus from wastewater which are both inexpensive and sustainable. It is expected that the technique and the media investigated in this project will accomplish all these aims which would allow for their potential introduction in the wastewater treatment industry. This chapter presents the key conclusions and recommendations that the current study has led to.

Cardiff University process:

A carbonation process was tested for the removal of phosphorus from wastewater. In the lab runs, phosphorus concentration was reduced for all solutions, promising that the carbonate process works as a treatment to remove phosphate from solution. Within the Uk, the most common methods of phosphate removal are chemical dosing and biological treatment. The technology involved with these processes is trusted and largely understood. However, the infrastructure, monitoring and material cost requirements restrict the application of these methods to large treatment works only. Furthermore, the disposal of sludge produced as a by product of this treatment phase can be troublesome and expensive. Other novel treatment methods for P removal do exist, including the controlled precipitation of struvite, magnetic separation and electro coagulation. However, these methods often require additional precursors to treatment such as pH adjustment, the addition of expensive additives like iron, aluminium, magnetite or high energy inputs. Thus, they are also not suitable to be fitted to smaller WWTWs. The process investigated within this study uses a relatively low cost materials (limestone) and it is feasible that it may adapted to a low energy treatment system and suitable to small and large WWTWs alike. Based on the research carried within this part of the study, the following key conclusions can be drawn.

- The laboratory results clearly showed that as both the volumetric CO_2 flow rate and the duration increased, then $CaCO_3$ dissolution increased up to a maximum in line with expected equilibrium solubility of $CaCO_3$. It was also observed that calcium concentration in DI water of 340 mg/l can be achieved in optimum conditions.
- When solutions from the carbonation stage were aerated at different volumetric flow rates and durations it was found that the pH always increased but that precipitation was only

observed when aeration rate of 2 l/min (per litre of solution) was used. The reason why aeration rate is so critical for producing precipitate seems to be related to pH.

- The precipitate formed from mixture of limestone and water was shown by XRD to be calcite of particle size D_{10} of 12.2 μm, D_{50} of 27.6 μm, D_{90} of 46.1 μm and was relatively depleted in Fe and Al compared to the original limestone.
- Results showed that by running the proposed laboratory process using 1 L P solution under 40 min carbonation of 750 ml/min, 40 min aeration of 2 l/min and 48 hr settlement, phosphate ions are reduced from solution to a concentration as low as 0.6mg/l and a precipitation of HAP was formed with the kinetics corresponding to a theoretical interpretation proposed previously.
- High load removal obtained by running the laboratory system with high initial phosphorus concentration highlighting the potential of treating a flow with higher concentration of phosphorus.
- The presence of phosphate ions clearly retarded the dissolution of limestone in agreement with observations from other studies. The mechanism of retardation suggested by other studies is possibly the formation of calcium phosphate on the surface.
- The length of quiescent settling time appeared to influence further uptake of P from solution. This is probably due to further precipitation of HAP.
- The presence of elevated Mg and SO_4 ions in tap water and in real wastewater appear to retard the rates of calcium phosphate formation. The mechanism of retardation suggested by other studies is possibly the formation of other calcium components like calcium sulfate.
- XRD analysis performed on precipitate samples taken from the bottom of the settlement beaker after the process had been completed proved that the calcium and phosphorus precipitation/sorption process was occurring. Furthermore, the precipitate formed from phosphate solution was different depending on starting concentration of phosphate as the concentration of dissolved phosphorus increases, calcite precipitation deceases and there is evidence from the changes in the precipitate composition, for the formation of calcium carbonate/ calcium phosphate phase.
- XRD, total digest and total carbon analysis showed that calcium carbonate is the main precipitate when P concentration were 2,10 and 20 mg while calcium phosphate and calcium carbonate were the precipitant when P concentration of 100mg/l was used as an initial concentration for all P solutions.
- ESEM analysis showed that the morphology of the precipitate changes from crystalline to amorphous by increasing initial P concentration indicating the formation of amorphous

calcium phosphate at high initial P concentration. This analysis also showed that the foreign ions presented in tap water and real wastewater do not affect the morphology of the precipitate.

- FEG-SEM analysis showed surface coverage of P on all precipitates indicating that phosphate ions were replacing carbonate ions to form calcium phosphate and indicated close association between Ca and P as there were no patches of P concentrated in one spot, so the P coverage was uniform. This analysis also showed that the presence of the foreign ions in tap water and real wastewater samples did not affect the distribution of P in precipitate.
- Zeta potential experiment showed that the newly formed calcium carbonate precipitate had negative surface charge. This is therefore preventing electrostatically unfavourable surface for phosphate adsorption. Addition of phosphate make the zeta potential even more negative. This could suggest some adsorption of phosphate or it could be the formation of thin surface layer of HAP which make the surface more negative as the XPS analysis indicated. Adsorption experiment using calcite precipitate showed small uptake of phosphate but not huge although the mechanism between adsorption and precipitation is difficult to be decided from these tests because calcium was being released at the same time as P. Sequential extraction experiment showed very little loosely sorbed phase and most in apatite phase. All this evidence clearly points towards precipitation as the major mechanism of removal in the system.
- Although, it is difficult to assess the performance of the carbonation precipitation process in the field due to the challenges on implementing the system on site, a number of key findings can be concluded:
    1. It has been shown that calcium concentration in the limestone reactor can be increased by increasing the circulation flow for the same CO_2 flow rate.
    2. pH dropped in the carbonation stage to almost the same level obtained in the laboratory experiment indicating the formation of carbonic acid.
    3. Noticeable increase in pH during passive aeration indicating the CO_2 degassing although the final maximum pH of 6.9 was not sufficient to promote precipitation.

ARM Ltd apatite media:

Two apatite media were tested for the removal of phosphorus from wastewater. Both media showed effectiveness in removing phosphorus from wastewater. Based on the research carried out on this part of the study, the following conclusions can be drawn:

- XRD analysis of apatite media 1 and 2 showed that the dominant mineral in media 1 was hydroxyapatite with a minor amount of silicon dioxide, and the dominant component in media 2 was fluorapatite with gypsum.
- Adsorption test carried out on ARM media suggested the adsorption as the dominant removal mechanism for both media with pH less than 9 which is the minimum pH required to precipitate calcium phosphate. This test also showed the high Ca concentration released from Media 2 comparing with Media 1.
- The data of real wastewater obtained from West Bonvilston site showed that often ortho phosphate was the major component, but the presence of other phosphate forms was indicated up to 25%.
- Although, the P loading rate was very low (79.2 and 191.5 l/d) the column Media 1 in field application was effective in removing almost 100% phosphate for 6 months trial. this media elevated pH to high levels of up to 11.3. Mechanism of P removal by this media is therefore likely to be precipitation as the media releases Ca at high pH. Media 2 was also very effective in removing phosphate. As the media is releasing high Ca concentration and pH level in the zone of precipitation HAP indicating the precipitation as the possible removal mechanism. The change in morphology of both media before and after use on site examined by ESEM images confirmed the formation of crystalline hydroxyapatite.
- The high pH values caused by the Media 1 pellets would likely be a hindrance to their practical implementation.

The introduction of such a process and media to eliminate phosphorus from wastewater into industry would offer significant financial advantages to water companies which would be passed onto the general public. The investigated process and media would also enable water boards to meet treatment goals set under the Water Framework Directive. Furthermore, environmental benefits are realised via an improvement in water quality and potentially a reduction in greenhouse gas emission associated with fertilizer production.

7.2 Recommendations for further work

Other different adaptations, tests, and experiments could not been targeted due to lack of time could be recommended for future work:

- It has been reported by Aziz et al. (2001) that the removal increased marginally with decreasing particle size and this is due to the greater surface area per volume of smaller diameter limestone chips available to come into contact with the effluent solution. Further experimentation could be carried out to determine if the process will work as effectively

when P solution is carbonated in a limestone column bed containing chips with diameter larger to 2-5 mm. the use of bigger size chip sizes would result in the limestone column being more porous thus allowing a larger volume of water to be treated per area of limestone. Tests could also be performed using chips with a smaller diameter than 2-5 mm in order to determine if their increased surface area per volume will results in more $CaCO_3$ being dissolved in solution during carbonation and hence more phosphorus being co precipitated with calcium during aeration.

- Initial results in section 4.2.2.1 showed that by increasing CO_2 flow rate and duration, limestone dissolution increased. As a result of this finding and towards increasing the efficiency of the CO_2 in dissolving limestone, test could be conducted with variable limestone column height might result in more calcite dissolution as a result that carbon dioxide being injected into a column having more time to dissolve in solution.
- Results presented in section 4.3 showed that limestone dissolution was occurring during carbonation stage and precipitation was occurring mainly during aeration stage. Further experimentation is required to determine if the addition of air and CO_2 simultaneously into the limestone column can consistently produce effective results at reducing phosphate concentration from solution by combining both carbonation and aeration stages.
- Results in section 4.4.1 showed that limestone dissolution was retarded by increasing P concentration in solution. More analysis could be carried out to determine the mechanism of inhibition and if there is a directly proportional link between the concentration of calcium dissolved in solution during carbonation stage and the subsequent removal of phosphorus from solution during aeration stage.
- Precipitate characterisation test in section 5.2.1 showed that hydroxyapatite and calcite are the precipitates with initial P concentration of 100 mg/l and FEG-SEM analysis in section 5.2.4 showed that Ca was uniformly distributed across the samples. Further research is needed to identify the order of the phases formed and how the presence of CO_3^{2-} ions control the reaction kinetics.
- Testing should be continued in trying to establish if effective P removal from wastewater can be obtained in shorter carbonation, aeration and settlement time than discovered in this study. Results obtained from tests performed during this project would suggest that mixing limestone with gypsum would almost double the concentration of calcium and reduce the CO_2 flow rate from 750 ml/min to 100 ml/min. More investigation on replacing limestone with gypsum might avoid the use of CO_2 completely.

- Regarding the field trial system, it has been identified that the Ca concentration generated by the limestone reactor is low and further investigation is required to increase calcium concentration in the limestone reactor to achieve the calcium concentration obtained in batch experiments.
- There would be a considerable scope to improve the efficiency of CO_2 utilisation through better design to further reduce costs. Using a CO_2 based system has the advantage over conventional chemical treatment, that it is impossible to overdose, eliminating the risk of the discharge consent breaches. Furthermore, it is possible that CO_2 from on site combustion of digester gas (which is rich in CO_2) could be used in the process eliminating the need to purchase CO_2. The carbonation system might be useful for retrofitting to existing tertiary ponds/ wetlands where improved P removal is required.
- As the lab experimentation indicated that pH is an important factor to achieve high removal and It has already been identified from the field trial that the degree of aeration generated by the current aeration stage appears to be limiting its treatment performance. it is essential to increase aeration efficiency by either applying an air blower to the current aeration stage to degas the CO_2 and elevate the pH to the required level or increase aeration time by changing the design of the aeration stage.
- The effective P removal achieved by using the apatite media was attributed to the introduction of a calcium phosphate precipitation removal mechanism as a result of the high Ca concentration and high pH. Prolonged operation time is required to assess the performance of ARM media. The high pH values would likely be a hindrance to their practical implementation. The avoidance of this could be investigated.

References

Abbona, F. and Baronnet, A. 1996. A XRD and TEM study on the transformation of amorphous calcium phosphate in the presence of magnesium. Journal of Crystal Growth 165(1–2), pp. 98–105. doi: 10.1016/0022-0248(96)00156-X.

Ádám, K. et al. 2007. Phosphorus retention in the filter materials shellsand and Filtralite P®-Batch and column experiment with synthetic P solution and secondary wastewater. Ecological Engineering 29(2), pp. 200–208. doi: 10.1016/j.ecoleng.2006.09.021.

Agyei, N.M. et al. 2003. Reply to the discussion by A. Demirbas of the paper "The removal of phosphate ions from aqueous solution by fly ash, slag, ordinary Portland cement and related blends". Cement and Concrete Research 33(6), p. 937. Available at: http://linkinghub.elsevier.com/retrieve/pii/S0008884602010724.

Alkattan, M. et al. 2002. An experimental study of calcite dissolution rates at acidic conditions and 25 °C in the presence of $NaPO_3$ and $MgCl_2$. Chemical Geology 190(1–4), pp. 291–302. doi: 10.1016/S0009-2541(02)00121-3.

Amor, M. Ben et al. 2004. Influence of water hardness, substrate nature and temperature on heterogeneous calcium carbonate nucleation. Desalination 166(1–3), pp. 79–84. doi: 10.1016/j.desal.2004.06.061.

Arias, C.A. et al. 2003. Phosphorus removal in constructed wetlands: can suitable alternative media be identified Society (c), pp. 267–273. doi: 10.2166/wst.2005.0335.

Aziz, H.A. and Smith, P.G. 1996. Removal of manganese from water using crushed dolomite filtration technique. Water Research 30(2), pp. 489–492. doi: 10.1016/0043-1354(95)00178-6.

Aziz, H.A. et al. 2001. Removal of copper from water using limestone filtration technique determination of mechanism of removal. Environment International 26(5–6), pp. 395–399. doi: 10.1016/S0160-4120(01)00018-6.

Battistoni, P. et al. 1997. Phosphate removal in anaerobic liquors by struvite crystallization without addition of chemicals: Preliminary results. Water Research 31(11), pp. 2925–2929. doi: 10.1016/S0043-1354(97)00137-1.

Bellier, N. et al. 2006. Phosphorus removal from wastewater by mineral apatite. Water Research 40(15), pp. 2965–2971. doi: 10.1016/j.watres.2006.05.016.

Benitez-Nelson, C.R. 2000. The biogeochemical cycling of phosphorus in marine systems. Earth Science Reviews 51(1–4), pp. 109–135. doi: 10.1016/S0012-8252(00)00018-0.

Berner, R.A. and Morse, J.W., 1974. Dissolution kinetics of calcium carbonate in sea water; IV, Theory of calcite dissolution. *American Journal of Science*, *274*(2), pp.108-134.

Blaney, L.M. et al. 2007. Hybrid anion exchanger for trace phosphate removal from water and wastewater. Water Research 41(7), pp. 1603–1613. doi: 10.1016/j.watres.2007.01.008.

Boudreau, B.P. and Canfield, D.E. 1993. A comparison of closed- and open-system models for porewater pH and calcite-saturation state. Geochimica et Cosmochimica Acta 57(2), pp. 317–334. doi: 10.1016/0016-7037(93)90434-X.

Bowes, M. et al. 2016. Climate change and eutrophication risk in English rivers. Available at: www.gov.uk/government/publications.

Brix, H. et al. 2001. Media selection for sustainable phosphorus removal in subsurface flow constructed wetlands. Water Science and Technology 44(11–12), pp. 47–54.

Brooks, A.S. et al. 2000. Phosphorus removal by wollastonite: A constructed wetland substrate. Ecological Engineering 15(1–2), pp. 121–132. doi: 10.1016/S0925-8574(99)00056-7.

Buhmann, D. and Dreybrodt, W. 1985. The kinetics of calcite dissolution and precipitation in geologically relevant situations of karst areas. 2. Closed system. *Chemical Geology* 53(1–2), pp. 109–124. doi: 10.1016/0009-2541(85)90024-5.

Bunce, J.T. et al. 2018. A review of phosphorus removal technologies and their applicability to small-scale domestic wastewater treatment systems. *Frontiers in Environmental Science* 6(FEB), pp. 1–15. doi: 10.3389/fenvs.2018.00008.

Burau, R.G. and Zasoski, R.J. 2002. Chemistry of carbonate systems. SSC 102 - Soil and Water Chemistry, pp. 5.1-5.27.

Cabeza, R. et al. 2011. Effectiveness of recycled P products as P fertilizers, as evaluated in pot experiments. Nutrient Cycling in Agroecosystems 91(2), pp. 173–184. doi: 10.1007/s10705-011-9454-0.

Cao, X. and Harris, W. 2008. Carbonate and Magnesium Interactive Effect on Calcium Phosphate Precipitation. Environmental science & technology 42, pp. 436–442. doi: 10.1021/es0716709.

Cao, X. et al. 2007. Inhibition of calcium phosphate precipitation under environmentally-relevant conditions. Science of the Total Environment 383(1–3), pp. 205–215. doi: 10.1016/j.scitotenv.2007.05.012.

Carliell-Marquet, C. et al. 2010. Inorganic profiles of chemical phosphorus removal sludge. Proceedings of the Institution of Civil Engineers - Water Management 163(2), pp. 65–77. doi: 10.1680/wama.2010.163.2.65.

Chaturvedi, D. and Sahu, O. 2014. Minimization of Phosphate from Ocean Water. 2(1), pp. 1–4. doi: 10.12691/jor-2-1-1.

Chazarenc, F. et al. 2007. Slag columns for upgrading phosphorus removal from constructed wetland effluents. Water Science and Technology 56(3), pp. 109–115. doi: 10.2166/wst.2007.499.

Chen, J. et al. 2007. Phosphate immobilization from aqueous solution by fly ashes in relation to their composition. *Journal of Hazardous Materials* 139(2), pp. 293–300. doi: 10.1016/j.jhazmat.2006.06.034.

Chong, T.H. and Sheikholeslami, R. 2001. Thermodynamics and kinetics for mixed calcium carbonate and calcium sulfate precipitation. Chemical Engineering Science 56(18), pp. 5391–5400. doi: 10.1016/S0009-2509(01)00237-8.

Chris P. Minstone and Parr., W. 2002. Phosphorus in rivers — ecology and management. doi: 10.1016/s0048-9697(01)00937-8.

Clark, T. et al. 1997. Phosphorus removal by chemical precipitation in a biological aerated filter. Water Research 31(10), pp. 2557–2563. doi: 10.1016/S0043-1354(97)00091-2.

Coelho, J.P. et al. 2004. Phosphorus speciation and availability in intertidal sediments of a temperate estuary: Relation to eutrophication and annual P-fluxes. Estuarine, Coastal and Shelf Science 61(4), pp. 583–590. doi: 10.1016/j.ecss.2004.07.001.

Commission of the European Communities 1999. Implementation of Council Directive 91/271/EEC of 21 May 1991 concerning urban waste water treatment, as amended by Commission Directive 98/15/EC of 27 February 1998. (February 1998), pp. 1–27. Available at: http://aei.pitt.edu/6709/1/6709.pdf.

Corbridge 2016. Chemistry, Biochemistry and Technology.

Corbridge Dec, C., 1995. Phosphorus: an outline of its chemistry, biochemistry and technology.

Corbridge, D.E.C., 1966. The structural chemistry of phosphorus compounds. Topics in phosphorus chemistry, 3, p.57.

Cordell, D. et al. 2009. The story of phosphorus: Global food security and food for thought. Global Environmental Change 19(2), pp. 292–305. doi: 10.1016/j.gloenvcha.2008.10.009.

Cordell, D. et al. 2011. Chemosphere Towards global phosphorus security: A systems framework for phosphorus recovery and reuse options. Chemosphere 84(6), pp. 747–758. Available at: http://dx.doi.org/10.1016/j.chemosphere.2011.02.032.

Corre, L. 2009. PHOSPHORUS RECOVERY FROM WASTEWATER BY STRUVITE CRYSTALLISATION: A REVIEW. 39(6), pp. 433–477.

Cowan, C.E. et al. 1990. Solution ion effects on the surface exchange of selenite on calcite. Geochimica et Cosmochimica Acta 54(8), pp. 2223–2234. doi: 10.1016/0016-7037(90)90047-O.

Cucarella, V. et al. 2008. Effect of reactive substrates used for the removal of phosphorus from wastewater on the fertility of acid soils. Bioresource Technology 99(10), pp. 4308–4314. doi: 10.1016/j.biortech.2007.08.037.

Curl 1968. [no date].

Dandurand, J.L. et al. 1982. Kinetically controlled variations of major components and carbon and oxygen isotopes in a calcite-precipitating spring. Chemical Geology 36(3–4), pp. 299–315. doi: 10.1016/0009-2541(82)90053-5.

de Kanel, J. and Morse, J.W. 1978. The chemistry of orthophosphate uptake from seawater on to calcite and aragonite. Geochimica et Cosmochimica Acta 42(9), pp. 1335–1340. doi: 10.1016/0016-7037(78)90038-8.

De-Bashan, L.E. and Bashan, Y. 2004. Recent advances in removing phosphorus from wastewater and its future use as fertilizer (1997-2003). Water Research 38(19), pp. 4222–4246. doi: 10.1016/j.watres.2004.07.014.

Desmidt, E. et al. 2015. Global phosphorus scarcity and full-scale P-recovery techniques: A review. Critical Reviews in Environmental Science and Technology 45(4), pp. 336–384. doi: 10.1080/10643389.2013.866531.

Dove, P.M. and Hochella, M.F. 1993. Calcite precipitation mechanisms and inhibition by orthophosphate: In situ observations by Scanning Force Microscopy. Geochimica et Cosmochimica Acta 57, pp. 705–714. doi: 10.1016/0016-7037(93)90381-6.

Doyle, J.D. and Parsons, S.A. 2002. Struvite formation, control and recovery. Water Research 36(16), pp. 3925–3940. doi: 10.1016/S0043-1354(02)00126-4.

Dreybrodt, W. et al. 1992. Geochemically controlled calcite precipitation by CO2 outgassing: Field measurements of precipitation rates in comparison to theoretical predictions. Chemical Geology 97(3–4), pp. 285–294. doi: 10.1016/0009-2541(92)90082-G.

Dreybrodt, W., 1981. 1981. KINETICS OF THE DISSOLUTION OF CALCITE AND ITS APPLICATIONS TO KARSTIFICATION. 31, pp. 245–269.

Drizo, A. et al. 1999. Physico-chemical screening of phosphate-removing substrates for use in constructed wetland systems. Water Research 33(17), pp. 3595–3602. doi: 10.1016/S0043-1354(99)00082-2.

Drizo, A. et al. 2002. Phosphorus saturation potential: A parameter for estimating the longevity of constructed wetland systems. Environmental Science and Technology 36(21), pp. 4642–4648. doi: 10.1021/es011502v.

Drizo, A. et al. 2006. Phosphorus removal by electric arc furnace steel slag and serpentinite. Water Research 40(8), pp. 1547–1554. doi: 10.1016/j.watres.2006.02.001.

Dueñas, J.F. et al. 2003. Characterisation of phosphorous forms in wastewater treatment plants. Journal of Hazardous Materials 97(1), pp. 193–205. doi: 10.1016/S0304-3894(02)00260-1.

Faul, K.L. et al. 2005. Phosphorus distribution in sinking oceanic particulate matter. Marine Chemistry 97(3–4), pp. 307–333. doi: 10.1016/j.marchem.2005.04.002.

Feenstra, T.P. and De Bruyn, P.L. 1981. The ostwald rule of stages in precipitation from highly supersaturated solutions: a model and its application to the formation of the nonstoichiometric amorphous calcium phosphate precursor phase. Journal of colloid and interface science. 84(1), pp. 66–72.

Froelich, P.N. 1988. Kinetic control of dissolved phosphate in natural rivers and estuaries: A primer on the phosphate buffer mechanism'. Limnology 33(July)

Fytianos, K. et al. 1998. Modelling of phosphorus removal from aqueous and wastewater samples using ferric iron. Environmental Pollution 101(1), pp. 123–130. doi: 10.1016/S0269-7491(98)00007-4.

Gal, J.Y. et al. 2002. Mechanisms of scale formation and carbon dioxide partial pressure influence. Part I. Elaboration of an experimental method and a scaling model. Water Research 36(3), pp. 755–763. doi: 10.1016/S0043-1354(01)00270-6.

Goldsmith, T. and Rubin, A.J., 1980. Aqueous chemistry and precipitation of aluminum phosphate in. Chemistry of Water Tech. pp. 59, 79.

Hanna, A.A. et al. 2008. Phosphate Removal From Wastewater By Calcite and Dolomite Ores. Phosphorus Research Bulletin 22, pp. 7–12. doi: 10.3363/prb.22.7.

He, Y. et al. 2016. Simultaneous removal of ammonium and phosphate by alkaline-activated and lanthanum-impregnated zeolite. Chemosphere 164, pp. 387–395. Available at: http://dx.doi.org/10.1016/j.chemosphere.2016.08.110.

Heal, K. V. et al. 2005. Enhancing phosphorus removal in constructed wetlands with ochre from mine drainage treatment. Water Science and Technology 51(9), pp. 275–282.

HELEEN J. DANEN-LOUWERSE 1995. Coprecipitation of Phosphate With Calcium. 29(7), pp. 1781–1785.

Herman, J.S. and Lorah, M.M. 1987. CO2 outgassing and calcite precipitation. Chemical Geology 62, pp. 251–262. doi: Doi: 10.1016/0009-2541(87)90090-8.

Herrmann, I. et al. 2014. Effect of temperature on the performance of laboratory-scale phosphorus-removing filter bEDX in on-site wastewater treatment. Chemosphere 117(1), pp. 360–366. Available at: http://dx.doi.org/10.1016/j.chemosphere.2014.07.069.

Hoffer-french, K.J. et al. 1989. EVALUATION OF HYDROLOGICAL AND BIOLOGICAL INFLUENCES ON CO2 FLUXES FROM A KARST STREAM. 108, pp. 189–212.

Hollett, M.J. [no date]. The Spectroscopic Analysis of Vaterite and Other Forms of Calcium Carbonate.

Hong, D. et al. 2018. An experimental study simulating the dissolution of gypsum rock. Energy Exploration and Exploitation 36(4), pp. 942–954. doi: 10.1177/0144598717751927.

House, W.A. 1984. The kinetics of calcite precipation and related processes. (1977), pp. 75–90. doi: 10.1007/s11837-014-1109-6.

House, W.A. 1987. Inhibition of calcite crystal growth by inorganic phosphate. Journal of colloid and interface science. 119(2), pp. 505–511.

House, W.A. 1990. The prediction of phosphate coprecipitation with calcite in freshwaters. Water Research 24(8), pp. 1017–1023. doi: 10.1016/0043-1354(90)90124-O.

House, W.A. et al. 1986. Factors affecting the coprecipitation of inorganic phosphate with calcite in hardwaters-I Laboratory studies. Water Research. doi: 10.1016/0043-1354(86)90181-8.

Huang, J. et al. 2017. Nitrogen and phosphorus losses and eutrophication potential associated with fertilizer application to cropland in China. *Journal of Cleaner Production* 159, pp. 171–179. Available at: http://dx.doi.org/10.1016/j.jclepro.2017.05.008.

Huang, W. et al. 2008. Phosphate removal from wastewater using red mud. Journal of Hazardous Materials 158(1), pp. 35–42. doi: 10.1016/j.jhazmat.2008.01.061.

Hussain, S. et al. 2011. Orthophosphate removal from domestic wastewater using limestone and granular activated carbon. Desalination 271(1–3), pp. 265–272. Available at: http://dx.doi.org/10.1016/j.desal.2010.12.046.

Inskeep, W.P. and Bloom, P.R. 1985. An evaluation of rate equations for calcite precipitation kinetics at pCO2 less than 0.01 atm and pH greater than 8. Geochimica et Cosmochimica Acta 49(10), pp. 2165–2180. doi: 10.1016/0016-7037(85)90074-2.

Ishikawa, M. and Ichikuni, M. 1981. Coprecipitation of phosphate with calcite. GEOCHEMICAL JOURNAL . doi: 10.2343/geochemj.15.283.

Jacobs 2017. Wastewater Treatment Cost drivers. (December)

Jaffer, Y. et al. 2002. Potential phosphorus recovery by struvite formation. Water Research 36(7), pp. 1834–1842. doi: 10.1016/S0043-1354(01)00391-8.

Jang, H. and Kang, S.H. 2002. Phosphorus removal using cow bone in hydroxyapatite crystallization. Water Research 36(5), pp. 1324–1330. doi: 10.1016/S0043-1354(01)00329-3.

Jenkins, D. et al. 1971. Chemical processes for phosphate removal. Water research 5(June 1970), pp. 369–389. Available at: http://scholar.google.com/scholar?hl=en&btnG=Search&q=intitle:CHEMICAL+PROCESSES+FOR+PHOSPHATE+REMOVAL#0.

Johansson Westholm, L. 2006. Substrates for phosphorus removal - Potential benefits for on-site wastewater treatment? Water Research 40(1), pp. 23–36. doi: 10.1016/j.watres.2005.11.006.

Johansson, L. and Gustafsson, J.P. 2000. Phosphate removal using blast furnace slags and opoka-mechanisms. Water Research 34(1), pp. 259–265. doi: 10.1016/S0043-1354(99)00135-9.

Jonasson, R.G. et al. 1996. Effect of phosphonate inhibitors on calcite nucleation kinetics as a function of temperature using light scattering in an autoclave. *Chemical Geology* 132(1-4 SPEC. ISS.), pp. 215–225.

Kagalou, I. et al. 2008. Long term changes in the eutrophication process in a shallow Mediterranean lake ecosystem of W. Greece: Response after the reduction of external load. Journal of Environmental Management 87(3), pp. 497–506. doi: 10.1016/j.jenvman.2007.01.039.

Kang, M. et al. 2018. Effects of dissolved oxygen and nutrient loading on phosphorus fluxes at the sediment–water interface in the Hai River Estuary, China. *Marine Pollution Bulletin* 130(June 2017), pp. 132–139. Available at: https://doi.org/10.1016/j.marpolbul.2018.03.029.

Karaca, S. et al. 2006. Adsorptive removal of phosphate from aqueous solutions using raw and calcinated dolomite. Journal of Hazardous Materials 128(2–3), pp. 273–279. doi: 10.1016/j.jhazmat.2005.08.003.

Karageorgiou, K. et al. 2007. Removal of phosphate species from solution by adsorption onto calcite used as natural adsorbent. Journal of Hazardous Materials 139(3), pp. 447–452. doi: 10.1016/j.jhazmat.2006.02.038.

Karapinar, N. et al. 2006. P-recovery by secondary nucleation and growth of calcium phosphates on magnetite mineral. Water Research 40(6), pp. 1210–1216. doi: 10.1016/j.watres.2005.12.041.

Karunanithi, R. et al. 2015. Phosphorus recovery and reuse from waste streams. Elsevier LTD. Available at: http://dx.doi.org/10.1016/bs.agron.2014.12.005.

Kathleen C. Ruttenberg 1992. Development of a sequential extraction method for different forms of phosphorus in marine sediments. Prevention & Treatment 37(7), pp. 1460–1482. doi: 10.4319/lo.1992.37.7.1460.

Kaufmann, G. and Dreybrodt, W. 2007. Calcite dissolution kinetics in the system CaCO3-H2O-CO2 at high undersaturation. *Geochimica et Cosmochimica Acta* 71(6), pp. 1398–1410. doi: 10.1016/j.gca.2006.10.024.

Kemenade, M.J.J.M. van and Bruyn, P.L. de 1987. A kinetic study of precipitation from supersaturated calcium phosphate solutions. Journal of Colloid and Interface Science 118(2), pp. 564–585. Available at: https://dspace.library.uu.nl/handle/1874/16857.

Kim, E.H. et al. 2006. Recovery of phosphates from wastewater using converter slag: Kinetics analysis of a completely mixed phosphorus crystallization process. *Chemosphere* 63(2), pp. 192–201. doi: 10.1016/j.chemosphere.2005.08.029.

Kim, J.O. and Chung, J. 2014. Implementing chemical precipitation as a pretreatment for phosphorus removal in membrane bioreactor-based municipal wastewater treatment plants. KSCE Journal of Civil Engineering 18(4), pp. 956–963. doi: 10.1007/s12205-014-0070-9.

Kitano, Y. 1978. Uptake of phosphate ions by calcium carbonate. 12(1969)

Kleiner, J. 1988. Coprecipitation of phosphate with calcite in lake water: A laboratory experiment modelling phosphorus removal with calcite in Lake Constance. Water Research 22(10), pp. 1259–1265. doi: 10.1016/0043-1354(88)90113-3.

Kõiv, M. et al. 2010a. Phosphorus removal using Ca-rich hydrated oil shale ash as filter material - The effect of different phosphorus loadings and wastewater compositions. Water Research 44(18), pp. 5232–5239. doi: 10.1016/j.watres.2010.06.044.

Kõiv, M. et al. 2010b. Phosphorus removal using Ca-rich hydrated oil shale ash as filter material - The effect of different phosphorus loadings and wastewater compositions. Water Research 44(18), pp. 5232–5239. doi: 10.1016/j.watres.2010.06.044.

Korchef, A. et al. 2011. Phosphate recovery through struvite precipitation by CO2 removal: Effect of magnesium, phosphate and ammonium concentrations. Journal of Hazardous Materials 186(1), pp. 602–613. Available at: http://dx.doi.org/10.1016/j.jhazmat.2010.11.045.

Koutsoukos, P.G. [no date]. Current Knowledge of Calcium Phosphate Chemistry and in Particular Solid Surface-Water Interface Interactions.

Langmuir, D. 1971. The geochemistry of some carbonate ground waters in central Pennsylvania. Geochimica et Cosmochimica Acta 35(10), pp. 1023–1045. doi: 10.1016/0016-7037(71)90019-6.

Langmuir, D. 1997. Aqueous environmental Geochemistry. Available at: https://www.researchgate.net/profile/Bayan_Hussien/post/how_pH_is_related_to_metal_solubility_in_solution_Is_there_anyway_to_compare_metal_solubility_in_acidic_and_basic_solutions/attachment/5aace3ecb53d2f0bba589203/AS%3A605106244423680%401521279979315/do.

LECKIE, J.O. and Stumm, W., 1970. Phosphate precipitation.

Lee, C.-K. et al. 2005. the Removal of Heavy Metals Using Hydroxyapatite. Environmental Engineering Research 10(5), pp. 205–212. doi: 10.4491/eer.2005.10.5.205.

Letshwenyo, M.W. 2014. Phosphorus removal in passive treatment technologies for tertiary wastewater treatment. (January), pp. 2010–2013. doi: 10.1007/s13398-014-0173-7.2.

Li, Z. et al. 2017. Phosphate adsorption and precipitation on calcite under calco-carbonic equilibrium condition. Chemosphere 183, pp. 419–428. Available at: http://dx.doi.org/10.1016/j.chemosphere.2017.05.139.

Littler, J. 2012. Removal of phosphorus from water using treated acid mine drainage solids and pellets made thereof. (March), pp. 1–328. Available at: http://orca.cf.ac.uk/22605/.

Liu, N. et al. 2017. Quantitative fluorescence techniques for investigating hydrocarbon charge history in carbonate reservoir. Energy Exploration and Exploitation 35(3), pp. 356–375. doi: 10.1177/0144598717700081.

Liu, Y. et al. 2012. Removal of high-concentration phosphate by calcite: Effect of sulfate and pH. Desalination. doi: 10.1016/j.desal.2012.01.011.

Lopez-Valero, I. et al. 1992. Effects of sodium and ammonium ions on occurrence, evolution and crystallinity of calcium phosphates. Journal of crystal growth 121(3), pp. 297–304.

Loste, E. et al. 2003. The role of magnesium in stabilising amorphous calcium carbonate and controlling calcite morphologies. Journal of Crystal Growth 254(1–2), pp. 206–218. doi: 10.1016/S0022-0248(03)01153-9.

Letshwenyo, M.W. 2014. Phosphorus removal in passive treatment technologies for tertiary wastewater treatment. (January), pp. 2010–2013. doi: 10.1007/s13398-014-0173-7.2.

Lürling, M. and Oosterhout, F. Van 2013. Controlling eutrophication by combined bloom precipitation and sediment phosphorus inactivation. Water Research 47(17), pp. 6527–6537. doi: 10.1016/j.watres.2013.08.019.

M.Lorah, J.S.H. 1988. Calcite precipitation rates in the field: Measurement and prediction for a travertine-depositing stream. 52

Ma, B. et al. 2016. Origin of carbonate cements with implications for petroleum reservoir in Eocene sandstones, northern Dongying depression, Bohai Bay Basin, China. Energy Exploration and Exploitation 34(2), pp. 199–216. doi: 10.1177/0144598716629871.

Maher, W. and Woo, L. 1998. Procedures for the storage and digestion of natural waters for the determination of filterable reactive phosphorus, total filterable phosphorus and total phosphorus. Analytica Chimica Acta 375(1–2), pp. 5–47. doi: 10.1016/S0003-2670(98)00274-8.

Mangwandi, C. et al. 2014. Removal of ortho-phosphate from aqueous solution by adsorption onto dolomite. Journal of Environmental Chemical Engineering 2(2), pp. 1123–1130. Available at: http://dx.doi.org/10.1016/j.jece.2014.04.010.

Maryutina, T.A. 1999. PHOSPHORUS SPECIATION IN WATER AND SEDIMENTS. (December)

Martin, B.D. 2010. Removal and recovery of phosphorus from municipal wastewaters using a ferric nanoparticle adsorbent. (November), p. 185. Available at: http://dspace.lib.cranfield.ac.uk/handle/1826/5767.

Mayer, B.K. et al. 2013. Innovative strategies to achieve low total phosphorus concentrations in high water flows. *Critical Reviews in Environmental Science and Technology* 43(4), pp. 409–441. doi: 10.1080/10643389.2011.604262.

Mekmene, O. et al. 2009. Effects of pH and Ca/P molar ratio on the quantity and crystalline structure of calcium phosphates obtained from aqueous solutions. Dairy Science and Technology 89(3–4), pp. 301–316. doi: 10.1051/dst/2009019.

Meldrum, F.C. 2003. Calcium carbonate in biomineralisation and biomimetic chemistry. International Materials Reviews 48(3), pp. 187–224. doi: 10.1179/095066003225005836.

Melikhov, I. V et al. 1989. The effect of dissolved impurity on calcium phosphate nucleation in supersaturated medium. Journal of colloid and interface science. 127(2), pp. 317–327.

Meybeck, M. 1993. C, N, P and S in Rivers: From Sources to Global Inputs. In: Wollast, R. et al. EDX. Interactions of C, N, P and S Biogeochemical Cycles and Global Change. Berlin, Heidelberg: Springer Berlin Heidelberg, pp. 163–193.

Millero, F. et al. 2001. Adsorption and desorption of phosphate on calcite and aragonite in seawater. Aquatic Geochemistry 7, pp. 33–56.

Mino, T. et al. 1998. Microbiology and biochemistry of the EBPR process. Water Researches 32(11), pp. 3193–3207.

Molle, P. et al. 2005. Apatite as an interesting seed to remove phosphorus from wastewater in constructed wetlands. Water Science and Technology 51(9), pp. 193–203.

Montes-Hernandez, G. et al. 2009. Removal of oxyanions from synthetic wastewater via carbonation process of calcium hydroxide: Applied and fundamental aspects. Journal of Hazardous Materials . doi: 10.1016/j.jhazmat.2008.11.120.

Morse, G.K. et al. 1998. Review: Phosphorus removal and recovery technologies. Science of the Total Environment 212(1), pp. 69–81. doi: 10.1016/S0048-9697(97)00332-X.

Murphy, J., and J.P. Riley. 1962. A modified single solution method for the determination of phosphate in natural waters. Anal. Chim. Acta 27:31-36.

Murphy, T.P.K.J.H. and I.Y. 1983. Coprecipitation of phosphate will marl in a naturally eutrophic lake. Manuscript? 28(i), pp. 58–69.

Nancollas, G.H. and Koutsoukos, P.G. 1980. Calcium phosphate nucleation and growth in solution. Progress in Crystal Growth and Characterization 3(1), pp. 77–102.

Nassef, E. 2012. Removal of Phosphates from Industrial Waste Water by Chemical Precipitation . International Journal 2(3), pp. 409–413. Available at: http://www.estij.org/papers/vol2no32012/8vol2no3.pdf.

Ofwat 2017. Wastewater Treatment Cost drivers. (December)

Ogino, T. et al. 1987. The formation and transformation mechanism of calcium carbonate in water. Geochimica et Cosmochimica Acta 51(10), pp. 2757–2767. doi: 10.1016/0016-7037(87)90155-4.

Oguz, E. 2004. Removal of phosphate from aqueous solution with blast furnace slag. Journal of Hazardous Materials 114(1–3), pp. 131–137. doi: 10.1016/j.jhazmat.2004.07.010.

Okano, K. et al. 2013. Novel technique for phosphorus recovery from aqueous solutions using amorphous calcium silicate hydrates (A-CSHs). Water Research 47(7), pp. 2251–2259. Available at: http://dx.doi.org/10.1016/j.watres.2013.01.052.

Ooi, K. et al. 2017. Comparative study on phosphate adsorption by inorganic and organic adsorbents from a diluted solution. Journal of Environmental Chemical Engineering 5(4), pp. 3181–3189. Available at: http://dx.doi.org/10.1016/j.jece.2017.06.015.

Panthi, S. 2003. Carbonate Chemistry and Calcium Carbonate Saturation State of Rural Water Supply Projects in Nepal. Water-Observatory.Net (April), pp. 545–560. Available at: http://www.water-observatory.net/sources/iwtc2003/08-5.pdf.

Paytan, A. and McLaughlin, K. 2007. The oceanic phosphorus cycle. Chemical Reviews 107(2), pp. 563–576. doi: 10.1021/cr0503613.

Patrick M. Melia, Andrew B. Cundy, Saran P. Sohi, Peter S. Hooda, Rosa Busquets, Trends in the recovery of phosphorus in bioavailable forms from wastewater, (2017), doi: 10.1016/j.chemosphere.2017.07.089

Perassi, I. and Borgnino, L. 2014. Adsorption and surface precipitation of phosphate onto CaCO3-montmorillonite: Effect of pH, ionic strength and competition with humic acid. Geoderma 232–234, pp. 600–608. Available at: http://dx.doi.org/10.1016/j.geoderma.2014.06.017.

Plant, L.J. and House, W.A. 2002. Precipitation of calcite in the presence of inorganic phosphate. Colloids and Surfaces A: Physicochemical and Engineering Aspects 203(1–3), pp. 143–153. doi: 10.1016/S0927-7757(01)01089-5.

Plummer, L.N. and Busenberg, E. 1982. The solubilities of calcite, aragonite and vaterite in CO2-H2O solutions between 0 and 90°C, and an evaluation of the aqueous model for the system CaCO3-CO2-H2O. Geochimica et Cosmochimica Acta 46(6), pp. 1011–1040. doi: 10.1016/0016-7037(82)90056-4.

Quintana, M. et al. 2008. Removal of phosphorus through struvite precipitation using a by-product of magnesium oxide production (BMP): Effect of the mode of BMP preparation. Chemical Engineering Journal 136(2–3), pp. 204–209. doi: 10.1016/j.cej.2007.04.002.

Reddy, M.M. et al. 1981. Crystal growth of calcite from calcium bicarbonate solutions at constant PCO2 and 25°C: a test of a calcite dissolution model. Geochimica et Cosmochimica Acta 45(8), pp. 1281–1289. doi: 10.1016/0016-7037(81)90222-2.

Renman, A. and Renman, G. 2010. Long-term phosphate removal by the calcium-silicate material Polonite in wastewater filtration systems. Chemosphere 79(6), pp. 659–664. Available at: http://dx.doi.org/10.1016/j.chemosphere.2010.02.035.

Rittmann, B.E. et al. 2011. Capturing the lost phosphorus. Chemosphere 84(6), pp. 846–853. Available at: http://dx.doi.org/10.1016/j.chemosphere.2011.02.001.

Sabliy, L. et al. 2019. New Approaches in Biological Wastewater Treatment Aimed at Removal of Organic Matter and Nutrients. *Ecological Chemistry and Engineering S* 26(2), pp. 331–343. doi: 10.1515/eces-2019-0023.

Saidou, H. et al. 2009. Struvite precipitation by the dissolved CO2 degasification technique: Impact of the airflow rate and pH. Chemosphere 74(2), pp. 338–343. Available at: http://dx.doi.org/10.1016/j.chemosphere.2008.09.081.

Segnit, E.R. et al. 1962. The solubility of calcite in aqueous solutions-I The solubility of calcite in water between 75° and 200° at CO2 pressures up to 60 atm. Geochimica et Cosmochimica Acta 26(12), pp. 1301–1331. doi: 10.1016/0016-7037(62)90057-1.

Serruya, C. 1971. the Sediments Chemistry of. Limnology and Oceanography 16(May), pp. 510–521.

Sharpley, A. and Haygarth, P. 1991. Terminology for Phosphorus Transfer. Journal of Materials 26(4), pp. 441–446.

Shilton, A.N. et al. 2006. Phosphorus removal by an 'active' slag filter-a decade of full scale experience. Water Research 40(1), pp. 113–118. doi: 10.1016/j.watres.2005.11.002.

Shuster, E.T. and White, W.B. 1971. Seasonal fluctuations in the chemistry of lime-stone springs: A possible means for characterizing carbonate aquifers. Journal of Hydrology 14(2), pp. 93–128. doi: 10.1016/0022-1694(71)90001-1.

Sibrell, P.L. et al. 2007. An Innovative Carbonate Coprecipitation Process for the Removal of Zinc and Manganese from Mining Impacted Waters. Environmental Engineering Science 24(7), pp.

881–896. Available at: http://dx.doi.org/10.1089/ees.2006.0126%5Cnhttp://www.liebertonline.com/doi/abs/10.1089/ees.2006.0126.

Sindelar, H.R. et al. 2015. Effects of natural organic matter on calcium and phosphorus co-precipitation. Chemosphere . doi: 10.1016/j.chemosphere.2015.05.008.

Smith, D.R. et al. 2006. Changes in sediment-water column phosphorus interactions following sediment disturbance. Ecological Engineering 27(1), pp. 71–78. doi: 10.1016/j.ecoleng.2005.10.013.

Sø, H.U. et al. 2011. Sorption of phosphate onto calcite; results from batch experiments and surface complexation modeling. Geochimica et Cosmochimica Acta 75(10), pp. 2911–2923. Available at: http://dx.doi.org/10.1016/j.gca.2011.02.031.

Song, Y. et al. 2002. Effects of solution conditions on the precipitation of phosphate for recovery: A thermodynamic evaluation. Chemosphere 48(10), pp. 1029–1034. doi: 10.1016/S0045-6535(02)00183-2.

Song, Y. et al. 2006. Calcite-seeded crystallization of calcium phosphate for phosphorus recovery. Chemosphere 63(2), pp. 236–243. Available at: http://linkinghub.elsevier.com/retrieve/pii/S0045653505010210.

Stabel, H. 1986. Calcite precipitation in Lake Constance: Chemical equilibrium, sedimentation, and nucleation by algae l. 31(5), pp. 1081–1093.

STEEN, I. 1998. Phosphorus availability in the 21st century : Management of a non-renewable resource. Phosphorus Potassium 217(Cl), pp. 25–31.

Strong, A.E. and Eadie, B.J. 1978. Satellite observations of calcium carbonate precipitations in the Great Lakes. Limnology and Oceanography 23(5), pp. 877–887. doi: 10.4319/lo.1978.23.5.0877.

Stumm, W. and Morgan, J.J. 1996. Chemical Equilibria and Rates in Natural Waters. Aquatic chemistry , p. 1022.

Stumpf, D. et al. 2008. Phosphorus recovery in aerated systems by MAP precipitation: Optimizing operational conditions. Water Science and Technology 58(10), pp. 1977–1983. doi: 10.2166/wst.2008.549.

Su, Y. et al. 2013. Strong adsorption of phosphate by amorphous zirconium oxide nanoparticles. Water Research 47(14), pp. 5018–5026. doi: 10.1016/j.watres.2013.05.044.

Sundareshwar, A.P. V et al. 1999. Phosphorus sorption characteristics of intertidal marsh sediments along an estuarine salinity gradient. Limnology 44(7), pp. 1693–1701.

Suzuki, K. et al. 2002. Removal of phosphate, magnesium and calcium from swine wastewater through crystallization enhanced by aeration. Water Research 36(12), pp. 2991–2998. doi: 10.1016/S0043-1354(01)00536-X.

Suzuki, T. et al. 1986. Adsorption of Phosphate on Calcium Carbonate. Journal of the Chemical Society, Faraday Transactions 1 82, pp. 1733–1743.

Tahmazi, T. Al et al. 2017. Characteristics and mechanisms of phosphorus removal by dewatered water treatment sludges and the recovery.

Tervahauta, T. et al. 2014. Calcium phosphate granulation in anaerobic treatment of black water: A new approach to phosphorus recovery. Water Research 48(1), pp. 632–642. doi: 10.1016/j.watres.2013.10.012.

Tran, A.T.K. et al. 2014. P-recovery as calcium phosphate from wastewater using an integrated selectrodialysis/crystallization process. Journal of Cleaner Production 77, pp. 140–151. Available at: http://dx.doi.org/10.1016/j.jclepro.2014.01.069.

Tu, Y.J. and You, C.F. 2014. Phosphorus adsorption onto green synthesized nano-bimetal ferrites: Equilibrium, kinetic and thermodynamic investigation. Chemical Engineering Journal 251, pp. 285–292. Available at: http://dx.doi.org/10.1016/j.cej.2014.04.036.

Ugurlu, A. and Salman, B. 1998. Phosphorus removal by fly ash. Environment International 24(8), pp. 911–918. doi: 10.1016/S0160-4120(98)00079-8.

Usdowski 1979. RELATIONSHIP BETWEEN 13C and 1So FRACTIONATION AND CHANGES IN MAJOR ELEMENT COMPOSITION IN A RECENT CALCITE-DEPOSITING SPRING - A MODEL. Changes 42, pp. 267–276.

Vanderesse, R. et al. 2011. Calcium Phosphate and Calcium Phosphosilicate Mediated Drug Delivery and Imaging. Available at: http://www.springerlink.com/content/h182281q101615jl/.

Verbeeck, R.M.H. and Devenyns, J.A.H. 1992. The kinetics of dissolution of octacalcium phosphate II. The combined effects of pH and solution Ca/P ratio. Journal of crystal growth 121(3), pp. 335–348.

Walter, L.M. and Morse, J.W. 1985. The dissolution kinetics of shallow marine carbonates in seawater: A laboratory study. Geochimica et Cosmochimica Acta 49(7), pp. 1503–1513. doi: 10.1016/0016-7037(85)90255-8.

Wang, J. et al. 2005. Engineered struvite precipitation: Impacts of component-ion molar ratios and pH. Journal of Environmental Engineering 131(10), pp. 1433–1440. doi: 10.1061/(ASCE)0733-9372(2005)131:10(1433).

Wang, K. et al. 2012a. Theoretical analysis of protein effects on calcium phosphate precipitation in simulated body fluid. CrystEngComm 14(18), pp. 5870–5878. doi: 10.1039/c2ce25216c.

Wang, L. et al. 2012b. Kinetics of calcium phosphate nucleation and growth on calcite: Implications for predicting the fate of dissolved phosphate species in alkaline soils. Environmental Science and Technology 46(2), pp. 834–842. doi: 10.1021/es202924f.

Wei, X. et al. 2008. Phosphorus removal by acid mine drainage sludge from secondary effluents of municipal wastewater treatment plants. Water Research 42(13), pp. 3275–3284. doi: 10.1016/j.watres.2008.04.005.

Wigley, T.M.L. and Plummer, L.N. 1976. Mixing of carbonate waters. Geochimica et Cosmochimica Acta 40(9), pp. 989–995. doi: 10.1016/0016-7037(76)90041-7.

Wood, E. et al. 2007. The Application of ViroFilter Technology at Yorkshire Water. *European Water & Wastewater Management* , p. 16.

Wu, D. et al. 2017. Investigation of productivity decline in inter-salt argillaceous dolomite reservoir due to formation damage and threshold pressure gradient: Laboratory, mathematical modeling and application. Energy Exploration and Exploitation 35(1), pp. 33–53. doi: 10.1177/0144598716684308.

Xiong, J. et al. 2008. Phosphate removal from solution using steel slag through magnetic separation. Journal of Hazardous Materials 152(1), pp. 211–215. doi: 10.1016/j.jhazmat.2007.06.103.

Xu, N. et al. 2014. Mechanisms of phosphate retention by calcite: Effects of magnesium and pH. Journal of Soils and Sediments . doi: 10.1007/s11368-013-0807-y.

Yagi, S. and Fukushi, K. 2012. Removal of phosphate from solution by adsorption and precipitation of calcium phosphate onto monohydrocalcite. Journal of Colloid and Interface Science . doi: 10.1016/j.jcis.2012.06.063.

Yoshimura, T. et al. 2007. Distributions of particulate and dissolved organic and inorganic phosphorus in North Pacific surface waters. Marine Chemistry 103(1–2), pp. 112–121. doi: 10.1016/j.marchem.2006.06.011.

Yu, Y. and Paul Chen, J. 2015. Key factors for optimum performance in phosphate removal from contaminated water by a Fe-Mg-La tri-metal composite sorbent. Journal of Colloid and Interface Science 445, pp. 303–311. Available at: http://dx.doi.org/10.1016/j.jcis.2014.12.056.

Zhang, Y. and Grattoni, C.A. 1998. Comment on “Precipitation kinetics of calcite in the system CaCO3-H2O-CO2:The conversion to CO2 by the slow process H1 1 HCO32 3 CO2 1 H2O as a ratelimiting step” by W. Dreybrodt, L. Eisenlohr, B. Madry, and S. Ringer. Geochimica et Cosmochimica Acta 62(23/24), pp. 3789–3790. doi: 10.1016/S0016-7037(98)00257-9.

Zhang, Y. et al. 2004. The biogeochemical cycling of phosphorus in the upper ocean of the East China Sea. Estuarine, Coastal and Shelf Science 60(3), pp. 369–379. doi: 10.1016/j.ecss.2004.02.001.

Zuddas, P. and Mucci, A. 1994. Kinetics of calcite precipitation from seawater: I. A classical chemical kinetics description for strong electrolyte solutions. Geochimica et Cosmochimica Acta 58(20), pp. 4353–4362. doi: 10.1016/0016-7037(94)90339-5.

Appendices

Table 1: parameters measured during the field experimentation of Cardiff University system at 1 l/min inlet flow and 7 l/min circulation flow

System Stages	Sample point No.	TSS mg/l	Alkalinity mg/l as $CaCO_3$	Acidity g/l	DO (mg/l)	Temp °C	pH	Conductivity μScm^{-1}
Inlet Flow	1	34	135	85	1.3	17.7	7.1	613
After Carbonation	2	15	388	838	0	18	5.8	944
After Aeration	3	11	380	337	7.3	17.6	6.7	795
Outlet Flow	4	7	320	218	0.8	17.4	7.2	286

Table 2: Other elements average total concentrations (mg/l) measured from Cardiff university system during the field experimentation

System Stage	Sample Point No.	Fe	K	Mg	Mn	Na	Zn	S
Inlet Flow	1	0.1	17.3	7.9	0.0	56.9	0.0	15.7
After Carbonation	2	0.1	16.8	7.7	0.0	55.5	0.0	15.3
After Aeration	3	0.1	17.0	7.6	0.0	55.2	0.0	15.1
Outlet Flow	4	0.1	16	7.4	0.0	53.6	0.0	13.8

Table 3: Other elements average dissolved concentrations (mg/l) measured from Cardiff university during the field experimentation

System Stage	Sample Point No.	Fe	K	Mg	Mn	Na	S	F	Cl	SO_4^{-2}	NO_3^-
Inlet Flow	1	0.1	17.0	7.7	0.0	56.2	15.6	0.2	50.9	39.9	55.5
After Carbonation	2	0.1	16.6	7.6	0.0	55.3	15.1	0.7	47.7	40.7	54.1
After Aeration	3	0.1	16.9	7.6	0.0	54.9	15.0	1.0	48.4	39.9	54.8
Outlet Flow	4	0.1	16.2	7.4	0.0	53.1	13.7	0.9	47.1	39.3	50.0

Table 4: Average of related parameters measured from ARM system during the field experimentation

System Stages	Sample point No.	TSS mg/l	Alkalinity Mg/l as $CaCO_3$	Acidity g/l	DO (mg/l)	Temp °C	pH	Conductivity μScm^{-1}
Inlet Flow	1	32.6	119.5	84.5	4.6	16.5	7.3	548.6
IBC	2	16.3	124.3	80.0	7.1	16.8	7.8	455.2
C 1	3	7.5	230.0	0.0	4.6	16.7	11.6	1273.8
C 2	4	9.8	113.8	0.0	4.8	16.8	11.3	813.9
C 3	5	8.7	129.2	81.4	1.7	17.1	8.0	962.1
C 4	6	11.3	111.8	81.4	3.0	17.1	7.7	664.3

Table 5: Other elements average total concentrations (mg/l) measured from ARM system during the field experimentation

System Stage	Sample Point No.	Fe	K	Mg	Mn	Na	S
Inlet Flow	1	0.12	14.6	8.4	0.0	50.3	15.1
IBC	2	0.02	12.8	8.6	0.0	49.9	15.5
C 1	3	0.0	12.6	0.0	0.0	49.1	43.3
C 2	4	0.0	11.7	0.2	0.0	49.2	39.7
C 3	5	0.0	15.3	11.8	0.1	55.8	185.8
C 4	6	0.0	12.7	9.2	0.0	49.9	76.2

Table 6: Other elements average dissolved concentrations (mg/l) measured from ARM system during the field experimentation

System Stage	Sample Point No.	Fe	K	Mg	Mn	Na	S	F	Cl	SO_4	NO_3
Inlet Flow	1	0.1	14.4	8.1	0.0	49.8	14.9	0.2	44.9	38.2	37.1
IBC	2	0.0	12.7	8.5	0.0	49.7	15.4	0.9	44.4	36.5	48.7
C 1	3	0.0	12.6	0.0	0.0	48.8	43.1	4.6	44.1	112.0	32.1
C 2	4	0.0	11.6	0.1	0.0	49.0	39.2	2.5	43.5	102.5	34.7
C 3	5	0.1	15.2	11.1	0.1	54.7	175.5	6.1	47.8	448.1	33.5
C 4	6	0.0	12.6	9.0	0.0	49.4	75.7	4.3	44.1	201.3	35.9